AN EQUIPMENT FOR GEOMAGNETIC MEASUREMENTS IN A ROCKET VEHICLE

Thesis

Submitted by

K. BURROWS, M.Sc.

for the

Degree of Doctor of Philosophy

in the

Faculty of Science

UNIVERSITY OF LONDON

DECEMBER, 1962

Department of Geophysics,
Imperial College,
London, S.W.7.

ABSTRACT

The geophysical reasons for requiring magnetic measurements in the upper atmosphere are outlined and the scientific, technical and administrative problems involved in using a Skylark rocket for the purpose are described. The principles and advantages of a measuring technique utilising the free precession of protons in a hydrogenous liquid are discussed and this technique is applied to the design and construction of a portable magnetometer, which was used for general magnetic measurements.

A series of experiments, designed to investigate the effect of a rocket's rotational motions on the proton magnetometer data, is described and the results presented.

The application of the preliminary work to the design, construction and testing of an early valve/transistor magnetometer and of a later, completely transistorized, version is described, together with their associated equipment for pre-flight testing and post-flight data processing.

The results of the first, partially successful, instrument-proving flight of a single coil transistorized

proton precession magnetometer are presented and discussed. The evaluation of the flight data involved carrying out a ground survey, at the Woomera rocket range, and also an investigation into the effect of magnetic field gradients on the rocket-borne magnetometer.

Where possible the various stages of the project are described in chronological order.

CONTENTS

	Page.
CHAPTER 1. INTRODUCTION	7
CHAPTER 2. PRELIMINARY INVESTIGATIONS	15
2.1 Estimated Geomagnetic Effects	15
2.2 Rocket Magnetism	18
2.3 Instrumental Considerations	26
2.4 Nuclear Magnetic Resonance	27
2.5 Proton Precession Magnetometer	31
CHAPTER 3. THE PORTABLE MAGNETOMETER	44
3.1 Introduction	44
3.2 General Description of the Instrument	47
3.3 The Sensing Head	49
3.4 The Switching Circuit	51
3.5 The Amplifier	52
3.6 Frequency Measurement	55
3.7 Testing and Evaluation	58
3.8 Applications	60
3.9 Abridged Specification	61
CHAPTER 4. THE ROTATION EXPERIMENTS	62
4.1 Introduction	62
4.2 Apparatus	64
4.3 Results	71
4.4 Conclusions	79

	Page.
CHAPTER 5. THE ROCKET-BORNE MAGNETOMETER Mk. I	81
5.1 Introduction	81
5.2 The Sensing Head	83
5.3 Electronic Circuitry	87
5.4 Laboratory Evaluation	97
5.5 Installation and Compatibility Tests	107
CHAPTER 6. THE ROCKET-BORNE MAGNETOMETER Mk. II	124
6.1 General Considerations	124
6.2 The Sensing Head	125
6.3 Electronic Circuitry	125
6.4 Monitoring circuits	140
6.5 Mechanical Construction	141
6.6 Laboratory Testing and Evaluation	144
6.7 Compatibility Tests	151
CHAPTER 7. AUXILLIARY EQUIPMENT	154
7.1 Ground Recording Magnetometer	154
i) Double Channel Installation	154
ii) Single Channel Installation	158
iii) The Sensing Head	158
iv) The Head Unit	160
v) Frequency Measurement	165
vi) Sequence Timing	165
7.2 Test Oscillator	169
7.3 Standard Reference Frequency Source	172
7.4 Filter/Mixer Unit	174

Page

CHAPTER 8. TRIAL B.67 - FLIGHT OF SKYLARK SL40 180

8.1 Abridged Round Specification 180

8.2 Pre-flight Tests 181

8.3 The Flight of SL40 181

8.4 Timing Sequences 184

8.5 Data Recording 185

8.6 Performance of Rocket Instrumentation 186

8.7 Performance of Proton Magnetometers 188

8.8 Data Processing 191

CHAPTER 9. RESULTS OF TRIAL B.67 (SL40), DISCUSSION AND INTERPRETATION 198

9.1 Diurnal Variation 198

9.2 Rocket-borne Data 198

APPENDIX I. GRADIENT EXPERIMENTS 230

APPENDIX II. MAGNETIC SURVEY OF THE WOOMERA RANGE 241

BIBLIOGRAPHY 249

ACKNOWLEDGMENTS 252

CHAPTER 1

INTRODUCTION

The generally accepted basis for the explanation of the observed daily variations in the earth's magnetic field is to be found in the dynamo theory, first postulated by Balfour Stewart in a famous article in the 1882 edition of the Encyclopaedia Britannica.[1] His suggestion arose from the observation that the amplitude of the daily variations increased by a factor of two or more during a sunspot maximum, as compared with that during a sunspot minimum. Since this large factor could not be explained in terms of any known physical changes near the surface of the earth, he concluded that the source of the variations must lie in the upper atmosphere and must, therefore, be an electric current. Schuster[2], Chapman[3] and other workers later elaborated the dynamo theory and, using magnetograms recorded at various observatories throughout the world, they were able to represent the complex and changing array of magnetic variations by a relatively simple system of horizontally stratified sheet currents, stationary relative to the sun, but, relative to an observer on the earth, continuously moving westwards and varying in intensity with a predominantly twenty-four hour period. (Fig. 1).

According to the dynamo theory the electric currents

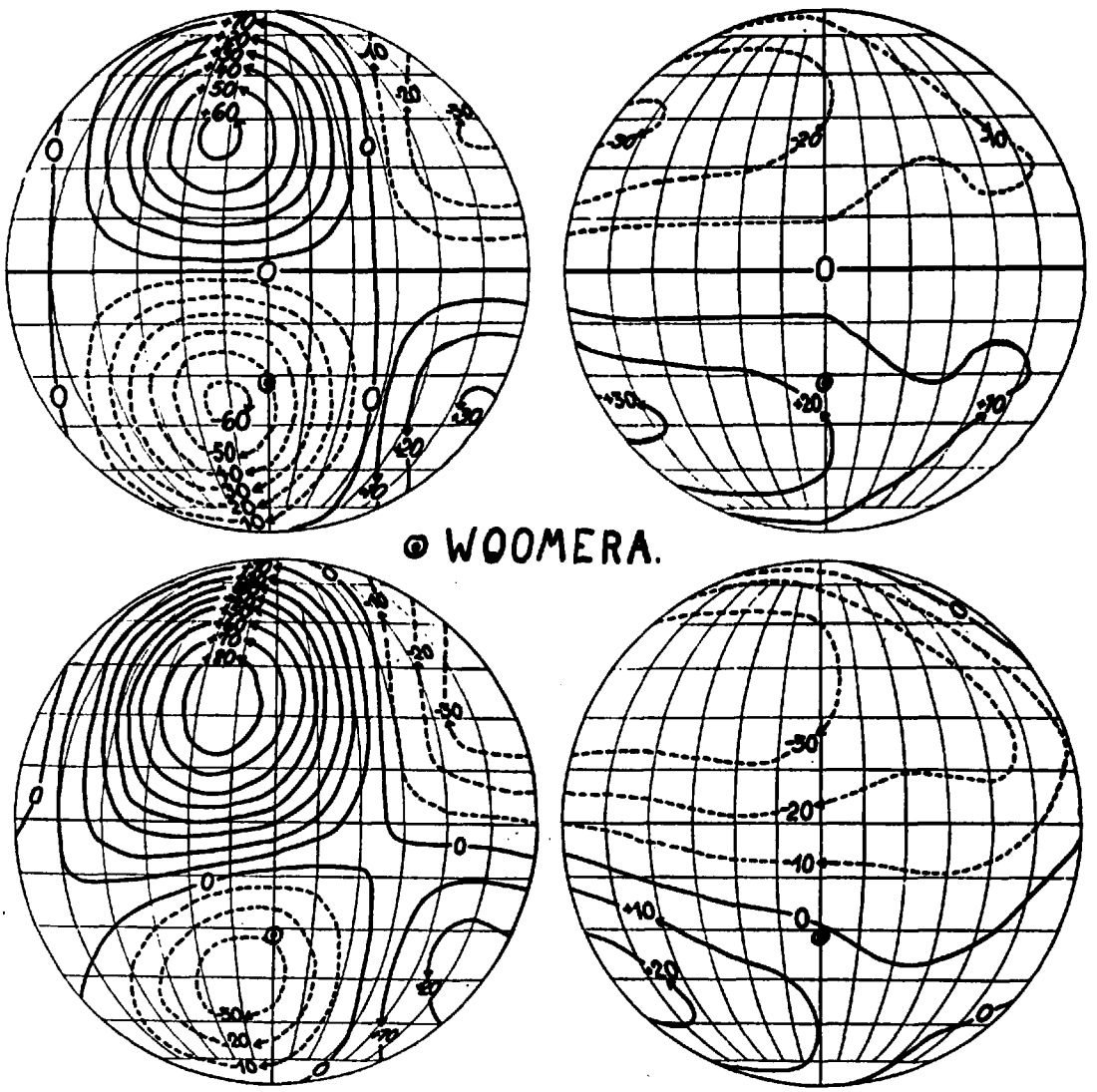


Fig. 1. Current diagram, for the electric current system responsible for the quiet-day solar daily magnetic variation S (or Sq), over the sunlit hemisphere, as viewed from the Sun (on the left), and over the night hemisphere (right). The flow between adjacent current-lines is 10,000 A. Above, for sunspot minimum, equinox; below, sunspot minimum, northern summer

are initiated and maintained by a combination of the action of solar tidal winds and the effects of solar radiations on the upper atmosphere. As charged particles are transported across the lines of force of the earth's magnetic field electromotive forces deflect the positively charged particles in the opposite direction from the negative ones, thereby generating a current. The current system is identified by the symbol Sq to differentiate it from other proposed currents responsible for lunar (L) variation and storm-time (D) variation. Since the source of the charged particles is to be found in the horizontal layers of the ionosphere it follows that, on a world-wide scale, the current systems must be predominantly horizontal. The current density at any point then depends on the velocity of the tidal winds producing the electromotive forces, on the conductivity of the ionised gases and on the strength and direction of the earth's magnetic field.

From an analysis of routine observatory magnetograms it is possible to estimate the integral, with respect to height, of the postulated current system; a detailed analysis is, however, not possible from ground data alone. In particular it is difficult to assess such features as the height, vertical thickness and any possible stratification of the currents.

With the advent of high altitude sounding rockets in

1946, direct in situ measurements of atmospheric properties became possible and in 1947 Vestine and others[4] first suggested that rocket-borne magnetometers could be used to investigate the distribution of the electric currents with height. Accurate determinations of the current density as a function of height at several geographical locations would then establish the validity of the dynamo theory and assist in its further development.

In addition to the measurements of the various atmospheric current systems, rocket-borne magnetometers could be used to obtain more detailed information on the morphology of the earth's main magnetic field. When corrected for the effects of the electrical currents, the data should reveal whether the main field decreases as a dipole field at the place of measurement, or whether the decrease deviates from that of a dipole, because of some large scale anomaly.

A comprehensive summary of the various circumstances in which worth-while magnetic measurements should be carried out from rockets has been given by Chapman[5]. In addition to his recommendations for flights during magnetic disturbances he further suggests that measurements of the current system be undertaken in low and middle latitudes during periods of magnetic calm.

A few flights of rockets carrying magnetometers have already been reported by various American authors.

At the time when the present work started (November, 1957 the only flights which had been reported were a series of three by Singer, Maple and Bowen, one from White Sands, New Mexico and two from a ship at a point very close to the magnetic equator (-1° latitude) [6,7]. Three mutually orthogona fluxgate elements were mounted in the fibre-glass nose cone of an Aerobee rocket and reached a height of 105 km. The outputs of the three fluxgates were squared and combined to measure the total scalar field, thereby making the data almost independent of fluxgate attitude, however, since at certain orientations the measured value of total force is very sensitive to the precise orthogonality of the fluxgate elements, some modulation of the field with rocket rotation was inevitable and this error had to be adjusted in the data analysis. The authors minimised the error due to dynamotors in the rocket power supplies by winding three mutually orthogonal coils round the magnetic detectors and adjusting the currents in the coils for the best attitude compensation, when the power supply was energised. Drifts in the three elements were corrected in the data reduction by means of in-flight calibration signals. The final accuracy of the data, after adjustments for the various heading errors and drifts, was in the region of 100 gamma. (1 gamma = 10^{-5} oersted).

The first flight was merely an instrument proving

flight; it was not expected that any current sheet would be detected as the experimental error was considerably larger than the anticipated effect of the current sheet. Of the two flights near the geomagnetic equator the first one was during the local evening and merely recorded an approximately dipole field profile but the second one, at local noon, succeeded in detecting a discontinuity of 400 gamma due to the equatorial electrojet, a local intensified current which occurs during the middle day-light period, in a narrow band (approximately 3° of latitude wide) along the magnetic equator. This pioneering flight represents the first successful direct detection of an ionospheric current by means of a rocket-borne magnetometer.

The first reported flight of a proton magnetometer was that by Heppner, Stolarik and Meredith who used an instrument developed by Varian Associates, Palo Alto, California, in an Aerobee flight. The rocket was fired to a height of 163 Km. from White Sands, New Mexico[8]. No ionospheric discontinuity was detected, but the measurements indicated that, at a height of 150 Km. the intensity of the geomagnetic field was approximately 200 gammas lower than that which would be predicted assuming a dipole source.

Meredith, Davis, Heppner and Berg also have reported a series of proton precession magnetometer flights through, or close to, auroral arcs in the Northern Auroral zone[9].

The instruments were carried in Aerobee rockets fired from the Fort Churchill rocket launching site in Northern Canada. They were able to demonstrate that aurorae are associated with intense electric currents, which can have comparatively small dimensions. The anomalous magnetic fields detected by the magnetometers, on passing through auroral arcs, were of the order of a few hundred gamma.

The first attempt at a more detailed investigation of the equatorial electrojet was by Cahill in a series of "rockoon" flights launched from the USS Glacier, during a cruise through the Pacific[10]. A proton precession magnetometer was developed for this purpose by the State University of Iowa. In particular two flights from the vicinity of Jarvis Island reached heights of 120 and 130 Km. and detected anomalous departures from a dipole field of -150 gamma and -300 gamma respectively, the experimental error in the observations being $\pm$20 gamma. The second flight also indicated some stratification of the electrojet into two layers, though the upper layer was not completely penetrated.

The Earth's main magnetic field above Fort Churchill was measured, on a magnetically quiet day, by Conley[11], using a "Varian" proton magnetometer in a Nike-Cajun rocket flight. The data revealed that the field departs from that of a geocentric dipole by approximately -200 gamma at a height of 150 Km. The scatter of the readings was approximately

±35 gamma and no discontinuity was detected.

The most recently reported flight is one from the Holloman Missile Development Centre, New Mexico. Hutchinson and Shuman[12] installed a "Varian" proton precession magnetometer in an Aerobee-Hi rocket which was fired to a height of 236 Km. An anomaly of the order of -80 ±20 gamma was detected during the ascent but not during the descent and, to explain this inconsistency in the results, the authors suggest that the rocket may have passed through a cloud of "Sporadic E" of approximately 60 Km. vertical thickness but with much smaller horizontal dimensions. No discontinuity which could be attributed to the postulated Sq current system was detected.

At the present time the existence of the normal diurnal (Sq) current system has not been confirmed, by means of a rocket-borne magnetometer, in middle latitudes.

In 1957 it was proposed that a British rocket-borne magnetometer should be developed, under the auspices of the Gassiot Committee of the Royal Society, to be fired from the Woomera rocket range in "Skylark" research rockets. The project would form part of the Royal Society's upper-atmospheric research programme, already commenced in connection with the International Geophysical Year[13].

The Skylark[14] is a single-stage uncontrolled rocket propelled by a "Raven" solid-fuel motor. It can carry 150 lb of payload to a height of approximately 160 Km.

CHAPTER 2

PRELIMINARY INVESTIGATIONS

2.1 Estimated Geomagnetic Effects.

Assuming, as discussed previously, that the current system shown in Fig. 1 is contained within the ionized layers of the upper atmosphere, it follows that the height and thickness of the current must each be small compared with its lateral dimensions and that therefore, to an observer on the earth, it can be approximated to a thin sheet of infinite horizontal extent. The magnitude of the external field is therefore approximately independent of height but its direction above the sheet will be opposite to that below. Hence on passing through the current sheet there will be a discontinuous change in the horizontal component of the geomagnetic field, the direction of the change being at right angles to the lines of current flow. Unfortunately it is not yet possible to stabilize the Skylark rocket, within the limits which would be necessary for useful in-flight measurements of components of the magnetic field, and hence measurements are limited to the scalar magnitude of the total force.

A rough estimate of the amplitude of the discontinuity which might be expected in the total scalar force at

Woomera can be made as follows. Since the focus of the Southern Hemisphere current system passes very close to Woomera (Fig. 1) Z, the vertical component of F, shows the greatest diurnal variation, at ground level, but it is continuous through the current sheet and so cannot contribute appreciably to any discontinuity. Fig. 2.1 shows the mean monthly variations in X and Y, the horizontal components of F, for quiet days during 1938 (sunspot maximum) at ~~Woomera~~ WATHEROO magnetic observatory (30°19'S, 115°53'E, Geomagnetic Lat. -41.8° Long. 185.6°). Since the observatory at Watheroo (now removed to Gnangara) was at approximately the same magnetic latitude as Woomera (-41.0°) it is reasonable to assume that the magnetograms from a geomagnetic observatory at Woomera would be very similar at corresponding local times. In Fig. 2.1, Y, the E-W component, shows maximum variation but since this component is almost normal to F, it will contribute very little and hence it is the variation in X which can be expected to be mainly responsible for any discontinuous change in F. As would be expected from a consideration of Fig. 1, the magnitude of the maximum diurnal variation in X varies with the season and occurs at different local times in each month (Fig. 2.1), the maximum being of the order of $\pm$20 gamma, at 09.00 $\pm$ 1 hours in August. Since at least 25% of this will be due to induced earth currents, the

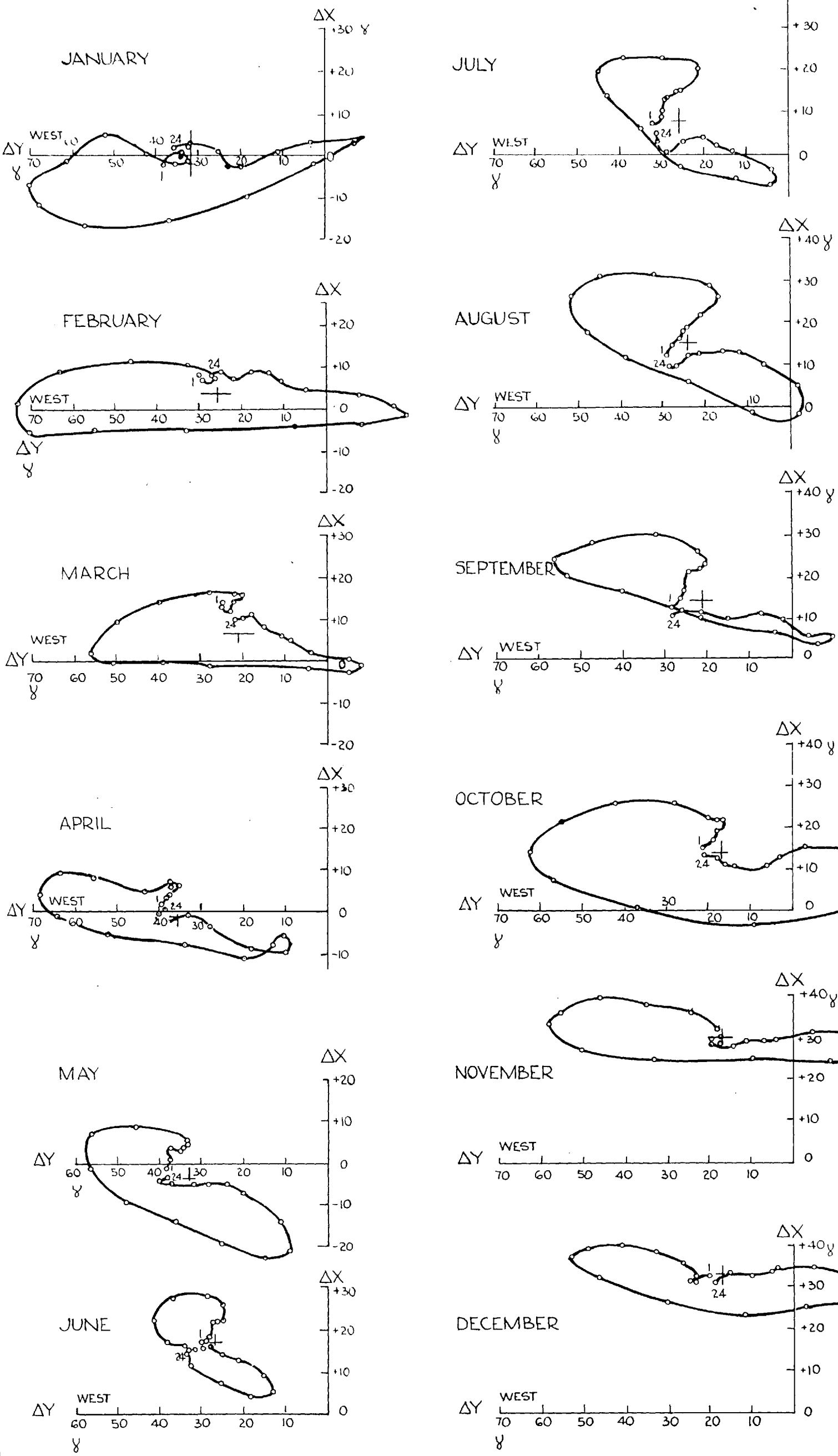


FIG. 2.1. ΔX- ΔY WATHEROO 1938

actual discontinuity in X will be roughly -0.75 x 2 x 20 = -30 gamma and this leads to an estimated discontinuity in F of 30. cos 63° = 14 gamma, since the angle of dip at Woomera = 63°. This estimate is furthermore rather optimistic since it applies only when time of day, time of year and sunspot cycle are all optimised; it further assumes that the current sheet is of negligible thickness and that the rocket flight penetrates right through all current carrying layers (neither assumption is strictly valid). It is likely therefore that the actual discontinuity present on any given day will, in general, be considerably less than this value.

2.2 Estimates of Magnetic-Field Perturbations due to Rocket Magnetism

The first problem was to decide whether the local magnetic field perturbations, due to unavoidable magnetic fields associated with the rocket, would make it impracticable to instal a sensitive magnetometer (i.e. one capable of resolving the estimated discontinuity of the order 10 gamma) in the rocket itself, or whether it would be necessary to separate a non-magnetic package from the main rocket. The latter alternative would involve many problems with regard to data recovery and either maintenance or monitoring of the package attitude; for these reasons it

was most undesirable and would only be entertained should it prove impracticable to remove, or compensate for the rocket magnetism.

The various possible sources of magnetic fields are:-

i) Permanent and induced magnetism of the rocket motor.

ii) Permanent and induced magnetism of the structure of the nose cone and instrumented parts of the rocket.

iii) Any permanent magnets.

iv) Electro-magnets in field windings of electric motors.

v) Unbalanced current loops supplying power to instruments.

vi) Induced eddy currents in the structure of the round.

i) Raven Rocket Motor.

The permanent and induced fields associated with a sample Raven motor were measured at the Royal Aircraft Establishment at Farnborough (hereafter referred to as R.A.E.). A recording fluxgate magnetometer, kindly loaned by Hunting Geophysics Ltd., was set up in the centre of a flat area at R.A.E. and the fields due to the combination of the induced and permanent magnetisation of the motor were measured at various orientations of the motor relative to magnetic north, with the motor positioned to the North, East, South and West of the magnetometer and with the motor both "end-on" and "broadside" relative to the magnetometer.

The motor was found to have some permanent magnetisation

orientated mainly along the longitudinal axis of the tube. The results of two of the experiments are illustrated in Fig. 2.2 which shows δF, the magnetic field perturbations

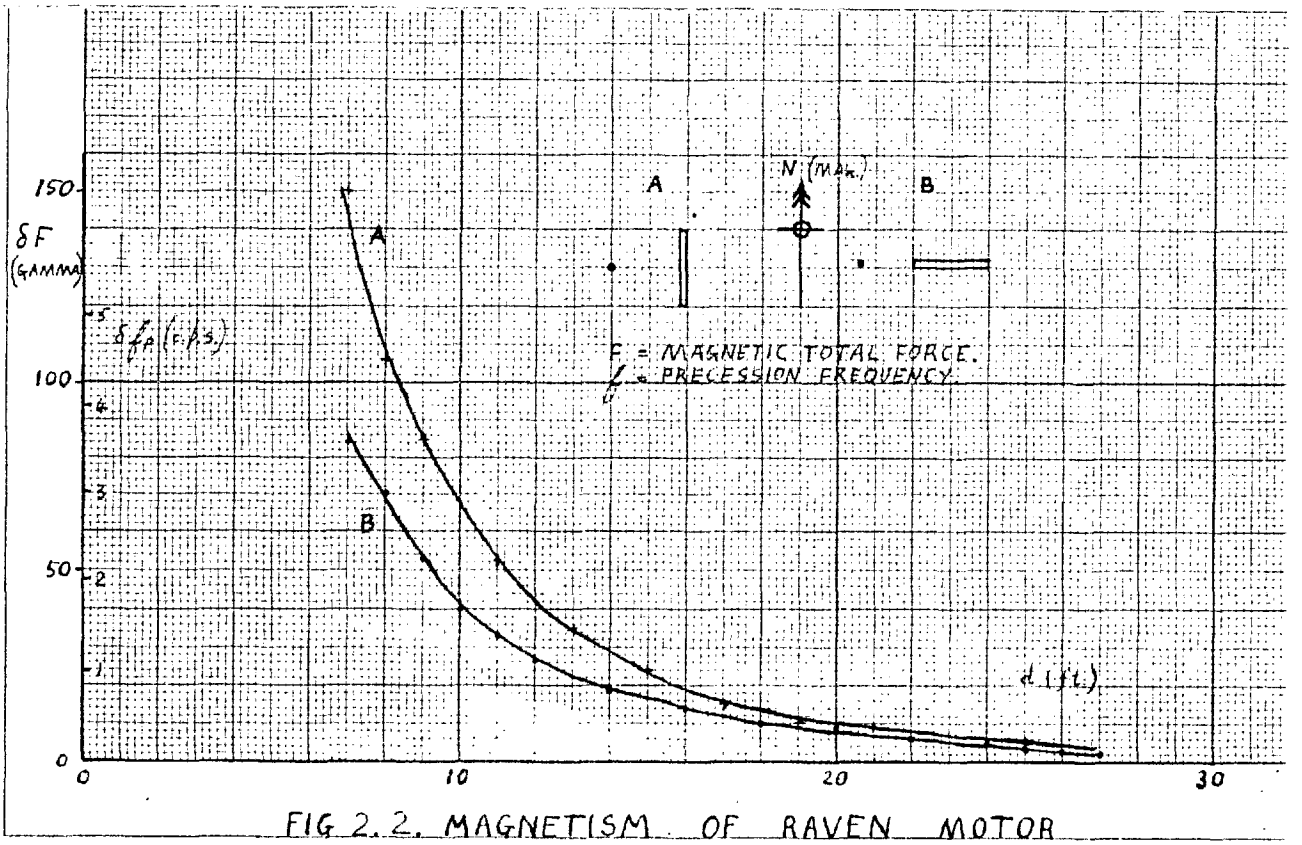


FIG 2.2. MAGNETISM OF RAVEN MOTOR

due to the induced magnetisation of the motor, plotted against d, the distance between the magnetometer sensing head and the nearest point of the motor. In this graph the effect of the permanent magnetisation has been taken out,

to a first approximation, by taking the mean of two opposite orientations of the motor tube. The key shows the relative orientations of motor tube, fluxgate and magnetic North for the two experiments. In these experiments the motor tube was, of necessity, always horizontal whereas in flight the rocket could be expected to take up any attitude relative to the magnetic vector. In order to estimate the magnetic perturbations in the vicinity of the motor tube which would occur when the motor axis is parallel to the magnetic vector, a series of model experiments was performed using a piece of mild steel tube, having appropriate dimensions, to simulate magnetically the Raven motor. A correction factor calculated from the model experiments, together with a further factor to take into account the relative field strengths at Farnborough and Woomera, enabled estimates to be made of the minimum magnetic field perturbations which might be experienced in the vicinity of the motor tube in flight. Assigning an arbitrary value of 5 gamma to the maximum permissible variation of measured field values with rocket attitude, an effect which will be called the "heading error", the corresponding minimum values of d can readily be calculated.

The various measurements yielded estimates of d within the range 41 - 68 ft. and it was therefore decided that it would be necessary to separate the instrumented

head of the rocket from the motor with as large a separation velocity as possible and as early in the flight as possible.

ii) Magnetism of the structure of the instrumented sections of the rocket.

Since most of the components used in constructing the instrumented sections of a Skylark rocket are non-magnetic this presented no problem. The only magnetic items were small (nuts, bolts, studs, etc.) and it was decided to manufacture these from austenitic (non-magnetic) stainless steel. In a confirmatory test a skeleton assembly (without instruments) was found to produce an external field which was quite negligible compared with that expected from instrumentation in the round.

iii) Permanent Magnets.

By far the strongest magnet used in a standard rocket instrumentation is that for the magnetron of the 6 cm "Missile Tracking System" transmitter (M.T.S.). At a distance of 9 ft. the perturbation in F due to this horseshoe magnet was 76.8 $\pm$ 0.5 gamma and therefore to reduce the heading error to ± 5 gamma or ± 1 gamma the sensing head would have to be situated 22.4 ft. or 38.3 ft. away from the magnetron respectively. Furthermore the magnet was subjected to long and short period vibration tests and to

temperature cycling, to simulate both the transit flight from England to Australia and the environment during the rocket flight. These tests indicated that any attempt to compensate for the field within a few feet of the rocket would have to be done at the launcher site and even then the compensation could change by a few gamma due to the environmental changes during the rocket firing. Fortunately the M.T.S. is not an essential tracking facility and it was decided that it could be omitted from the proposed flight.

The external field of the 24 way rotary switch, used for multiplexing the data from different instruments, was found to be negligible.

iv) Fields due to rotary power converters.

The external field of a standard rotary converter, powered by a standard battery but with no load, was found to be 12 $\pm$ 2 gamma at a distance of 5 ft., and it was anticipated that two converters would be required to provide all the H.T. power for the round. Application of a load on the H.T. output terminals increased this by a factor lying between 1.56 (80mA load) and 1.9 (130mA load). This is well outside the specified tolerance. This difficulty could be overcome by extending the sensing head of the magnetometer on a probe protruding from the tip of the nose cone. The maximum permissible length of a fixed

probe, determined by considerations of the aerodynamic stability of the rocket, is 4 ft., making the separation between sensing head and rotary converter about 10 ft. At this distance the combined fields of the two rotaries running with the anticipated loads would be approximately 5.2 gamma; however, if they were mounted in such a way that their external fields cancelled, to a first order, this heading error would be reduced to approximately 0.5 gamma.

v) Unbalanced current loops.

The heading error due to a single turn of wire carrying 10 amps round the circumference of the round (say 8 " radius) at a point near the base of the nose cone (say 10 ft. from the sensing head) would be of the order of 10 gamma. It would, therefore, be necessary to keep the area turns of any current loops to a minimum by using twisted or co-axial wires for any inter-connections carrying large currents.

vi) Eddy currents in the rocket skin.

As the rocket rotates about a transverse axis circulating eddy currents will be induced in the skin of the rocket and these, in turn, will generate magnetic fields in the vicinity of the sensing head. A rough estimate of the order of magnitude of the heading error

can be derived by approximating the parallel section of the head to a ring of diameter roughly equal to the rocket and of resistance equal to that of the rocket skin. If this ring is rotating with angular frequency ω about an axis in the plane of the ring but normal to F and if the instantaneous angle between the plane of the ring and F is ωt, then the flux through the coil $= \phi = FA \sin \omega t$. The induced e.m.f. is $\omega FA \cos \omega t$ and the component of the magnetic field parallel to F, at a distance a, is given by $2A^2 \omega FR^{-1} a^{-3} \sin \omega t \cos \omega t$, where A is the area of the ring in sq.cm., R its resistance in e.m.u. and a is the distance, in cm., between the point of measurement and the ring, measured along the axis of the ring perpendicular to its plane.

Substituting appropriate values for the parameters and taking a value for ω of 2π radians per second leads to the conclusion that the heading error due to this cause in the proposed rocket configuration would be of the order 10^{-4} gamma. It can therefore be stated with confidence that eddy currents in the main body of the rocket are not likely to induce a serious heading error in the results.

On the basis of these calculations and experiments it was decided that, in the first instance at least, it would not be necessary to eject a non-magnetic package from the round and that it should be possible to compensate for the

unavoidable rocket magnetism by means of correction magnets. Any residual heading error would then be measured by means of a pre-flight calibration and appropriate corrections could be applied to the flight data.

2.3 Instrumental Considerations

The requirements for the rocket-borne magnetometer can be summarized as follows:

i) Accuracy. To resolve a change of 10 gamma the error in each reading must not be greater than, say, $\pm$ 5 gamma.

ii) Resolution. Assuming the rocket reaches a height of 150 Km. it will be travelling at a speed of approximately 1 Km/sec. at a height of 100 Km. (the region where the greatest density of the postulated electric currents might be expected). Therefore to resolve any fine structure the readings from the instrument, if not continuous, must be at least one per second.

iii) It must be as simple as possible, as this will normally lead to good reliability, and must be capable of withstanding the severe environmental conditions experienced in a rocket, particularly during the boost phase. Intricate adjustments, such as are required in conventional ground observatory magnetometers, will obviously greatly decrease the chances of a successful flight.

iv) As the rocket can assume any attitude in space relative to the vertical the functioning of the instrument and the data it produces must be independent of the rocket attitude; or at least capable of being corrected for the motions of the rocket.

v) The temperature changes likely to be encountered must not affect the instrument in any way which might be detrimental to the scientific value of the data.

vi) The data must be in a form which will either survive the rocket's impact with the ground, or can be transmitted back to ground, without loss of accuracy, by the standard radio-telemetry system[15].

The disadvantages of the fluxgate as a magnetic sensor for rocket use have already been mentioned with particular regard to its attitude and drift characteristics, and it was decided to develop an instrument using the principle of proton free precession. Van Allen[16] had suggested that this technique could be used as the basis of a rocket-borne magnetometer and that it potentially satisfied all the requirements mentioned above.

2.4 Nuclear Magnetic Resonance.

Packard and Varian[17] in America and subsequently Waters and Francis[18,19] in England were the first to report the successful detection of nuclear free precession. Three

distinct operations are required to induce and detect coherent precession in a sample of a hydrogenous liquid.

1. A strong polarizing magnetic field H_o is created through the sample, preferably at a large angle to the earth's field F, by passing a direct current through a coil wound round the sample. This results in a magnetisation parallel to H_o of $M = \chi H_o [1 - \exp(-t/T_1)]$ where χ is the nuclear susceptibility and T_1, is the thermal relaxation time ($H_o \gg F$).

2. The polarizing field H_o is reduced to a value of the same order of magnitude as F, in a time short compared with T_1 and is then removed in a time short compared with $T_p/4$, where T_p is the period of the precession signal in the magnetic field present. If this condition is not fulfilled, the polarization in the sample follows the direction of the resultant vector $\vec{H}_o + \vec{F}$, the final orientation of $\vec{M}$ is therefore parallel to $\vec{F}$ and no coherent precession can ensue. This switching operation can be performed conveniently and simply, by the opening of a pair of relay contacts, since the final rapid removal of the polarizing current is achieved when the spark is extinguished. It is evident that the resonant frequency of the combination of polarizing coil and connecting cable must be high compared with the expected precession frequency.

3. The polarized protons in the sample now precess

in phase, round the direction of $\vec{F}$, at a frequency given by the well known Larmor formula, $f_p = \gamma F/2\pi$ where γ is the gyromagnetic ratio of the proton. The behaviour of the spinning protons in the magnetic field is analagous to that of a gyroscope precessing in the earth's gravitational field. The rotating resultant of the proton magnetic vectors induces an e.m.f. (of the order of a few microvolts) in a pick-up coil wound round the sample. When space is limited, as in the present application, it is convenient to use the same coil for detecting the precession as that used for polarizing. The signal finally decays exponentially as a result of the gradual loss of phase coherence in the precessing protons, caused by atomic interactions, any inhomogeneity in the magnetic field and absorption of energy by the pick-up coil. The time constant, T_2 of the decay envelope of the precession signal is called the transverse relaxation time. Fig. 2.3 shows a sample signal recorded at a film speed of 4"/sec.



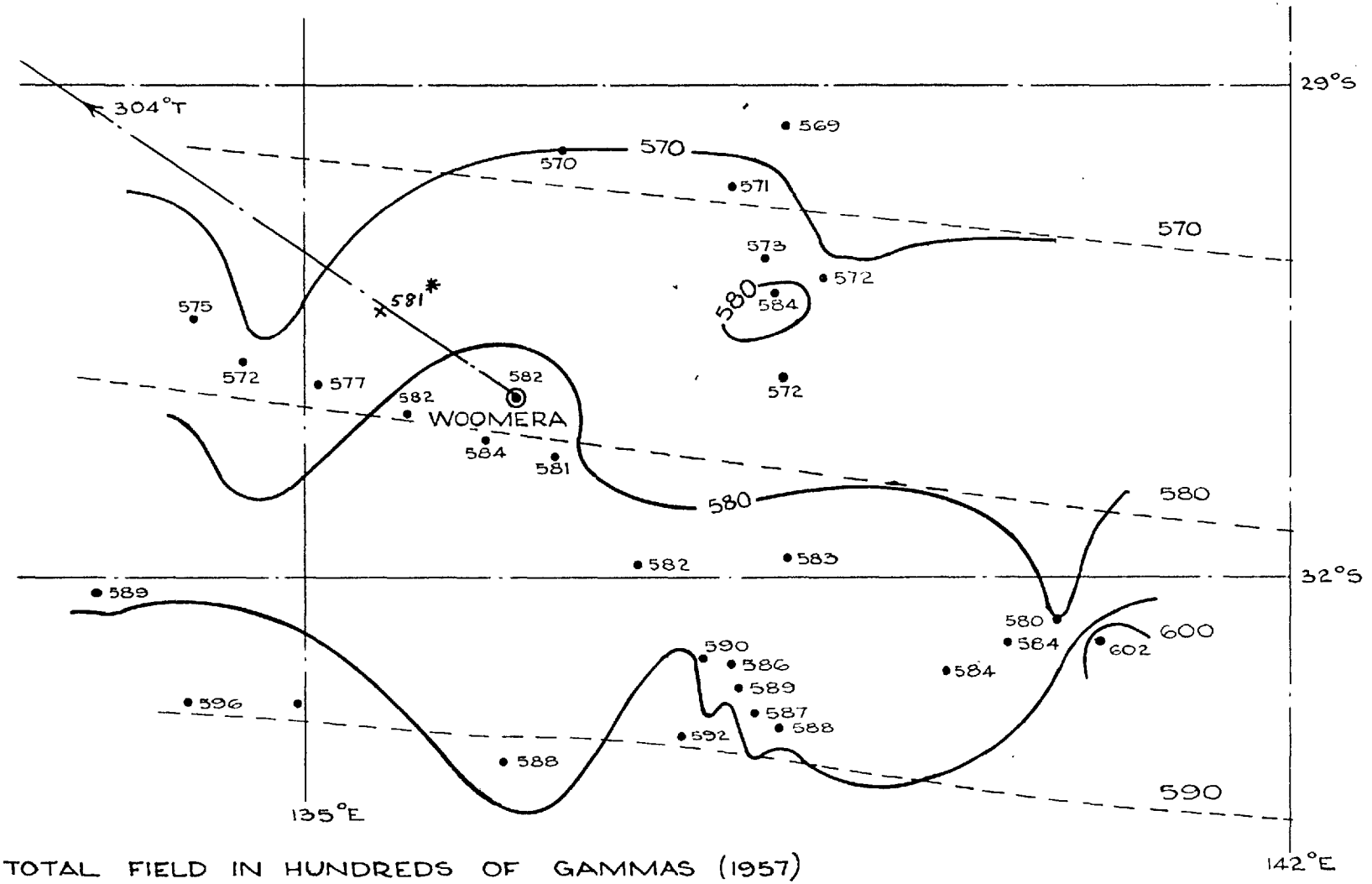
Fig. 2.3 Decay envelope of precession signal from protons in paraffin (2,000 c.p.s. unresolved).

Substituting the value of the latest determination of γ (2.67513×10^4 radian gauss^{-1} second^{-1})[20] yields an expression for the precession frequency of fp = 4257.8F = 2478.0 c.p.s. at Woomera (ground level) since the mean total field there is 0.582 gauss (Fig. 2.4). In London (F = 0.476 gauss) the precession frequency is approximately 2020 c.p.s. A change of 1 c.p.s. in the precession frequency corresponds to a change of 23.5 gamma in the field.

The advantages of using nuclear free precession as the basis for a magnetometer to be flown in a rocket can therefore now be summarised. The precession frequency, and hence the field measurements, will be independent of the rocket's orientation (though, as will be discussed later, the signal amplitude is profoundly affected).

Since the data is a frequency analogue of the field, problems of changes in calibration due to slow drifts in the gain of associated amplifier circuits, data transmission and processing systems, etc., are eliminated and no in-flight calibration is required. Furthermore as the frequency lies conveniently in the audio spectrum no particularly difficult requirements are imposed on the performance of data handling equipment. The sensing head is a passive element consisting merely of a coil containing a suitable sample, and is therefore inherently rugged and reliable and requires no intricate adjustments. The accuracy of such an instrument,

FIG. 2.4. TOTAL MAGNETIC INTENSITY NEAR WOOMERA



TOTAL FIELD IN HUNDREDS OF GAMMAS (1957)

SMOOTHED CONTOURS - - - - - - - -

POSSIBLE DETAILED CONTOURS ——————

× SL40 IMPACT POINT * FROM GROUND SURVEY (APPENDIX II)

SCALE : 111 Km.

both as an absolute standard and for measuring relative changes, is potentially very high because the precession frequency depends only on F, and on the constant γ; in general the accuracy will therefore be limited only by the associated electronic circuitry and not by the basic data; furthermore environmental changes will have a negligible effect on the precession frequency itself.

2.5 Proton Precession Magnetometer

The design of a practical instrument to measure the total scalar magnetic field can conveniently be considered under four headings:

i) The sensing head

ii) The switching arrangement

iii) The amplifier circuitry

iv) The frequency measuring circuits or techniques.

The special features of each of these sections, as they apply to each of the various types of instrument which have been developed, will be discussed in the relevant chapters; but before any practical instruments could be designed it was necessary to carry out some preliminary investigations into the basic techniques involved.

i) The sensing head

With the sensing head mounted at the tip of a 4 ft.

long probe (Ch. 2 Sec. 2(iv)) severe restrictions were imposed on its size and weight by considerations of the aerodynamic stability of the rocket. It was therefore necessary to optimise the design of the coil/sample combination to achieve the maximum ratio of wanted to unwanted signals.

The approximate precession signal voltage which will be induced into the pick-up coil can be estimated as follows. The effective magnetic flux ϕ threading the coil of N turns each of area A sq. cm. is given by $\phi = \eta$ N A B $\sin\omega t$ where ω is the angular velocity of the precessing protons and η is a filling factor which in general will be of the form

$$\int_{\text{sample}} H_o^2 \, dv \Big/ \int H_o^2 \, dv$$

But B = 4π M (M = intensity of magnetisation of sample) and, at normal temperatures, if H_o is much larger than F but still sufficiently small for the polarization to be assumed proportional to the field (i.e. $H_o \sim 100$ - 1000 gauss) then M = χH_o where χ is the nuclear susceptibility. χ is given by the formula $\chi = \frac{(j+1)}{3j} \cdot \frac{n\mu^2}{k'T}$ where j = spin quantum number, n = number of nuclei per cc., μ = magnetic moment of nucleus, k = Boltzman's constant and T = absolute temperature.

Thus $\phi = \eta\, N\, A\, B \sin\omega t$

$= 4\pi\eta\, N\, A\, M \sin\omega t$

$= (4\pi/3)(j+1).j^{-1}.\, n\mu^2.(kT)^{-1}.\eta\, N.A.\, H_o \sin\omega t$

and the peak induced e.m.f. is given by

$$\hat{V}_s = \frac{d\hat{\phi}}{dt}$$

$= (4\pi/3)(j+1).j^{-1}.n\mu^2(kT)^{-1}.\omega.\eta\,.\, N.A.\, H_o.$ e.m.u.

If we substitute the appropriate values of the parameters for the coil design which was eventually used in the first Skylark flight (Fig. 6.1) and make the simplifying assumption that H_o is constant throughout the volume of the sample, we find that the induced peak voltage, using a water sample in a field of 0.52 oersted and with polarizing volts = 15 v, lies within the range 2.9 - 7.7μV., depending on whether the coil shape is approximated to an infinite solenoid or a plane coil respectively. Having regard to the simplifying approximations made above, this figure agrees reasonably well with the experimental figure of 1.5μ V., which was subsequently obtained, using the measured gain and output volts of the rocket-borne amplifier to be described later.

It is now possible to investigate the way in which the signal/noise ratio of the sensing head depends on the geometrical configuration of the coil. In particular when the outside diameter of the coil is fixed (for the reasons stated above) at 2½" we need to investigate how much of the available volume should be taken up by sample and how much

by the coil itself; it is also not immediately obvious whether the coil should consist of a large number of turns of small gauge wire or a smaller number of larger gauge.

Neglecting all constants and parameters whose value is fixed by other considerations we have that $V_s \propto NAH_o v$, where v is the volume of sample, and from the well-known Nyquist formula we have v_n, the Johnson noise generated in the resistance of the coil, is proportional to $R^{\frac{1}{2}}$.
Therefore $V_s/V_n \propto N.A.H_o.v.R^{-\frac{1}{2}}$

If each of the parameters on the right hand side of this equation is expressed in terms of the geometrical configuration of the coil, this leads to an equation of the form

$$\text{Ratio of signal power to noise power} = (V_s/V_n)^2 \propto a^4 l^3 d^4 (b - a)(b + a)^{-1}$$

where: a = inside diameter of coil

b = outside diameter of coil

l = length of coil

d = diameter of wire.

This expression leads to the following conclusions for maximum signal to noise ratio .

a) The coil should be as long as practicable.

b) The wire should be of heavy gauge (the practical limit to this condition would be set by considerations such

as the current handling capacity of the switching system and the power which could be dissipated in the coil).

c) $a = 0.78b$

The way in which the expression $(a^4(b-a)(b+a)^{-1})^{\frac{1}{2}}$ varies with a/2 (the inside radius of the coil) when the outside diameter is fixed at 6.4 cm (=$2\frac{1}{2}$") is shown in Fig. 2.5, in which the maximum value (at $a = 0.78b$) has been normalized to 1.

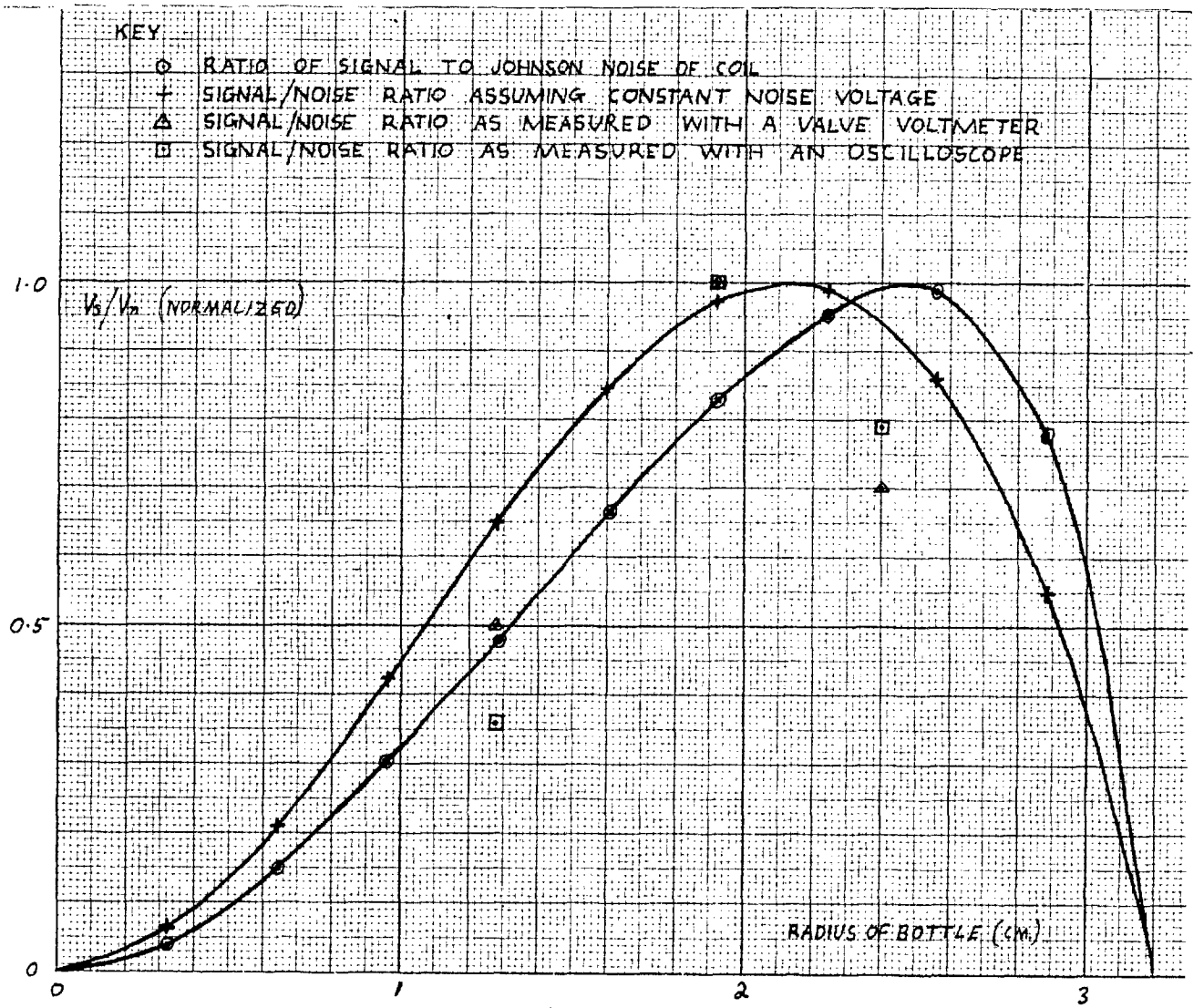


FIG 2.5. VARIATION OF SIGNAL/NOISE RATIO WITH DIAMETER OF BOTTLE.

In general, however, the shot noise of the first stage of the amplifier will be large compared with the thermal noise generated in the coil resistance. Since, for any given amplifier bandwidth, the shot noise will be constant the coil/sample combination should be designed for maximum signal rather than maximum signal/noise ratio.

As above $V_s^2 \propto (NAH_o v)^2$

$$\propto a^4 l^4 (b-a)^2$$

This leads to the following conclusions.

a). The coil should be as long as practicable.

b). The signal is independent of the gauge of wire used.

c). $a = 0.67b$.

For comparison the expression $a^2(b-a)$ is also plotted in Fig. 2.5, again the maximum value being normalized to 1.

In order to investigate empirically the above calculations and conclusions a set of experiments was carried out. It was designed specifically to investigate how the signal/noise ratio, in a practical sensing unit, depends on the wire gauge used and on the ratio of "a" to "b". Since each combination of wire gauge and ratio a/b requires a separate coil to be wound manually there is an obvious practical limit to the number of experiments which it is reasonable to conduct. For convenience the values of "a" were limited to the standard sizes of polythene bottles available and the maximum wire diameter was limited to

20 S.W.G., as that would result in a polarizing current of about 6 amps from a 12V battery. Nine coils were wound all with identical values of b ($2\frac{1}{2}$") and l ($2\frac{1}{2}$"), but with all possible combinations of the three bottle sizes available and using enamelled copper wire of 20, 28 and 32 S.W.G. No precession signal could be detected from any of the three coils wound with 32 S.W.G. and, of the three wound with 28 gauge, only the one with the smallest inductance (largest value of "a") gave a signal and that was only 3.2 times the noise. The explanation of this is believed to be that the resonant frequency of the coil/cable combination was too low in comparison with the 2 Kc.p.s. precession frequency (cf. Sec. 4, above). As a consequence of this the decay of the polarizing field was too slow and insufficient protons were left orientated normal to F for a signal to be detected.

The values of signal to noise ratio measured with the three coils wound with 20 S.W.G. wire are shown plotted, at the same scale as the theoretical curves in Fig. 2.5. It will be observed that the agreement is quite close and this confirms that the errors introduced in the calculations by making the simplifying assumptions discussed, are not excessive and that the conclusions are valid.

The principal considerations involved in the choice of proton sample are that the liquid is required to contain a

high concentration of protons and to have relaxation times somewhat longer than the time available for polarizing; this time will naturally vary with the application. It has already been stated that, for the rocket-borne application, the time available for polarizing is of the order of 0.5 sec. The effect of two different samples, with different relaxation times, is illustrated in Fig. 2.6 where the thermal relaxation times, T_1, of paraffin and water are reflected in the

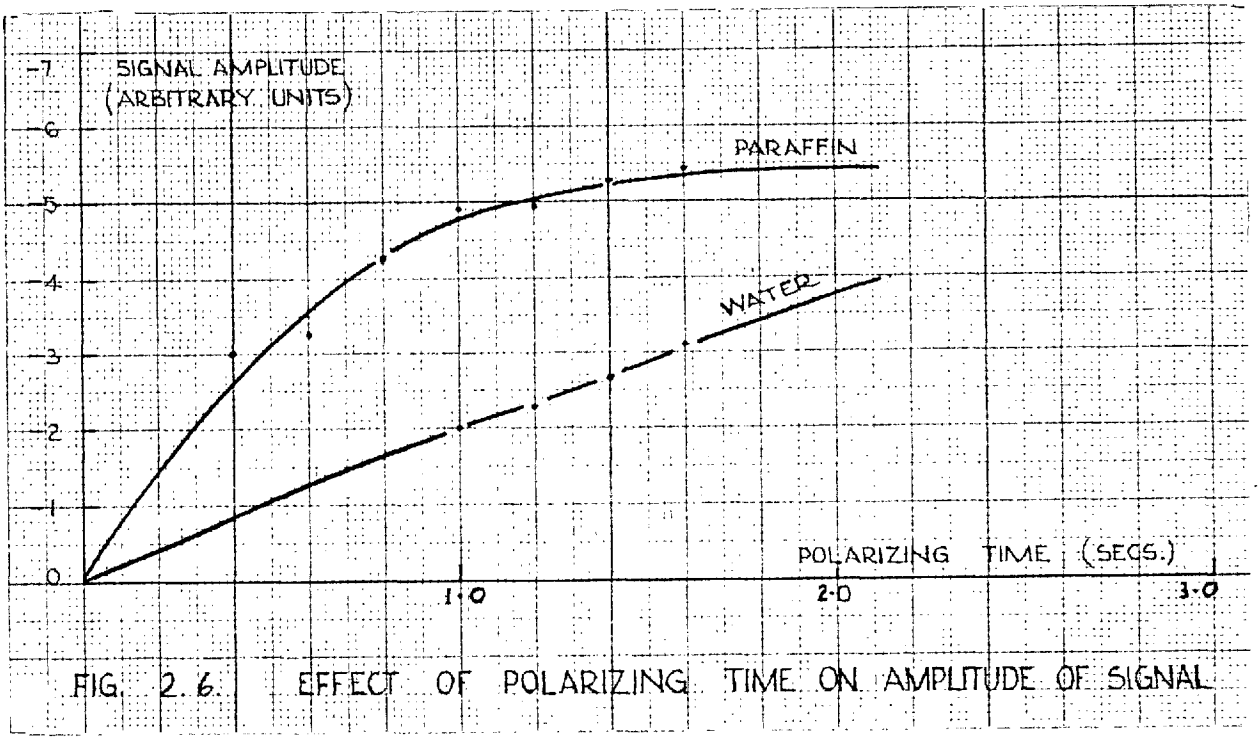


FIG. 2.6. EFFECT OF POLARIZING TIME ON AMPLITUDE OF SIGNAL

variation of the initial signal with polarizing time. Thus, although when each sample is polarized for a time long compared with T_1, water gives approximately 30% more signal than paraffin, when only 0.5 second is available

paraffin is the more suitable material of the two. Numerous liquids with differing values of relaxation time and of proton concentration were investigated but, colourless commercial paraffin was found to be most suitable.

A convenient method of achieving a continuous control on the relaxation times is by mixing two samples. Fig.2.7

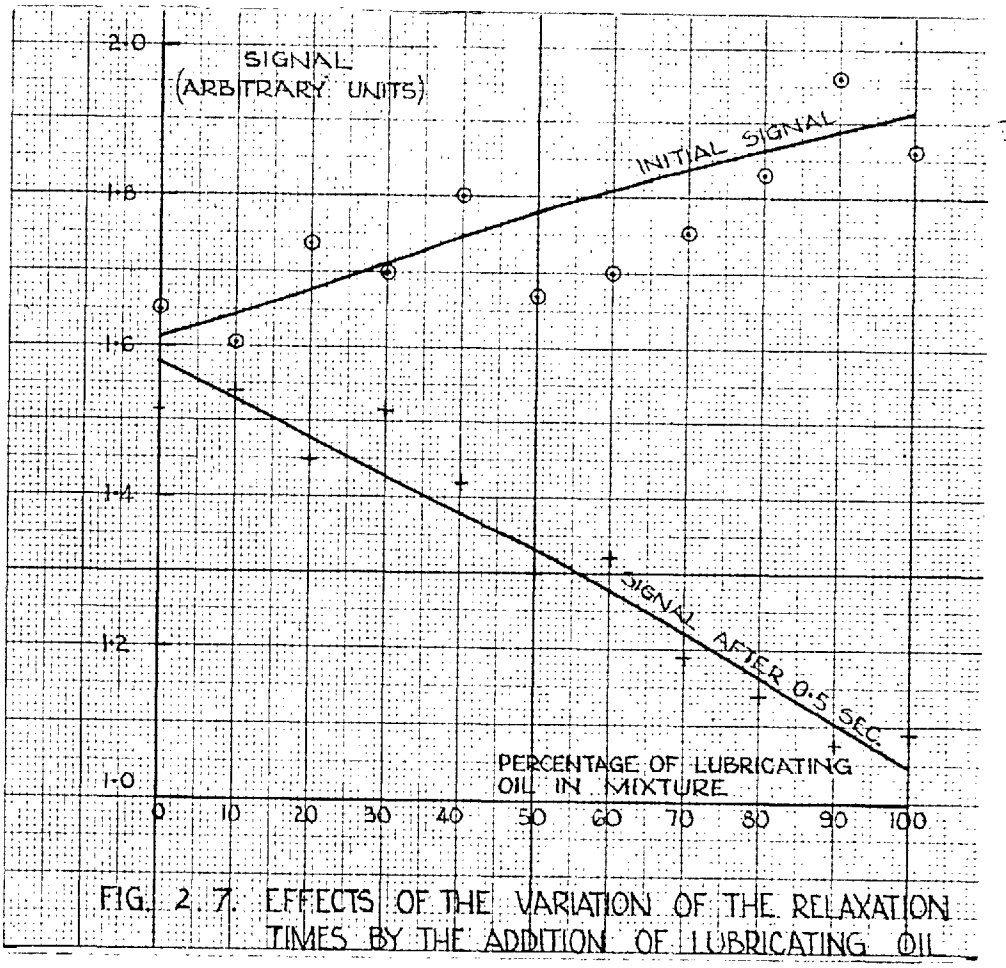


FIG. 2.7. EFFECTS OF THE VARIATION OF THE RELAXATION TIMES BY THE ADDITION OF LUBRICATING OIL

shows the effect of progressively reducing the relaxation times of paraffin by the addition of a quantity of heavy lubricating oil. In each of the experiments, from which

Fig. 2.7 was derived, the polarizing time was made a constant value of 0.5 sec. and the graphs show the initial amplitude of the precession signal, immediately after the decay of the switching transient, and the amplitude after 0.5 sec.

It is evident that an improvement in the initial signal (by reducing T_1) is more than counterbalanced by a degeneration of the final signal (by reducing T_2) and that, for 0.5 second polarizing and counting times, it is preferable to use pure paraffin.

ii The switching arrangement.

It has already been stated that the function of the switch is firstly to apply the polarizing current to the sensing head coil for a suitable period, then to switch off the current as rapidly as possible and finally to connect the coil into a suitable amplifier to detect the ensuing precession signal. The first signal was obtained using a morse key as a change-over contact, in which the key could be held in a position where it made contact with neither terminal for any required time; by this means it was possible to allow the large voltage transient, which inevitably occurs when a large current through an inductive circuit is broken, to decay before the amplifier was connected.

In order to investigate the way in which the timing of

the three switching operations might affect the amplitude and consistency of the switching transients and the precession signals the switching circuit of Fig. 2.8 was used. When

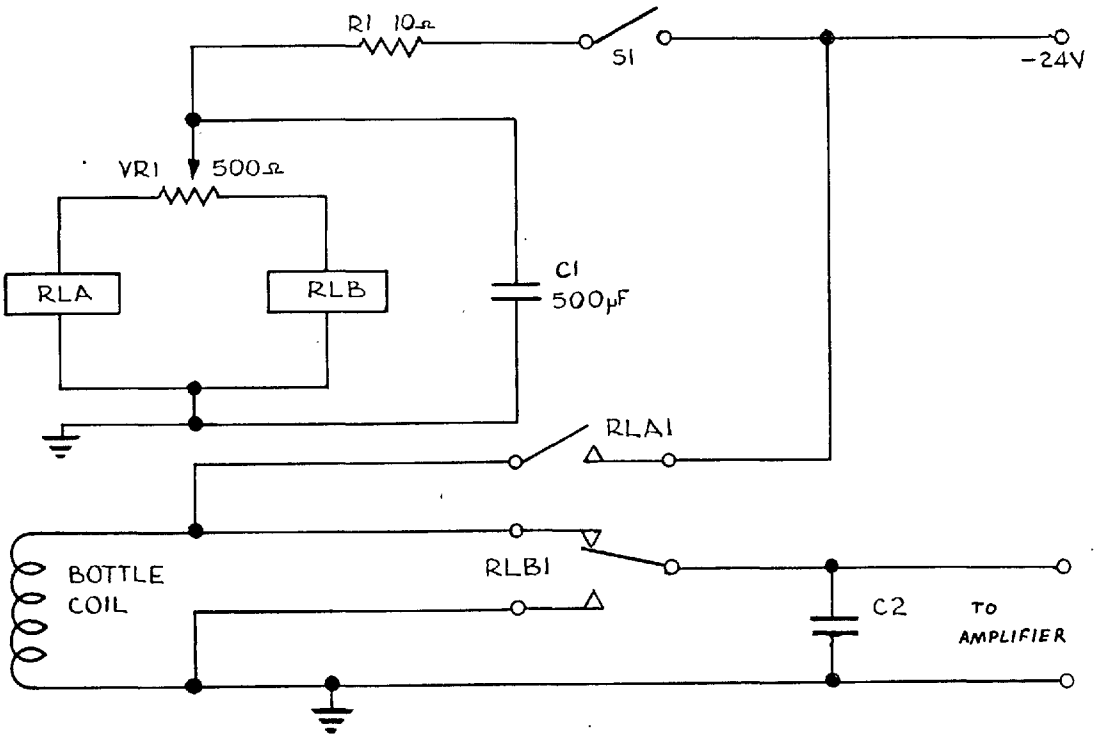


FIG. 2.8. EXPERIMENTAL SWITCHING UNIT WITH CONTINUOUSLY VARIABLE RELAY TIMING

the spring loaded switch S_1 is manually closed relays RLA and RLB close and C_1 is charged to almost the supply voltage, the charging current being limited by R_1. Contacts RLA1 then apply polarizing current to the sensing head coil, whilst RLB1 disconnects the coil from the amplifier and earths the amplifier input. Earthing the amplifier input terminals prevents any accumulation of charge on C_2; this

could be important as any charge on C_2 would subsequently discharge through the coil and could upset the polarization. When S_1 is released the capacitor C_1 discharges through RLA, RLB and VR_1 and this current holds in the relays until it falls below their respective drop-out ratings. By appropriate adjustment of VR_1 the relative times at which RLA and RLB de-energise can be continuously varied. When the relays drop out the polarizing current is switched off and the coil is connected to C_2, which tunes it to the anticipated precession frequency, and to the amplifier for measurement. This switching circuit was used for all the preliminary investigations described in this chapter.

Using the circuit of Fig. 2.8 the following conclusions were made:-

a) The simple action of opening a pair of relay contacts will remove the polarizing field sufficiently quickly to obtain a precession signal providing there is not too much capacitive loading on the coil during the switching operation.

b) Shorting out C_2 during the polarizing period was not essential but it did result in a slightly more consistent signal amplitude.

c) It is essential that RLA1 should remove the polarizing current before RLB1 connects the coil to its tuning capacitor C_2. The precise minimum value of delay

time required in practice was too small to be measured, without further refinements to the timing system; it was however evident that a delay of a few milliseconds was quite adequate. Any time delay in excess of the minimum did not increase the amplitude of the signal; indeed, as some loss of phase coherence could take place during this extra delay, the initial amplitude of the signal was decreased.

d) Various clipping and filtering circuits were tried in an effort to quench the spark at the relay contacts but it appeared that the most satisfactory method of switching off the polarizing current was simply to open a pair of contacts and to ensure that they had sufficient rating to cope with the inevitable spark. This confirms the conclusion made by Waters[18,19].

iii. The Amplifier and the Frequency Measuring Circuitry.

The amplifier used in the preliminary experiments consisted of two double triodes with the four triode sections connected in cascade. An L/C filter with a bandwidth of 50 c.p.s. in the anode of the final triode, rejected unwanted noise whilst passing the precession signal. The circuit was of conventional design and is not reproduced.

The special features of the various amplifiers used in the subsequently developed instruments and the associated frequency measuring techniques will be discussed in the relevant sections.

CHAPTER 3

THE PORTABLE MAGNETOMETER

3.1 Introduction

It soon became evident that some form of portable magnetometer would be essential in order to carry out the numerous magnetic measurements on materials and equipment, and also to conduct any possible site surveys which might be required in England or Australia. Accordingly, one was developed using the principles of Nuclear Free Precession discussed in Chapter 2.

The requirements of such an instrument may be summarized as follows.

i. It must be light in weight in order that it can be readily carried and operated by one man.

ii. Power consumption must be small enough to allow for, say, 8 hours continuous operation when powered by a battery which is also readily portable. In view of requirements i. and ii. a completely transistorized system is desirable and was in fact adopted.

iii. It must give reliably consistent readings, each reading should be accurate to the order of $\pm$ 1 gamma and it must maintain this accuracy over the range of field values encountered in England and Australia. This requirement

implies certain limitations to the performance of the frequency measuring equipment, as will be discussed in detail later.

iv. The operations involved in setting up a station and in taking a reading should be as simple and rapid as possible. If any processing of the data is required, in order to arrive at a measure of the magnetic field, it must be simple and rapid. A proton free precession instrument can readily be adapted to fulfill this requirement.

v. It must be reliable and substantially unaffected by the wide variations in temperature, humidity and atmospheric pollution of England and Australia. The use of transistors can lead to some temperature compensation problems but these are easily overcome by suitable design of the circuits.

vi. It must be sufficiently rugged to withstand reasonable rough handling in transport. Again this condition can be fulfilled because of the inherently robust nature of the sensing head and of the transistor.

vii. Fault diagnosis must be straightforward and, where possible, any likely faults must be easily remedied "in the field" without access to specialised equipment.

For this reason a modular construction was adopted, in which the various sections of the circuitry are independent plug-in units and can be readily replaced.

Fig. 3.1 The Portable Magnetometer.



3.2 General Description of the Instrument

A photograph of the complete instrument is shown in Fig. 3.1. A simplified block diagram, which illustrates the frequency measuring technique, is shown in Fig. 3.2 and the detailed wiring diagram, showing the switching circuit and the inter-connections of the various modules, is shown in Fig.3.3.

The various types of modular plug-in stages were manufactured by Venner Electronics Ltd., to their standard designs and will not be described in detail. The plug-in stages used were as follows.

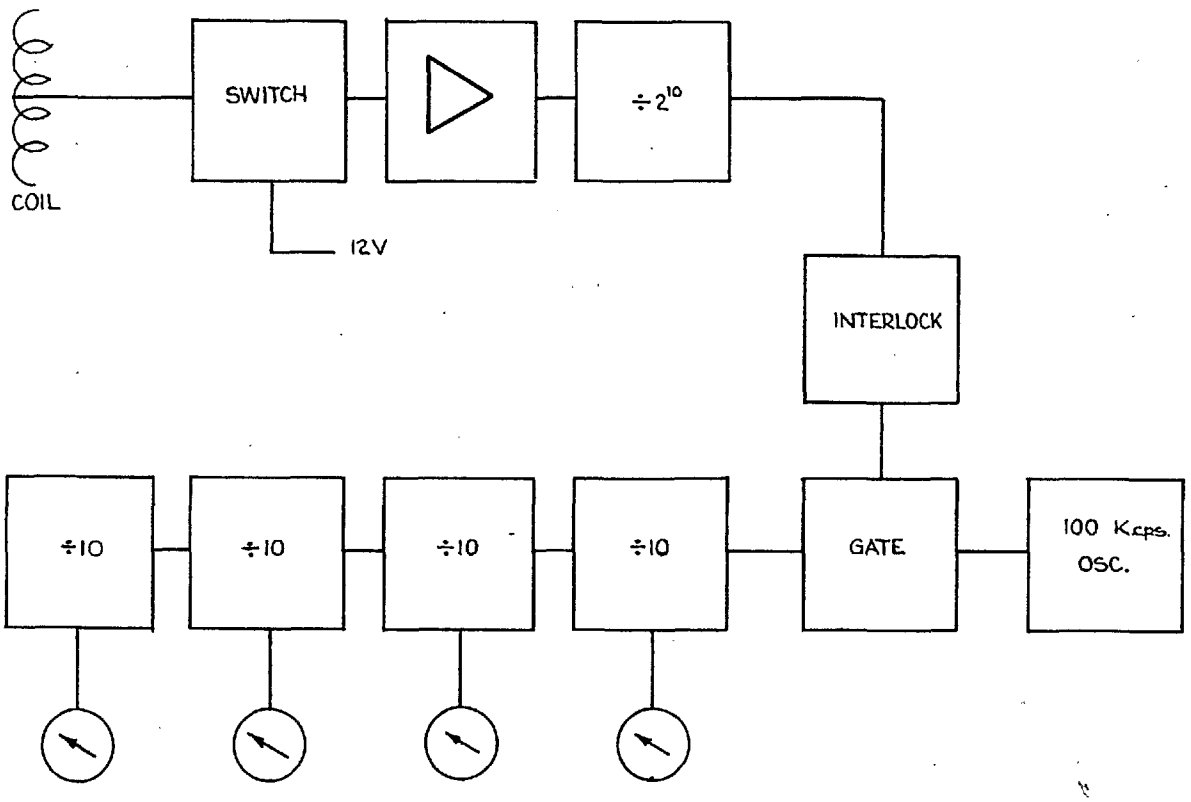
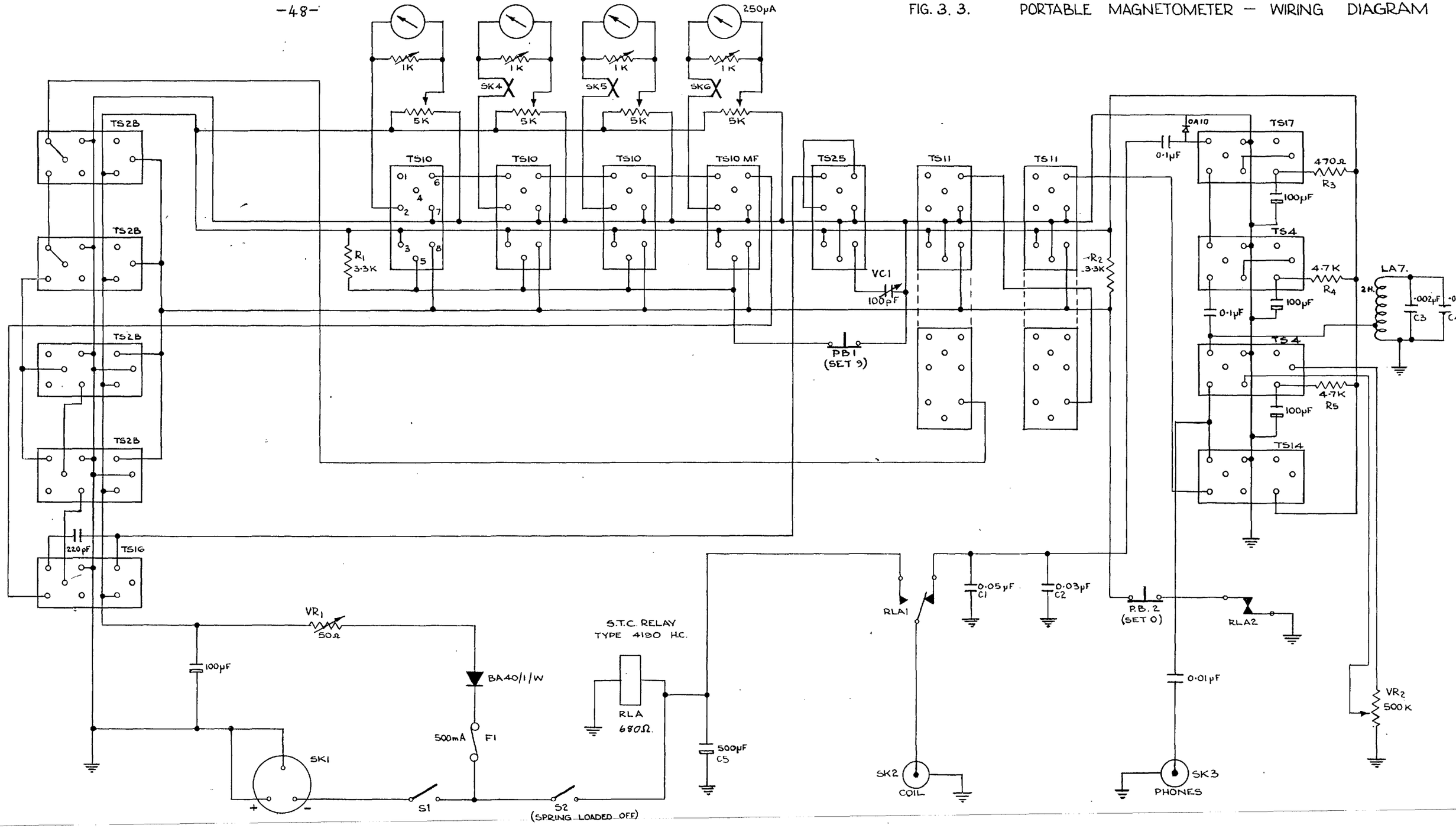


FIG. 3.2. PORTABLE MAGNETOMETER — SIMPLIFIED BLOCK DIAGRAM

FIG. 3. 3. PORTABLE MAGNETOMETER — WIRING DIAGRAM



TS17 Twin Emitter follower. Two D.C. coupled emitter followers in cascade.

TS4 Two stage amplifier. A two stage grounded emitter amplifier.

TS14 Pulse shaper. Essentially a Schmitt trigger circuit which converts a slowly varying waveform into a rapid switching action. In the present application it is used to convert a sine wave input to a square wave, of the same frequency.

TS11 Decade selector. Four Eccles Jordon circuits in one unit, with facilities for introducing feed-back loops to vary the division factor of the unit.

TS2B Eccles Jordon binary divider.

TS16 Universal Gate.

TS25 100 K.c.p.s. Oscillator with a selection of output waveforms.

TS10 Decade. Essentially 4 Eccles Jordon circuits in cascade with feedback loops to give a division of 10. Produces one output pulse for every 10 input pulses. A resistance network in the collectors of the binaries delivers a staircase waveform which indicates the state of the four binaries and hence provides an analogue of the number of input pulses.

3.3 The Sensing Head

The design of the sensing head was a question of a

compromise between its size, and hence its weight, and the power required to polarize the sample. A large polarizing power implies a larger, heavier battery in order to achieve a reasonable period of continuous use.

It was found that 1000 turns of 22 S.W.G. enamelled copper wire wound round a commercial polythene bottle, 2½" in diameter by 3½" long, formed a sensing head from which an adequate signal/noise ratio could be obtained with a 12V polarizing battery. The definition of an "adequate" signal/noise ratio is that, with the particular application in mind, the final accuracy of the readings is not limited by the precession signal but by some other consideration, such as the frequency measuring system. With this coil configuration the resistance was 13.5 ohms and hence less than one amp is required for polarizing. The coil inductance is 92 mH and with this value no difficulty was experienced in obtaining a signal when the coil was loaded with 25 ft. of screened cable; at this range the sensing head is unaffected by the magnetic fields associated with the rest of the instrument. Water was used as the sample, since it was anticipated that there would normally be no disadvantage in spending several seconds in obtaining each reading. The entire unit was encapsulated in "Araldite" epoxy resin type D, cured with hardener 951. This ensures a mechanically robust unit, which will withstand being accidentally dropped

from a height of a few feet to the ground, and effectively prevents the water sample from leaking away under varying atmospheric conditions (Fig. 3.1). The smooth surface also minimises the risk of the head becoming contaminated with dirt, which might contain magnetic particles and would interfere with the operation of the instrument.

The size of the encapsulated coil/bottle combination is 5" long by $3\frac{1}{4}$" diameter and its weight is 4 lbs.

3.4 The Switching Circuit

The switching operation is performed by the plug-in sealed relay RLA (Fig. 3.3) which is energised by closing the spring-loaded toggle switch S2. It was discovered that it was possible to obtain sufficient delay between switching off the polarizing current and connecting the coil to its tuning capacitor, by a single relay change-over contact, providing the operation of the relay was "slugged" with a suitable reservoir capacitor; since relays are a notorious source of unreliability in electro-mechanical equipment this represents a significant improvement on the double relay circuit described previously. The switching sequence is as follows.

i. When S_2 is closed, RLA is energised and C_5 is charged to 12V. Contacts RLA1 apply the polarizing volts to the coil. S_2 is held closed for approximately

3 - 4 seconds and is then released.

ii. C_5 discharges through the polarizing coil and RLA in parallel, until the voltage falls to the "drop-out" voltage for RLA. The polarizing current is then broken by RLA1 and immediately the discharge rate of C_5 is reduced by a factor of 500 since it now only discharges through the RLA coil. This slows down the change-over action of RLA1 contacts and allows time for the polarizing field to decay before the next operation.

iii. The normally-closed contacts of RLA1 close and connect the coil to its tuning capacitor, $C_1 + C_2$, and to the amplifier. Capacitors $C_1 + C_2$ in parallel tune the sensing head coil to 2 K.c.p.s., which is the approximate precession frequency in England. The removal of C_2 increases f_o to approximately 2.5 K.c.p.s. for use in Australia.

3.5. The Amplifier

The amplifier section consists of the TS17 emitter follower and the two TS4's connected in cascade (Fig. 3.3). The emitter follower acts as an impedance converter to match the parallel resonant circuit into the comparatively low input impedance of the TS4 amplifier (approximately 2 K ohms). With this configuration the amplifier input impedance is approximately 800 K ohms, which does not appreciably load the source. Noise occuring outside the

required bandwidth of the amplifier is rejected by the L/C filter consisting of a 2 Henry coil of copper wire wound on a Mullard Ferroxcube pot core type LA7 and either C_3 alone (in Australia) or C_3+C_4 (in England). Since the low (approximately 2K ohms) impedance characteristics of the transistor amplifier reduce the Q of the filter it is necessary to match the tuned circuit into the amplifier with a 10:1 tapping on the coil, to maintain the required selectivity. The gain of the amplifier is controlled by VR_2, though the setting of this control is not critical since a high gain merely results in "clipping" the precession waveform and, since it is required to be converted to a square wave of the same frequency to drive the binary stages, this is not detrimental. The reverse biassed OA10 diode, across the input terminals of the TS17, clips the positive excursions of the switching transient and effectively prevents an excessive reverse bias from being applied across the base-emitter diode of the first transistor. Such a reverse bias, of the large voltage generated on switching off the polarizing current, would rapidly destroy the transistor.

R_3, R_4 and R_5, together with their associated 100μF capacitors, provide the decoupling essential to prevent instability. The TS17 and the first TS4 were selected for low noise. The band-pass characteristics of the complete amplifier are shown in Fig. 3.4. The output waveform of

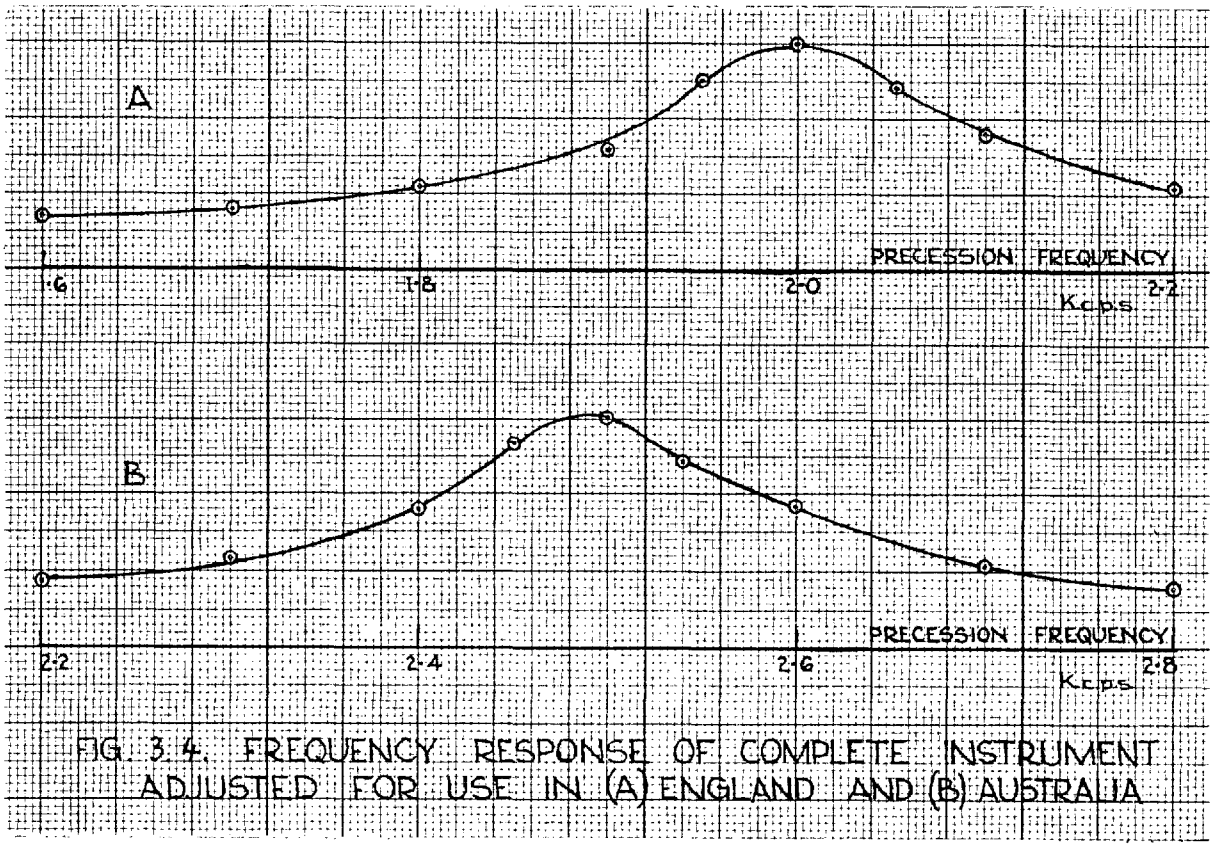


FIG. 3.4. FREQUENCY RESPONSE OF COMPLETE INSTRUMENT ADJUSTED FOR USE IN (A) ENGLAND AND (B) AUSTRALIA

the amplifier can be examined at SK3. This provides a convenient aid to fault diagnosis "in the field" since, if a pair of high impedance headphones are plugged into this jack socket, the precession signal can be heard. Thus if the amplitude of the signal is too small in relation to the hoise level (perhaps due to its frequency being outside the pass band of the amplifier), or if the decay is too rapid (due to the presence of an excessive field gradient in the vicinity), or if the precession signal is absent altogether (due perhaps to the presence of ferromagnetic material close

to the coil or due to the coil being positioned too close to a conducting medium) then these faults can be diagnosed and appropriate measures taken.

3.6 Frequency Measurement

To determine the value of the earth's magnetic field to, say, ± 1 gamma a measurement of the precession frequency to 1 part in 50,000 is necessary and, as the frequency is approximately 2 K.c.p.s., the accuracy of frequency measurement must be about 0.04 c.p.s. As the signal, at best, only remains above the noise level for a few seconds it is evident that direct counting of the cycles of precession for a given fixed period is not adequate. Accordingly the technique illustrated in Fig. 3.2 is used. The precession signal is squared by the TS14 and passed through 10 Eccles-Jordon binary divider circuits in cascade, giving a total division in the frequency of 1024. This divided down signal is used to control the TS16 gate, through which 100 K.c.p.s. pulses from the TS25 oscillator are passed and are subsequently counted by the four TS10 decades with their associated meter displays. In effect, therefore, the meters measure the period of 1024 cycles of the input signal in units of 10^{-5} second.

It is inevitable that the rapid switching of the polarizing current will cause the polarizing coil to "ring" at a frequency which is un-related to the precession frequency.

It is essential, therefore, that the counting circuits should reject these spurious oscillations and so a delay is incorporated, in order that the switching transient will have completely decayed before the TS16 gate opens and the counting of the precession signal begins. This delay is achieved simply by re-setting the first eight binaries (i.e. the two TS11's) to "0" but the remaining two binaries in the counter chain, which divides down the precession signal, are set to "1" (a "1" state is that which, on receipt of an input pulse, will also change the state of the next binary in the chain). Thus the first 2^8, or 256, pulses set all 10 binaries to "1" and the TS16 gate is opened by the 257th pulse. The operation of re-setting the binaries, and the decades in the crystal counter chain, is performed by RLA2 during the period when S_2 is closed.

Re-setting the binaries (or decades) involves arranging which transistor in each pair, comprising an Eccles-Jordon circuit, is bottomed and which is cut-off. This is simply achieved by taking the potentials of the appropriate transistor bases to a value close to the supply potential, which then ensures that it is bottomed. Thus, when RLA2 opens (or PB2 is pushed), the resistor R2 connects the appropriate transistor bases to the supply line.

The current through the meters can be adjusted to zero when the corresponding decades are in the "0" state by the appropriate 5 Kohm potentiometer. Similarly PB1 sets all the

decades to "9" and the currents are adjusted by the 1 Kohm potentiometers.

Another important feature of an instrument of this type is that, once having "counted" an unknown frequency, the information should be displayed for a sufficiently long time. In the arrangement described above the count would only be displayed for a period corresponding to 2^{10} cycles of the precession signal (i.e. approximately 0.5 sec) after which time the TS16 gate would open again and the decades would count the 100 Kcps pulses for a further 2^{10} precession cycles, this count being added to the first one; this cycle of operations would then carry on until the precession signal had decayed to a level which was insufficient to trigger the counter chain. This is prevented by the latching circuit, consisting of two inter-connected Eccles-Jordon circuits type TS2B. which are triggered by the last two binaries in the precession divider chain.

The two Eccles-Jordon circuits A and B are both re-set by RLA2 or PB2 into the "0" state and it is arranged that the first positive pulse they receive has no direct effect on B but switches A into the "1" state, A then in turn switches B into the "1" state and the output of B opens the gate. The next pulse has no effect on A but switches B back into the "0" state and closes the gate. Since all subsequent pulses are fed to the sides of A and B which are now cut off they

have no further effect and the gate remains closed until A and B are re-set.

The staircase waveforms can be examined at the jack sockets SK4,5 and 6, and, if required, any of the last three digits of the count can be recorded by plugging in a suitable recorder at the appropriate socket.

Variations in battery state can be compensated by means of VR_1 which is adjusted to bring all four meters to "9" when the decades are in the "set 9" condition; the counter thus acts as its own voltmeter.

In the event of the battery being connected the wrong way round, damage to the transistors is prevented by the diode in the supply line.

The various plug-in stages are arranged in the box in a similar lay-out to that of Fig. 3.3. In this arrangement units of corresponding sizes are grouped together and can be securely clamped in position. The entire electronic circuitry is contained in a strong steel box with a removable lid which protects the meters from damage in transit, (Fig. 3.1).

3.7 Testing and Evaluation

Providing all the electronic circuitry is functioning correctly the three possible sources of inaccuracy in the data are as follows.

i. Inadequate signal/noise ratio. This trouble manifests itself as erratic readings, in rapid consecutive measurements. In practice it is found that, over the bandwidth specified and with a bottle temperature of 50°C, the readings are self-consistent to ± 1 count during magnetically quiet conditions.

ii. Heading error. This is the name given to any variations in the readings which result from changes in orientation of the sensing head relative to the magnetic vector. In the present application, orientation, or heading errors, could be introduced by the presence of minute quantitie of ferromagnetic substances in any of the materials used in the construction of the head or by a leakage current through the coil during the counting period. Such a current would result from poor insulation between the normally open contacts of RLA1 (a few micro-amps could introduce significant errors).

Any error due to these two causes is, during normal operation of the instrument, less than one count.

iii. Errors in the reference frequency. The frequency of the 100 K.c.p.s. oscillator (TS25) was adjusted at room temperature, using the 200 K.c.p.s. RF carrier of the B.B.C. Droitwich transmission as reference. The TS25 oscillator drift is specified at 2 parts per million per °C; this will therefore lead to a systematic error in the readings at 50°C of approximately 3 counts which (in Australia)

corresponds to about 4 gamma. The error introduced into relative measurements will however be quite negligible.

3.8 Applications

Since its construction the portable magnetometer has been used for the following purposes.

i. To examine the various materials to be used in the construction of the rocket magnetometer probes and sensing heads.

ii. To measure the external fields of various other instruments to be flown in the rocket.

iii. To calibrate the signal generator used in the accurate adjustments of the tuned circuits used in the various instruments described in this paper.

iv. To survey the area at the Weapons Research Establishment, Salisbury, South Australia (hereafter referred to as "W.R.E.")where it was proposed to construct a non-magnetic rotatable frame to carry out magnetic measurements and compensations on the completely assembled rocket.

v. To survey the sites, both at Woomera and in England, for the sensing head of the Ground Recording Magnetometer (Chapter 7) for presence of any local sharp anomalies.

vi. To carry out a magnetic traverse from the vicinity of the launcher to the impact area of Skylark No.40 (discussed in Appendix II).

vii. To provide standard 1 K.c.p.s. and 100 c.p.s. pulses for the rotation experiments described in Chapter 4. This can readily be done by replacing the TS16 by a shorting plug which connects pins 1 and 6. The TS25 oscillator then feeds 100 K.c.p.s. pulses into the counter chain continuously and frequencies of 10 Kpps, 1 Kpps, 100 pps or 10 pps can be extracted from the appropriate points.

3.9 Abridged Specification

For convenience the most important features of the instrument are summarised.

Ranges of measurements of F	a) England 0.446-0.506 Oersted
	b) Australia 0.560-0.620 "
Accuracy of measurements	a) England ± 0.94 gamma
	b) Australia ± 1.43 gamma
Size. a) Electronics	16½" x 7½" x 9"
b) Head	5" x 3½" diameter
Maximum separation of Head and Electronics	25 ft.
Weight. a) Electronics	23 lbs.
b) Head	4 lbs.
Power Supply	12V (positive earth) Standing current = 175 mA Polarizing current (3 seconds per reading)= 890 mA
Temperature range	$0^{o}C$ - $50^{o}C$.

CHAPTER 4

THE ROTATION EXPERIMENTS

4.1 Introduction

A theoretical investigation of the effects of rotations of the sensing coil of a proton magnetometer reveals that when the rocket is rolling, precessing or tumbling the precession signal, in addition to being amplitude modulated as discussed elsewhere, will also in general be frequency modulated. On the assumption that the interactions between the molecules in the sample can be neglected, it can be shown that the instantaneous frequency deviation is, in the general case, a function of the coil orientation and is given by $(fr \cos \phi)/\sin^2 \theta$ where fr = frequency of rotation of the coil, ϕ = angle between $\vec{F}$ and the axis of rotation of the coil and θ = angle between $\vec{F}$ and the coil axis[21].

In order to verify the fundamental assumptions made in the calculations, to investigate the performance of a prototype rocket-borne magnetometer under the simulated conditions of a rotating rocket and, at the same time, to gain experience in the techniques of handling the data, a series of experiments illustrated in Fig. 4.1 was conducted.

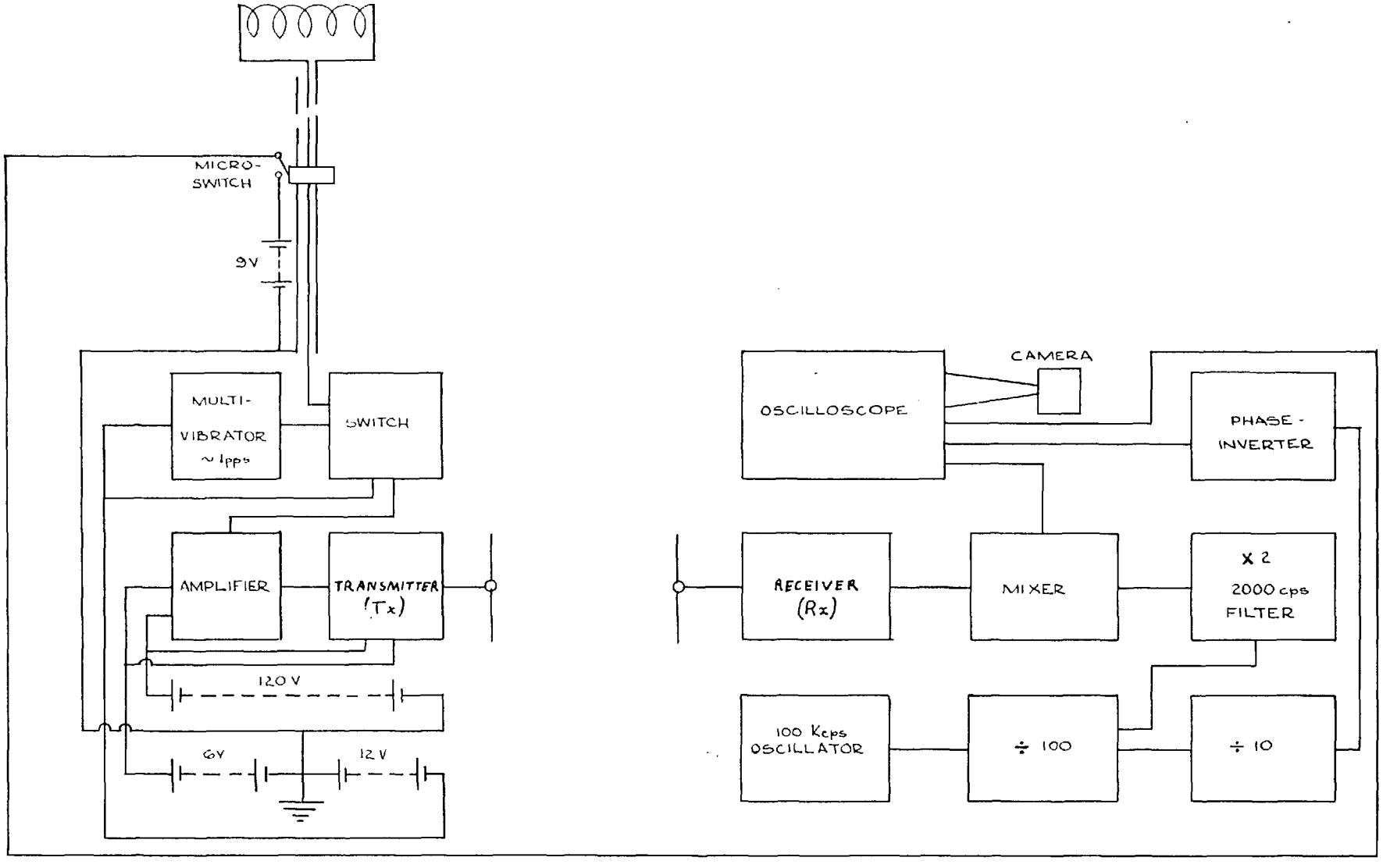


FIG. 4.1. BLOCK DIAGRAM OF THE ROTATION EXPERIMENTS

4.2 Apparatus

The "rocket-borne" instrumentation consisted of the multi-vibrator and the switch, which controlled the polarizing of the sensing head; the amplifier and the transmitter (Tx), which transmitted the data to the receiver (Rx) for processing and recording. The magnetometer, transmitter and batteries were mounted on a rotatable platform in a "Dexion" framework. Fig. 4.2 shows the arrangement of units on the platform and Fig. 4.3 shows the coil mounting and the rotating mechanism. The entire structure could be tilted at various angles to the magnetic vector F. With this arrangement the platform carrying the electronic units could be rotated manually at speeds in the range 0-4 revolutions per sec.

The circuit diagram of the complete "rocket-borne" equipment is shown in Fig. 4.4. The coil, switching circuit and valves V_1 and V_2 in fact constitute the prototype flight instrument, which was constructed for preliminary tests in the actual rocket.

The multi-vibrator, consisting of V_3 and V_4, energises the relays RLA and RLB at approximately one pulse per second. When the relays are energised the polarizing current is switched on by RLA1, RLA2, and RLB1. At the same time RLB2 earths the input to the amplifier. When the relays de-energise RLA drops out first and the polarizing current is

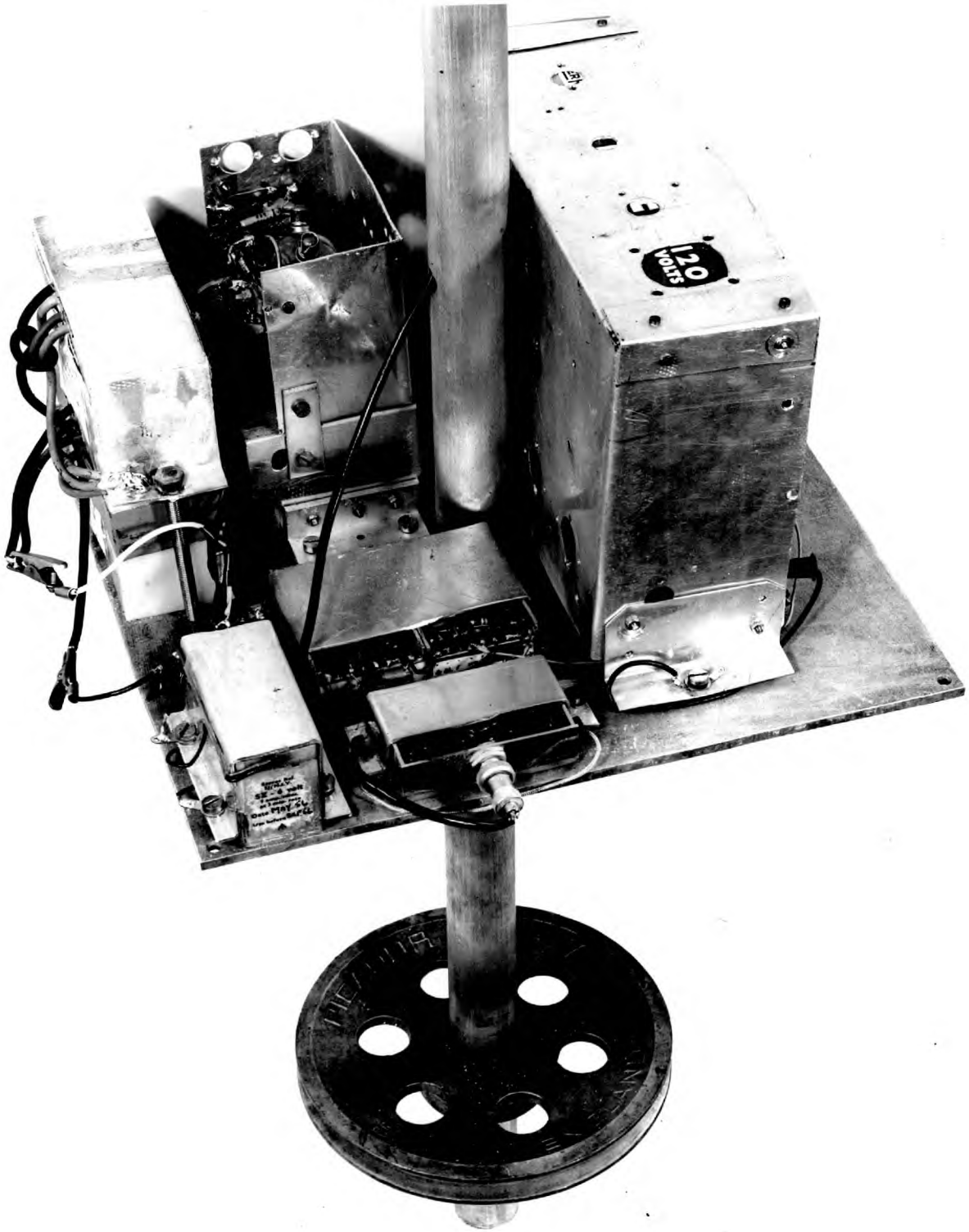


Fig.4.2. The Electronic Units Mounted on the Rotatable Platform.

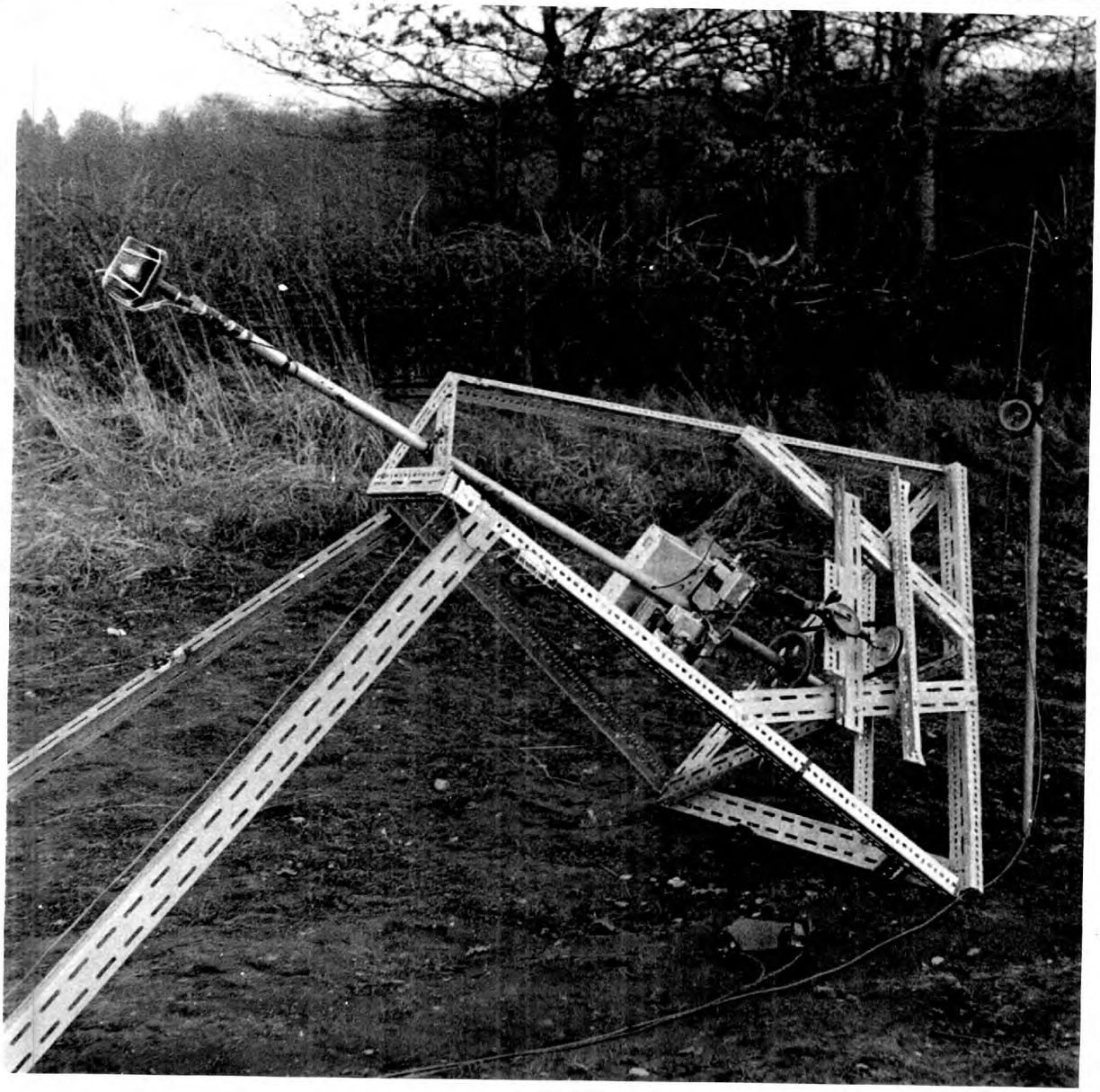


Fig. 4.3. Apparatus for the Rotation Experiments.

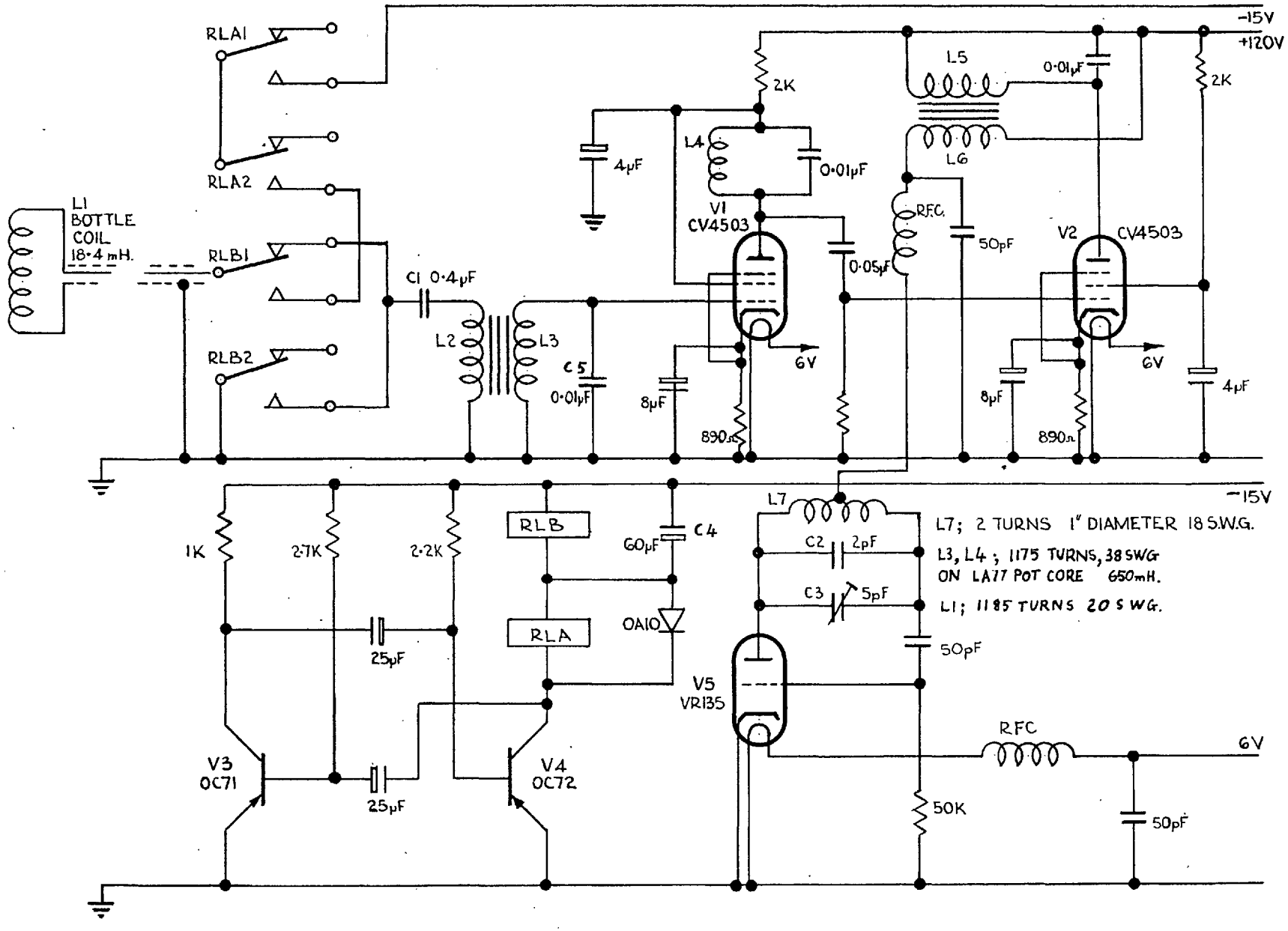


FIG. 4.4. ROTATION EXPERIMENTS – CIRCUIT DIAGRAM

switched off by RLA1 and RLA 2. The use of two contacts in series assists in the rapid breaking of the polarizing current and reduces the risk of contact welding. RLB is slugged by C_4 and therefore the required delay is achieved before RLB1 connects the pick-up coil, L1, into its tuning capacitor C1. L3 is also tuned to 2 K.c.p.s. (the anticipate precession frequency in England) by C5, and the two resonant circuits consisting of L1/C1 and L3/C5 are loosely coupled by L2, a few turns wound on the same pot core as L3. This arrangement produces a "double humped" frequency characteristic curve, the top of which is somewhat flattened by L4/C6 to give a roughly rectangular characteristic of the required bandwidth. The OA10 diode across RLA damps down the transient oscillations on de-energising the relay coil; this diode was found to be essential to prevent erratic triggering of the multi-vibrator.

The amplified precession signal is applied as plate modulation to V5, a simple R.F. oscillator which radiates at a frequency of approximately 120 M c.p.s. The frequency of the transmitter was adjusted to that of the crystal-controlled receiver by means of the pre-set capacitor C3. It was found necessary to shield the oscillator valve from the draughts, caused by the rotations, to prevent its frequency from drifting outside the band-pass of the receiver.

The apparatus was positioned in a field, approximately

30 ft. from the laboratory containing the receiving and recording equipment. In this position it was out of the range of the 50 c.p.s. interference, which had proved troublesome when an attempt was made to conduct the experiment inside the laboratory.

The "telemetered" data were detected by means of a government-surplus crystal controlled receiver type 1392.

To select the precession signal a 2 K c.p.s. filter was incorporated in the anode circuit of the output valve.

Fig. 4.5 shows the circuit which was used to obtain

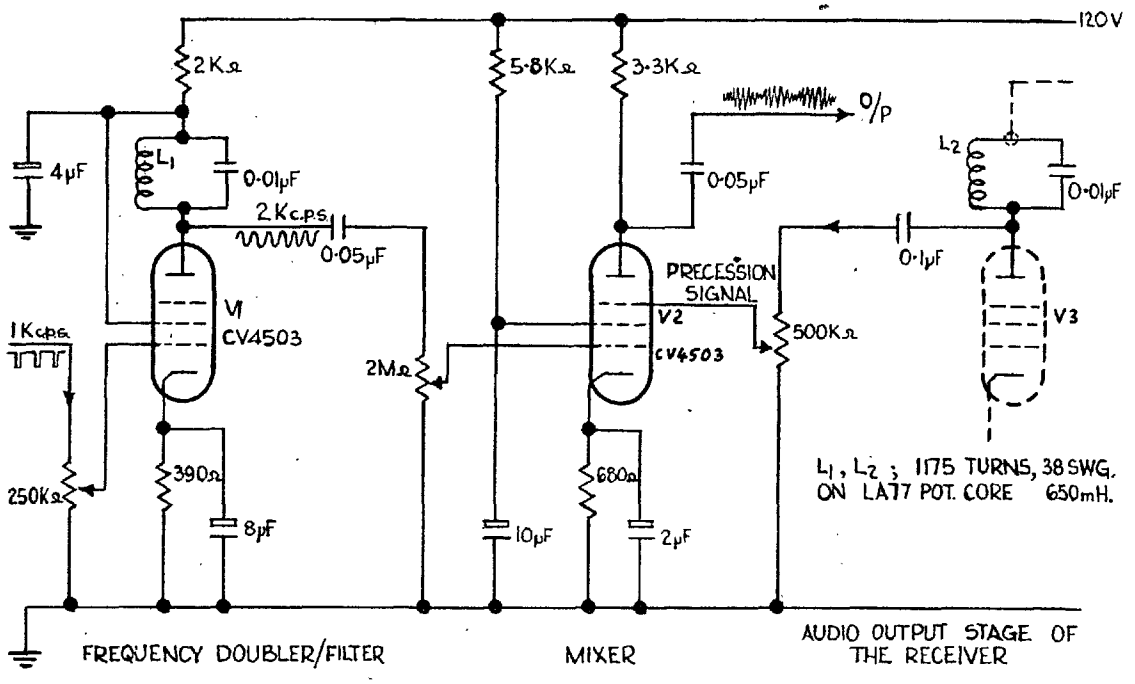


FIG. 4.5. ROTATION EXPERIMENTS DOUBLER/FILTER/MIXER UNIT

beats, of the frequency given by the difference between the precession signal and a reference 2 K.c.p.s. sine wave derived from 1 K.c.p.s. pulses extracted from the portable magnetometer, as described in Chapter 3. V1 together with its L/C anode load extracts the second harmonic from the 1 K.c.p.s. pulses and V2 mixes this 2 K c.p.s. sine wave with the precession signal extracted from V3, the audio output stage of the receiver type 1392.

The relative amplitudes of each can be controlled by the 2MΩ and the 500 KΩ potentiometers. The output from the mixer was applied to one pair of plates of a double beam "Nagard" oscilloscope.

The revolution rate of the sensing coil and its instantaneous position at any given time were monitored by means of a micro-switch mounted on the Dexion frame and operated by a cam on the rotating shaft. The pulses from the micro switch were applied to the second beam of the oscilloscope.

To enable the periods of the beats to be measured a time base in the form of 100 p.p.s. brightening pulses, also derived from the Portable magnetometer, was applied to the oscilloscope and the three sets of data were recorded on continuously moving 35 mm paper; Fig. 4.6 shows a typical record.



Fig. 4.6 Rotation Experiments. Typical record.

4.3 Results

Figures 4.7 to 4.13 inclusive show the reduced data derived from the records. In these diagrams the mean frequency deviation during each beat (normalized by dividing by fr) is plotted against β, the angle between the coil axis and the projection of $\vec{F}$ on the plane of revolution of the coil. Superimposed on each diagram is the theoretical curve for each value of ϕ for which an experiment was performed. It should be stressed that each reading involves a compromise between the accuracy of the determination of the precession frequency and the resolution of the variations in frequency deviation with β. Thus, for example, if the period of a single beat is measured the period of the measurement covers roughly 1/20 sec. (since the precession frequency is very nearly 2020 c.p.s.) and if the coil is rotating at, say, 2 revolutions per second this represents a range of β of 36°. The accuracy of the frequency determination can be increased by measuring two

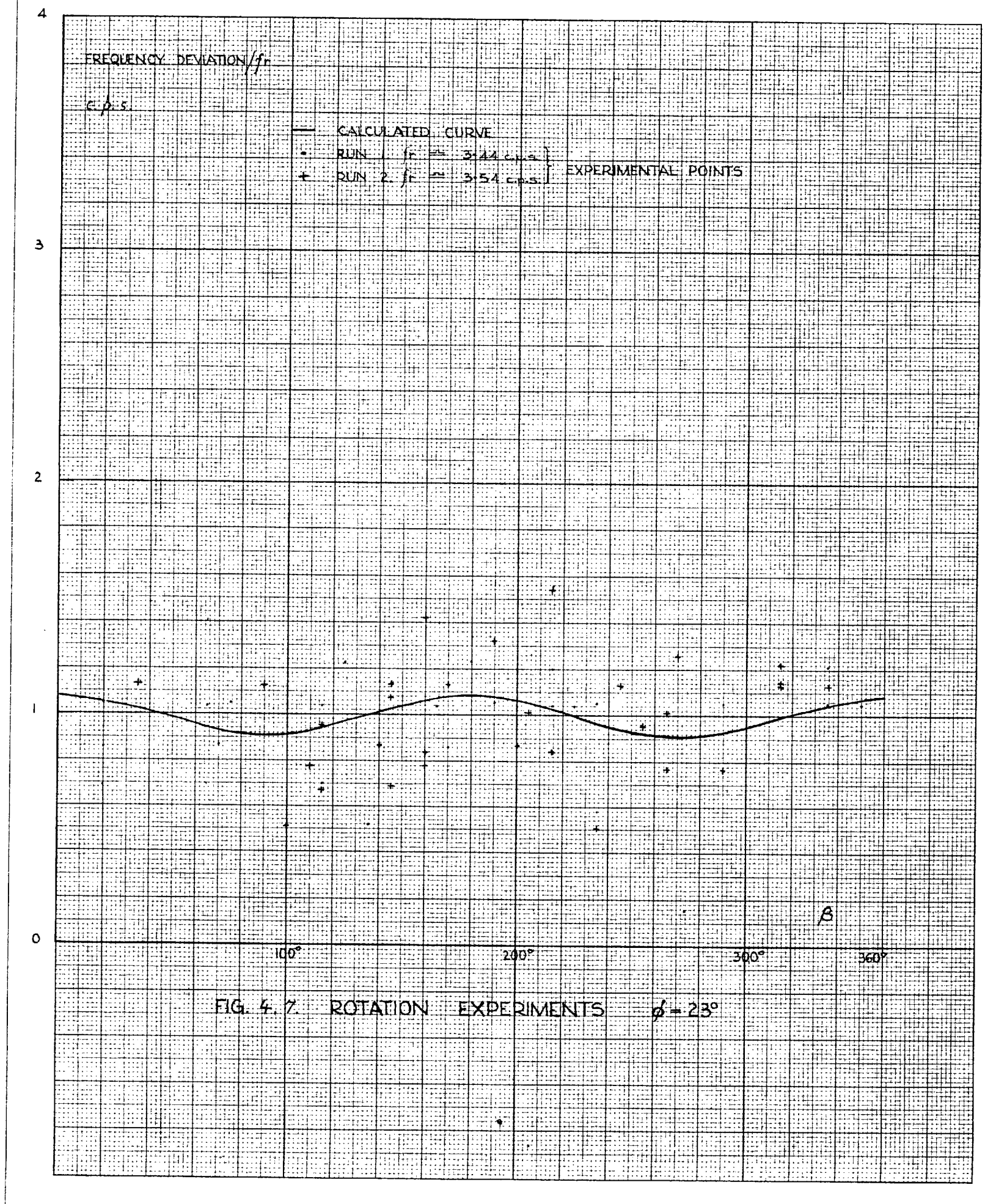


FIG. 4. 7. ROTATION EXPERIMENTS $\phi = 23°$

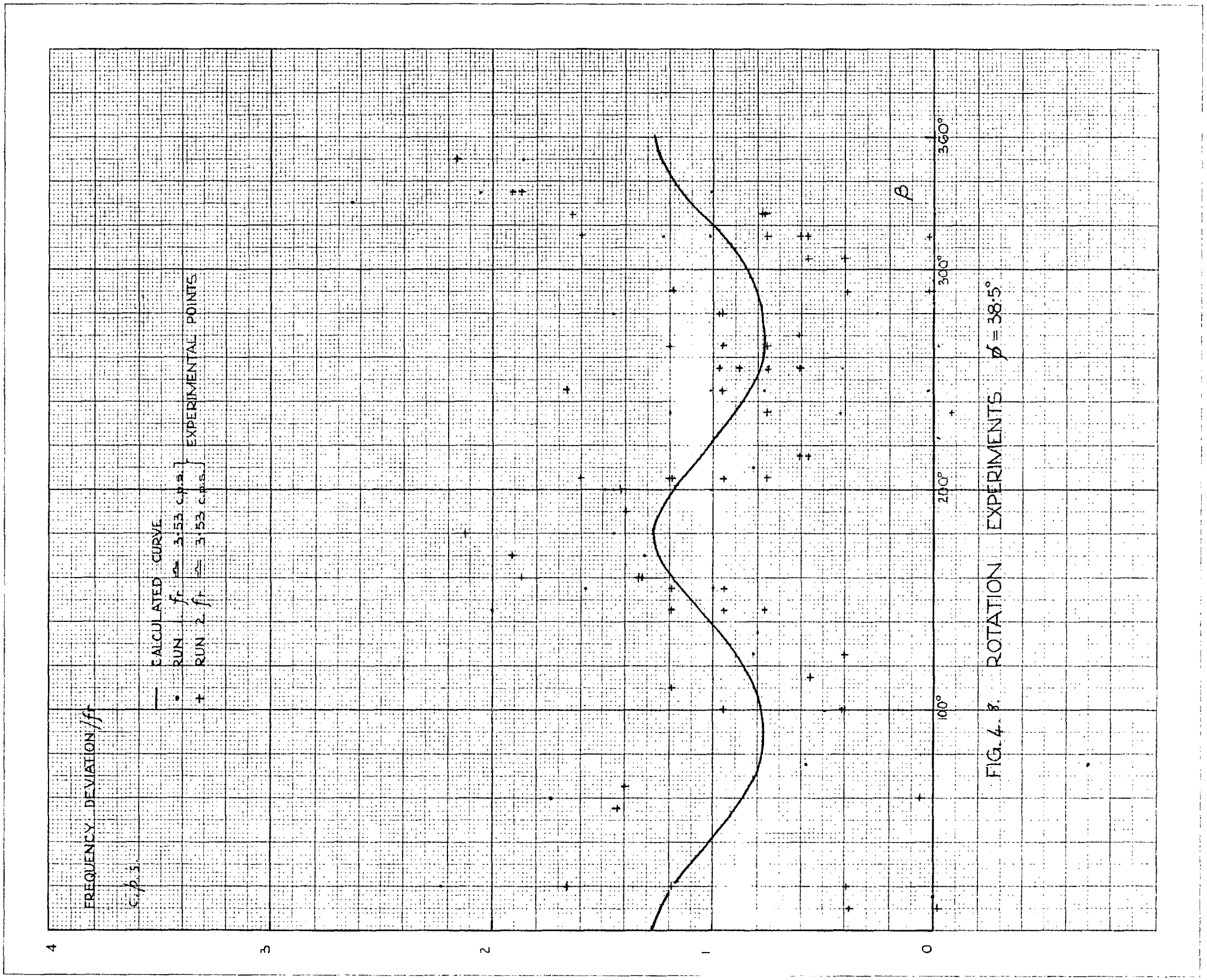


FIG. 4. 8. ROTATION

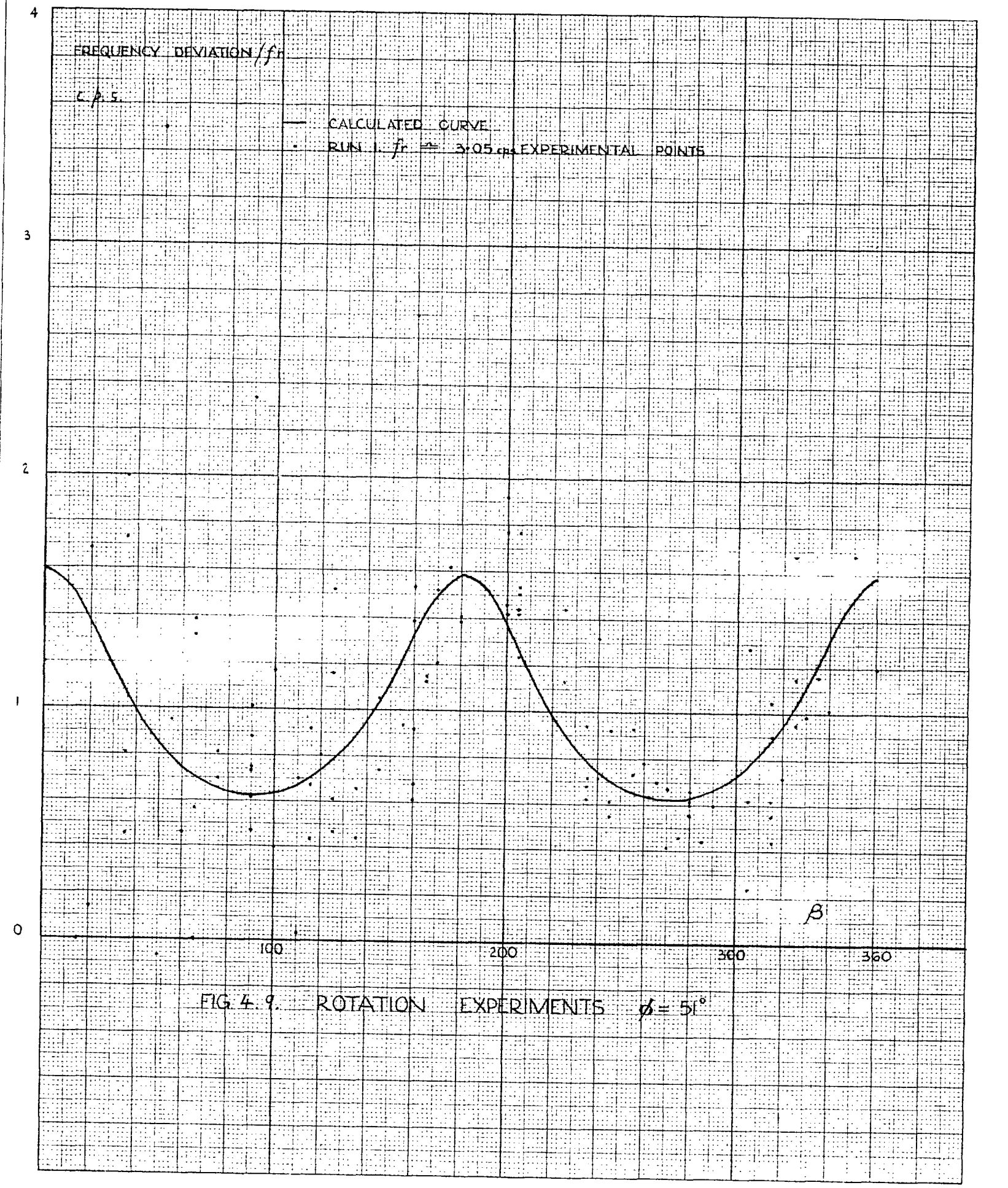


FIG. 4.9. ROTATION EXPERIMENTS $\phi = 51°$

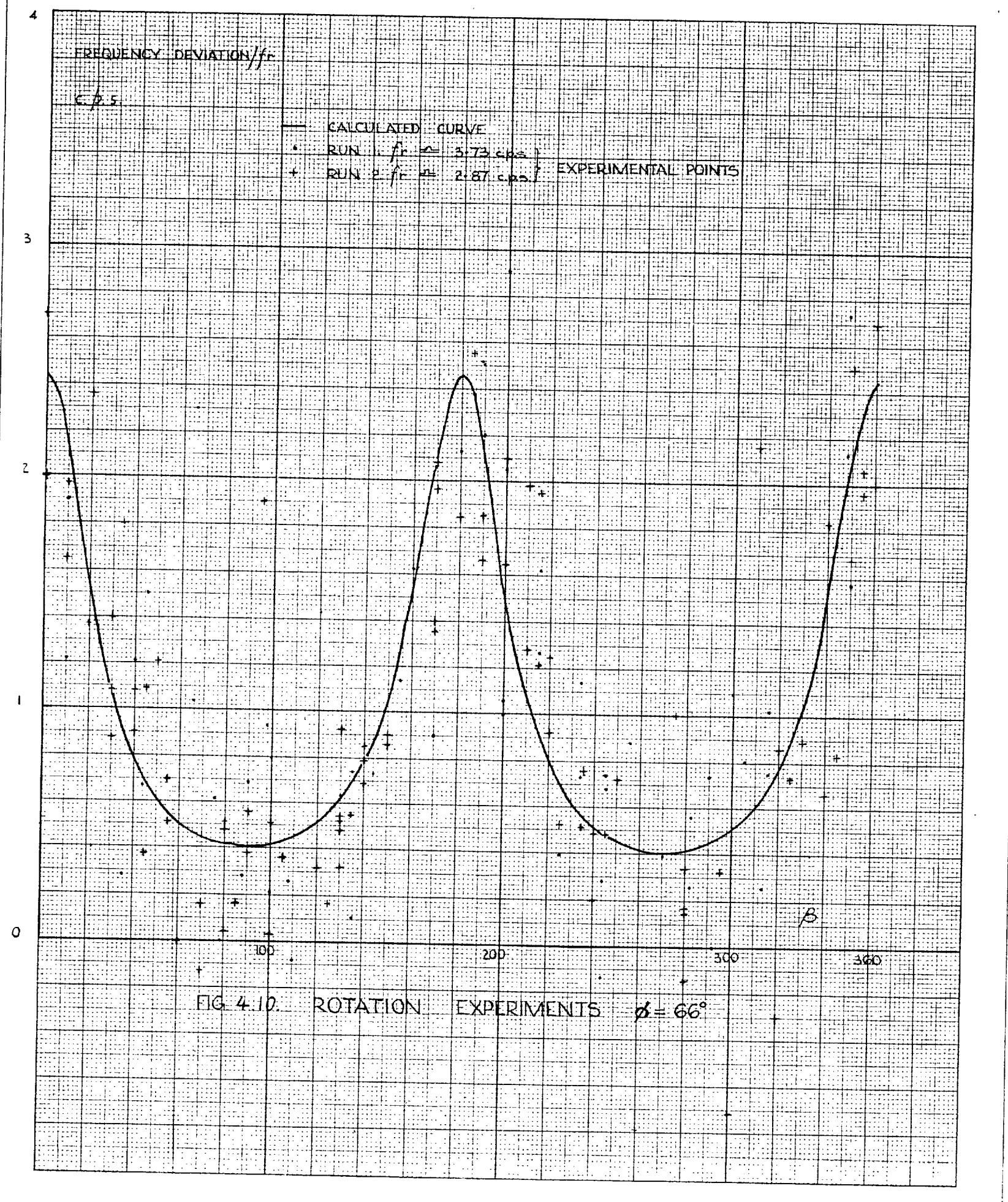


FIG 4.10. ROTATION EXPERIMENTS $\phi = 66°$

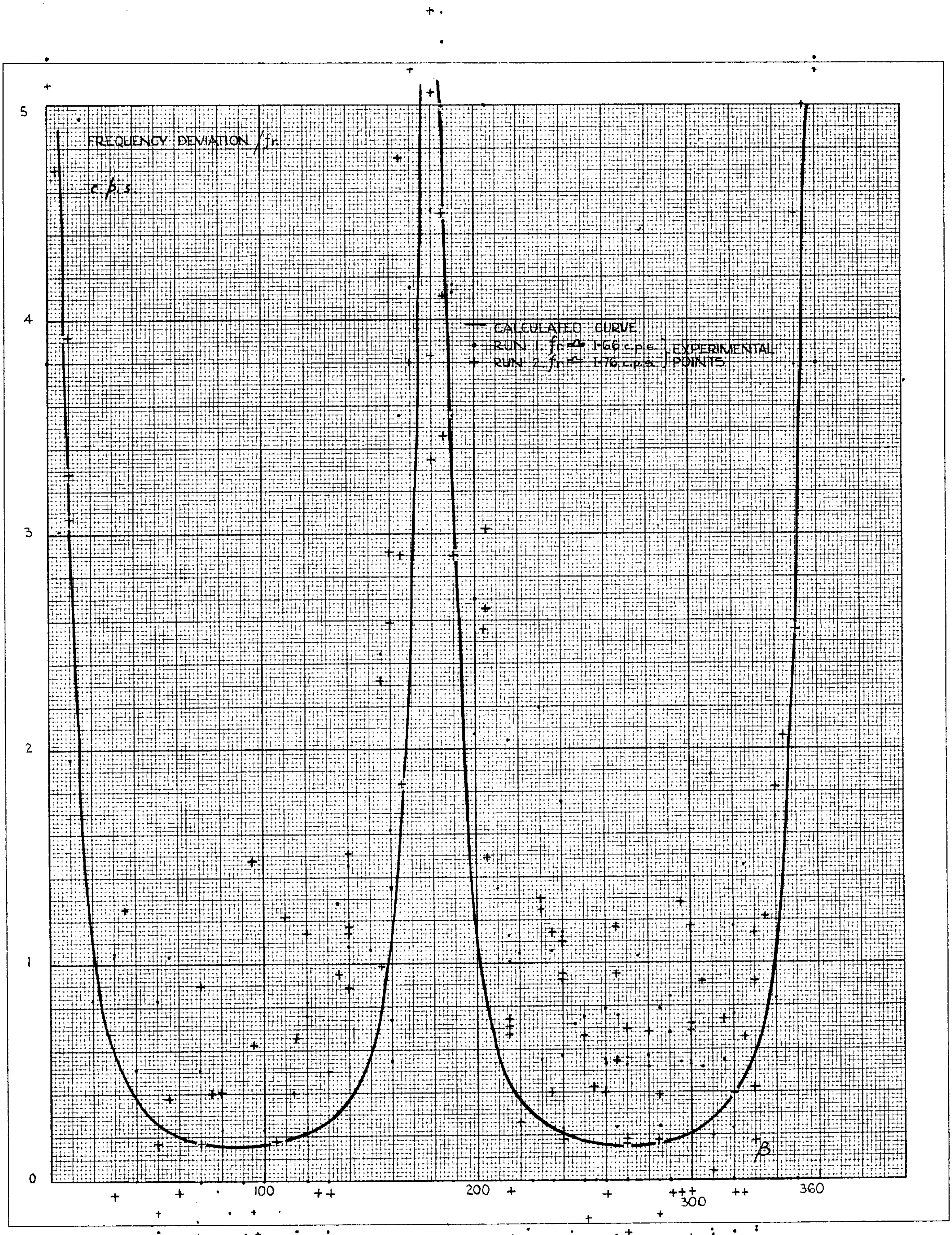


FIG. 4.11. ROTATION EXPERIMENTS $\phi = 81°$

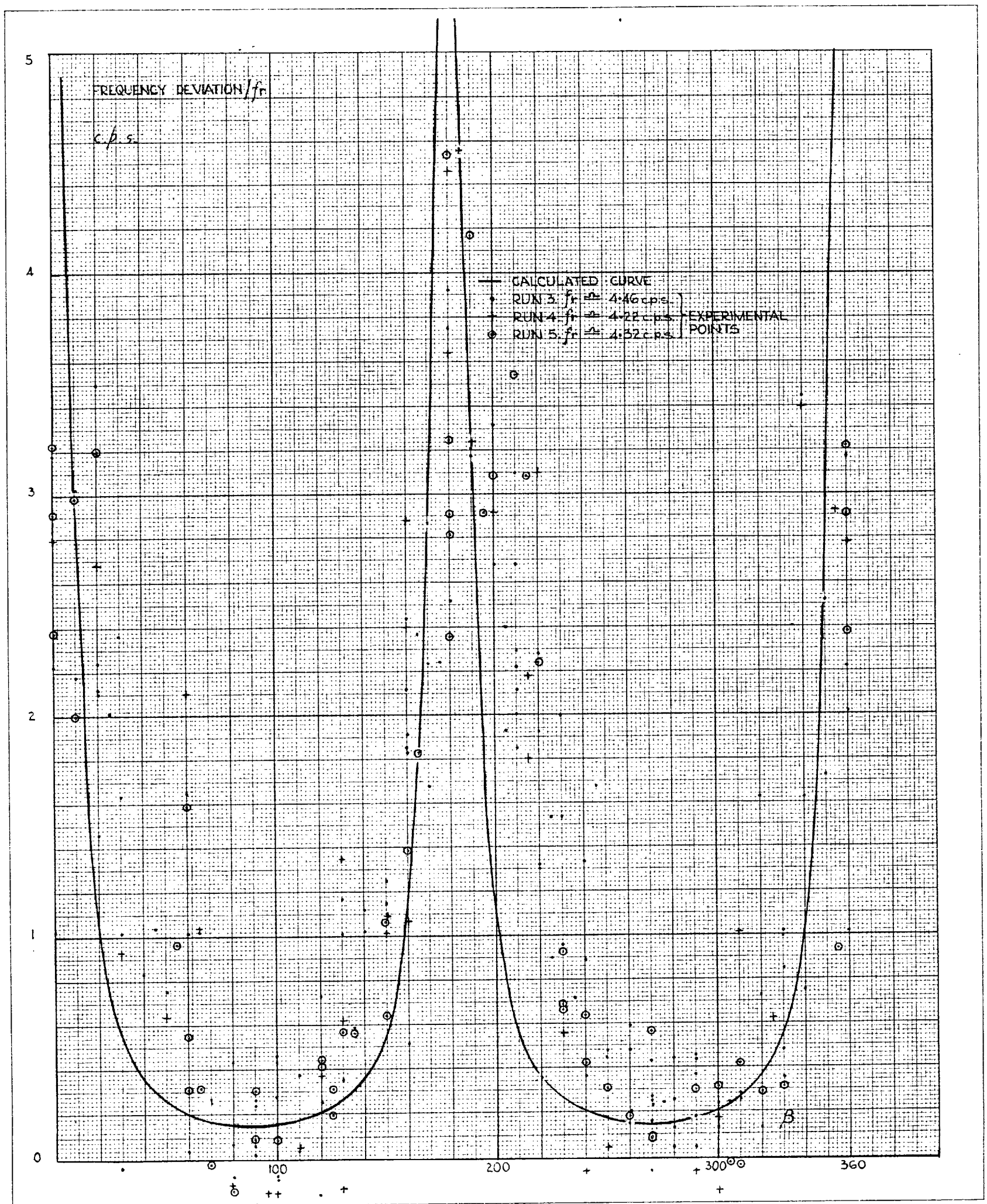


FIG. 4.12. ROTATION EXPERIMENTS $\phi = 81°$

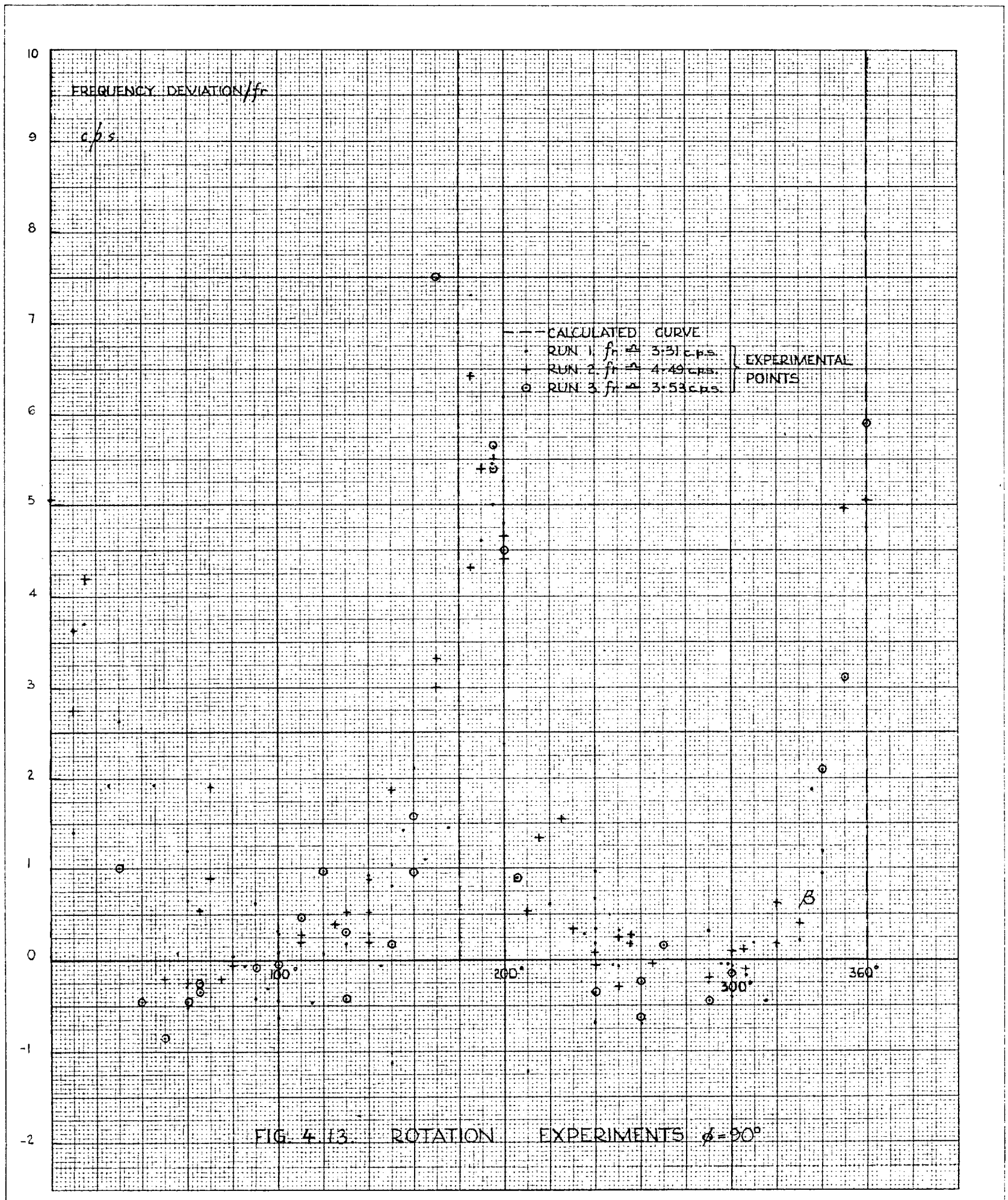


FIG. 4.13. ROTATION EXPERIMENTS $\phi = 90°$

beats, instead of one, but the inaccuracy in the determination of β would be increased correspondingly. For similar reasons a compromise has to be accepted with regard to the optimum value of fr. This is well illustrated by a comparison of Figs. 4.11 and 4.12, where the values of fr were roughly 1.7 and 4.5 respectively. As a result of the higher revolution rate in Fig. 4.12 the frequency deviation is larger and easier to measure which, when the data are normalized, leads to a reduced scatter of the points about the theoretical curve. On the other hand the values of β are averaged over a correspondingly larger range and this results in a flattening of the curve where the frequency deviation is changing most rapidly - i.e. at β = 0 and 180°.

At φ = 90° the "frequency modulation" is more accurately described as a phase change of π, in the precession signal induced into the pick-up coil, each time the coil axis passes through the position where its axis is parallel to $\vec{F}$. However, to some extent this effect has still shown up in Fig. 4.13 whenever β has passed through the value of 0 or 180° during the measurement period (Note the change of vertical scale).

4.4 Conclusions

Within the limits of the experimental errors involved the results of the rotation experiments agree with the

theoretically derived curves and confirm that the signal from a rocket-borne proton precession magnetometer will be frequency modulated by the rocket's rotational motions. A frequency deviation of only 1 c.p.s. corresponds to an error in the measured value of F of approximately 23.5 gamma. It is therefore essential that the rocket should remain as stable as possible throughout the flight and in particular the resultant thrust at head-separation (discussed in Chapter 1) must be orientated along the line joining the centres of gravity of the instrumented section of the rocket and the motor. Within limits it is, however, possible to apply corrections to the data using the results discussed in this Chapter - wherever the combination of β and fr is such that the assumption of a constant frequency deviation during the counting period does not introduce unacceptable errors. At other times it would still be possible to apply corrections but the data reduction would become somewhat cumbersome.

It was therefore decided, on the basis of these conclusions, that the rocket used for the proposed flight should be equipped with the standard attitude monitoring systems, which have been developed by the R.A.E., in order that at all times during the flight the attitude of the rocket relative to the magnetic vector could be established and, if necessary, corrections could be applied to the data to allow for the errors introduced by the rocket's rotations.

CHAPTER 5

ROCKET-BORNE MAGNETOMETER MARK 1

5.1 Introduction

Some of the general design requirements of a rocket-borne magnetometer have already been discussed in Chapter 2, Section 3.

The special requirements for an instrument to be fired from Woomera in a Skylark rocket concern mainly, the frequency band-pass characteristics. The precession frequency at Woomera (ground level) is 2478 c.p.s. since the mean total field there is 0.582 gauss. Approximating the geomagnetic field to that of a dipole located at the centre of the earth, the frequency excursion during the flight, calculated on the basis of the trajectory originally specified, is approximately -170 c.p.s. The instrument must therefore accommodate at least this frequency range.

When the same coil is used both for polarizing and as a pick-up coil, the signal amplitude is proportional to $\sin^2\theta$, where θ is the angle between the coil axis and $\vec{F}$, since the component of polarization normal to $\vec{F}$ and the induced signal, for a given polarization, are each proportional to $\sin\theta$. It therefore follows that there is a solid cone within which orientations of the coil axis will not yield a

detectable signal. For this reason (and to increase the reliability of the installation) it was decided to use two independent coils mounted with their axes respectively along and perpendicular to the rocket longitudinal axis.

In order to obtain an accurate measure of the frequency of the precession signal it is necessary to count the number of cycles which occur in a known time. A convenient manual technique is to mix the precession signal with a signal, of known frequency, and to record the resulting beat envelope, concurrently with a time base, as was done in the case of the rotation experiments (Chapter 4). Using this method the precise relation between the beat envelope and the time base need only be known at the beginning and at the end of the counting period, providing the number of intervening beats is also known. In practice comparatively short sections of record, at the start and end of a counting period, are adequate to enable the beat envelope to be extrapolated through out the intervening period; it is not therefore essential to record the intervening beats and the unwanted telemetry time can be used to transmit other data, such as the signal from the second sensing head. With suitable choice of the sub-switching speeds a time division multiplexing technique can, therefore, be used to telemeter the data from two independent magnetometers concurrently, providing that the two independent sensing heads can be arranged to perform satisfactorily in

close proximity to each other - a significant improvement on previous techniques. The instrument described in this chapter is based on this principle[22].

5.2 Design of the Sensing Head

Fig. 5.1 shows the two coils and the platform which was used to mount the complete sensing head on the tip of the probe. The 12.4 mH coil (Channel I) was wound with 20 S.W.G. aluminium wire, because of the low specific gravity of aluminium, and was mounted along the x (longitudinal) axis of the rocket. The small diameter of the probe made it necessary to use copper for the transverse coil (Channel II) in order to obtain an adequate signal and, to keep the polarizing current within reasonable limits, the wire diameter was reduced to 24 S.W.G. Furthermore, in order to fit the complete unit into the $2\frac{1}{2}$" diameter cylindrical space available, it was necessary to wind the Channel II coil in a roughly spherical fashion.

Since the space available for the sensing head was severely restricted, by the aerodynamic considerations mentioned previously, it was essential to make the fullest use of it. To this end great care was taken in winding the coils to get the maximum possible number of turns within the specified dimensions; and, in spite of the fact that this led to difficulties in sealing them, the two coils were

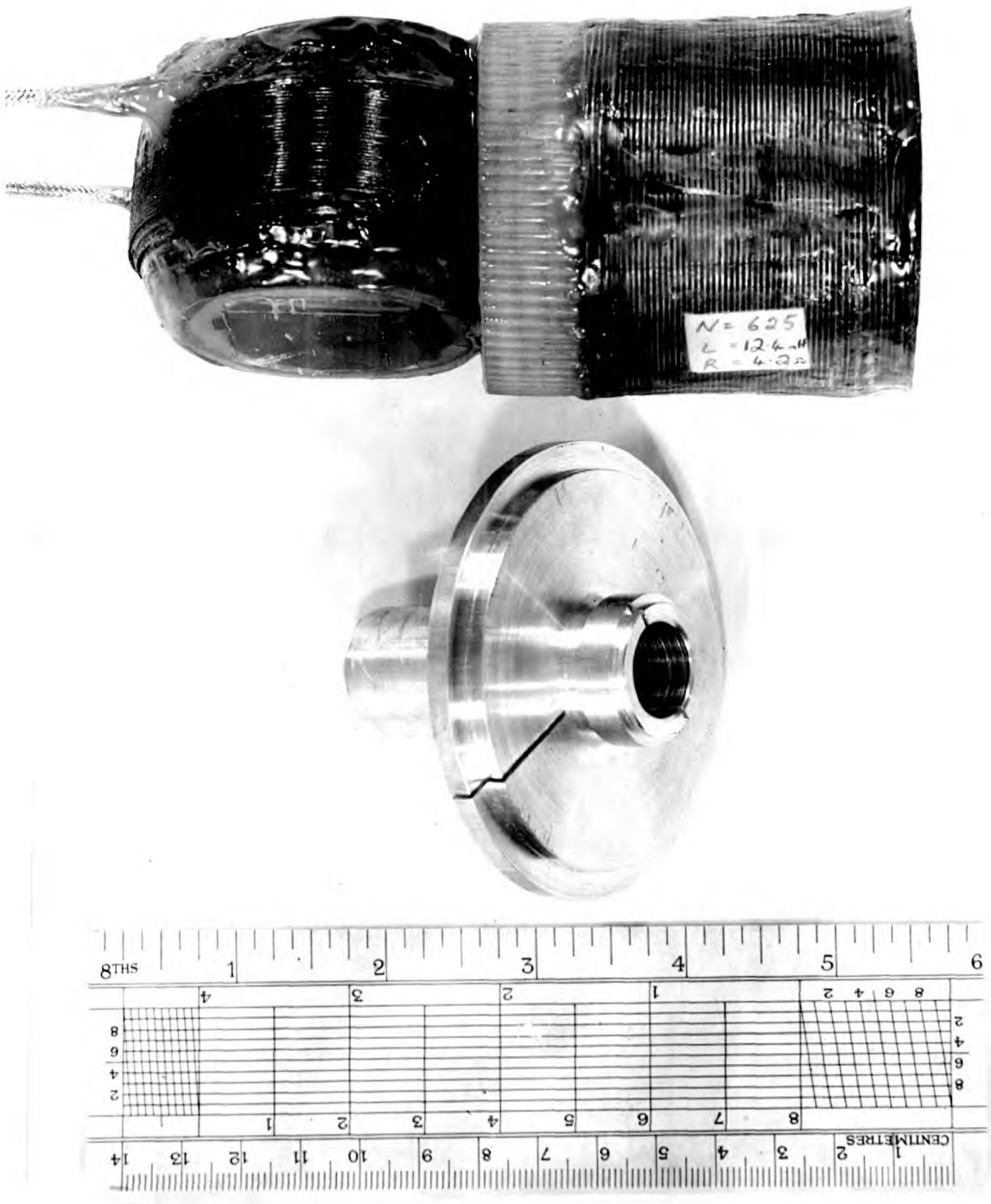


Fig. 5.1 Sensing coils and mounting platform.

themselves used as the walls of the bottles to contain the proton samples. As discussed in Chapter 2, Section 5, paraffin was used as the proton sample.

The two coils were embedded in Araldite high temperature casting resin type F and mounted on the platform machined from duralumin (Fig. 5.1). To make the whole assembly as mechanically strong as possible the platform was keyed into the resin by means of a keyway cut in the boss of the platform and four brass screws (4. B.A.) were arranged to protrude into the resin (Fig. 5.12).

The platform was attached to the nose cone by means of a 1 inch O.D., 18 S.W.G. austenitic stainless steel tube. Austenitic stainless steel proved to be unsuitable for the platform since it was discovered that machining it resulted in an appreciable magnetisation. To minimise electromagnetic damping of the coils due to the platform, the axial coil (Channel I) was mounted forward of the transverse coil and two saw-cuts were made in the duralumin platform.

In a later varsion the duralumin platform was replaced by one of fibreglass as this material was considered adequately strong for the purpose and problems associated with eddy currents (both due to switching off the polarizing current and to rocket rotations) were thereby eliminated. The relative position of the two coils was not changed, however, as it was desirable to arrange the centre of gravity

of the sensing unit to be as near as possible to the support.

The cables connecting the sensing head to the amplifier passed down the probe inside the stainless steel tube and, since any movement of the cable would generate an unwanted noise voltage, the tube was filled with a high temperature epoxy resin (Araldite F). In order that the probe could be removed for transit and to facilitate raising the rocket into the launcher, it was necessary to incorporate a plug in the lead-in cable at the base of the probe; this was done by the R.A.E.

To protect the coils during the rocket's ascent through the atmosphere the coil assembly was enclosed in a fibreglass sheath with $\frac{1}{4}$" thick walls. Durestos, which could more easily withstand the aerodynamic heating, was found to be slightly magnetic, due to the asbestos used in its manufacture.

It is well known that the adiabatic compression of the air caused by a vehicle moving at supersonic speeds results in severe heating at the surface of the vehicle. It has been calculated by the R.A.E. that this temperature rise would be sufficient to burn off the resin impregnation at the outside surface of the sheath and, at the inside surface, the temperature would reach a value of approximately 100°C in the absence of any heat sink. To accommodate this rise of temperature "Simgold M" high temperature insulated wire was used in the manufacture of the coils, a high temperature

resin (Araldite F) was used in the encapsulation, P.T.F.E. insulated connecting cables were used and, after filling with paraffin, the "bottles" were sealed at a temperature of 100°C. The co-axial cables also had to be manufactured specially as the standard range of P.T.F.E. insulated high temperature cables are nickel plated and therefore quite unsuitable from the magnetic point of view.

5.3 Electronic Circuitry.

Fig. 5.2 shows the complete circuit diagram of the double channel magnetometer. Each sensing coil is associated with its own independent amplifier and the information from each is sampled alternately, at approximately ten times per second, by means of the switching diodes V10 and V11 with their associated multivibrator circuit, V8 and V9. Whilst it would have been perfectly feasible to perform the channel switching in the input circuit and to use a common amplifier, with resultant saving in weight and space, this duplicated system is preferred as being inherently more reliable. The circuitry was developed from that already described in connection with the rotation experiments (Chapter 4), the main modification being that the later stages of the amplifiers are transistorized.

The cycling of the sensing coils L1 and L2 is performed by relays RLA and RLB. Contacts RLA1 and RLA2 alternately select polarizing current and switch the coils into their

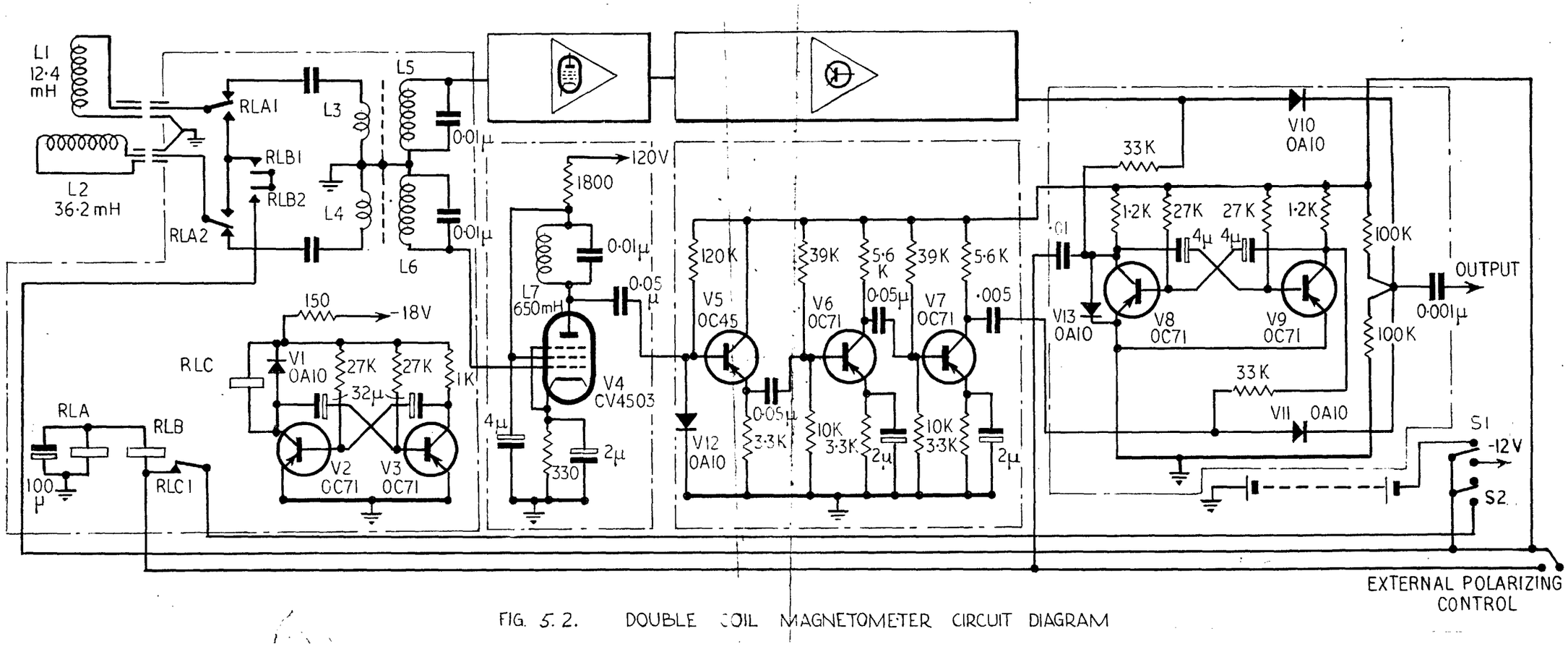


FIG. 5.2. DOUBLE COIL MAGNETOMETER CIRCUIT DIAGRAM

respective amplifiers, while RLB1 and RLB2 remove the polarizing fields as previously described. Since a current in one coil would result in a severe field gradient across the other coil, with consequent rapid loss of phase coherence in the precessing protons, it is essential that the two polarizing currents are switched off simultaneously, which implies that the same set of relay contacts must be used to switch both currents. There is thus a limit to the degree of independence, and hence increase in reliability, which can be achieved by the use of this double coil system, though this consideration is partially offset by duplicating both relays and operating the two pairs of relays in a series-parallel arrangement. The series-parallel arrangement of the contacts also assists in the rapid breaking of the polarizing current and reduces the risk of contact welding. To ensure that the sensing coils are not connected to their respective tuning capacitors before the polarizing fields have been completely removed a 100 μF capacitor is connected across the two relays RLA, thereby delaying their operation by a few milli-seconds.

The coupling constants in each pair of resonant circuits, formed by the sensing coils and the grid coils with their respective tuning capacitors, can be adjusted by varying the number of turns in L3 and L4. (Fig. 5.3). Twelve turns were used in each coupling coil and this, together with the

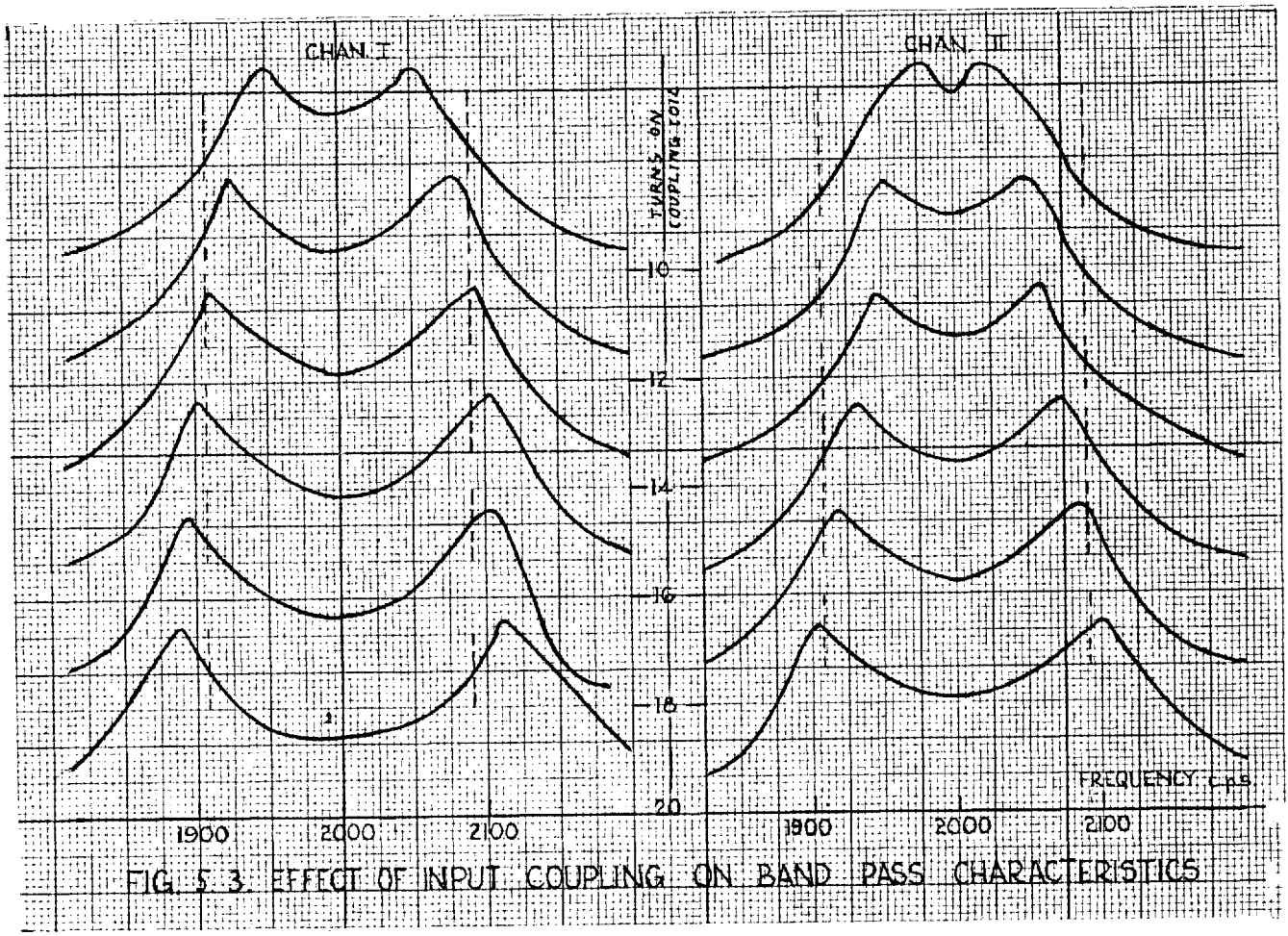


FIG. 5.3. EFFECT OF INPUT COUPLING ON BAND PASS CHARACTERISTICS

tuning of L7 (and its equivalent in Channel 1), enabled the band pass characteristics shown in Fig.5.4 to be obtained.

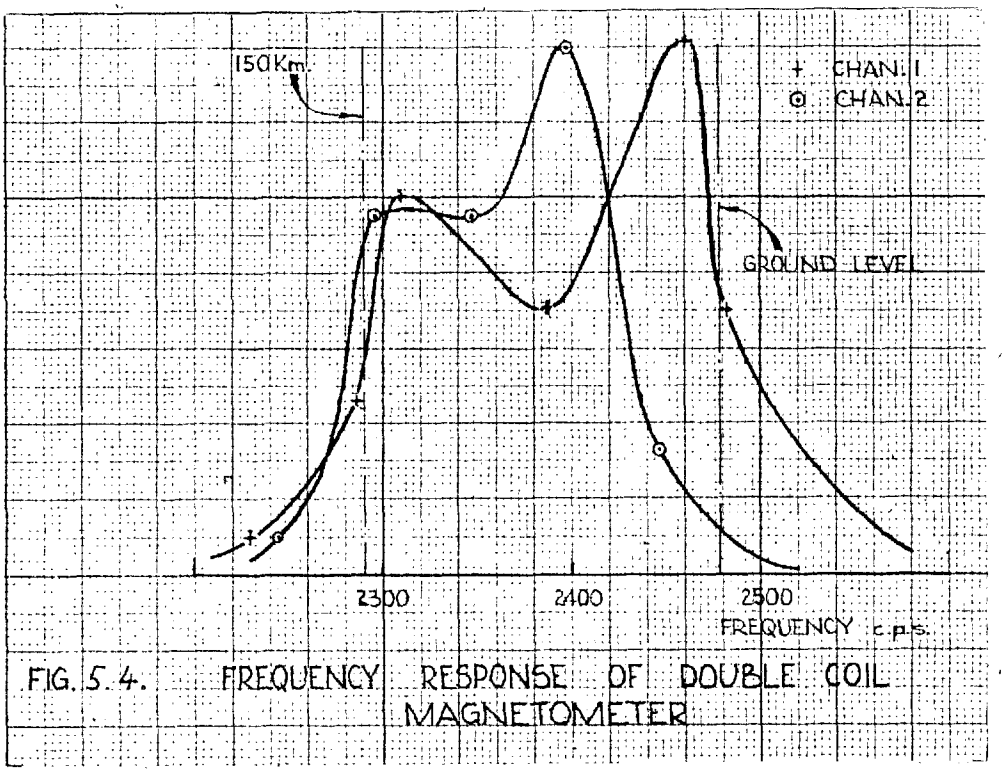


FIG. 5.4. FREQUENCY RESPONSE OF DOUBLE COIL MAGNETOMETER

Since the amplitude of the signal obtainable from the Channel II magnetometer is restricted, because of the small size of the coil, its bandwidth was limited to the upper part of the rocket trajectory in order to reduce the noise (Fig.5.4). The Channel I magnetometer was however tuned to cover the entire anticipated frequency excursions. Electrostatic shields in the form of earthed sheets of copper foil(0.001 inch) were incorporated between the primary and secondary windings of the input transformers (Fig.5.2).

A sub-miniature low microphony pentode, of a specially rugged construction, (CV4503) was used in the first stage of each amplifier in order to minimise loading of the input circuit and to achieve the maximum signal/noise ratio consistent with adequate gain. This is followed by an emitter follower, to maintain the high Q of the pentode anode load, and two stages of standard transistor amplificatio The voltage gain of each complete amplifier channel is 4×10^5.

In the prototype version the multiplexing circuit and the two sections of each amplifier channel were built as separate plug-in potted units (Fig. 5.5) and the switching relays and input circuits were an integral part of the chassis (Fig. 5.6). In the final version the two input circuits were also wired in separate modules and the mechanical lay-out was rearranged as shown in Fig. 5.7, in which the flight instrument is at the front right hand side of the table. On its lid, behind the main chassis, can be seen a set of spare modules.

In "potting" the modules a flexible polyester resin was used, to reduce contraction pressure and to provide a slight degree of cushioning thereby minimising the effects of severe transient accelerations. A thin glaze of epoxy resin was finally applied to seal the units against moisture penetration. In the first experimental version Araldite D

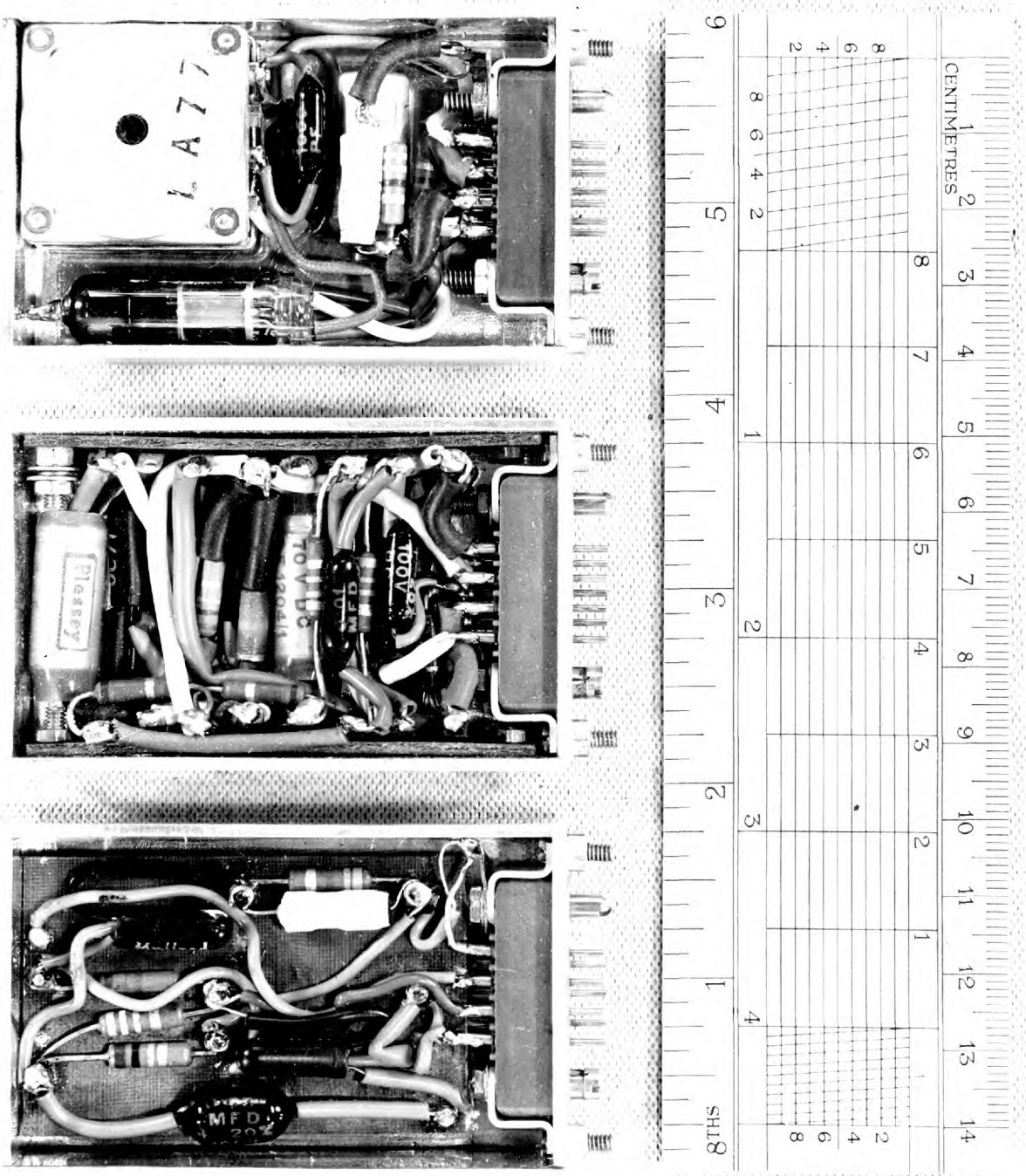


Fig. 5.5. Plug-in units. Transistor amplifier, electronic switch and valve amplifier.

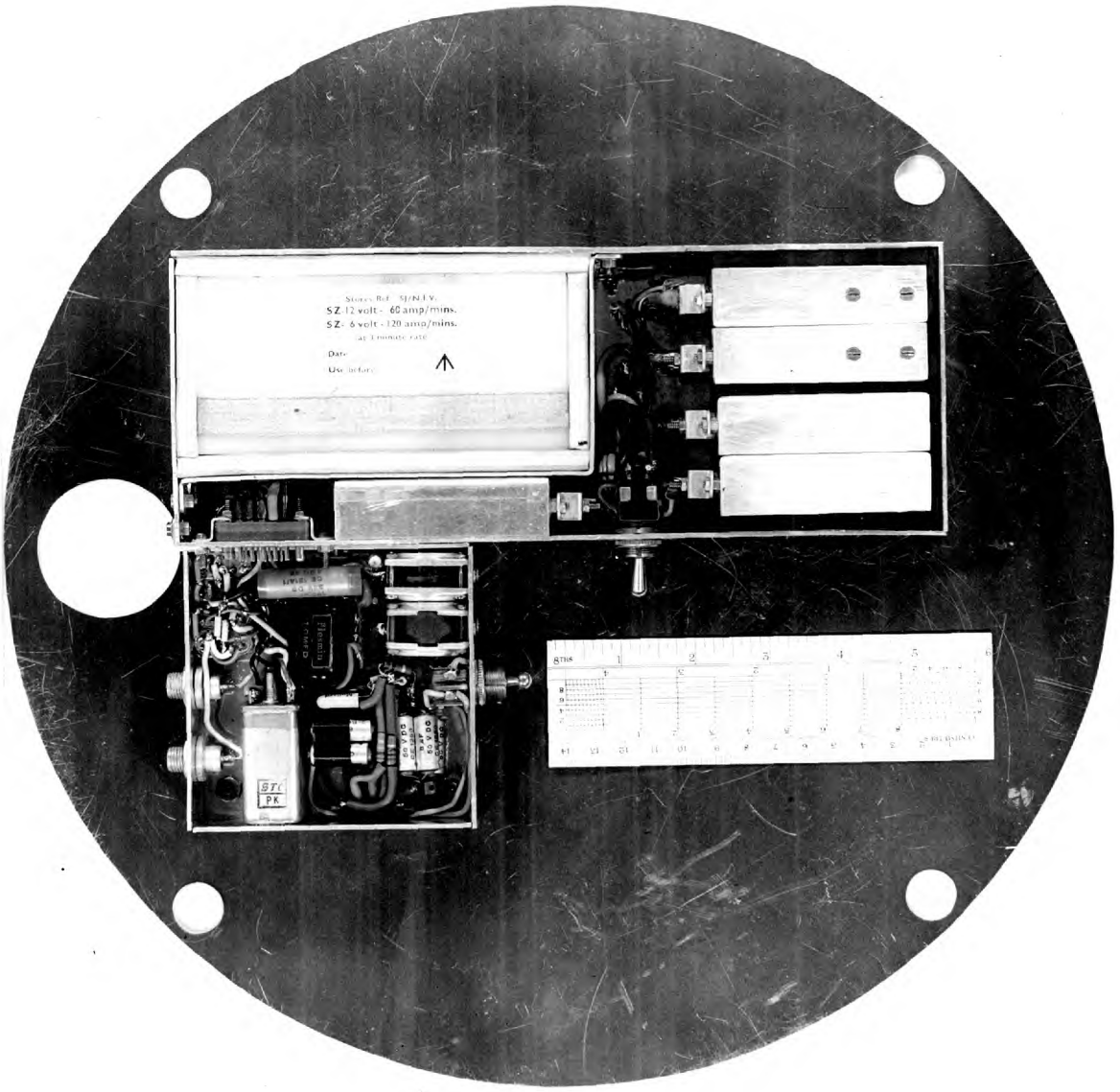


Fig. 5.6 Rocket-borne instrumentation mounted on a "Skylark" bulkhead.

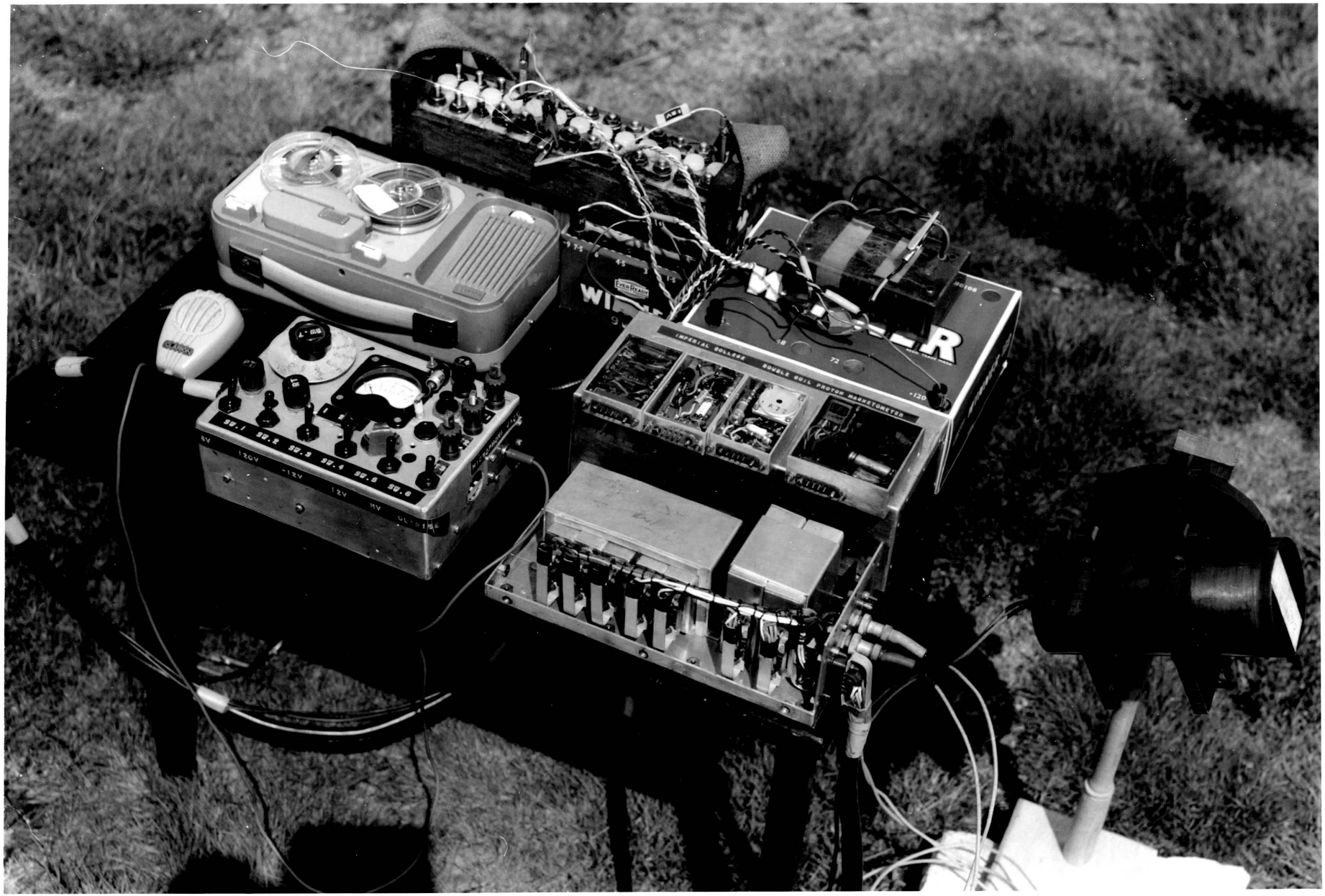


FIGURE 5.7.

epoxy resin was used throughout, but it was soon discovered that this led to troubles due to the contraction pressure cracking the glass envelope of the valves and causing severe changes in the temperature coefficients of the ferroxcube pot cores.

It was originally intended that the timing of the polarizing pulses should be carried out by the programme motor (external polarizing control - Fig. 5.2) and accordingly the multivibrator circuit V2 and V3 was incorporated to perform the cycling during testing. S1 selects internal or external battery and S2 is a spring loaded toggle switch whereby the polarizing can be controlled manually.

Fig. 5.8 shows sample records of the output of the

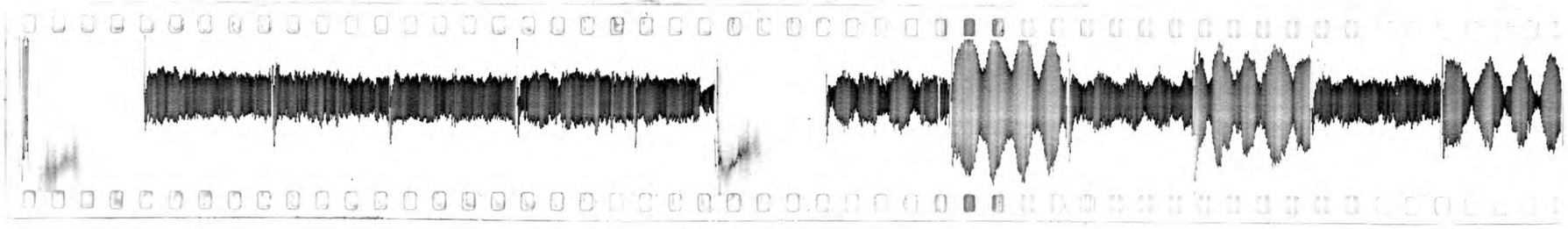


Fig. 5.8 Sample record of the output signal of a double coil magnetometer, beating with a local oscillator (Duration of record approx. 1 sec.).

instrument beating with a standard frequency local oscillator. The channel with the best signal/noise ratio can be selected and the number of missing cycles can then be interpolated.

The total weight of the magnetometer instrumentation is

9 lb. of which 4 lb. is accounted for by the sensing head.

Testing and Evaluation

The testing programme for a piece of rocket-borne equipment can conveniently be considered in two sections:

a) Laboratory tests prior to installation in the rocket.

b) Installation and compatibility tests in conjunction with other rocket-borne equipment.

5.4 Laboratory Evaluation

It has already been stated that one reason for developing the double channel instrument was in an attempt to make the quality of data less dependent on rocket attitude. In order to test to what extent this had been achieved the experiments depicted in Fig. 5.7 were performed. As already stated in connection with the rotation experiments, it is essential to position the instrument well out of the range of the 50 c.p.s. fields and magnetic field gradients normally present in a laboratory; this in turn creates problems of controlling and monitoring the various operations involved and the voltages and signals present.

The universal control/test unit, constructed to carry out the numerous tests which involved obtaining an actual precession signal, is shown in Fig. 5.7 and the circuit diagram is shown in Fig. 5.9. The various voltages can be

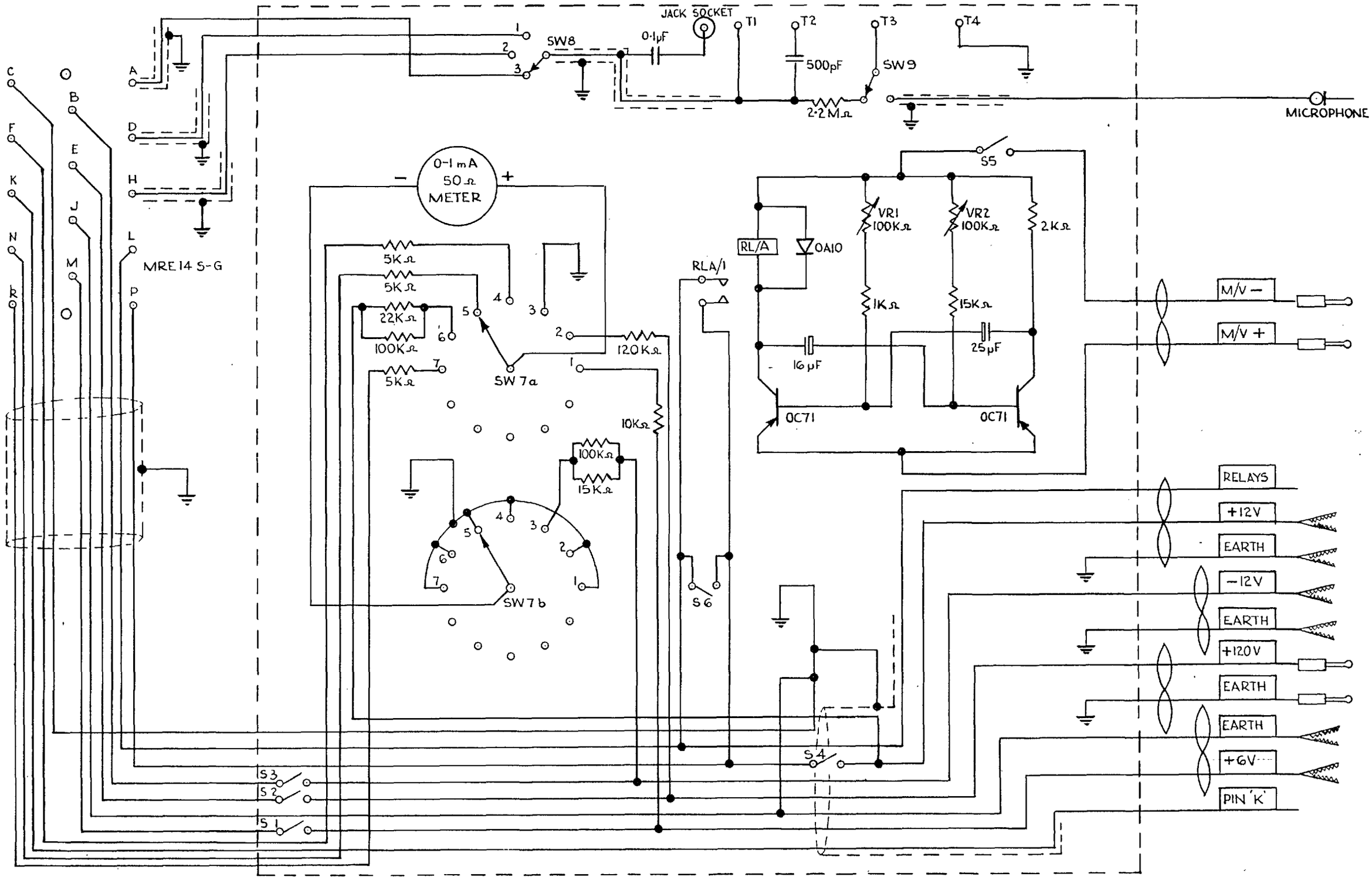


FIG 5.9. CONTROL/TEST UNIT

controlled by the switches and monitored on the meter by an appropriate setting of SW7. The polarizing is controlled manually, by S6, or automatically, by the multivibrator driving RL/A; the polarizing and recording times are independently variable by means of VR2 and VR1. The output of either channel separately, or the time-division multiplexed composite output, can be selected by means of SW8 and can either be heard in 'phones (in the jack socket), or fed to an oscilloscope from pins T1 or T2. If a permanent record is required, or if the equipment is "in the field" and no oscilloscope is available, the output at T3 is at a suitable level for recording on the "Clarion" transistorized battery operated tape recorder (Fig. 5.7) and it is in this application that the instrument was mostly used. The spring-loaded push button switch SW9 enables verbal comments to be incorporated quickly and conveniently at appropriate points during the recording.

In order to obtain actual precession signals in the magnetic field environment of London, the various tuned circuits were trimmed down in frequency, each by an equal number of c.p.s., by means of external capacitors.

Using the arrangement shown in Fig. 5.7 the sensing head was rotated about a horizontal axis perpendicular to both coil axes and perpendicular to the earth's field vector $\bar{F}$, an arrangement which would take the head through the most

unfavourable orientations. With both channels working concurrently, a recording was made of the signal from each channel in steps of 10° interval. The variation of signal amplitude with orientation is shown in Fig. 5.10 and Fig. 5.11

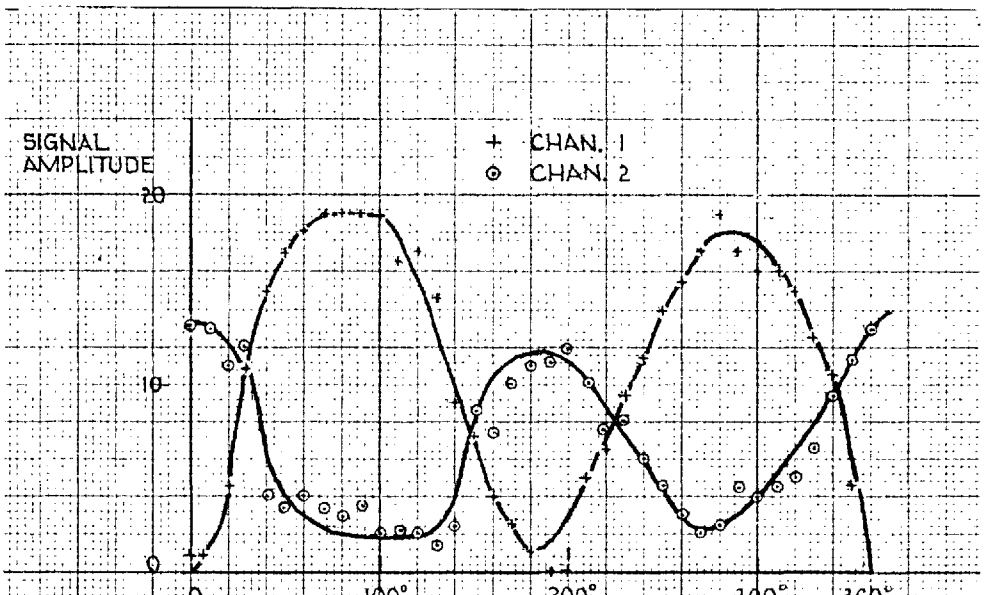


FIG. 5.10. AMPLITUDE OF SIGNAL AS A FUNCTION OF ROCKET ATTITUDE

shows samples of actual signals obtained in each position. It can therefore be stated that the instrument should produce a usable signal from one or other channel during each counting cycle regardless of the rocket's attitude relative to the geomagnetic vector.

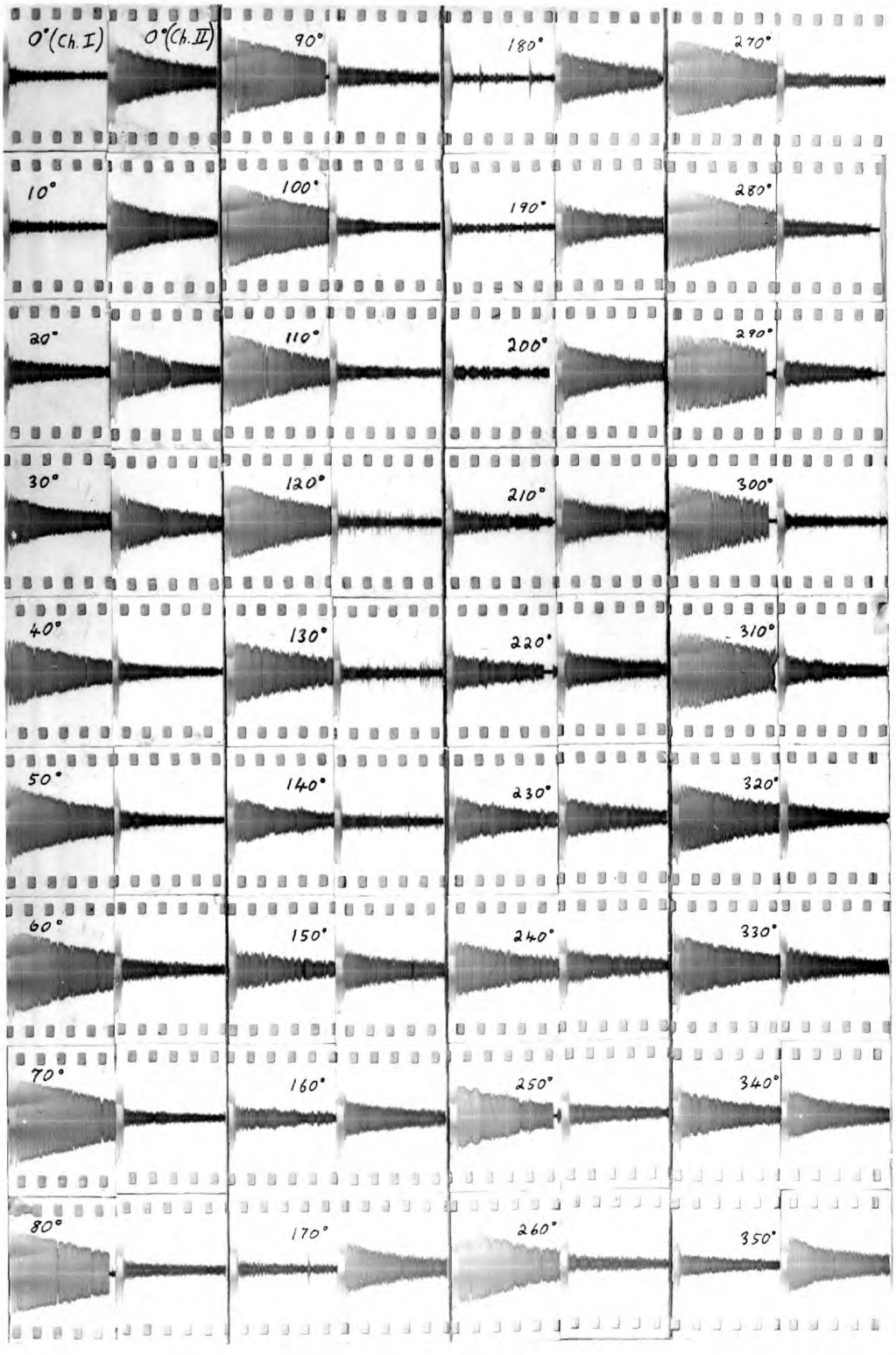


Fig. 5.11. Proton precession signals at various orientations of the sensing head relative to the geomagnetic field.

In the absence of any extraneous inductive pick-up, the signal/noise voltage ratio of the instrument, at room temperature, varies within the range 2 - 10 approximately, as the frequency changes through the pass band and with variation of rocket attitude. On the assumption that the maximum phase error ψ introduced into a signal of amplitude V_S by an unwanted sinusoidal signal of amplitude V_n is given by $\tan \psi = V_n/V_S$, it follows that the limiting accuracy of the instrument is approximately 0.03 c.p.s., which corresponds to an error in the measured field of less than one gamma. In the worst combination of precession frequency and rocket attitude this error would be increased to approximately 0.14 c.p.s., or 3.5 gamma, assuming the two errors introduced at the beginning and end of the counting period both add. It has already been stated that aerodynamic heating will result in an increase in the temperature of the sensing head to a value which might be of the order of 100°C. This temperature rise would lead to a reduction in the polarization of the sample, because of the reduced polarizing current and the higher thermal energies of the molecules, and the lower Q of the coils would result in a reduced voltage output, particularly at frequencies near the peaks of the frequency response curves. The higher coil temperature and resistance would also result in an increase in Johnson noise though, as discussed above, this will in general be negligible compared

with other sources of noise. In heating the sensing head from room temperature to 100°C these various effects would combine to reduce the available signal/noise voltage ratio by roughly 40 - 50%. It should, however, be possible to compensate for this loss of accuracy by replaying the signals through a narrower bandwidth than that of the flight instrument, when the signal/noise ratio would be increased by the square root of the ratio of the two bandwidths. Furthermore by drawing a best-fit curve through the plotted points the error in the curve would be correspondingly less than that of each individual determination, the actual improvement depending on the density of readings.

The ability of the device to resolve vertical changes is limited by the reading repetition rate. At one measurement per second, each reading taking 0.5 sec., the magnetometer will measure the mean field over the vertical distance traversed by the rocket in 0.5 sec. and the spatial separation of the readings will be twice this distance. The rocket was originally specified to reach a height of 150 Km, which implies that at a height of about 100 Km, where one would expect to find a significantly anomalous field, the readings will therefore be separated by approximately 1 Km in height.

The effect of the higher temperature during the rocket's flight, as compared with laboratory tests in England, will

be firstly to reduce the available signal, as discussed above, and secondly it might impair the performance of the electronic circuitry - in particular the increase in relay winding resistance will, at some temperature, prevent it from taking sufficient current to operate correctly and the increase of leakage current through the transistors (Fig. 5.2) will cause them to "bottom" at some temperature, determined by the type of transistor used and by the degree of temperature compensation employed. The complete instrument was designed to operate at a temperature of 60°C and was satisfactorily tested at this temperature.

To ensure as far as possible that the equipment can survive, though not necessarily function, during the initial part of the rocket flight, prototypes of each unit were subjected, whilst operating, to vibration tests covering the range 30 - 2000 c.p.s. at maximum accelerations of 10g (+20%, -0%), the rate of frequency sweep being adjusted continuously, throughout the range, to permit the full build-up of any resonances present. The instrument also received an unintentional "drop test" when the complete instrumented rocket was blown off its stand, during the open-air interference tests to be described in the next section. The electronics package fell a vertical distance of about 8 ft. and the sensing head about 17 ft. In spite of the fact that the fall bent the probe and caused extensive

damage to many other instruments inside the rocket, the magnetometer suffered no internal damage.

A possible mechanically weak part of the equipment is the potting of the sensing coils, in particular at the base, where severe aerodynamic forces will be present and the assembly relies solely on the resin for its strength. There are a number of possible manufacturing faults which could result in a weakness in this part. It was difficult to ensure that no bubbles of air were trapped during the encapsulation process. The exothermic reaction of curing the resin, if not carefully controlled, can cause strains in the potting and even slight mechanical and thermal stresses can cause paraffin to leak out of the coils during the curing process; the paraffin would collect asbubbles in the potting. To search for any weaknesses due to these three causes a series of X-rays was taken. These were of two types, firstly standard shadow-graphs along the two lateral axes of the head (Fig. 5.12 shows one of these), secondly a series of tomographs, in each of which the thickness of the sensing head "in focus" was 3 mm. None of the X-ray examinations revealed any flaw in the unit.

To ensure that there were no cracks through the potting, which could allow the sample to seep out during the flight, the sensing head was subjected to a "vacuum test" for a continuous period of 24 hours. The pressure during this

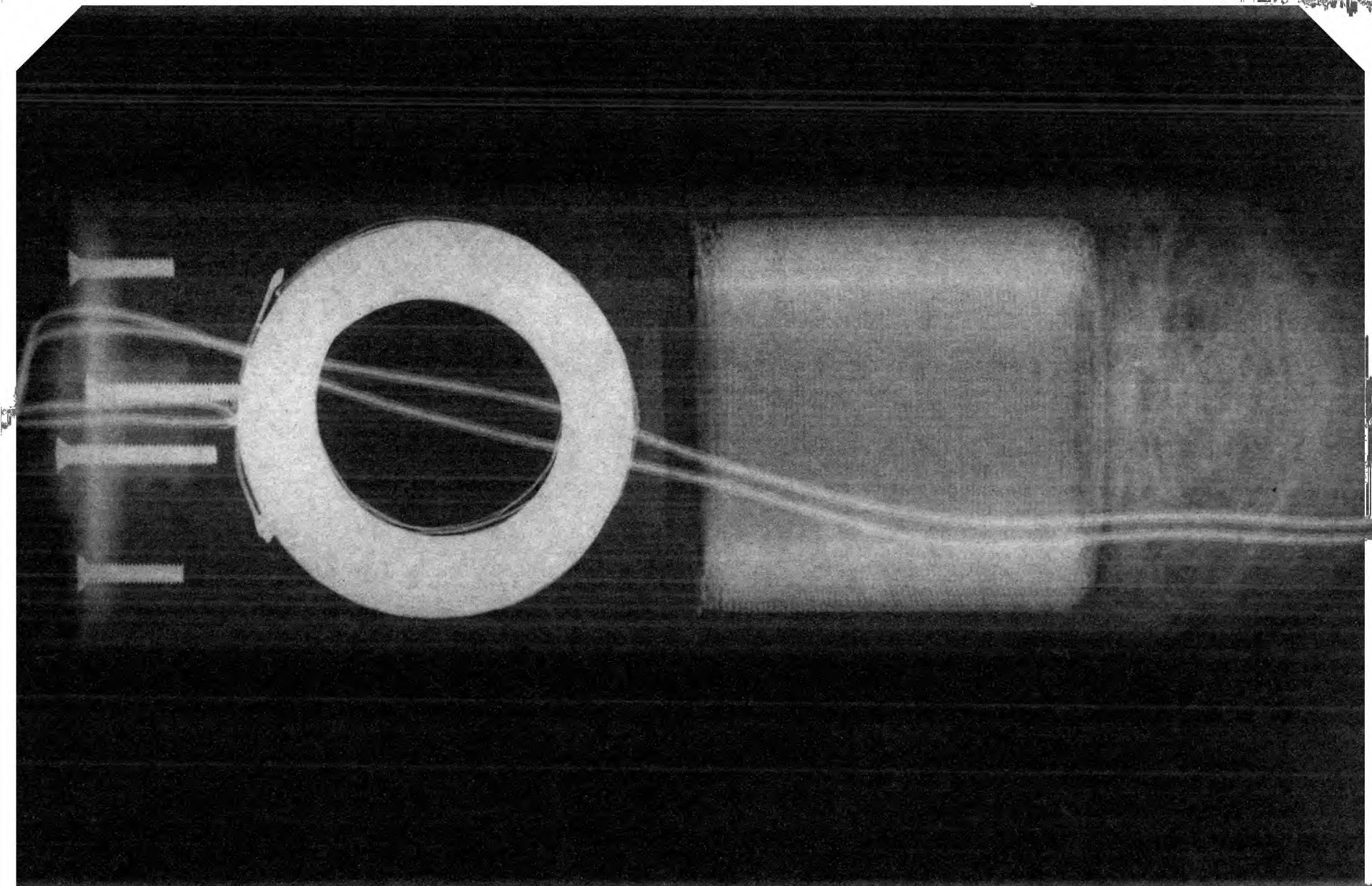


FIG 5.12. X-RAY OF SENSING HEAD.

test was approximately 0.1 mm. of mercury.

5.5 Installation and Compatibility Tests.

The problems which occur when an attempt is made to operate a sensitive magnetometer in close proximity to the other equipment in a rocket arise from the strong RF field radiated by the telemetry transmitter, from the alternating magnetic fields associated with the various electric motors and from the induced and permanent magnetic fields of any ferro-magnetic material.

The effects of the steady magnetic fields have been discussed previously (Ch.2, Sec.3).

When any new piece of sensitive laboratory apparatus is given its initial trials under realistic conditions trouble is often experienced as a result of instability and/or A.C. pick-up in high gain amplifiers. A similar situation exists when an instrument is first tried in a rocket, but in this case there are a number of administrative and technical difficulties, inherent in the system, which greatly increase the complexity of the problem:

i. As discussed in Chapter 4, the proton magnetometer is very susceptible to interference from mains powered equipment. For this reason the initial interference tests were carried out in a field well away from all buildings and later the operations were transferred to a disused wooden

tower at the Radio Transmitting Station at Cove, near the R.A.E.

ii. It had previously been discovered that, with the rocket powered from external generators, the alternating fields radiated from the power supply cables would cause unacceptable interference in a search coil positioned at the tip of the probe. It was therefore essential for the round to be powered by its internal batteries and for the external leads to be disconnected during the period of each test.

iii. In order to carry out, what in the laboratory would be a quick minor modification (such as unsoldering an earth connection), it was necessary partially to strip the rocket in order to gain access to the particular part and finally to reassemble it and go through the "run-up" procedure equivalent to an actual trial. As a general rule any alterations to the experimental conditions during the conduct of a run were out of the question.

iv. The interference level was found to vary widely under nominally identical circumstances. Thus it was often impossible to make consistently reproducible measurements from one day to the next. Fig. 5.13 shows samples of the various test runs which were made and records 1 and 2 show clearly how even during the course of a few seconds, the interference would vary, both continuously and discontinuously, from an almost negligible level to a

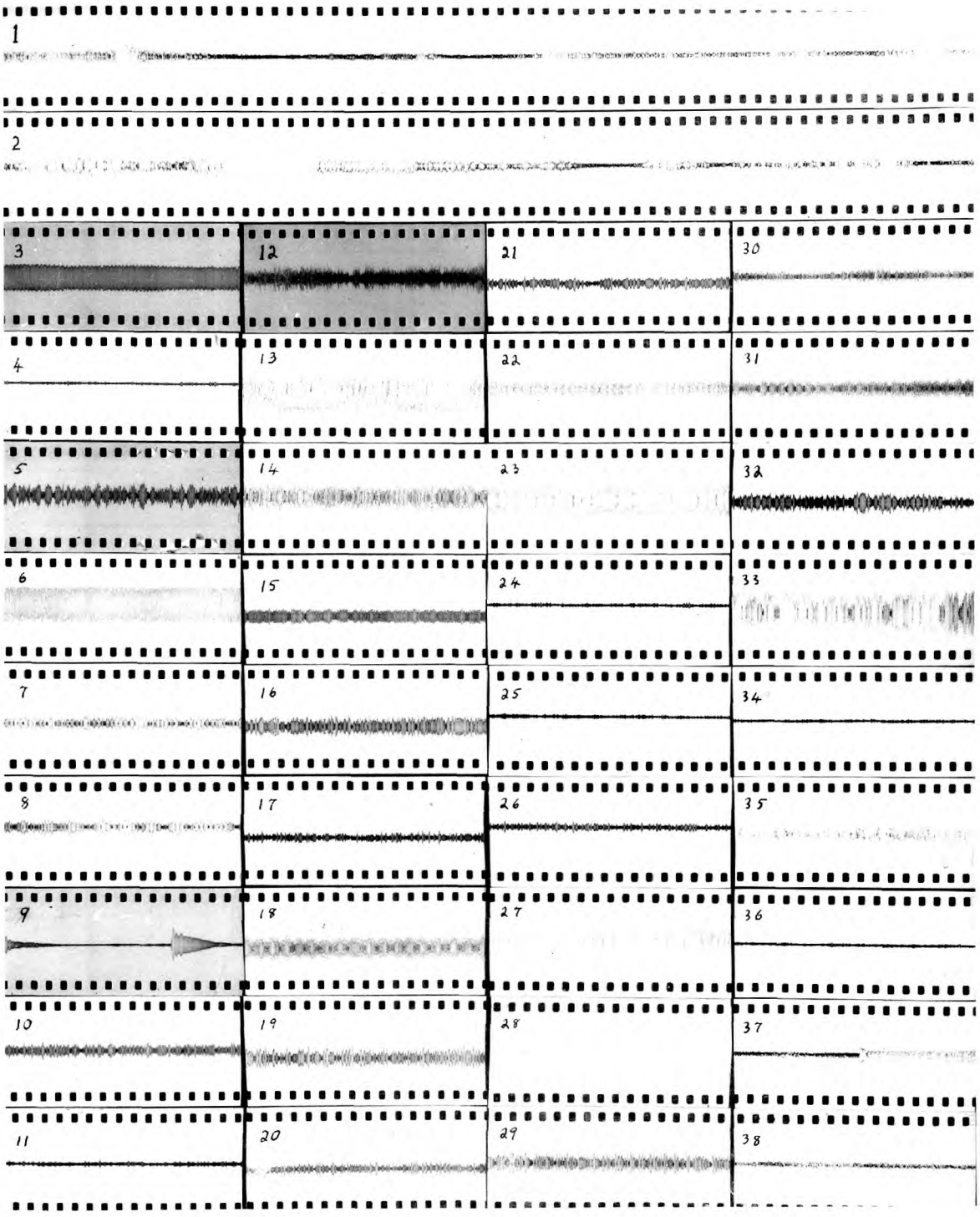


Fig. 5.13. Results of the Compatibility Tests. Magnetometer Output under Various Conditions of Interference.

level which saturated the amplifiers. It was therefore difficult to make quantitative assessments of the relative interference encountered under different experimental conditions. The causes of this effect are not clearly understood but it likely that several of the following factors were important:

i. Variations in the intensity of sparking at the brush contacts of the motors.

ii. Different earth returns for the various power supply currents resulting from slight differences in the assembling of the rocket skin.

iii. Variations in R.F. pick-up. It was discovered that R.F. energy fed back into the instrument would cause instability which would add to the general "ringing" of the resonant circuits caused by repetitive "spiky" interference. In particular standing waves were set up in the cable feeding the amplifier output to the control unit and varying R.F. loading of this cable would (apparently) cause variations in the general noise level; similar changes were experienced by covering up the various R.F. holes in the skin of the round.

iv. Variations of power supply impedances as a result of faulty plugs or battery ageing.

v. Variations in the relative rates of revolution of the electric motors.

The wide variations in interference level under,

nominally, identical test conditions led to certain incorrect conclusions being made on the basis of the results of the earlier tests.

In addition to the above unavoidable difficulties, considerable delays were also encountered as a result of unservicability of the rocket equipment viz:

i. The damage caused by the wind during the initial tests out of doors has already been mentioned.

ii. The limited life of the internal batteries severely curtailed the testing time available on any given day.

iii. On numerous occasions a day's testing was rendered abortive by failures in the rocket equipment, in particular rotary converters burning out and the occurrence of short circuits, which caused wiring to burn out. It is worth recording that the proton magnetometer remained serviceable throughout the duration of the testing programme.

iv. An unfortunate feature of the rocket instrumentation was that two "Ledex" rotary stepping switches were used on a single service way to control remotely the power supply to the inverters. This occasionally led to the two switches getting "out of step" and it was impossible to switch off the power supplies

The testing and tracing of the various causes of interference occupied six months altogether but, as a

consequence of these various technical and administrative difficulties during this period, the total time for which the rocket was in a suitable state for useful measurements (i.e. running on internal batteries and with everything serviceable) was only 31 min. 35 sec.

The tests were conducted using the apparatus shown in Fig. 5.7. The magnetometer and its sensing coils were mounted in the rocket and the control unit, tape recorder and batteries on a table close by. The recordings of the amplifier output could be played back immediately for a quick assessment and were subsequently transferred to 35 mm. paper for a more detailed evaluation (Fig. 5.13).

The noise level of the amplifier itself, in the absence of interference, was used as a means of standardizing the gain of the whole system in order that records taken on different days could be compared.

The various tests, which were carried out, will now be summarized.

Test No. 1.

To confirm that it was essential to remove the rocket from the vicinity of buildings, a test record was made of the 50 c.p.s. pick-up in the laboratory at the R.A.E., where Skylark rockets are normally tested. The results (Record 3, Fig. 5.13) confirm this point.

Test No. 2

Object To measure the degradation of the signal/noise ratio of each magnetometer channel which would result from A.C. pick-up with all the rocket equipment working.

Results

Record 4. Noise of amplifiers alone with no interference.

Record 5. Channel I. All rocket equipment functioning.

Record 6. Channel II. All rocket equipment functioning.

Conclusions

i. The interference level on both channels was intolerable.

ii. The level of pick-up in Channel II was much greater than Channel I and the character quite different. Since the amplifiers were nominally identical and the only difference between the two magnetometer channels was in the area-turns and orientation of the sensing coils (Fig. 5.1), this suggested that the pick-up was due to electro-magnetic induction in these coils.

iii. Since the level of interference in Channel II was such as to saturate the amplifier, Channel I was then used for the remaining quantitative measurements.

Test No. 3

Object To find the mechanism whereby the interference was being injected into the magnetometer.

Results

Record 7. Interference level with all rocket equipment running.

Record 8. All equipment ON. Sensing coil electrostatically screened by means of strips of 0.001" copper foil, 1 cm. wide, all connected to a common earth.

Record 9. All rocket equipment OFF. Noise level of amplifier I alone with a series of sharp taps on the skin of the rocket.

Record 10. All equipment ON. Magnetometer amplifier mechanically isolated by means of a cushion of foam rubber.

Record 11. All equipment ON. Sensing head magnetically screened by means of a μ-metal box.

Record 12. Repeat previous run but with μ-metal box removed.

Conclusions

i. The interference picked up as a result of the capacity between the sensing head and any other equipment was negligible. It did not appear that R.F. breakthrough into the sensing head was causing any trouble.

ii. A comparison of records 11 and 12, appears to confirm the conclusion that the principal method by which interference was picked-up by the magnetometer, was electromagnetic induction into the two sensing coils.

Effective electro-magnetic screening of the sensing head was obviously impracticable. It was therefore decided to investigate the possibility of suppressing the interference at its source.

Test No. 4

Object To measure the interference due to the three rate gyroscopes and their associated rotary converter power supply (E.D.C. rotary). This source was chosen first because it was a very large, heavy motor which took a large current; furthermore, since the data from the rate gyroscopes could be inferred from the other attitude sensitive devices, this equipment could be omitted from the rocket instrumentation without undue degradation of the scientific data.

Results

Record 13. Interference with all rocket instrumentation ON.

Record 14. Interference with all equipment except E.D.C. rotary.

Conclusions

The E.D.C. rotary converter and the rate gyroscopes together cause considerable interference but are not the only source.

In view of the redundancy of this data, the E.D.C. rotary was immobilized for the rest of the tests.

Test No. 5

Object To investigate the intensity and frequency spectrum of the alternating fields of the various remaining sources of interference.

Results

Record 15. Interference from telemetry sender No. 1. only.

Record 16. Interference from telemetry sender No. 2. only.

Record 17. Interference from Doppler transponder and fluxgate magnetometer (elements disconnected).

Record 18. Interference from Doppler transponder and fluxgate magnetometer (elements connected).

Record 19. Interference from 24 channel rotary switch used for time division multiplexing.

Record 20. Interference from a sub-switch motor only.

Record 21. Interference from the programme motor only.

Conclusions

Every electric motor was generating un-acceptable interference and the fluxgate elements also were radiating an intolerable alternating field.

Action The fluxgate elements were temporarily repositioned as far away from the proton magnetometer as possible and the R.A.E. undertook to suppress, as far as possible, the sparking of the various motor brushes.

Test No. 6

Object To evaluate the effectiveness of the measures taken as a result of test No. 5.

Results

Record 22. Interference level on Channel I of proton magnetometer.

Record 23. Interference level on Channel II of proton magnetometer.

Conclusion

The interference suppression measures had been ineffective.

Test No. 7.

Object To investigate the possibility of overcoming the interference problem by the use of a longer extendable telescopic probe. For convenience the 1185 copper coil, which had been used in the rotation experiments, was used with a continuous lead-in cable and both this cable and the amplifiers were positioned on a bench outside the rocket.

Result.

Record 24. Interference with coil 6 ft. from tip of nose cone.

Record 25. Interference with coil 4 ft. from tip of nose cone.

Record 26. Interference with coil 1 ft. from tip of nose cone.

Conclusion

The small variation between the three records, together with the fact that all three are a great improvement on previous records, suggested that voltages developed in the lead-in cable, as a result of earthing the screening in the plug at the tip of the nose cone, might have been appreciable.

Test No. 8.

Object To test the theory proposed above. The original Channel I coil, cable and amplifier was used; the amplifier again mounted inside the rocket but the plug at the tip of the nose cone was modified to enable the earthing of the braiding to be disconnected.

Results

Record 27. Braiding earthed at tip of nose cone, coil 10 ft from tip of nose cone.

Record 28. Braiding earthed at tip of nose cone, coil 1 ft. from tip of nose cone.

Record 29. Earthing of braiding open circuited. Coil 1 ft. from tip of nose cone.

Conclusion

Considerable interference resulted from earthing the screening braid of the input cable to the nose cone.

Action Screened twin cable was substituted for the lead-in cable. By this means the "earthy" side of the signal carrying wire was only earthed at one point - the input socket to the amplifier.

Test No. 9

Object To measure the interference level using the modified input cable.

Results

Record 30. Coil 10 ft. from tip of nose cone using twin screened input cable.

Record 31. Coil 1 ft. from tip of nose cone using twin screened input cable.

Conclusion

Comparing the results of Test No. 7 with tests 8 and 9, suggests that considerable interference must have been picked up by the amplifier.

Test No. 10.

Object To verify the conclusion of Test No. 9.

Results

Record 32. Amplifier alone mounted inside the rocket with lead-in cable replaced by a fully screened input plug (to reject R.F. pick-up). Channel I.

Record 33. Ditto. Channel II.

Conclusion

Considerable interference was being picked up by the amplifiers themselves. The only two possible mechanisms whereby this might happen were microphony (which early experiments had indicated was small, if not negligible) and electromagnetic - induction into the grid circuit. This latter mechanism also seems difficult to accept as the pot core constitutes an effectively enclosed magnetic loop and, furthermore, it was screened by the chassis of the relay unit and by the lid of the main chassis.

At this stage it was decided that only one more day could be allotted to testing the rocket. Accordingly both of the above possible sources of trouble were removed by replacing the valve stage by a transistorized amplifier, with an emitter follower input to maintain the input impedance and by screening the high impedance low level input circuit with a μ - metal box.

With these modifications record 34 was obtained.

The fluxgate elements were now repositioned at the tip of the nose cone. This led to a recurrence of noise (record 35) but as the character of the interference could

not be explained simply in terms of the energisation of the fluxgates the test was repeated. The repeat (records 1 and 2) showed clearly the intermittent character of the interference and it was concluded that dirty brush contacts on the motors were responsible. A further test run produced record 36 and confirmed that the various modifications had been effective.

Hitherto the power supplies and cycling of the magnetometer had been controlled by the Control unit (Fig. 5.9). When the installation was modified as for flight, record 37 was obtained; the change in interference level which occurred in synchronism with the switching of the polarizing current can clearly be seen.

When the lead from the energising coils of the relays RLA and RLB (Fig. 5.2) was disconnected from the programme motor record 38 was obtained. This shows that unacceptable interference was being picked up on the polarizing voltage supply lead and was being fed into the amplifier, via the capacity of the normally open contacts of RLA and RLB (Fig. 5.2).

It was therefore decided that a radical redesign of the rocket-borne magnetometer was necessary in order to incorporate the modifications already discussed and to control all power supplies and switching operations without reference to other rocket apparatus; the only connection

which appeared to be acceptable was one from the output of the magnetometer to the telemetry modulator.

The redesigned and re-engineered rocket-borne magnetometer will be discussed in Chapter 6.

CHAPTER 6

ROCKET-BORNE MAGNETOMETER MARK II

6.1 General considerations

Since the requirements and operation of this instrument are basically very similar to that discussed in the previous chapter only those features which constitute a significant modification from the previous design will be discussed.

Having regard to the severe interference problems discussed in Chapter 5, it was decided to revert to a single channel instrument and to employ a single coil occupying the entire space available in the sensing head. Such a device would give no signal at all in its worst orientation but, in its optimum orientation, would be considerably better than a transistorized version of the double-channel instrument discussed in Chapter 5. The probability of a satisfactory flight would then be dependent on the favourable orientation of the rocket head assembly in flight. Following the same policy of planning for less data, but in the expectation that some at least would be of better quality, the polarizing time was increased from 0.5 second to 0.6 second.

6.2 The Sensing Head

Fig. 6.1 shows a cross-section through the sensing head. The coil consisted of approximately 1500 turns of 20 S.W.G. Simgold "M" (high temperature) enamelled copper wire. This arrangement produced a coil with an inductance of 34.4 mH and a resistance of 6.5 ohms. The complete sensing head is shown mounted on the tip of the probe of Skylark No. 40 in Fig. 6.2.

6.3 Electronic Circuitry

As before a "modular" construction was used, the complete instrument being sub-divided into five plug-in stages, viz:

i. Relay unit (Fig. 6.3). The switching operation of the relays is similar to that described previously. The wiring of the two pairs of contacts RLA1 and RLA2 in parallel increases the reliability, since the signal voltages at this point are too small to break down any contact resistance. It is essential that the capacitor C2 should be as reliable as possible, particularly since its condition cannot be verified once the rocket has been raised into the launcher. Accordingly a tantalum electrolytic capacitor with a thickened anode plate, specially developed by the Plessey company for use in rockets, was used in this position.

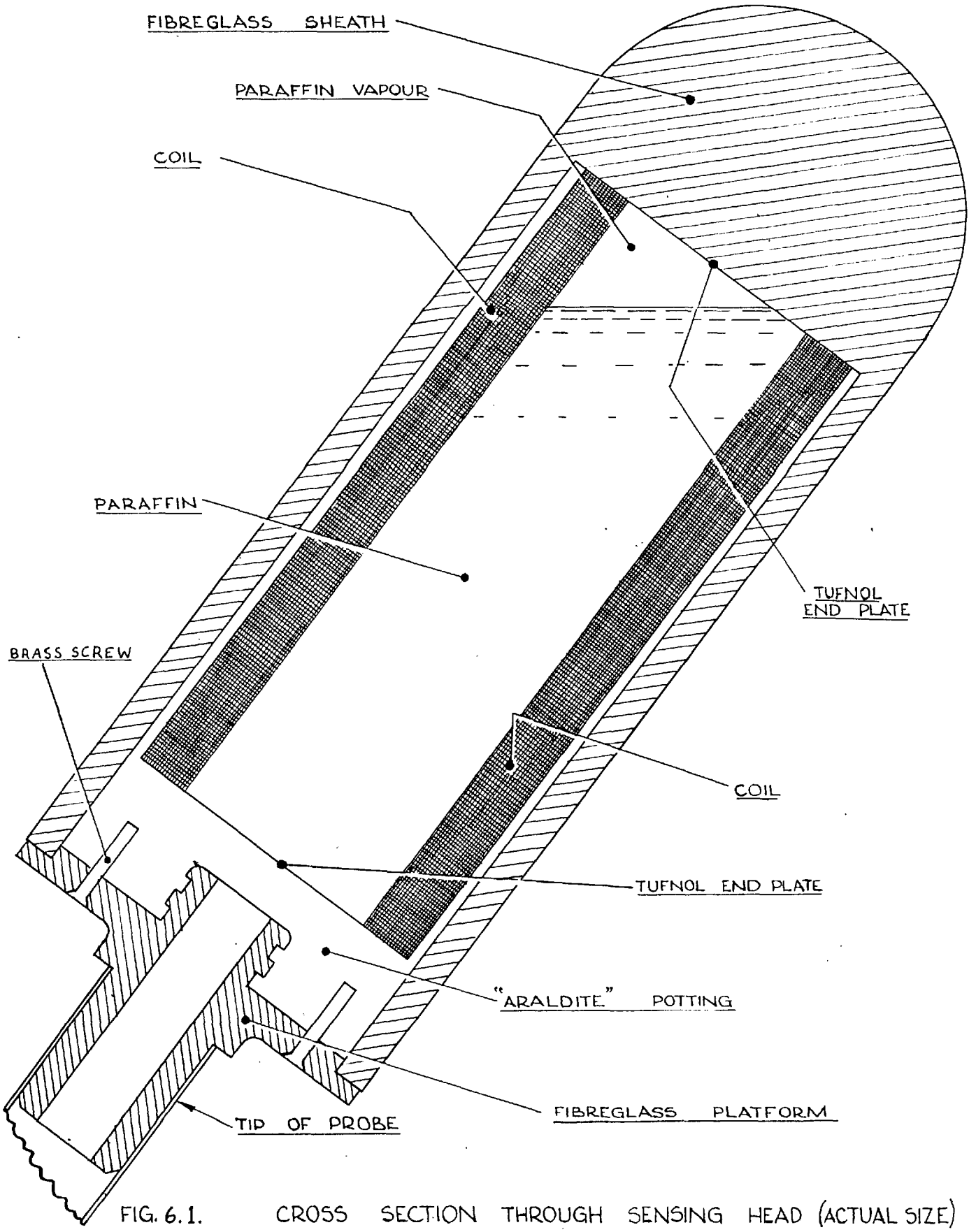
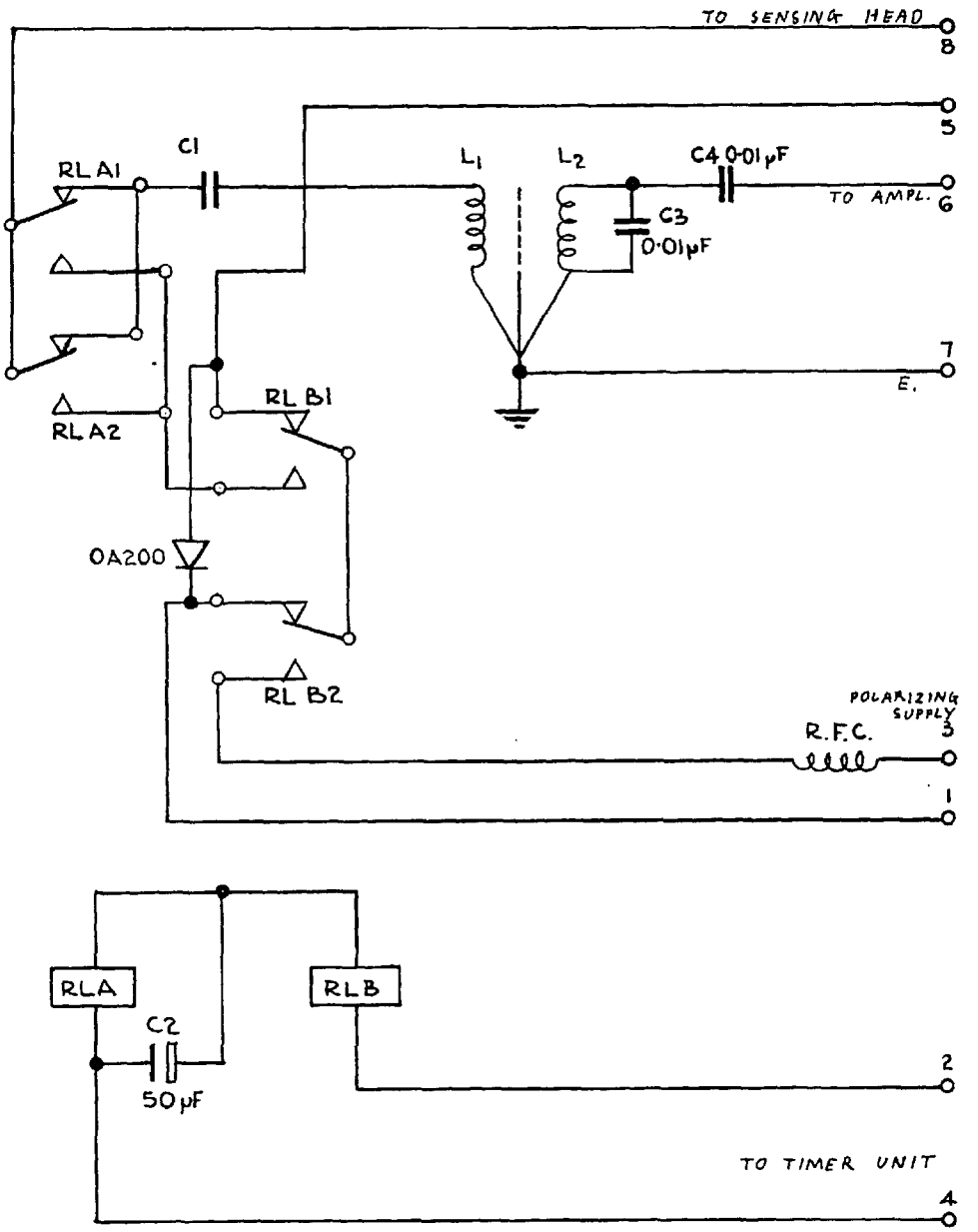


FIG. 6.1. CROSS SECTION THROUGH SENSING HEAD (ACTUAL SIZE)



Fig. 6.2. Probe and Sensing Head.



L_1 = 14 TURNS, 24 SWG.
L_2 = 725 TURNS, 35 SWG (SIMGOLD "M") } ON LA2103
C_1 = SELECTED TO TUNE SENSING COIL TO 2366 c.p.s.
f_0 = 2370 c.p.s.
R.F.C. = 12 TURNS ; ~ $\frac{1}{4}$" DIA: 20 SWG.

FIG. 6. 3. RELAY UNIT

The sensing head is connected via the high temperature lead-in cable to pin 8 and the signal is fed into the amplifier from pin 6. The polarizing supply is connected to pin 3 and the R.F. choke blocks any R.F. currents, which would cause instability if they were injected into the amplifier. The OA200 diode was included to enable the connections between pins 1 and 5 to be used to reset an electronic counter in the event of it being necessary to carry out the frequency measurements in flight. Such an arrangement would save telemetry bandwidth but would result in reduced reliability and quality of the data. RLA and RLB are miniature relays, of a specially rugged construction, and are specified to withstand accelerations of 50g. The entire circuit was enclosed in a box of 1/16" thick μ-metal.

ii. Emitter follower unit (Fig. 6.4): The circuit is a transistorized version of the well-known "White" cathode follower. High gain silicon transistors, selected for low noise, are employed in order to maintain a high input impedance over a wide temperature range. It was found that the noise factor of the circuit is critically dependent on the base current of V1 and accordingly the spread of transistor parameters is accommodated by selecting R1 to give each unit a optimum noise factor. The OA200 diode, V3, is incorporated to protect the transistors from the positive half cycles of the transient high voltage surges

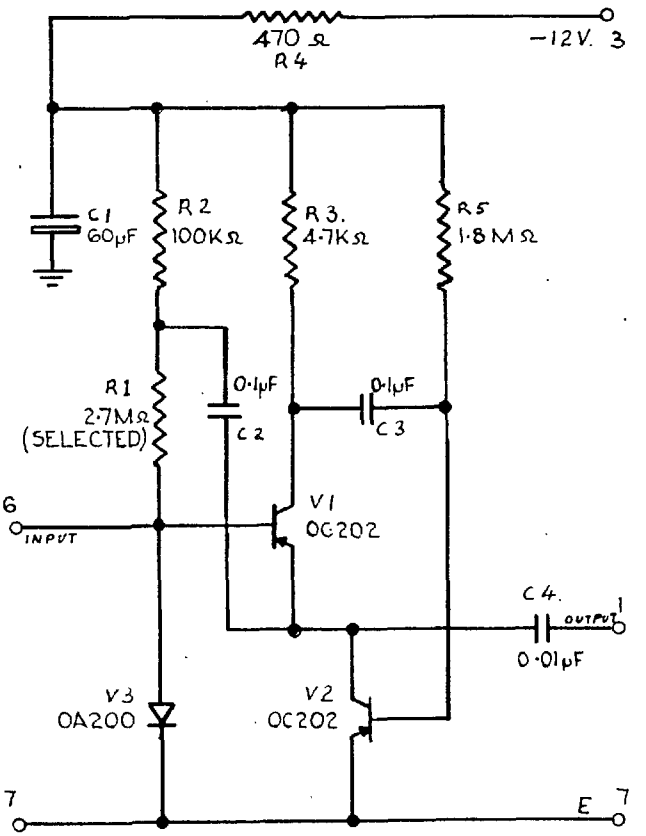
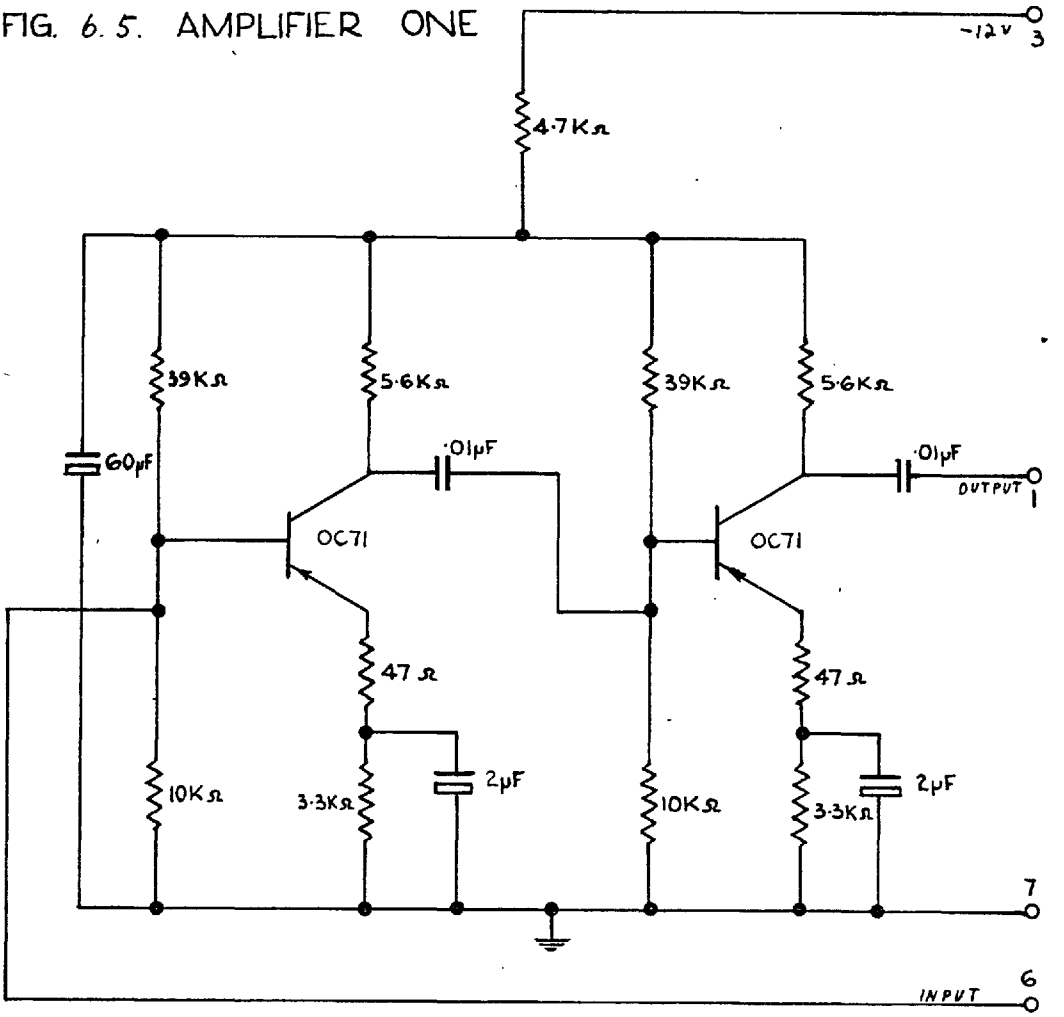


FIG. 6.4. EMITTER FOLLOWER UNIT

on switching off the polarizing current. When the emitter follower is loaded by the amplifier the input impedance is approximately 800 Kohms.

iii. Amplifier ONE (Fig. 6.5). This is of conventional design with temperature compensation to give a

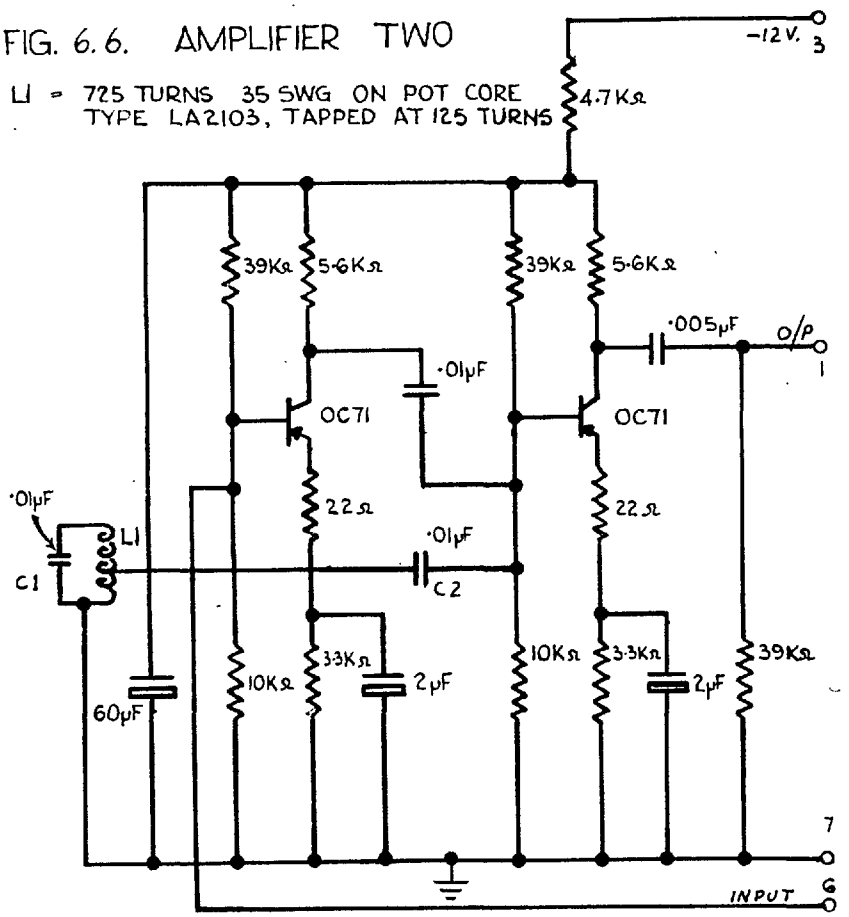
FIG. 6.5. AMPLIFIER ONE



satisfactory performance at temperatures up to 60°C. A low noise transistor is selected for the first stage.

iv. Amplifier TWO (Fig. 6.6): Noise occurring well outside the required pass band is rejected by means of the L/C filter L1 and C1 between the last two stages of the

FIG. 6.6. AMPLIFIER TWO



complete amplifier. The way in which the frequency response and resonant frequency are modified, as a consequence of the resistive and capacitive loading of the amplifier, with different tapping points, is shown in Fig. 6.7. The tapping point was chosen to give the required band pass in conjunction with the "double hump" of the input circuit characteristics. When all three resonant circuits are tuned to the same frequency the detuning effect results in a

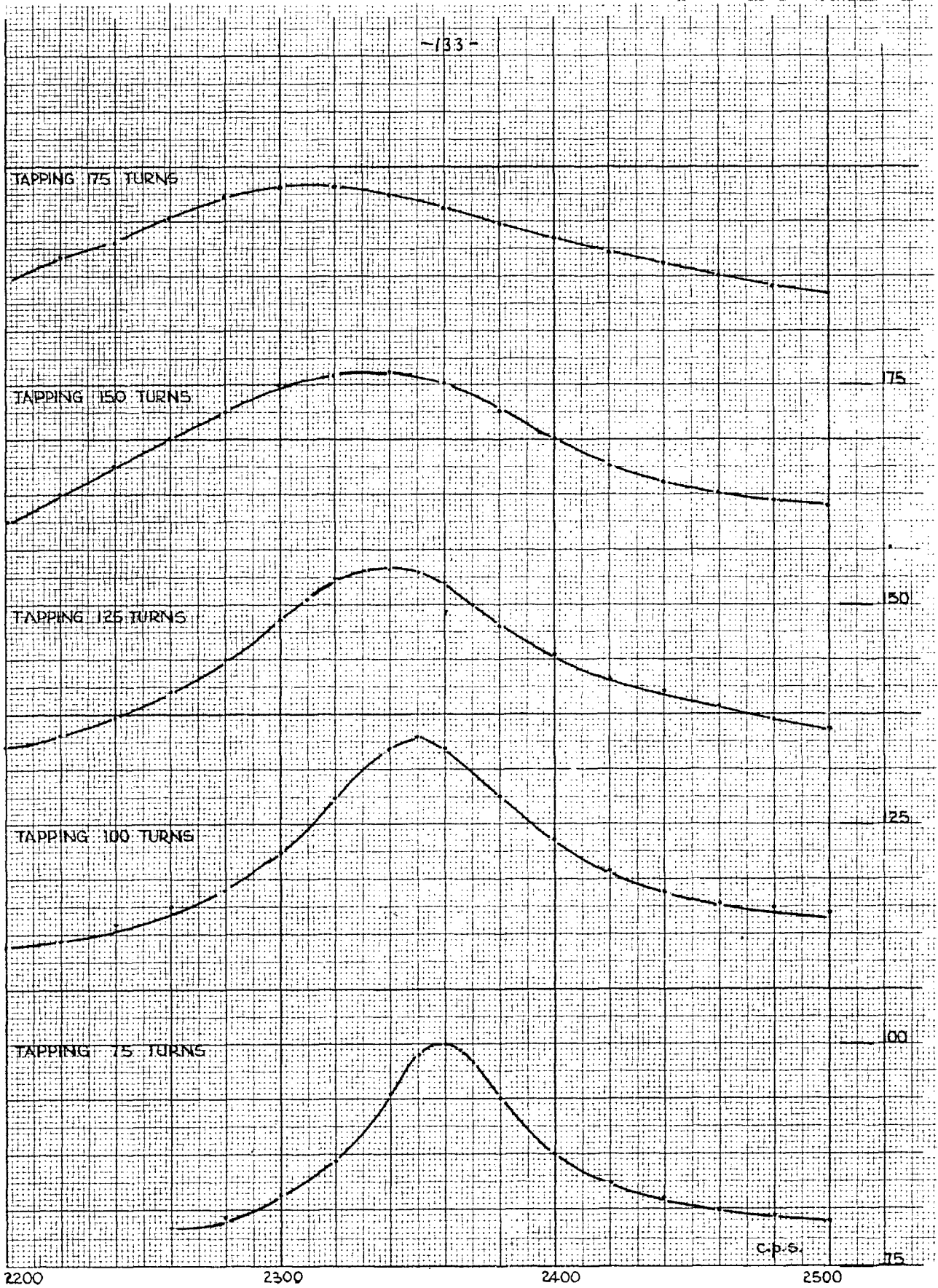


FIG. 6.7. EFFECT OF LOADING ON COIL 'Q' AND RESONANT FREQUENCY

useful slight increase in the amplitude of the lower frequency "hump" (Fig. 6.8) - the lower frequency corresponding to

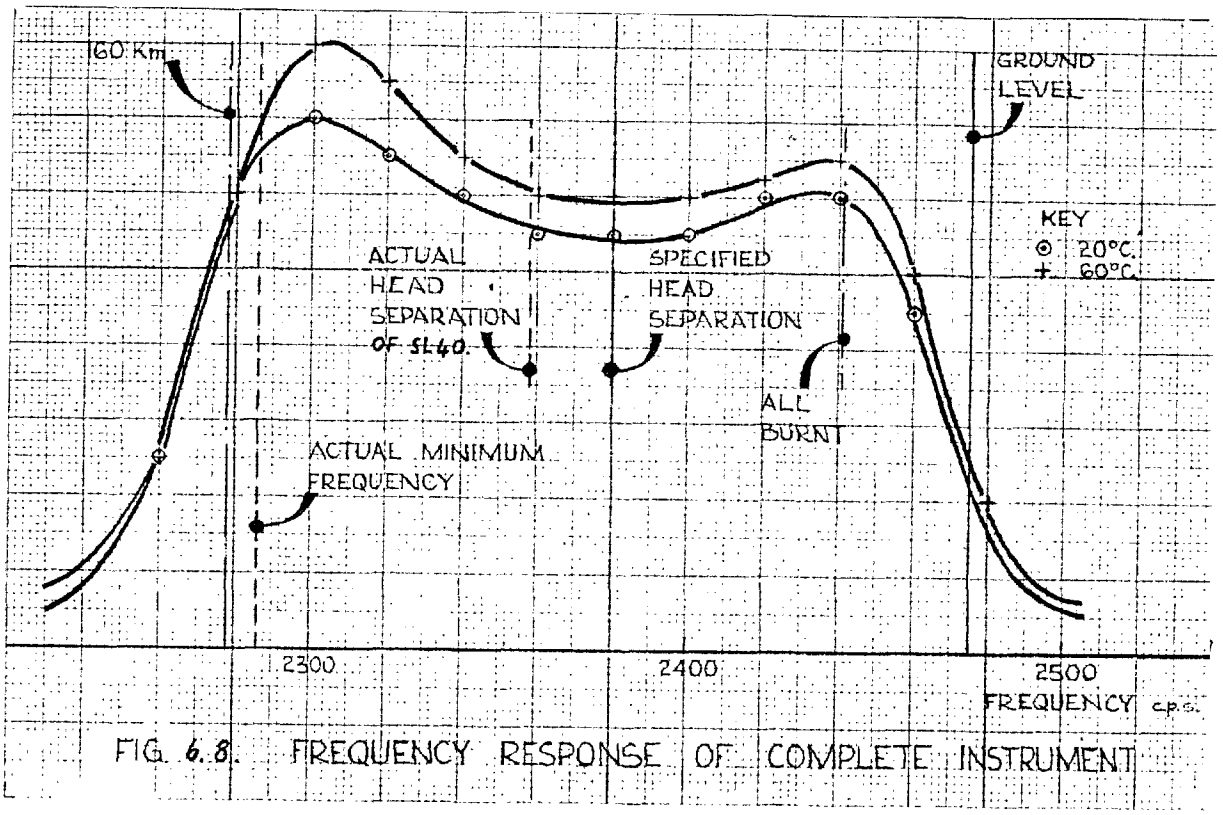


FIG. 6.8. FREQUENCY RESPONSE OF COMPLETE INSTRUMENT

the upper part of the flight. The pass band of the amplifier was adjusted to give the maximum signal between the heights where the Raven motor was expected to burn out ("All Burnt") and the maximum expected height. At the same time it was necessary to arrange for sufficient signal amplitude at ground level to enable the instrument to be given a final test before erection in the launcher (Fig.6.8)

In order to minimise the detuning effects of temperature changes in the two Ferroxcube pot cores, polystyrene tuning capacitors were used to tune the inductance (C3, Fig.6.3 and C1 Fig. 6.6); these have a negative temperature coefficient of -120 parts per million per ^{o}C which partly compensates for the +160 parts per million per ^{o}C coefficient of the LA2103 pot cores.

v. Timer unit (Fig. 6.9): This unit times the

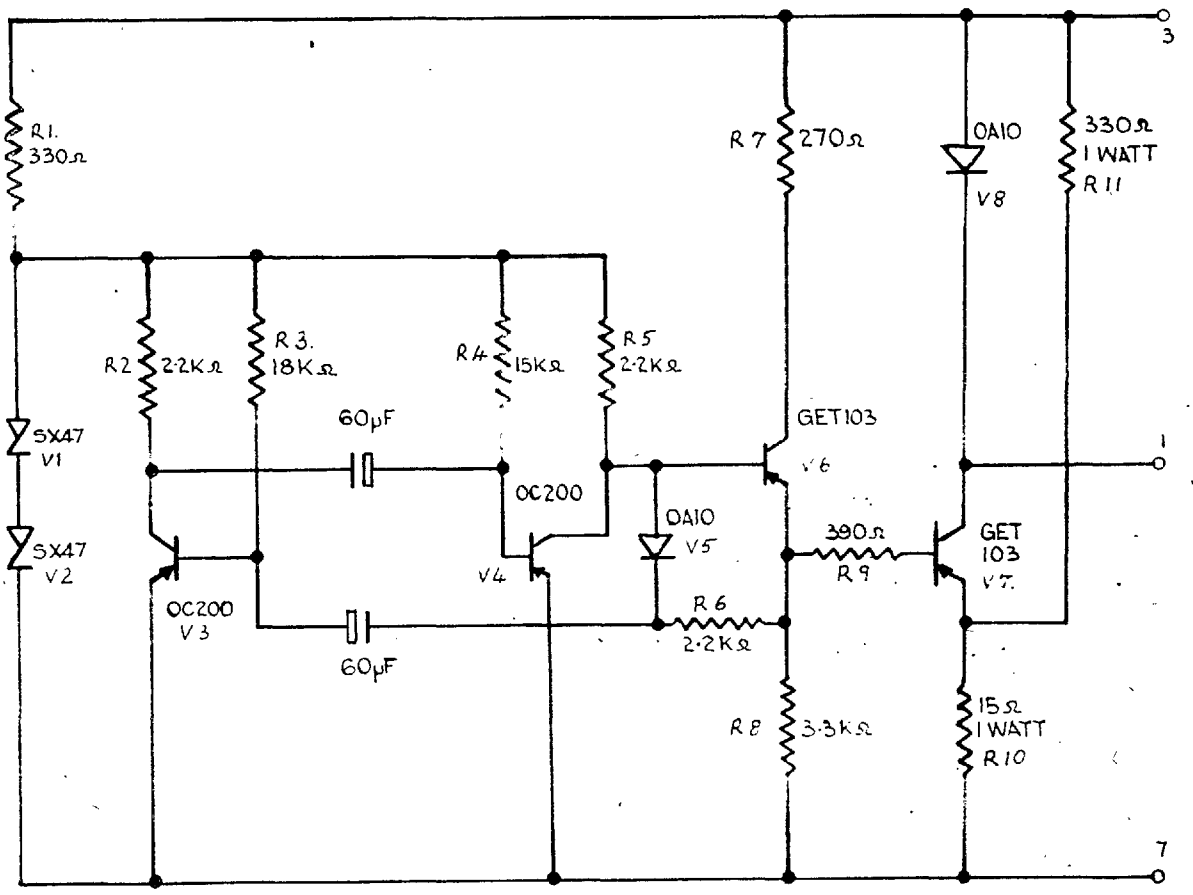


FIG. 6.9. TIMER UNIT

polarizing and counting periods and drives the two relays in the relay unit; the relays are connected between pins 1 and 3. Basically it is a conventional multivibrator in which the "ON" period is controlled by C1 and R4 and the "OFF" period by C2 and R3. (The "ON" and "OFF" periods refer to the state of the relays). In order to achieve constant timing periods throughout the specified voltage variations of the SZ6/12 silver-zinc battery (12-18 volts depending on age, temperature, load and state) the supply to the relaxation oscillators (V3 and V4) is stabilized by means of R1 and the zener diodes V1 and V2. Silicon OC200 transistors and tantalum electrolytic capacitors were used to ensure maximum stability with time and temperature changes. The output of the multivibrator is buffered from the output stage, V7, by means of the emitter follower V6, the low output impedance providing adequate current to bottom the output stage with the 70 ohm collector load, presented by the two relays in series. In order to maintain the buffering effect of V6 during the ON stage it is desirable to prevent it from bottoming and to this end the collector is taken to the unstabilized negative supply rail via R7 (R7 serves to limit the power dissipated in V6).

It is well known that the time during which a switching transistor is most liable to failure is during the period when it is changing from a "bottomed" to a

"cut-off" state or vice versa, since it is during this period that both appreciable currents and voltages are present concurrently. It is therefore essential to switch the transistors (in particular the output transistor V7) as rapidly as possible; this implies that no appreciable capacitive load can be applied to any point where the voltage is required to change rapidly. A normal multivibrator configuration produces alternating square and exponential waveforms at the collector of either transistor, the exponential time constant when the transistor switches OFF being determined by the collector resistance and the timing capacitor. In the circuit of Fig. 6.9 the capacitive load is removed from the collector of V4 during the ON period (i.e. the period when V4 is OFF) and is charged from the low output impedance point of V6 via R6, which serves to limit the base current through V3. Thus, whilst the junction of V5 and R6 changes with a time constant C2 . R6, the emitter of V6 (and hence the base of V7) are switched rapidly. During the OFF period V4 is bottomed and hence its collector presents a low impedance path to earth and the diode V5 clamps C2 to this collector, thereby again permitting the emitter of V6 to switch rapidly - if V5 were omitted the voltage change would follow a time constant C2 (R3 + R6 + R8).

As a further precaution to prevent "thermal run-away"

in the two GET 103 transistors, V6 and V7, they are mounted in a heat sink machined from a $\frac{1}{4}$" thick block of duralumin. The heat sink is mounted in good thermal contact with the aluminium chassis of the unit.

In order to ensure that the output transistor V7 is held off at high temperatures the emitter is biassed slightly negative by the potential divider R10 and R11. The impedance of this potentiometer is chosen to reduce the voltage across the relays, in the "ON" state, to a value within the specified working range.

The diode V8 damps down the voltage surge which would otherwise occur when the energising current is removed from the inductive load of the relays.

The inter-connections between the various stages are shown in the wiring diagram of Fig. 6.10.

For the flight of Skylark SL40 the -12V, 4 mA, and the -12V to 18V, 2-3A power supplies to the instrument were provided by Ever Ready B 1478 and Venner SZ6/12 batteries. The supplies could be switched, either manually or remotely, by means of a "Ledex" rotary stepping switch; a complete switching cycle occurred in three stages:

i. everything OFF

ii. amplifier only ON

iii. amplifier and timer ON (ready for flight).

Three complete magnetometers were produced, one being

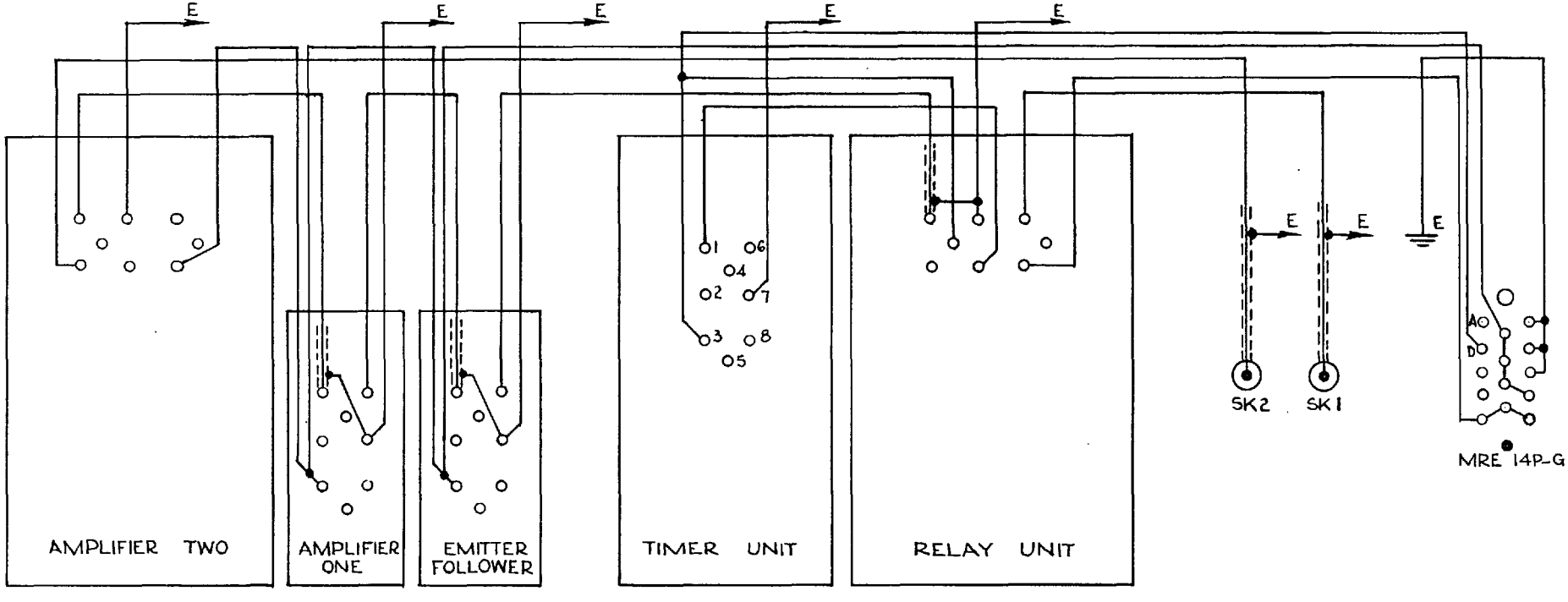


FIG. 6.10. SINGLE CHANNEL TRANSISTORIZED ROCKET-BORNE MAGNETOMETER — WIRING DIAGRAM.

for the flight and two spares.

6.4 Monitoring

It is normal practice with rocket-borne instrumentation to use some channels of the 24 channel switched telemetry sender to monitor voltages at one or more appropriate points in order to verify the satisfactory state of the equipment prior to flight and where possible, to diagnose the cause of any failure which might occur in flight, in order that appropriate measures can be taken to prevent a recurrence of the trouble.

In the present application the most likely causes of failure are to be associated with switching the sensing head coil between the polarizing supply and the input to the amplifier. It was therefore decided to monitor the voltage of the SZ6/12 polarizing battery and the voltage drop across the relays RLA and RLB. With an SZ6/12 power supply the voltages will drop by approximately 0.6 volts when the load of the polarizing coil is switched on, the precise voltage drop depending on the age, temperature and state of the battery and on the temperature of the polarizing coil. In the envent of a failure in the cycling of the polarizing supply the voltage across the relays would confirm whether the trouble was due to failure of the timer unit and relay energising coils or to some other cause.

It was not considered worth while to monitor the operation of the amplifier, as a failure here was much less likely and several possible failures could incidentally be diagnosed from the telemetered output signals of the amplifier, without the necessity for monitoring any voltages.

Since the modulator for the telemetry transmitter was designed to operate with input voltages within the range 0 to $+4\frac{1}{2}$V it was necessary to incorporate biassing batteries in the monitor leads. To prevent any interference picked up on these leads from being fed back into the amplifier, 70μF tantalum electrolytic capacitors were connected across the leads and fuses were incorporated in order that a short circuit occurring in the monitor leads should not immobilize the main instrument.

6.5 Mechanical Construction

Fig. 6.11 shows a complete electronics package with the lid removed and Fig. 6.12 shows a set of spare plug-in stages. The modules are rigidly clamped to the base plate and a strip of rubber lining on the clamps accommodates slight variations in the sizes of the boxes. For flight, locking screws ensure that the sockets cannot vibrate loose from the plugs. The "open" lay-out of the components permits ready access should any servicing be required and facilitates

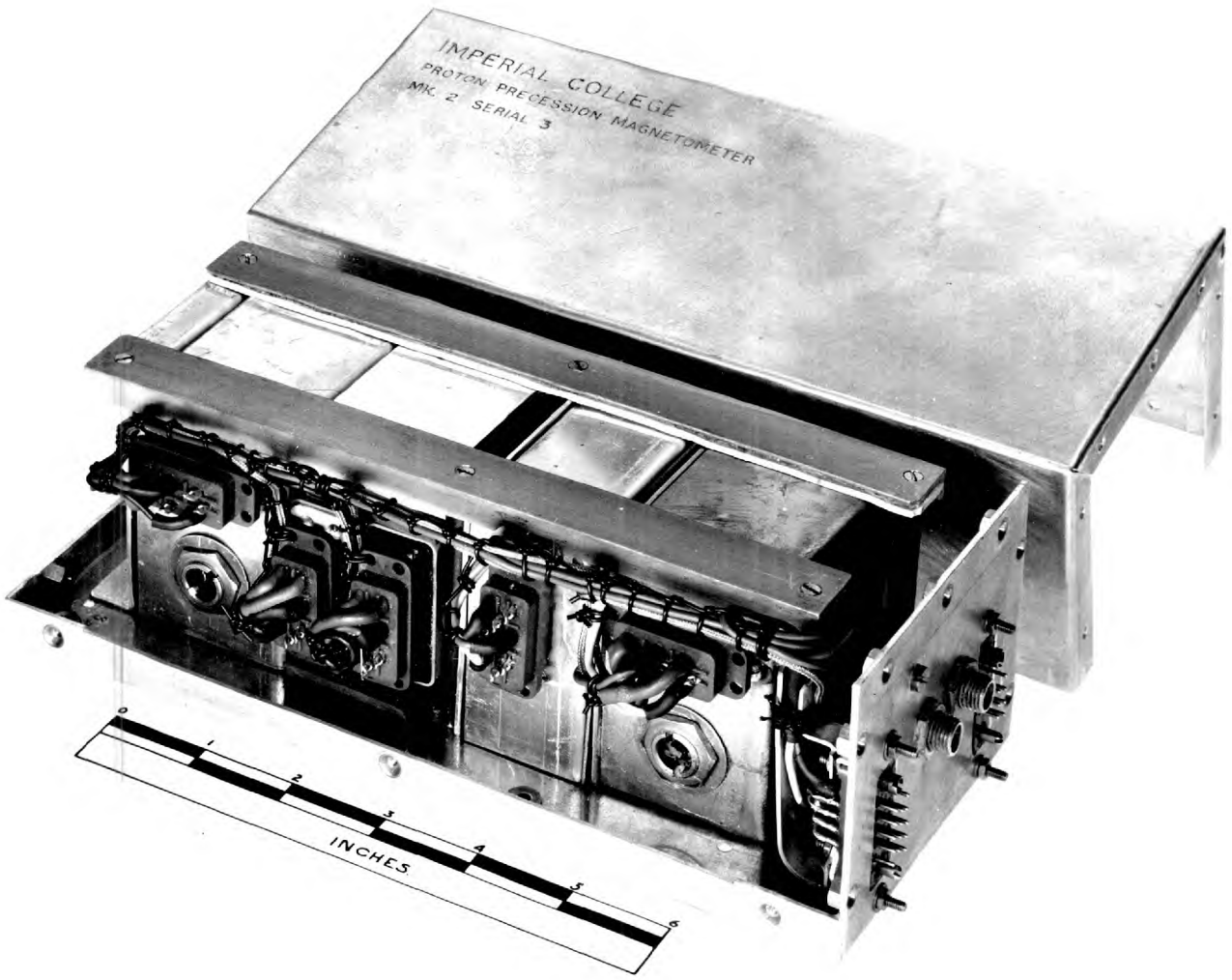


Fig. 6.11. The Proton Magnetometer Electronics Package.

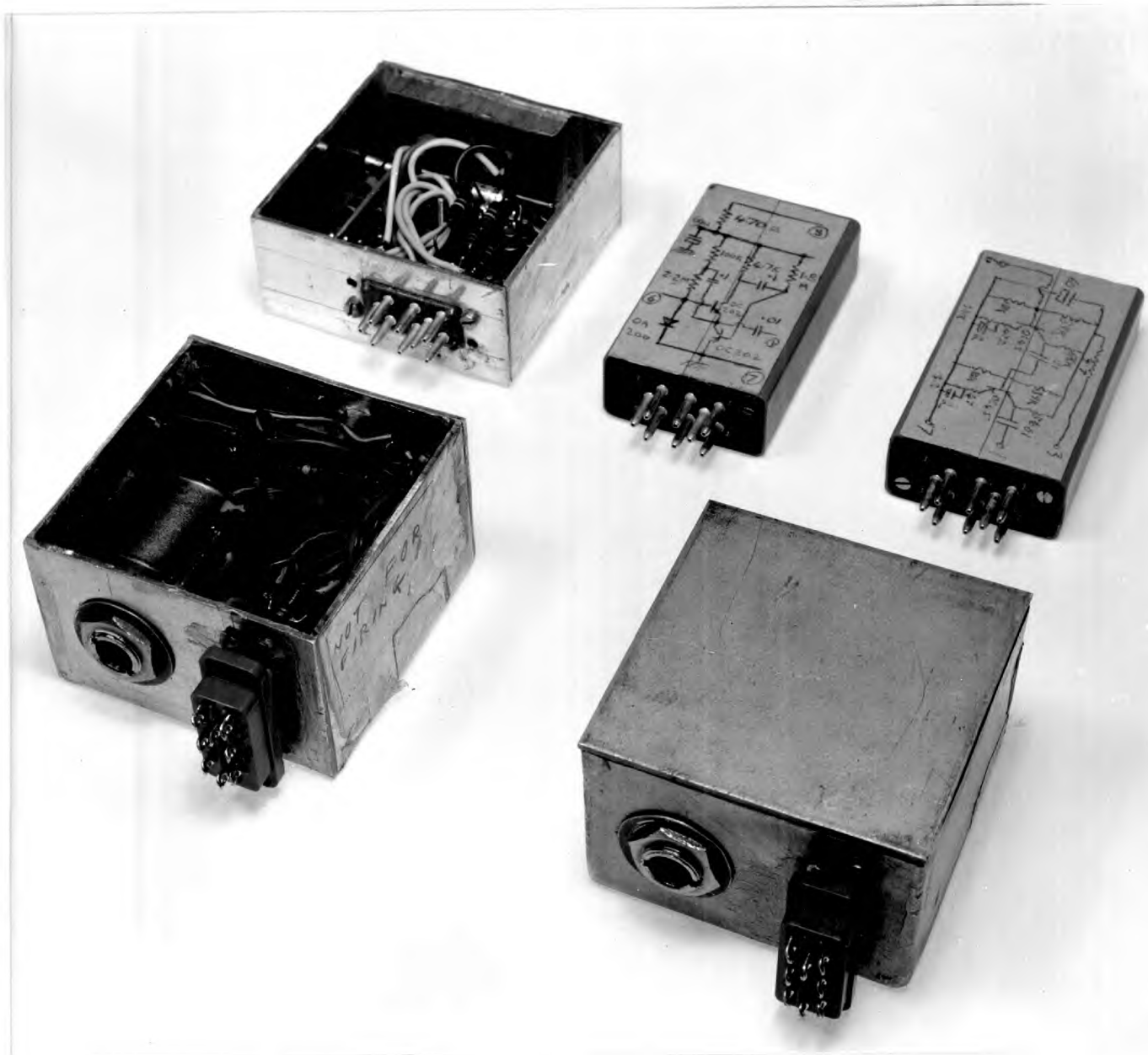


Fig. 6.12. Plug-in Stages.

the final adjustment of the two pot cores, under the correct working conditions prior to encapsulating the stages.

Negligible heat is developed in the transistor modules but the power dissipated in energising the two relays RLA and RLB causes a significant rise in the temperature of the relay unit. To keep this temperature rise within tolerance the relays are positioned in good thermal contact with the μ-metal box and the unit is clamped with the relays adjacent to the main chassis. As a further safe-guard the entire electronics package rests on a heat sink of $\frac{1}{4}$" thick duralumin and a plate of Tufnol is inserted between the relay unit and the timer unit. To reduce heat conduction from other rocket instrumentation into the magnetometer a sheet of rubber is inserted between the duralumin heat sink and the rocket bulkhead.

The complete instrument installed on a Skylark bulkhead ready for flight is shown in Fig. 6.13. Mounted on the lid of the electronics package can be seen the potted B1478 and Mallory biassing batteries and the "Ledex" switch. The lead-in cable from the sensing head is clamped to the nose cone struts.

6.6 Laboratory Testing and Evaluation

In order to test the flight equipment in the magnetic field it would experience during the actual rocket flight

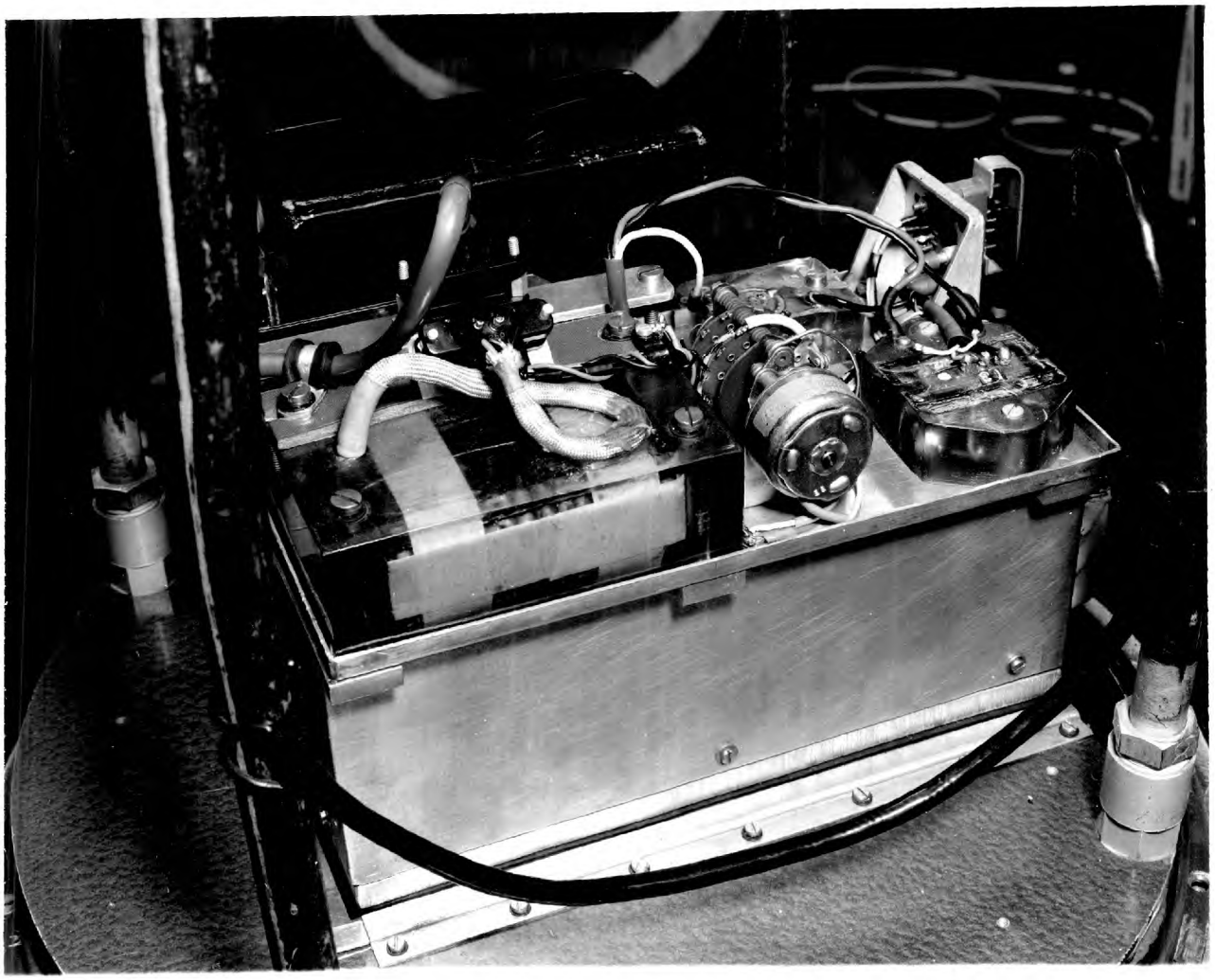


Fig. 6.13. The Electronics Package and Batteries installed in Skylark SL40.

a coil system was constructed according to the design of Rubens[23]. The space occupied by the set of five coils is 6 ft. cube and they produce a known magnetic field which is uniform to better than 0.1% within a cylinder 1.2 ft. in diameter and 2.7 ft. long. The sensing coil can be mounted in the centre of the coil system and can be rotated to any required value of θ, the angle between the coil axis and the magnetic vector. The axis of the coil system is arranged to be parallel to the Earth's magnetic field vector, and the entire installation is screened and protected from the weather by means of 20 S.W.G. Aluminium sheets. The field current through the coils can be controlled by means of a potentiometer with a 1000μ F capacitor across the terminals, to prevent noise from being induced into the search coil under test, as a result of changes in field current setting.

It has already been stated that the signal amplitude, from a single coil performing the dual role of polarizing and pick-up coil, will be a maximum when θ is 90° and will follow a sine-square law to zero when $\theta = 0°$. Fig. 6.14 shows actual records of the signal amplitude at various values of θ from 0° to 90°. In these experiments the field current through the field coils was adjusted to 100 mA, which corresponds roughly to a rocket altitude of 100 Km.

At this value of magnetic field the magnetometer can

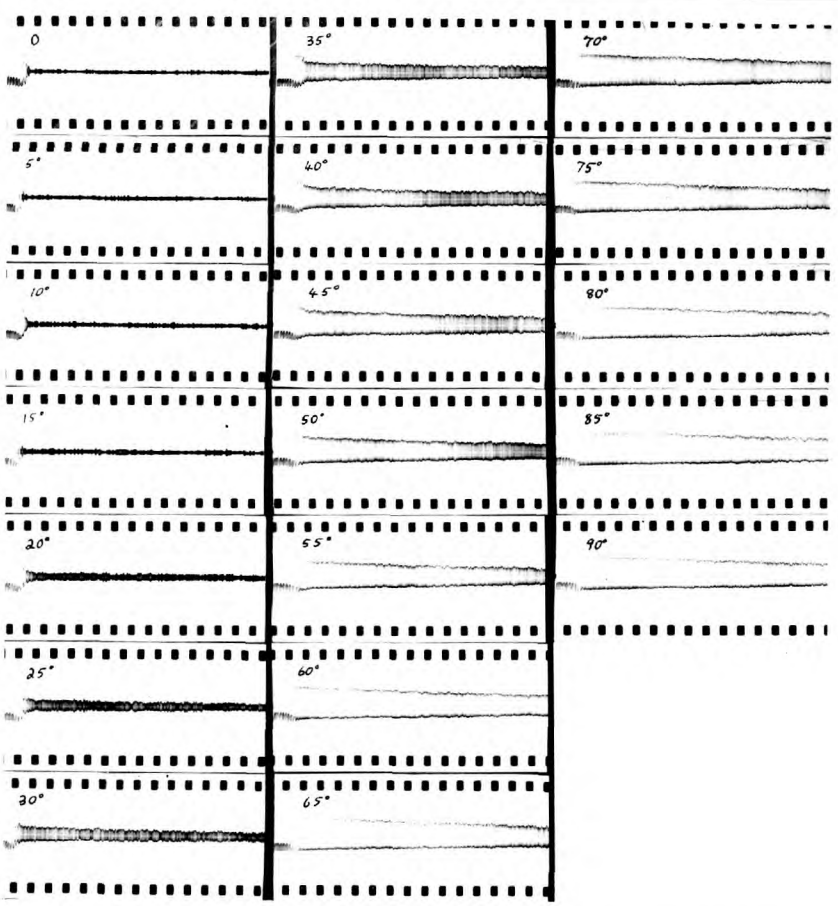


Fig. 6.14. Proton Precession Signals at Various Orientations of the Sensing Head.

be seen to produce a usable proton precession signal down to values of θ of approximately 25°, a range representing over 90% of all possible orientations.

The effect on the magnetometer of the high temperature environment during the rocket flight will be to reduce the signal amplitude slightly (see Ch. 5, Sec.4), to increase the noise in the system, to detune the three resonant circuits and to effect the polarizing and counting periods.

The way in which the signal/noise ratio is affected throughout the pass band is illustrated in Fig. 6.8. It will be observed that, as a result of the design features discussed above, the change in shape of the pass-band characteristic, in heating from room temperature to 60°C, is quite small. The elevated temperature does, however, result in a slight increase in the gain and the noise level of the amplifier, the final result being a slight degradation of the signal/noise ratio. The timing of the relay switching is constant to better than 0.1% with variations of temperature from room temperature up to 65°C, and with supply voltage variations within the range 15 - 18 volts.

The way in which the signal can be expected to change with field variations during the flight is illustrated in Fig. 6.15 which shows records of actual proton precession signals recorded with values of current through the field coils adjusted within the range 70 mA - 155 mA. The corresponding values of precession frequency are shown in parentheses.

The equipment was subjected to the same mechanical environmental tests as described in Chapter 5 for the double channel version. Fig. 6.16 shows a sample x-ray shadow graph of the sensing head. A section in the potting of lower density than the Araldite can clearly be

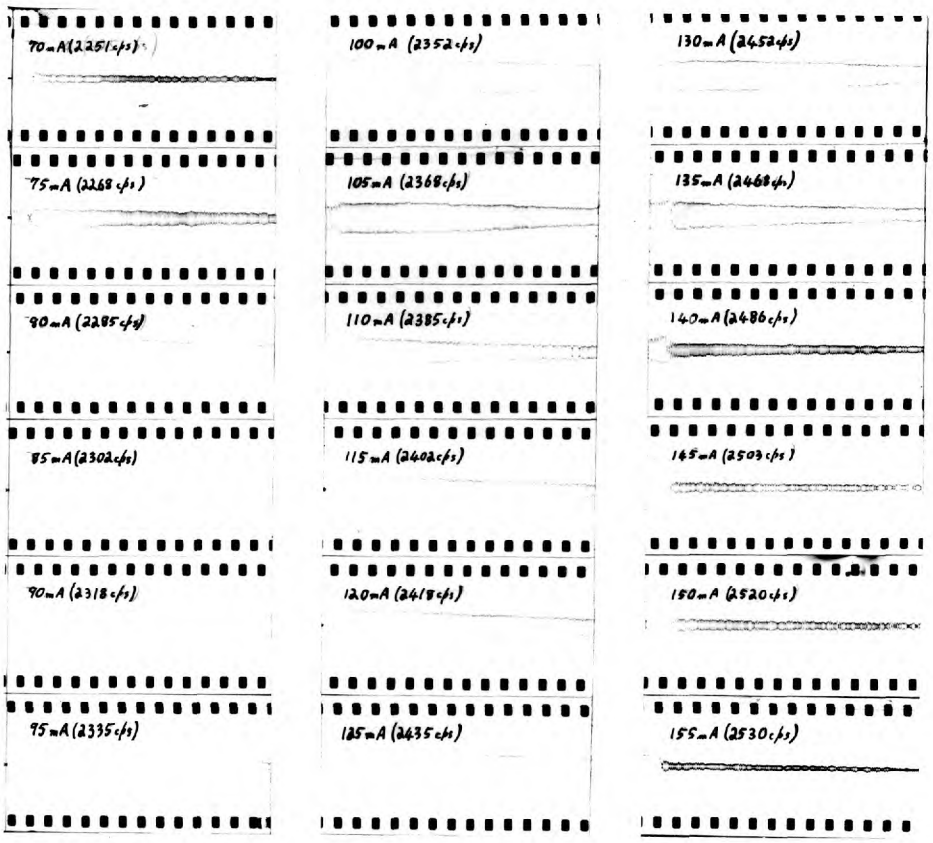


Fig. 6.15. Proton Precession Signals at Various Values of Magnetic Field Intensity.

seen near the platform. This could be a bubble of trapped air or a small quantity of paraffin which has leaked out of the coil as a result of the mechanical and thermal stresses during the curing process.

In view of the results in this test, a loading test, equivalent to a lateral acceleration of 10g, was carried out, by the R.A.E., on the sensing head. Since it survived this test it was considered adequately strong in spite of the flaw in manufacture.

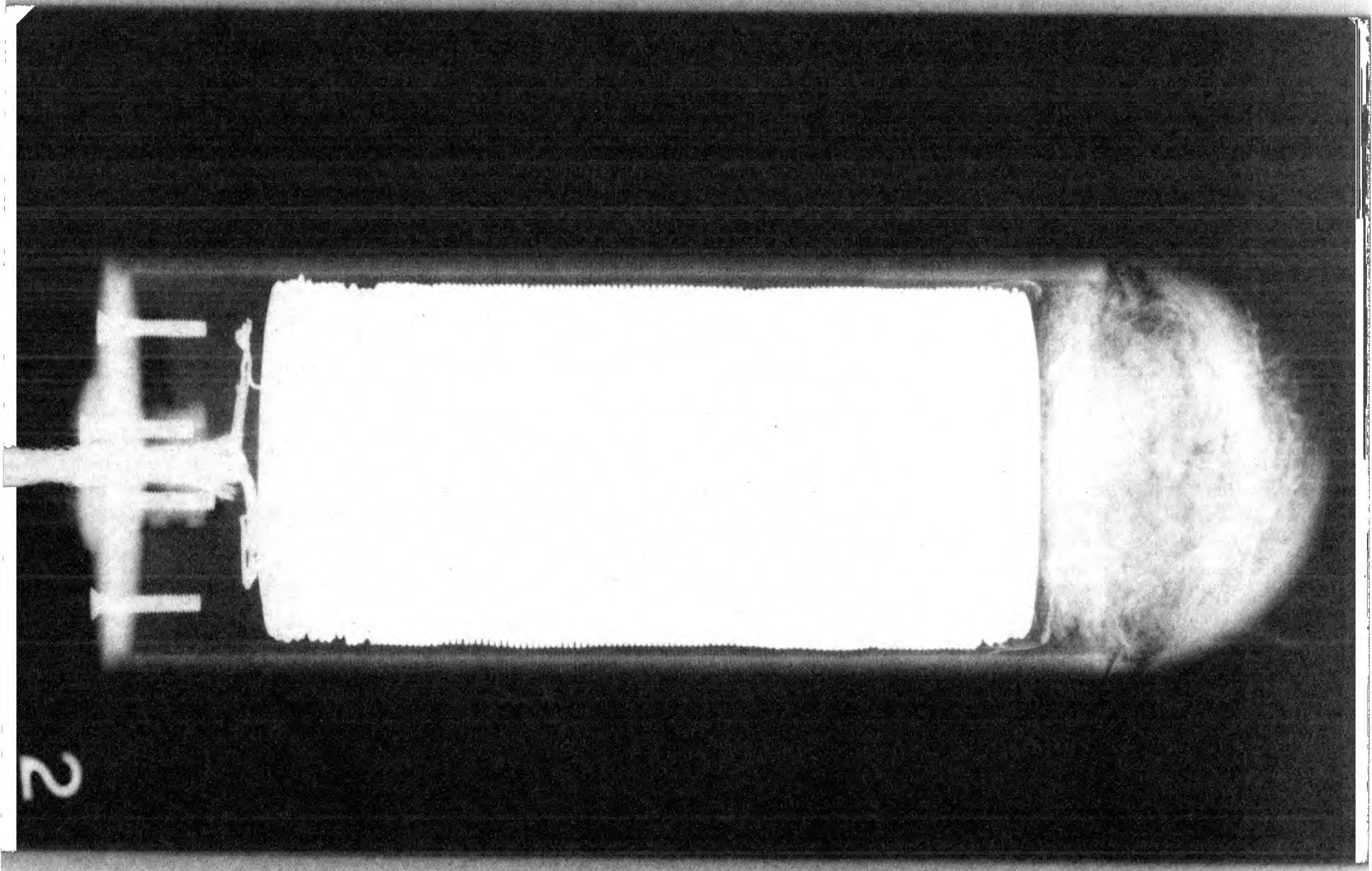


Fig. 6.16. X-RAY OF SENSING HEAD.

6.7 Compatibility Tests

In view of the time schedule involved it was not possible to carry out any interference tests on the complete refurbished rocket, with the modified proton magnetometer, before it was transported out to Australia.

A short test was, however, possible at the Weapons Research Establishment, Salisbury, just before the rocket was air-freighted to Woomera for firing. This test is shown in progress in Fig. 6.17. After a "run-up" the battery connectors were extracted and the demodulated telemetry output was monitored in the laboratory seen in the background. Unfortunately this test was abortive as a result of instability due to the R.F. energy being reflected into the sensing head from the steel trolley on which the rocket is standing.

The test illustrated in Fig. 6.17 was repeated at Woomera but this time the rocket was positioned horizontally with its axis East-West, on a wooden trolley. Under these circumstances a satisfactory record was obtained of a precession signal under near-realistic conditions, which confirmed (for the first time) that the modifications to the rocket-borne magnetometer had been effective in rejecting the interference.

It had originally been the intention to carry out a



Fig. 6.17. The Instrumented Head of Skylark SL40 being tested at the W.R.E.

series of magnetic "swings" on the complete rocket head assembly in order to investigate and, if necessary, to compensate for its induced and permanent magnetic fields. For this purpose a non-magnetic wooden rotatable frame was designed and constructed by the W.R.E. Unfortunately, as a result of the time schedule for the firing, these measurements were not possible and the rocket was fired without any knowledge of its magnetic properties beyond that obtained from the measurements carried out three years previously (Ch. 2. Sec. 2.).

CHAPTER 7

AUXILLIARY EQUIPMENT

7.1 Ground Recording Magnetometer

i. Double Channel Installation.

A geomagnetic survey involves the correlation of measurements taken by one instrument at different times and at different places. When the purpose of the survey is to measure the space-dependent changes in magnetic field, it is essential to allow for the time-dependent magnetic variations occurring in the survey area during the appropriate period, and for this purpose at least one stationary recording instrument is normally operated at a site as close as possible to the survey area. In the present application it is also desirable to record the diurnal variation for the day of the rocket flight for comparison with the flight data.

In view of the fact that very small variations in the rocket data are likely to be significant (Ch.2, Sec.1), it was considered advantageous to record the diurnal variations at two sites, one near the launcher and one at a point close to the impact area, in order, if necessary, that some allowance could be made for second order changes.

The use of a pair of land lines between the launcher area and the proposed site for the second instrument (at the H5 post, approximately 70 miles down the range) was arranged, with the proviso that all frequencies on the line should be contained within the bandwidth 0 - 320 c.p.s. The use of a land line to interrogate a remote magnetometer and to convey the information back to a central point offers the following advantages over the alternative of two independent recording instruments positioned at the two sites.

a). The two sets of data can be recorded on the same piece of chart paper for ease of comparison.

b). The timing and operation of both stations can be controlled and monitored by one man. This is particularly important during the "count down" when the reading repetition rate of each station has to be adjusted and time marks annotated.

c). The data from both head units can be processed and recorded by a single common system with consequent saving of cost and building effort.

d). The power saving at the remote station would enable the instrument to run continuously for longer periods without changing batteries.

A block diagram of the arrangement which was proposed is shown in Fig. 7.1 in which the facilities to be provided by the W.R.E. are shown in the dotted rectangle.

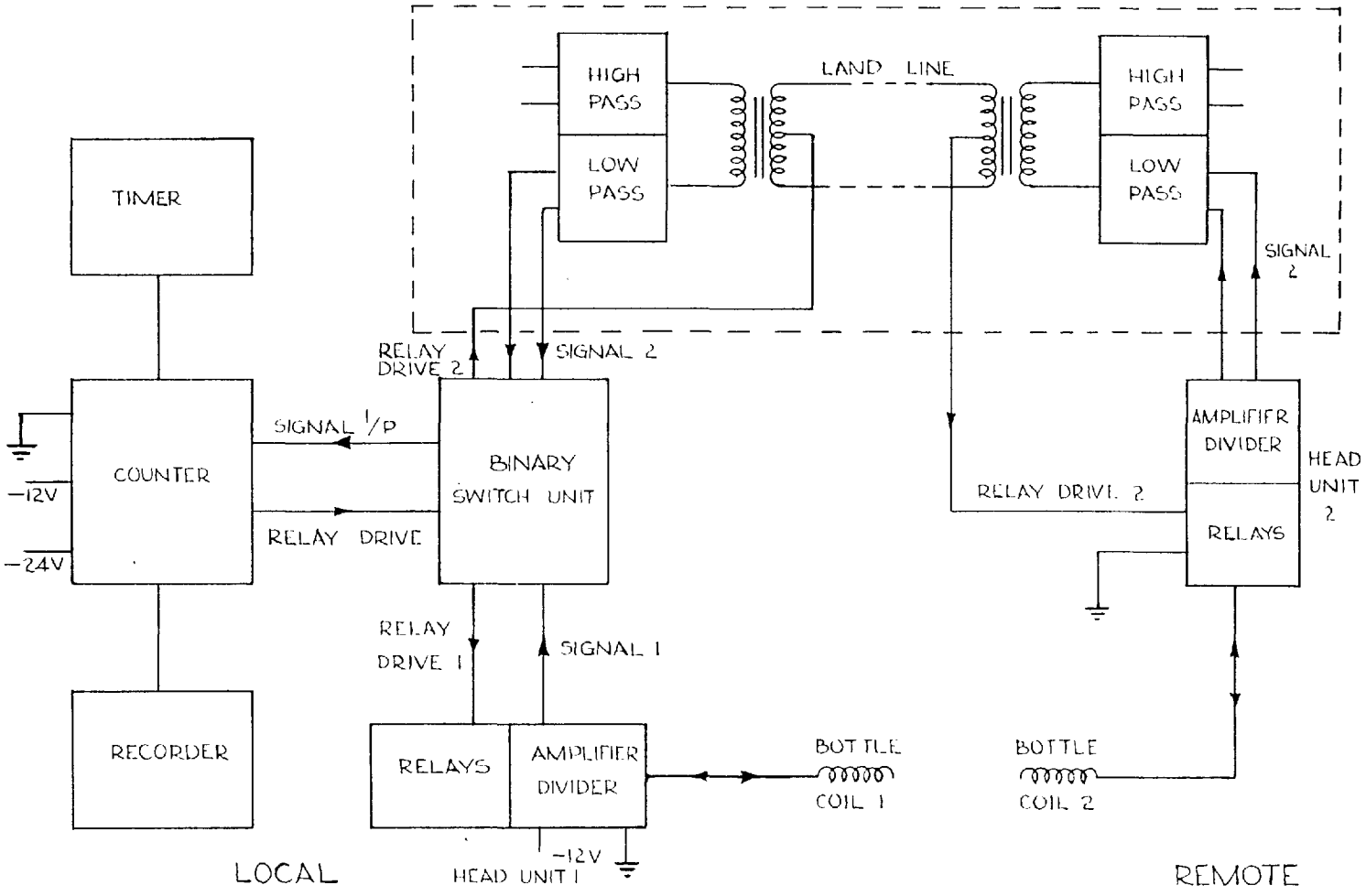


FIG. 7.1. BLOCK DIAGRAM OF A TWO CHANNEL GROUND MAGNETOMETER INSTALLATION

Each station consists of the bottle and sensing coil, a switching system, a tuned amplifier and three Eccles-Jordon binary circuits to divide down the precession signal to a frequency within the specified pass band. The timing and switching of both sets of relays is controlled by a single timer and the divided down signal from each head unit is counted and recorded. The binary switch unit (Fig. 7.2)

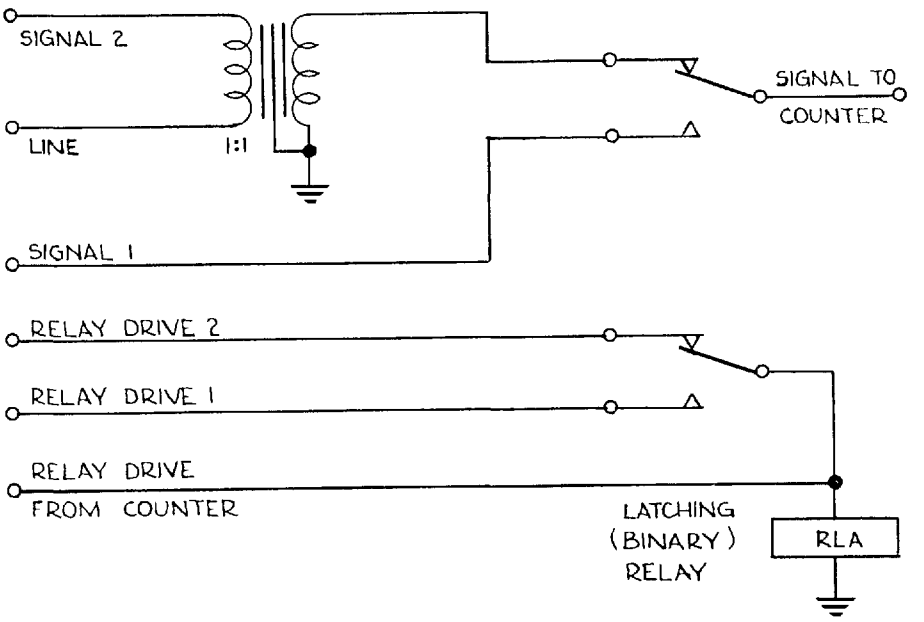


FIG. 7.2. BINARY SWITCH UNIT

selects each head unit in turn and also provides the balance-to-unbalance transformation necessary to match the counter circuits into the line. A similar balance-to-unbalance transformer is incorporated in the head unit

which was intended for use at the remote station.

Unfortunately the decision to provide land lines for this purpose was later reversed and, accordingly, only one of the head units which had been constructed could be used.

ii. Single channel installation.

The single channel instrument which was operated during the flight of Skylark SL40 consists of the timer, counter, recorder, head unit No.1 and bottle/coil No. 1 (Fig. 7.1).

iii. The sensing head.

In the consideration of the design of the sensing head the size and weight now assume secondary importance, as compared with the rocket-borne and portable versions discussed previously, and accordingly they were both increased in order to improve the signal/noise ratio of the system. A photograph of the sensing head is shown as mounted in a paddock at the Woomera range-head in Fig. 7.3. The water sample is contained in a polythene bottle, 2½" x 5" and the coil consists of four segments, each of 400 turns of 20 S.W.G. enamelled copper wire. The segmentation of the coil considerably reduces its self-capacity, thereby maintaining the rapid switch-off of the polarizing current. A further precaution to achieve a low self capacity was the interleaving of each layer of turns.

In order to prevent the water sample from freezing,



Fig. 7.3. The Sensing Head.

during operation in an English winter, 20% by volume of commercial "Anti-freeze" was added to it. It was found that this precaution did not appreciably affect either the amplitude or decay time constant of the precession signal.

The size of the complete sensing head is $4\frac{3}{4}$" x $5\frac{1}{2}$", its weight $10\frac{1}{2}$ lbs, its inductance 186 mH and its resistance 15 ohms.

iv. The Head Unit.

A block diagram of the head unit is shown in Fig. 7.4.

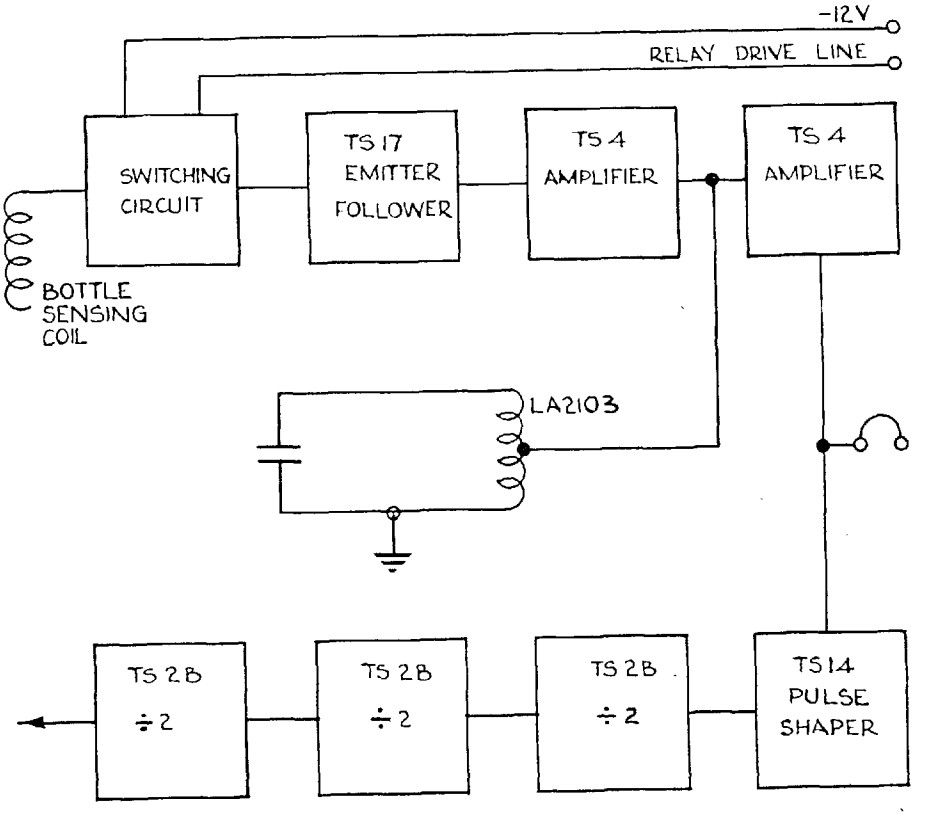


FIG. 7.4. SIMPLIFIED BLOCK DIAGRAM OF HEAD UNITS

and a photograph, also taken at Woomera, in Fig. 7.5. The electronic circuit elements are transistorized plug-in stages manufactured by Venner Electronics Ltd.

Two switching circuits were compared for use with the recording magnetometer and are shown in Fig. 7.6 . The operation of the two circuits is self explanatory though there are certain important differences. It has already been stressed that it is essential to remove the polarizing field before the pick-up coil is connected to its tuning capacitor. Circuit A achieves this delay by arranging that RLA should control RLB, thus contacts RLA1 must break the polarizing current before RLB changes over; in circuit B the delay is the result of the longer time constant formed by C2 and RLB, as compared with C3 and RLA. On the other hand, when the circuits are energised, RLB in circuit B closes first, since C2 is open circuit at this time; this has the advantage that the input to the amplifier is earthed before any large currents are switched and this reduces the risk of damage to the first transistor in the amplifier. It was also found that the unwanted transient oscillations on switching OFF were of lower amplitude and shorter duration with circuit B. In addition to protecting the amplifier this also reduces the risk of a pulse from this transient triggering any of the counters and thereby producing a spurious reading. Furthermore the amplitude of signals using

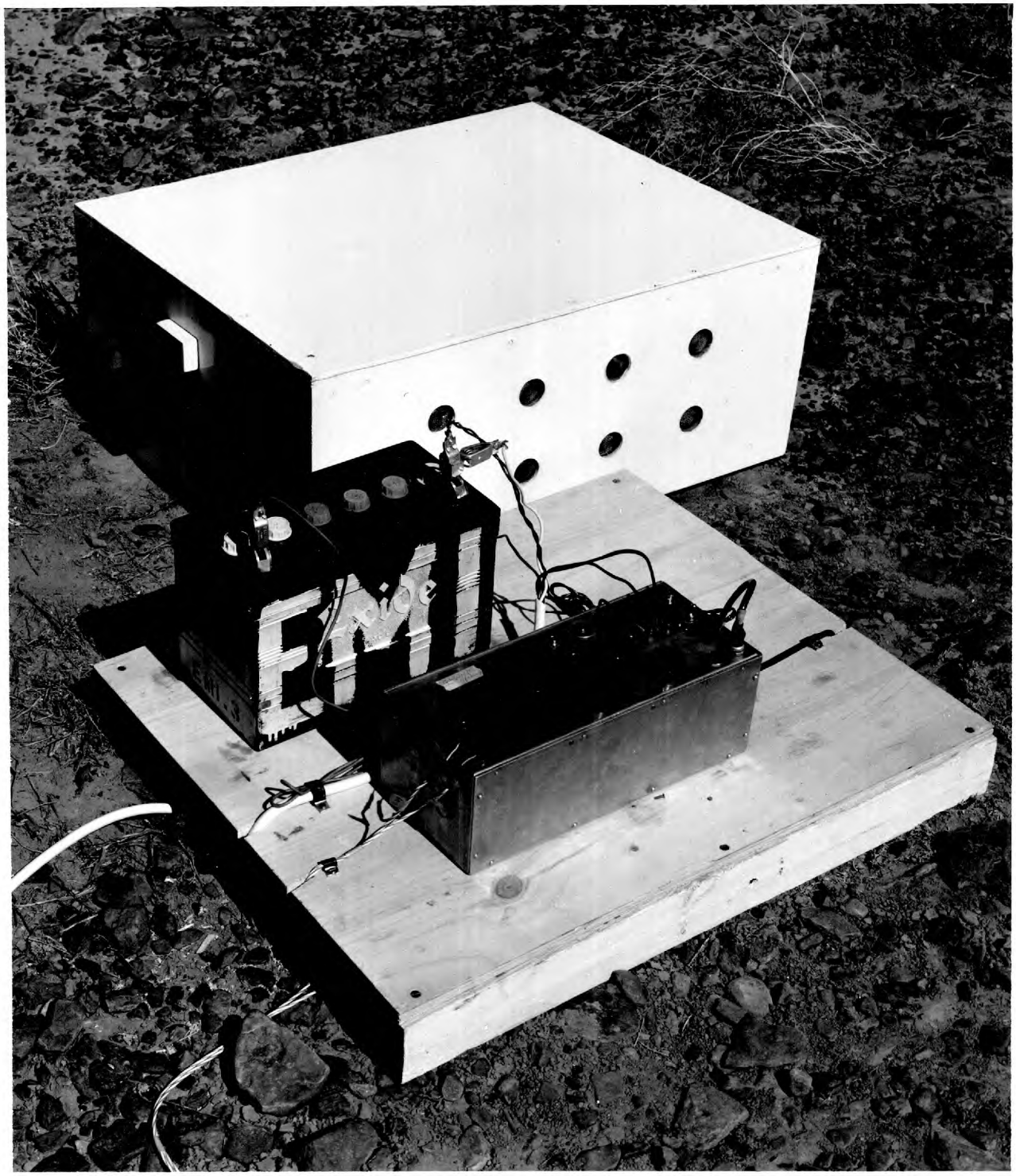


Fig. 7.5. Recording Magnetometer Head Unit.

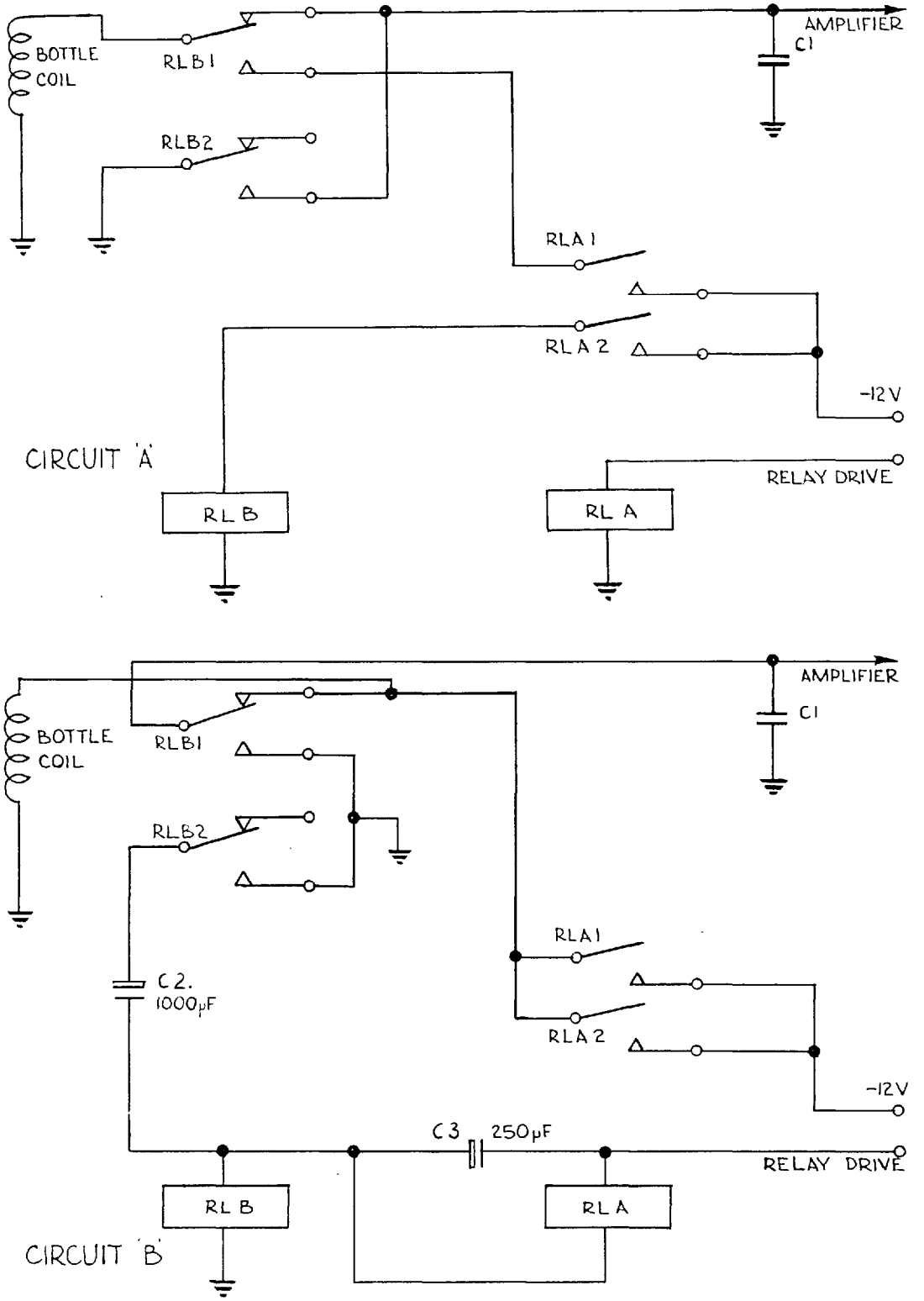


FIG. 7.6. RECORDING MAGNETOMETER, SWITCHING CIRCUITS

circuit B, whilst tending to be lower than those using circuit A, was somewhat more consistent. A further advantage of circuit B is that two pairs of contacts are used in parallel to switch the 0.8 amps polarizing current, as opposed to only one in circuit A; this will result in longer relay life. With these considerations in mind circuit B was used in the construction of the head units, in spite of the slightly larger signal from circuit A. Recordings of typical signals using each circuit are shown in Fig. 7.7

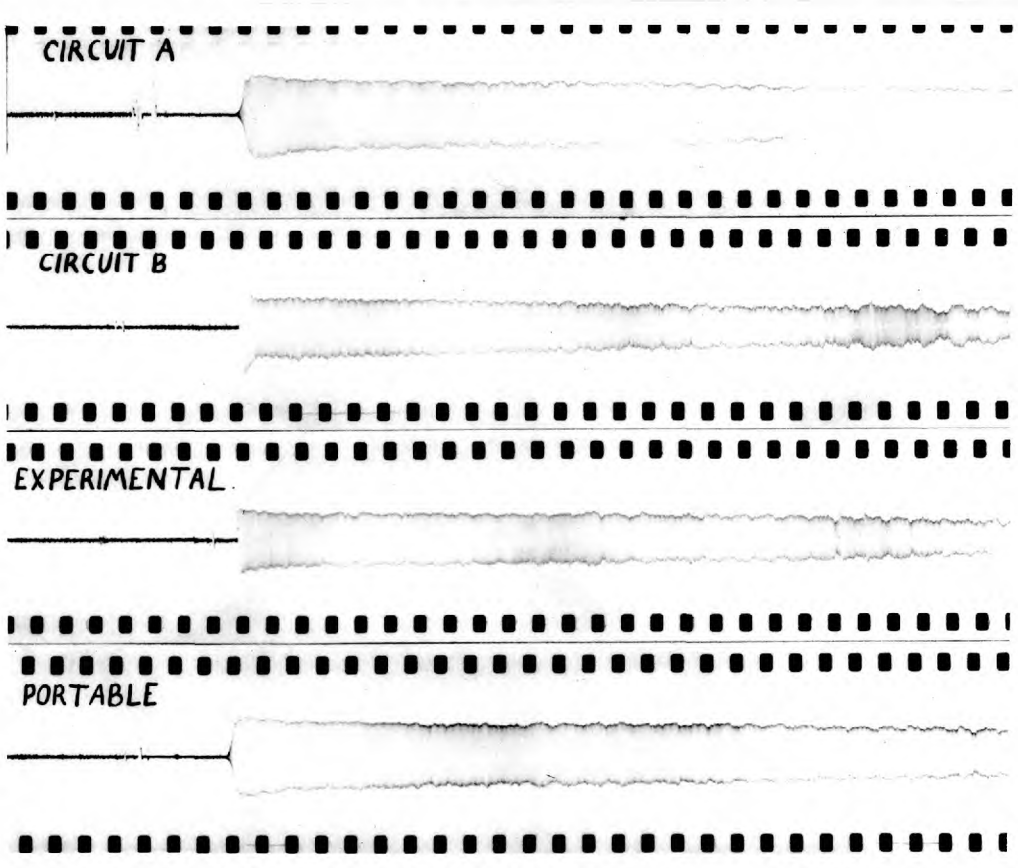


Fig. 7.7. Proton Precession Signals obtained from Various Designs of Switching Circuit.

Since the signal from the much larger coil of the recording magnetometer saturates the amplifier, the portable magnetometer sensing head (Ch. 3) was used in these comparative tests. For completeness, specimen records, taken under identical conditions, from the experimental circuit of Fig. 2.6 and from the portable magnetometer circuit of Fig. 3.3 are also presented in Fig. 7.7.

v. Frequency Measurement.

The frequency of the precession signal is counted electronically by a similar technique to that described in connection with the portable magnetometer (Fig. 3.2). The counter unit was manufactured by Venner Electronics Ltd., and will not be described in detail. The last two digits of the count are combined into a 100-step staircase waveform which is specified to be linear to within $\pm 0.5\%$ over the entire range and in ambient temperatures up to 50°C. This output is applied to a "Record" 0/250 microamperes pen recorder which has readily adjustable chart speeds of 1 inch and 6 inches per hour. The full scale of the chart paper therefore corresponds to 94 gammas in England and 143 gammas in Australia.

vi. Sequence Timing.

The timing of the instrument is controlled by a Venner time-switch, which is normally set to take one

reading every 5 mins. For more rapid readings an electronic timer was built using Venner plug-in stages. The wiring diagram is shown in Fig. 7.8. The two timer units type

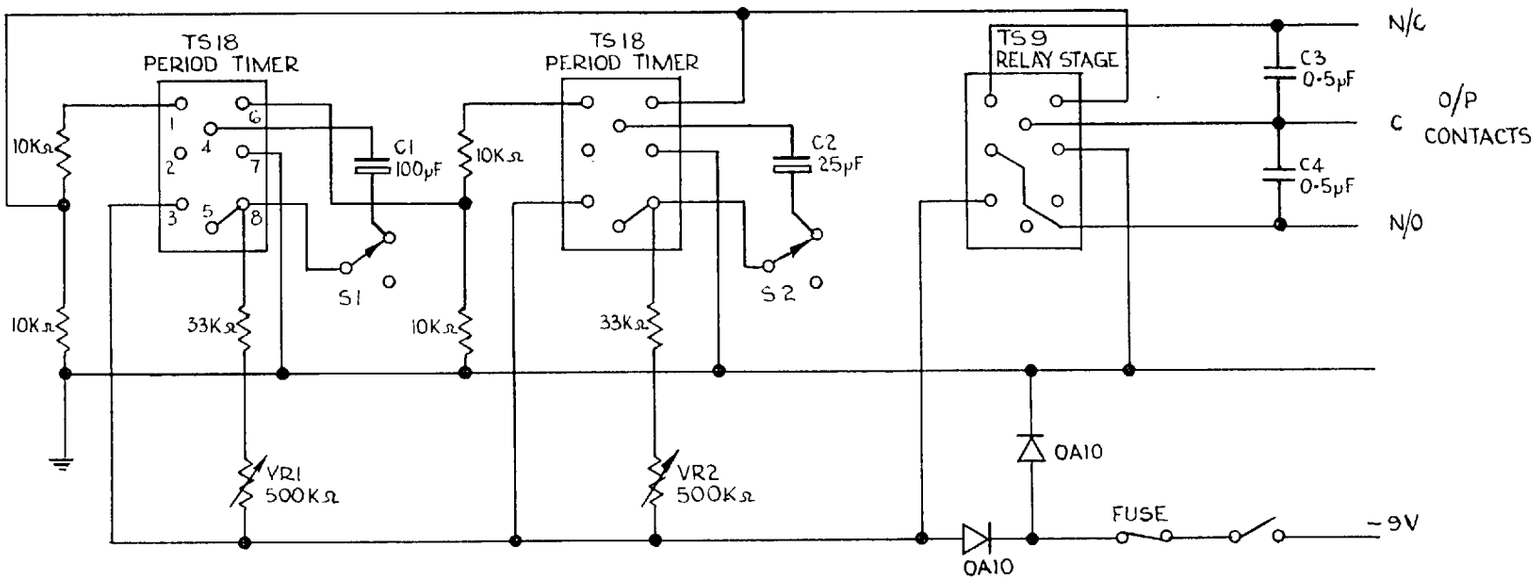


FIG. 7.8. CIRCUIT OF RE-CYCLING TIMER

TS18 consist essentially of flip-flop circuits with emitter follower output stages and they are arranged to cycle each other alternately. The output of step-waveform timing pulses is fed to the TS9, which consists of a Schmitt trigger circuit controlling an emitter follower, which

operates the relay. S1 and S2 provide a coarse control on the timing periods and VR1 and VR2 the fine control. The polarizing period can be continuously adjusted from 0.4 sec. to 20 sec. and the recording period can be varied from 0.4 seconds to 40 seconds. The two diodes in the power supply ensure that the fuse will blow in the event of the supply being connected in the wrong polarity.

Fig. 7.9 shows the complete equipment, as installed in test shop No. 7 at Woomera. From left to right the units are: 12V stabilized power pack; Venner counter unit; electronic timer; Venner time switch; Record recorder, high speed recorder; amplifier for high speed recorder and (on refrigerator) trickle charger to charge the battery powering the head unit.

The sequence of operation for each measurement is as follows.

a). When the contacts in either timer close, a relay (RLA) is operated and a flip-flop is triggered into its unstable state. The flip-flop drives a second relay (RLB) which resets the counters and switches the 12V relay drive supply down the line to operate the relays in the head unit. The relay RLA open circuits the output of the counter to the recorder.

b). The polarizing period is adjustable within the range

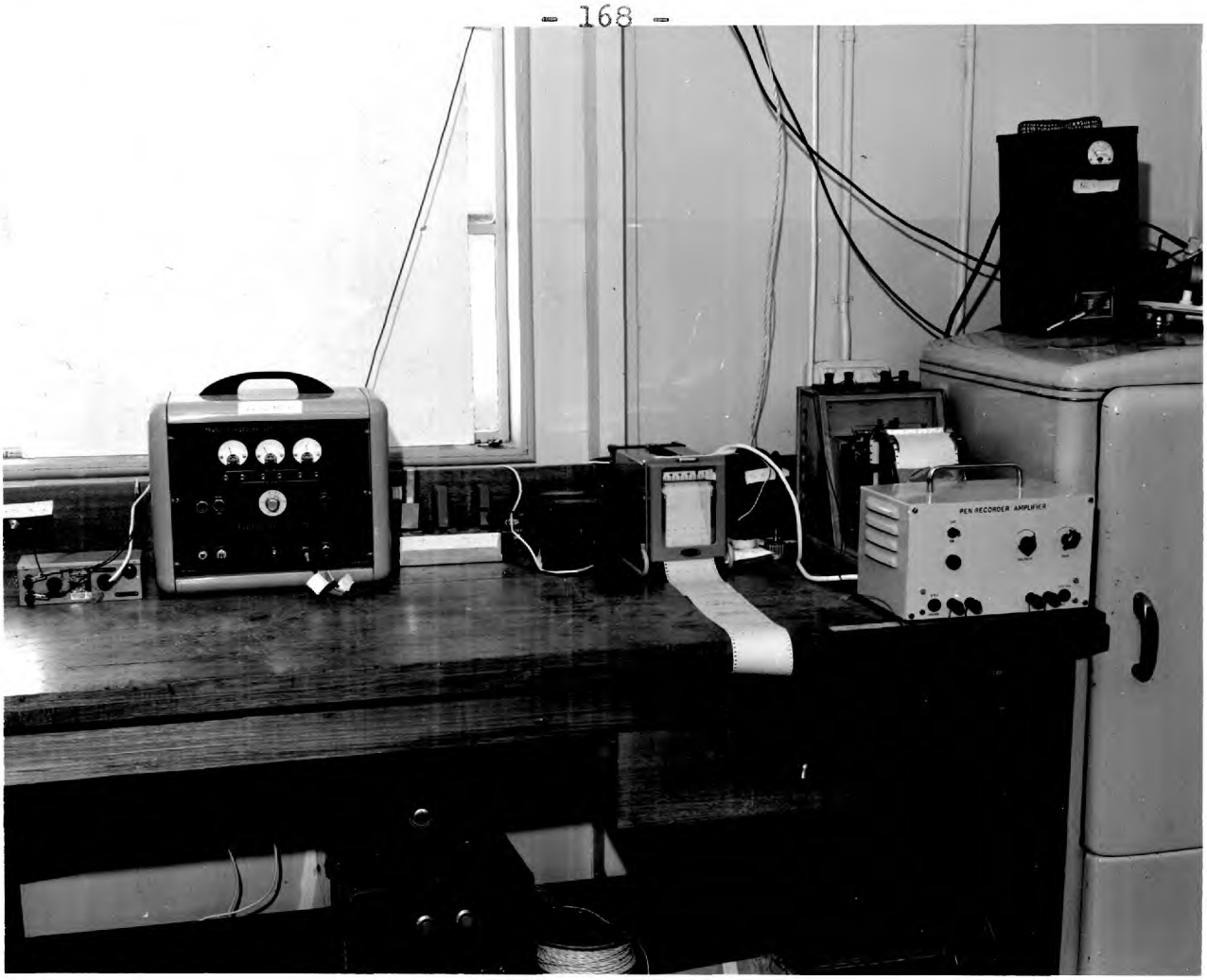


Fig. 7.9. The Recording Magnetometer Installation at Woomera.

1 - 10 seconds but is normally set at 3 seconds. At the end of this period the flip-flop changes into its stable state de-energising RLB. The precession signal is now counted in the way described previously, the last three digits being displayed on the meters.

c). When the clock, or timer, contacts open, RLA is de-energised and the current analogue of the combined last two digits is passed through the recorder. The use of RLA prevents the recorder from following the mid-scale value of the meters during the counting period. The instrument can also be used with a potentiometer recorder, in which case RLA can also be used to open circuit the motor during the polarizing and counting period. The pen therefore stays on the previous reading rather than returning to zero during this period.

Two specimen records, taken at chart speeds of 1 inch per hour (one reading every five minutes) and 6 inches per hour (one reading per 10 seconds) are shown in Fig. 7.10.

7.2 Test Oscillator

It has already been stated that magnetic field gradients in the vicinity of the launcher will prevent the detection of a coherent precession signal. In order to ensure, as far as possible, that the rocket borne magnetometer is serviceable during the count-down (in

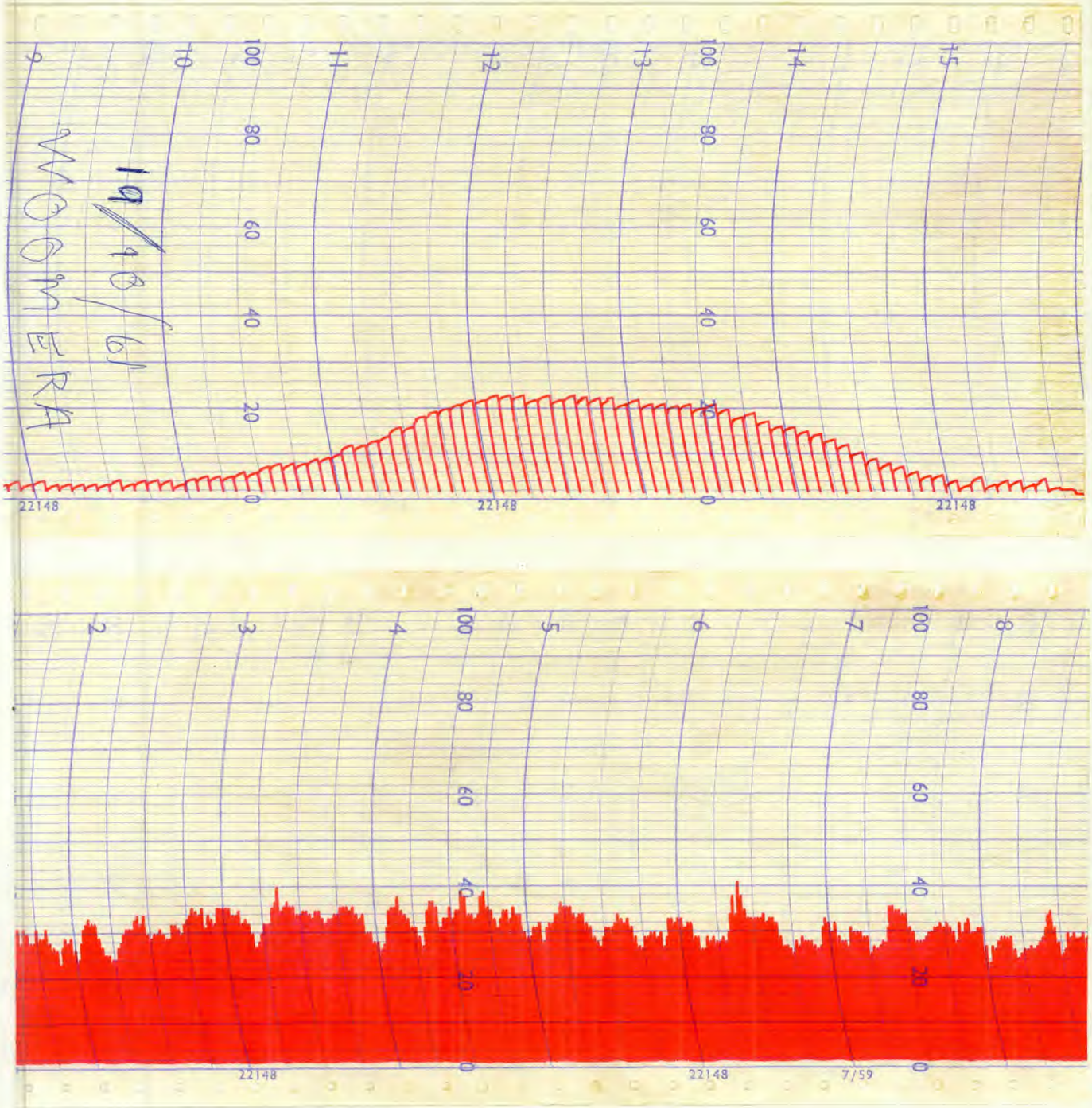


Fig. 7.10. Typical records from the Ground Recording Magnetometer.
Upper Record: One inch per hour. Full scale deflection = 143 gamma.
Lower Record: Six inches per hour. Full scale deflection = 94 gamma.

particular to ensure continuity of the data channel between the sensing head and the input to the amplifier), a small battery operated oscillator was built (Fig. 7.11).

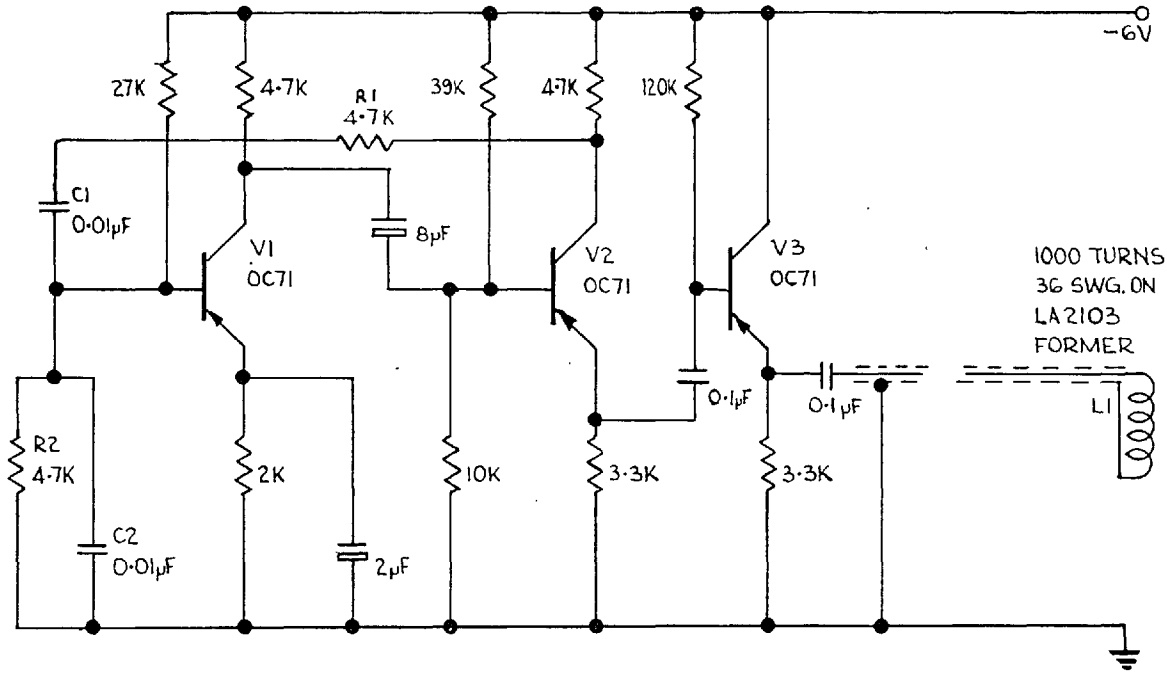


FIG. 7.11. TEST OSCILLATOR

V1 and V2 oscillate at a frequency (determined by R1, R2, C1 and C2) of 2.4 Kc.p.s. and the emitter follower, V3, buffers the load of the coil, L1, from the oscillator section. Within the temperature range 15 - 60°C the frequency of the oscillator drifts at the rate of approximately 0.5 c.p.s. per °C; it is, therefore, unsuitable as a

standard frequency source and it cannot be used to calibrate the amplifier gain accurately. This order of stability is, however, quite adequate for a"GO-NO-GO" test of the type envisaged.

The entire instrument, including battery is contained in an aluminium box 4" x 4" x 1". During the flight of SL40 the coil, L1, was attached to the launcher, in a position 3 ft. horizontally from the rocket sensing head and with its axis parallel to that of the rocket. The oscillator was sited in an under-ground room near the launcher.

7.3 Standard Reference Frequency Source

It has already been stated that a convenient manual technique for measuring the frequency of the precession signal is to beat the unknown frequency with a standard reference signal. This could be done during the flight of the rocket but is preferably left until a later time, in which case the reference frequency must be derived from the same tape as the signal in order that fluctuations in play-back speed should, to be a first order, have an equal effect on each of the two frequencies. It is normal practice to record accurate timing and frequency standards concurrently with information channels during each Skylark trial. When the magnetometer experiment was first conceived this standard frequency was 100 Kc.p.s. but was later changed

to 50 Kc.p.s.; accordingly the circuit of Fig. 7.12 was built

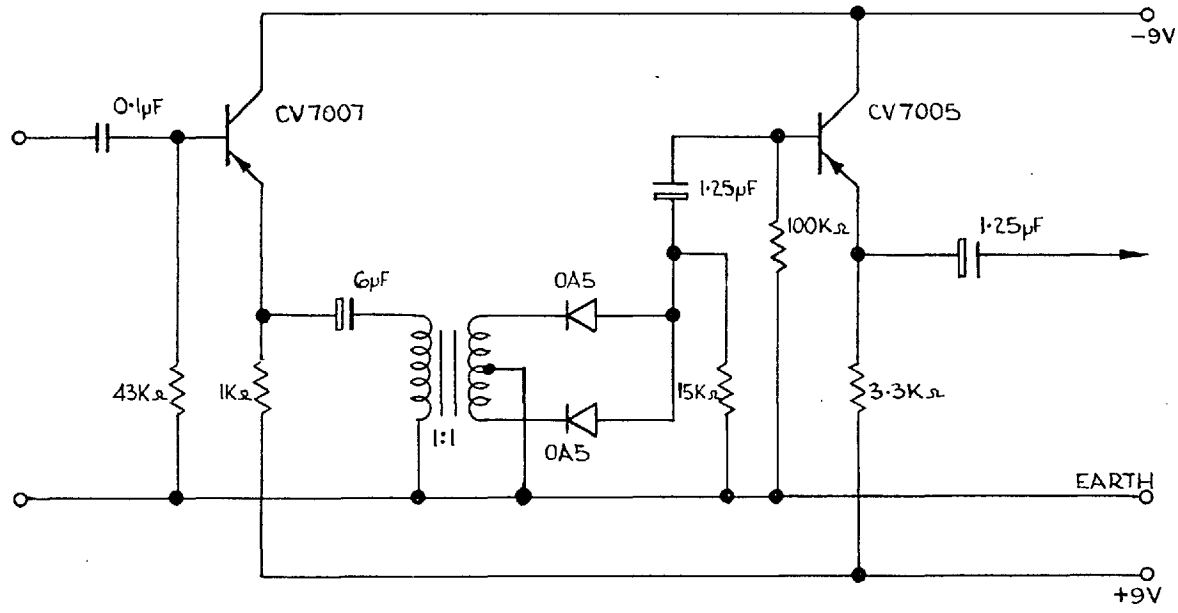


FIG. 7.12. CIRCUIT OF FREQUENCY DOUBLER

to double the 50 Kc.p.s. input and recover the original 100 Kc.p.s. In order to derive a suitable signal for beating with the precession frequency it is now necessary to divide the 100 Kc.p.s. by a factor of between 40 and 44, depending on the precise value of precession frequency. Dividing the standard frequency by 40, 41, 42, 43 and 44 gives reference frequencies of 2500.00, 2439.02, 2380.95, 2325.58 and 2272.73 c.p.s. respectively, and the difference between any two adjacent frequencies does not exceed 60.98 c.p.s.

Thus for any given precession frequency a standard reference frequency can be derived which will not differ from it by more than approximately 30 c.p.s. and the actual frequency measuring operation, during a half second period, will never involve the manual counting of more than 15 beats.

A transistorized divider capable of dividing any repetitive input waveform, of a frequency between random pulses and 100 Kc.p.s., by any whole number between 1 and 99 was obtained for this purpose. As it was designed and produced by Venner Electronics Ltd., it will not be described here.

7.4 Filter/Mixer Unit

The complete circuit diagram of this instrument is shown in Fig. 7.13 and a photograph of the chassis is shown in Fig. 7.14. The circuitry is designed to fulfill the following important requirements in the data handling process.

i. Shaping of the reference frequency waveform. The output of the 0 - 99 divider unit, mentioned above, is in the form of pulses, whose mark/space ratio varies with the division factor. In order to produce a pure sine wave, of frequency equal to that of the pulses, it is necessary to reject all higher harmonics. This is done by V1.

ii. Filtering of telemetered proton magnetometer data.

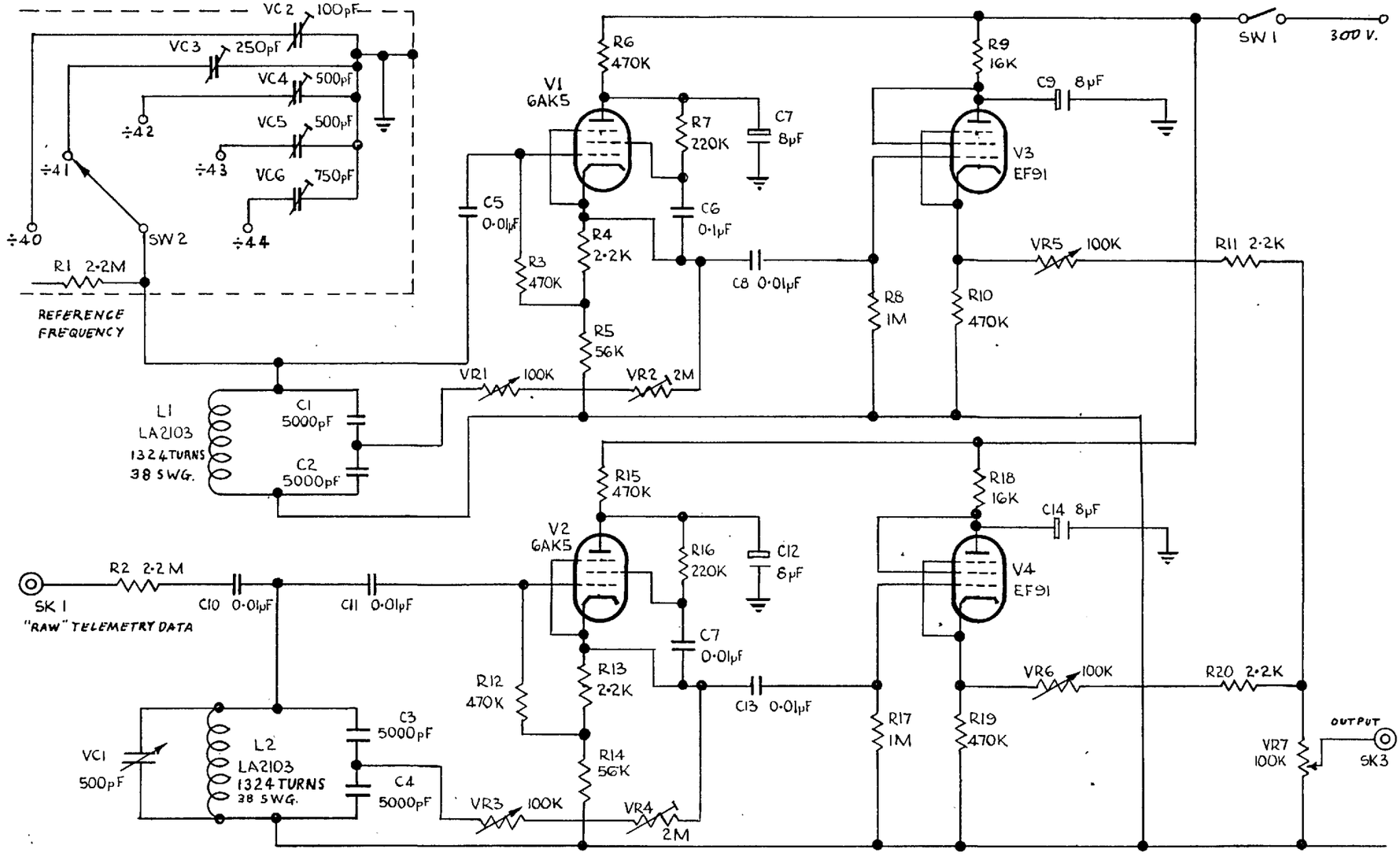


FIG. 7.13. CIRCUIT DIAGRAM OF FILTER CIRCUITS AND MIXER

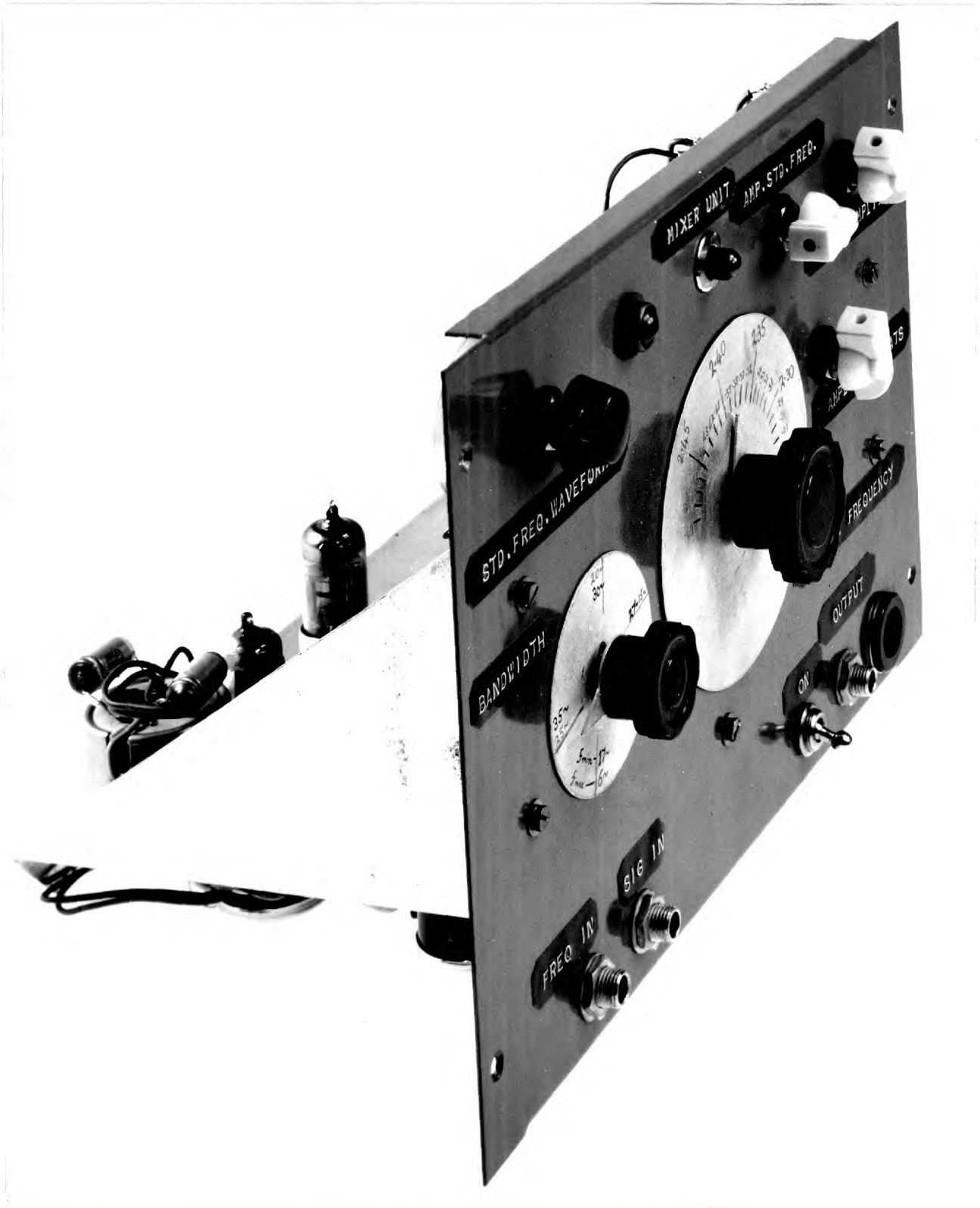


Fig. 7.14. The Filter/Mixer Unit.

Since the noise spectrum of the data from the rocket-borne proton magnetometer occupies a bandwidth of approximately 200 c.p.s. a considerable improvement in the quality of data can be achieved by reducing the bandwidth during play-back. Theoretically the signal/noise ratio should be improved by an approximate factor of $(200/B)^{\frac{1}{2}}$ where B is the 3db bandwidth of the data processing system, though there are certain practical considerations which limit the improvement attainable by this technique, as will be discussed later. This operation is performed by V2.

iii. Formation of "Beats". In order to measure the frequency difference between the sine waves, derived above, it is necessary to mix them and to obtain beats of a suitable frequency for manual counting. This is done simply by the resistance network in the cathode circuits of V3 and V4.

Each circuit associated with valves V1 and V2 works on the well known principle that positive feed-back from an active network can be used to compensate for the energy lost in the resistance of a resonant circuit, thereby increasing its Q. The effective Q multiplication can be adjusted continuously from 1 to infinity by varying the feedback factor. In the present case the valves are wired as cathode followers and the feedback is applied to the centre-taps of the resonant circuit tuning capacitors; thus the low output impedance of the active network enables

a voltage gain to be achieved in the passive network. The pre-set feed-back resistors, VR1 and VR2, set the bandwidth of the circuit of V1 (the reference frequency channel) and are adjusted to achieve a good sine waveform consistent with stability; similarly VR4 and VR3 serve as coarse and fine adjustment on the selectivity of the data channel.

Since changes in the setting of VC1 alter the feedback factor, the bandwidth of the instrument changes slightly through the working frequency range and VR3 is calibrated both at minimum and maximum frequency settings. This is, however, not a serious drawback and, if required, the two controls can be varied concurrently.

The variations in precession frequency can be accommodated, within the specified bandwidth, by manual adjustments of VC1, the dial of which is directly calibrated in Kc.p.s. As the reference frequency is changed, by adjustments of the division factor, (Section 7.3 above) it is also necessary to retune L1/C1/C2 to prevent distortion of the output waveform; this is achieved by switching in selected trimming capacitors VC2-6 by means of SW2, the wafer of which is physically situated on the "units" control of the Venner divider unit. By this means the resonant circuit is retuned in sychronism with changes in reference frequency.

C1-4 are polystyrene capacitors which temperature

compensate the inductances, as described previously. With this design it is found that the frequency calibration of the instrument changes by 42.5 parts per million per ^{o}C within the temperature range $15^{o}C$ to $65^{o}C$.

The 2.2 M ohm resistors, R1 and R2, prevent the Q of the coils from being loaded by the source impedances and the outputs of V1 and V2 are buffered from each other, and from the load impedance, by the two cathode followers V3 and V4.

The two filtered signals are linearly mixed by the resistive networks in the cathode circuits of V3 and V4. A combination of non-linear mixing and filtering could be used to extract the envelope of the beats but this was considered an unnecessary complication, providing a recording system of adequate bandwidth can be used, and, furthermore, it is desirable to keep the number of operations on the data to a minimum. The relative amplitudes of reference and signal waveforms can be varied by VR5 and VR6 and the output level controlled by VR7. In a later version of the instrument V3 and V4 are now rewired as amplifiers and the relative amplitudes of the two signals are controlled by potentiometers in their grid circuits. This arrangement means that the two signal amplitudes can be adjusted independently of each other and independently of the amplitude of beats, which is still determined by VR7. In the circuit of Fig.7.13 these adjustments were not independent.

CHAPTER 8

TRIAL No.B67 - FLIGHT OF SKYLARK SL40

8.1 Abridged Round Specification

In addition to the proton magnetometer, which was now classed as the secondary experiment, the rocket was instrumented with the following equipment: U.C.L./ Leicester University X-ray spectrometer (primary experiment); 3 rate gyroscopes, driven by E.D.C. rotary converter; 3 accelerometers; R.A.E. fluxgate magnetometer; R.A.E. Sun Slit Assembly; U.C.L. X-ray cameras; U.C.L. Sporadic E Probe; 24 channel telemetry transmitter; single channel telemetry transmitter for the exclusive use of the proton magnetometer; "Doppler" transponder and a "bomb slip" mechanism, with separation springs, to release and separate the instrumented head from the motor.

It has already been stated that the experiment required separation of the instrumented head from the motor at the lowest practicable height and with the maximum possible separation velocity. It was considered that the minimum height at which the head release could take place, without a serious adverse effect on the rocket's performance, was 75 Km and the calculated separation velocity, using three

standard separation springs, was approximately 1.5 ft./sec. It was therefore considered unlikely that the sensing head would be effectively out of range of the magnetic field perturbations due to the motor tube in time to detect a small discontinuity during the ascent of the rocket, but the required conditions should be present during the descent.

The total weight of the head assembly was 225 lbs. The motor was a Raven II.

8.2 Pre-flight Tests

The only pre-flight test of the rocket-borne proton magnetometer installation which was permitted was the brief interference level test described in Chapter 6, section 7. The ground recording magnetometer was fully tested and operated continuously for approximately four weeks prior to the flight.

8.3 Brief Description of the Flight of SL40

Skylark 40 was fired at Woomera (Lat.30°56'S. Long. 136°31'E; Geomagnetic Lat. -41.0°) on the 27th September, 1961 at 0955 hours C.S.T. (0025 hours G.M.T.). It was the 41st Skylark to be fired. A clear sky was a prerequisite of the trial since no M.T.S. was carried. The missile was tracked optically by kine-theodolites, from the instant of motor ignition (hereafter referred to as

"Zero Time Pip" and abbreviated to "Z.T.P.") to +42 seconds and the motor tube was tracked by radar, type FPS16 until +390 seconds.

The rocket reached a maximum height of 152.5 Km (predicted value 162 Km) and impacted at a point 113 Km down range (predicted value 131 Km), on a bearing of 303°T (predicted value 305°T). The effective Q.E. was 85°. A plot of the motor trajectory, determined mainly from the radar data, is shown in Fig. 8.1. This can be assumed to be coincident with the instrumented head up to the time of re-entry. In Fig. 8.1 the heights are relative to a plane tangential to the earth's surface and passing through the base of the launcher.

The motion of the rocket during the period +88 sec. to +150 sec. has been calculated from the fluxgate and sun-slit data by the R.A.E. and can be summarized as follows. The rocket executed the normal precessional motion but, as a consequence of the low roll rate, the "cone of precession" can for most purposes be regarded as a plane.

Roll rate = 8.09°/sec. (Period = 44.5 sec.)

Precession rate = 11.73°/sec (Period = 30.7 sec.)

Precession semi-cone angle = 88°

Angle between the axis of the cone of precession and the solar vector = 67°

Elevation of sun = 43.68°

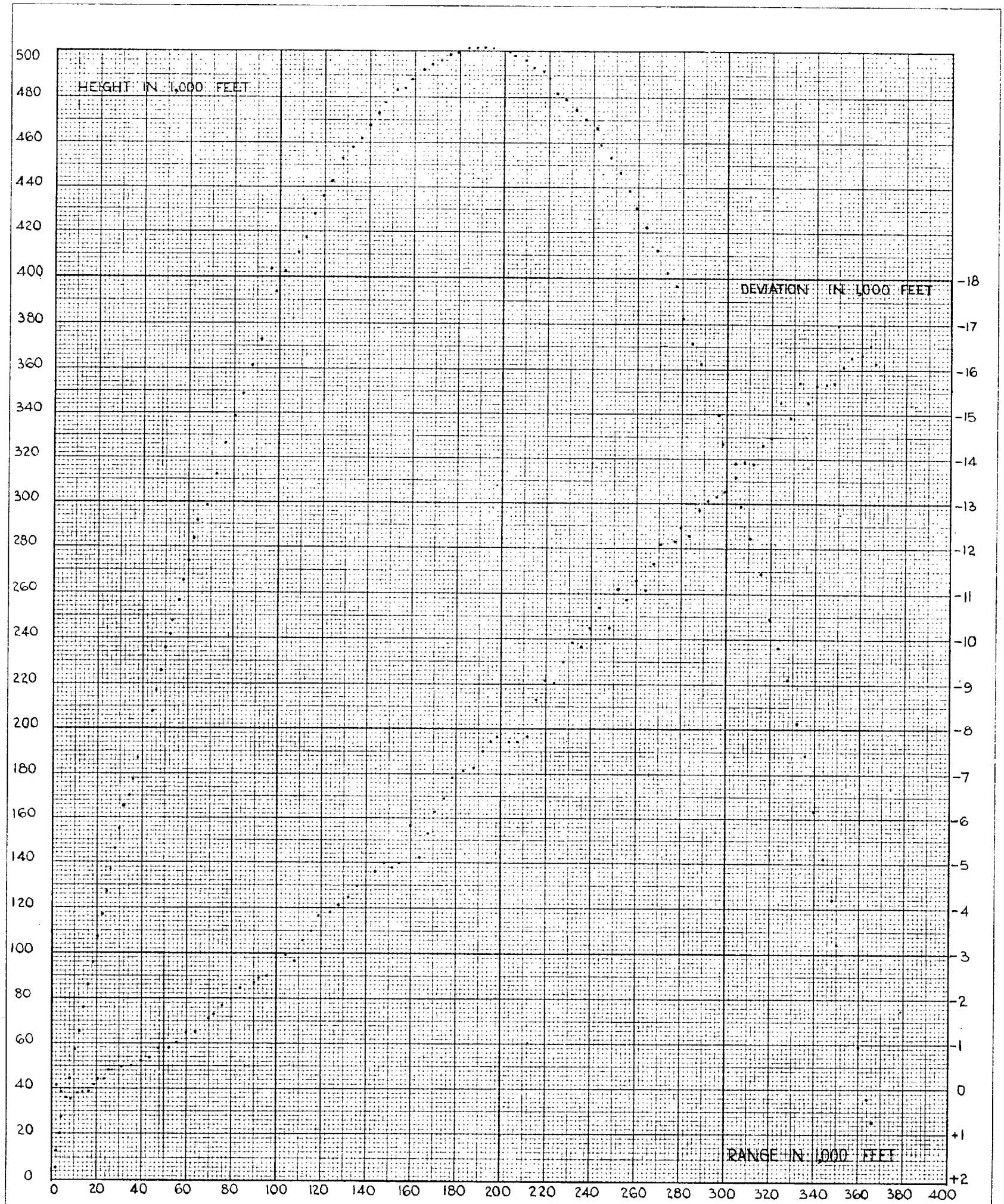


FIG 8.1. TRAJECTORY OF SL40 DEDUCED FROM FPS 16 RADAR.

Azimuth of sun = 52.08°

Angle between the axis of the cone of precession and the magnetic vector = 35°

Magnetic Inclination = 63°

Magnetic Declination = 6°E

Angle between the axis of the cone of precession and the vertical = 28°

Angle between the axis of the cone of precession and geographical North = 82°

Angle between the axis of the cone of precession and geographical East = 117°

Angles between rocket x axis and East, North and Vertical, at +88 seconds, = 115°, 42° and 115° respectively.

8.4 Summary of the Trial Programme - Timing Sequences.

All times are relative to "Z.T.P."

Event	Predicted Time	Actual Time
Proton Magnetometer amplifier switched ON	- 15 min.	- 15 min.
Test Oscillator switched ON	- 11 "	- 11 "
Timer unit of proton magnetometer switched ON (ready for flight)	- 64 sec.	- 64 sec.
High speed recorder of ground magnetometer started	- 62 "	- 62 "
Timing mark on ground magnetometer records	- 60 "	- 60 "
Motor ignited	0	0

Event	Predicted Time	Actual Time
Motor burnt out	+ 35 sec.	+ 35 sec.
Head separation	+ 77 "	+ 88 "
E.D.C. rotary and rate gyros switched off.	+ 80 "	+ 91 "
X-ray cameras opened	+ 98 "	+109 "
Apogee	+206 "	+200 "
X-ray cameras closed	+308 "	+319 "
Impact of motor tube	+410 "	~+410 "
Impact of instrumented head	+520 "	~+528 "
Ground magnetometer high speed recorder switched OFF	+540 "	+540 "
Spent motor and head assembly recovered and returned		+ 7 hour

8.5 Data Recording

The following records, relevant to the present topic, were produced by the W.R.E. either during the trial or, by playback, shortly afterwards.

i. Tape recordings, at a speed of 60" per second, of both the 24 channel and the single channel telemetry data, the Elapsed Time Code (E.T.C.) and the times of events. These data were recorded at both the rangehead and at Mirikata, approximately 175 km down range.

ii. Slow speed, 24" wide, records of the 24 channel time division multiplexed telemetry transmitter.
Figs. 8.2, 8.3, 8.4, 8.5 and 8.6 (in the rear pocket) show photographic copies of these records, reduced in scale, and annotated with times relative to Z.T.P.

iii. A 1" per second, 5½" wide, record showing the proton magnetometer monitor channels, fluxgate and sun slit data.

iv. Records of telemetry signal strength at the range head and Mirikata.

v. 35 mm film records of the single channel (proton magnetometer) data at a film speed of 64" per second.

8.6 Performance of Rocket Instrumentation

i. X-ray Spectrometer. No usable data were obtained from this instrument as a result of a faulty E.H.T. supply to the counters.

ii. Rate Gyros. These worked satisfactorily until switched off by the programme motor at +91 seconds (Fig. 8.2).

iii. Accelerometers. These appeared to function satisfactorily throughout the flight, though a zero shift of the $\dot{y}$ and $\dot{z}$ instruments during the re-entry phase is suspected.

iv. RAE Fluxgate magnetometer. At approximately 151 seconds the first element of this instrument failed, followed at 159 seconds by the second, and at 160 seconds by the third. (Fig.8.3). The cause of the failure is not known.

v. RAE Sun Slit Assembly. This failed at +250 seconds due to an unknown cause. This failure meant the loss of all positive accurate attitude data from this time for the rest of the flight.

vi. U.C.L. X-ray cameras. One of the two cameras was recovered in the open position and the other was half open. It was, however, later reported that a good photograph was obtained from the first camera and it is thought that the impact may have caused it to return to the open position.

vii. U.C.L. Sporadic E. probe. This appeared to function throughout the flight but no high levels of ionisation were detected.

viii. Telemetry reception from both senders was very good throughout the flight.

ix. The "Doppler" record was only satisfactory up to +62 seconds and, since good optical tracking had been achieved, it was not used in the trajectory calculations.

x. The head release monitor indicated that the bomb slip mechanism operated correctly, though, due to the slow running of the programme motor, this event occurred 10.2 seconds later than planned.

8.7 Performance of the Proton Magnetometers

i. Recording Magnetometer. The ground recording magnetometer (Chapter 7, Section 1) functioned satisfactorily for a continuous period of several weeks including the day of the rocket flight.

ii. Rocket-borne Magnetometer. The rocket-borne proton magnetometer failed at +18 seconds but started working again at +167 seconds, and thereafter the instrument functioned correctly for the remainder of the flight. The cause of this failure can be assessed by reference to the monitor records Mm1 and Mm2 of the low speed 24 channel records (Fig. 8.2 and 8.3) and by examining the recorded rocket-borne magnetometer signals during this period. The monitor records indicate that the relays RLA and RLB of Fig. 6.3 were being energised, but that there was a break somewhere in the polarizing circuit. The character of the noise at the output of the amplifier during this period also indicated a break somewhere in the series resonant circuit consisting of the polarizing coil, lead-in cable, contacts RLA1, contacts RLA2 and L1, the primary

of the input transformer (Fig. 6.3). This effect is most easily recognized by listening to the signal and is quite characteristic. Now since the failure and the "repair" both occurred abruptly, and since all the wiring and soldered joints were found to be secure on recovery of the equipment, the only possible places for this break in continuity are the relay contacts and the plug at the tip of the nose cone, which had been fitted by the R.A.E. in order to facilitate the loading of the rocket into the launcher. Of these alternatives the latter seems most likely as the former would require the failure of both pairs of normally closed contacts RLA1 and RLA2. A possible explanation of why the plug should break the continuity of the circuit during this period is to be found in the fact that one section was rigidly attached to the struts inside the nose cone, whereas the other section was rigidly attached to the nose cone itself. Thus, as a result of the severe aerodynamic heating during the early part of the flight, the nose cone expanded and pulled the two sections of the plug apart. As the nose cone later cooled and its heat was re-distributed, the two parts then remade contact. It was later revealed that some failures in early Skylark flights had also been attributed to a similar mechanism, which tends to confirm this diagnosis.

A selection of specimen records of the output of the

amplifier of the proton magnetometer at different periods of the flight is shown in Fig. 8.7 (in rear pocket). These were transcribed, along with the E.T.C., on to 35 mm film moving continuously at 8" per second. In each record the first (left hand) section is the polarizing period and the second section is the signal. The section of the flight represented by each record is as follows.

A. Whilst the rocket was travelling up the launcher.

B. +4 sec. No signal due to unfavourable attitude. Noise induced by vibration.

C. +21 sec. Severe hoise induced by vibration. The rocket was now travelling at approximately 2,400 ft./sec. at a height of 26,000 ft.

D. +35 sec. to +167 sec. Instrumental failure due to circumstances described above.

E. +168 sec. The first productive signal. This quality of data is typical of the period whilst the rocket was close to apogee.

F. +237 sec. The lowest amplitude signal which was, nevertheless, used to obtain a field measurement in good agreement with other determinations.

G. +319 sec. A good signal but with short T2. This will be discussed later.

H. +320 sec. to +356 sec. During this period the instrument was working correctly but only two usable precession

signals were detected (at about +335 sec.) and they were similar to record G in that they were of short duration. The reasons for this will be discussed later.

I. +356 sec. to +390 sec. Noise induced by the vibration of "re-entry".

J. +390 sec. to +423 sec. The instrument appeared to be working correctly but no usable signals were obtained. The reason for this is believed to be that during this period the rocket was in an unfavourable attitude.

K. +423 sec. to impact. Quite good quality data.

A post-flight examination of the recovered magnetometer revealed that the top, sides and rear of the fibreglass sheath had been severely ablated (as expected) and on impact the sensing head had severed from the probe. The only unserviceability incurred by the electronics package during the entire flight was that the contacts RLA (Fig.6.3) were jammed in the normally closed position by the force of the impact. All the modular electronics circuits were still in a fully serviceable state on recovery.

8.8 Data Processing

A preliminary plot of precession frequency against time was obtained by using the 64" per second film records

of the un-processed proton magnetometer data, as recorded during the actual flight. This was done manually by estimating, by means of the E.T.C., the period of 100 precession cycles in each of 22 signal periods distributed uniformly throughout the appropriate sections of the flight. This was a low-accuracy determination but it facilitated the subsequent more accurate measurements.

A block diagram which illustrates the techniques used in obtaining high-accuracy measurements of the frequency of the precession signals is shown in Fig. 8.8. The tape

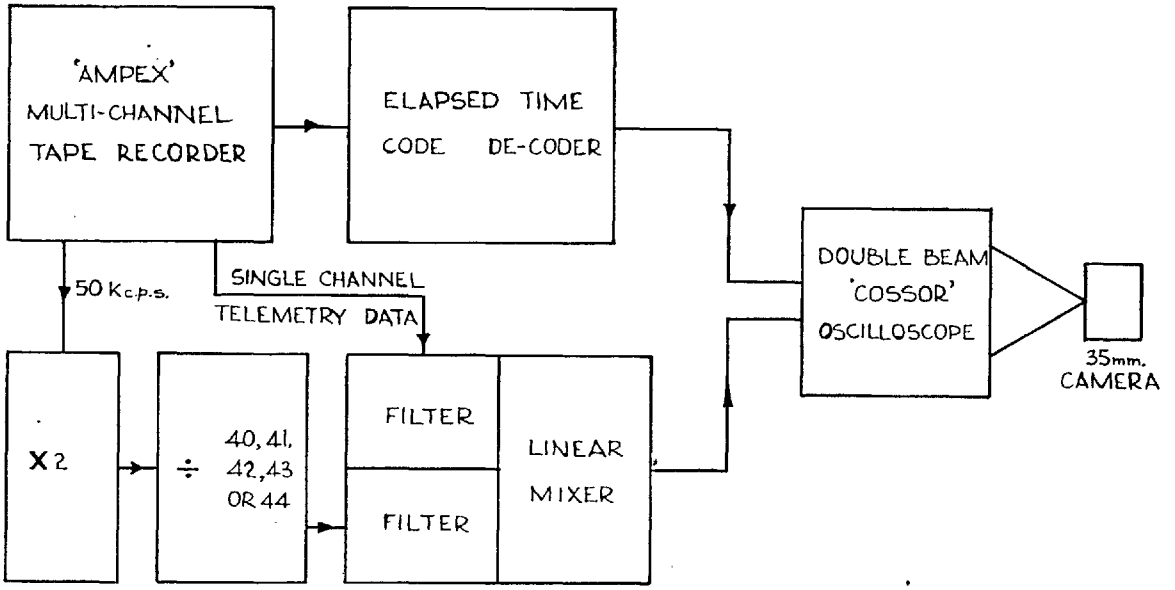


FIG. 8.8. BLOCK DIAGRAM OF DATA PROCESSING EQUIPMENT

play-back facilities, E.T.C. de-coder, oscilloscope and camera were provided by the W.R.E. The 50 Kc.p.s. pulses were fed through the frequency doubler (Fig. 7.12) and then through the Venner divider unit (not described). The standard reference frequency thereby derived was then mixed with the filtered telemetry signals, in the way which was described in Chapter 7, Section 4, by means of the Filter/Mixer unit (Figs. 7.13 and 7.14). The beats thereby obtained were recorded on 35 mm film at a speed of 8" per second . Fig. 8.9 shows sample records, derived from the same precession signal as that shown in record E of Fig. 8.7, using different settings of reference frequency and relative signal amplitudes. The improvement in signal/noise ratio resulting from the reduction in band-width is immediately evident.

In order to confirm the self-consistency of the data handling process, and to investigate the way in which the final data were affected by variations in signal band-width and standard reference frequency, the play-back process was repeated a number of times. The data reduction consisted of counting manually the number of beats in each precession signal period and measuring the total period of the beats with reference to the E.T.C. The limit to the accuracy of the determinations was set by the clarity of the beat envelope and hence by how accurately the times of maxima and

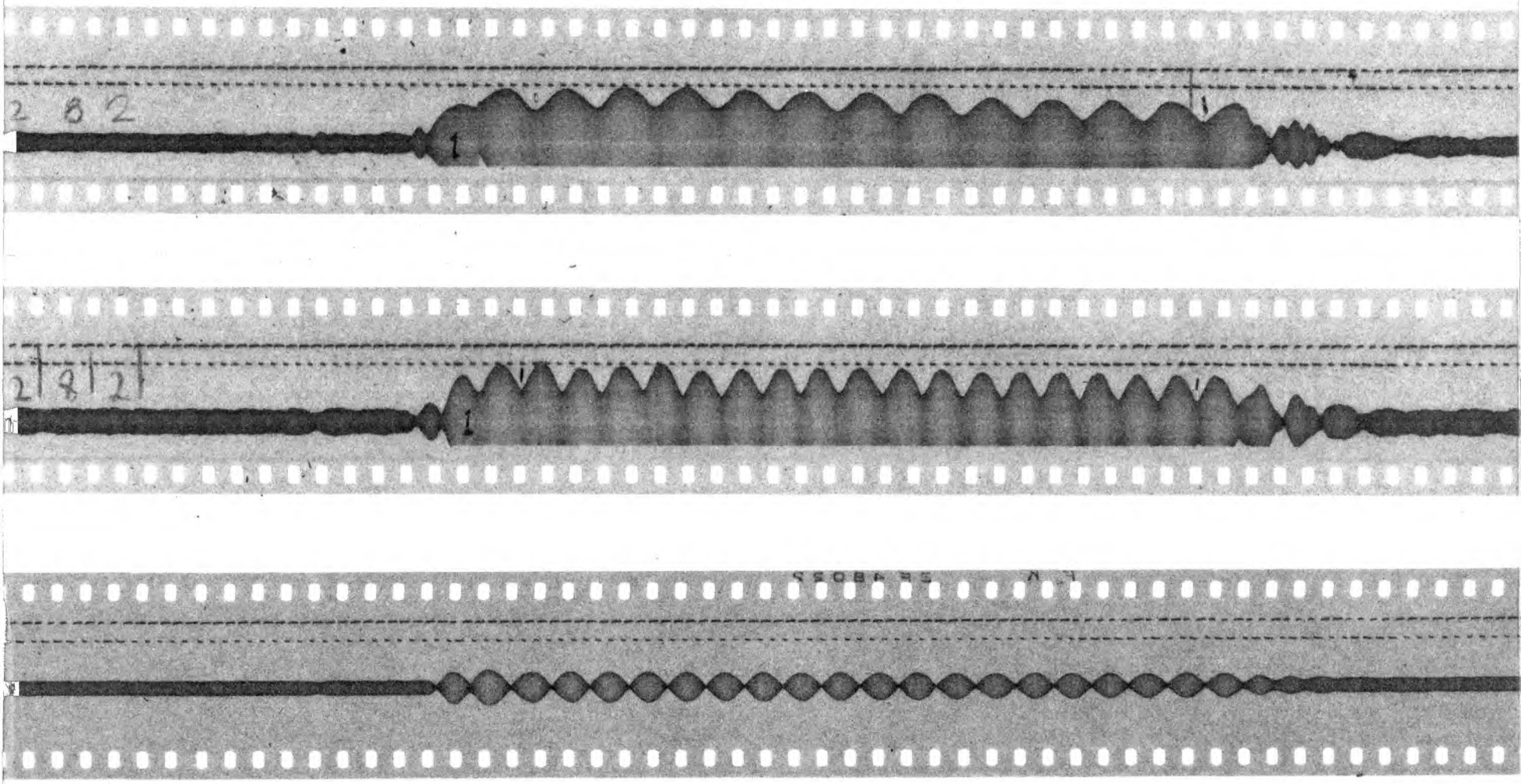


FIG 8.9. SAMPLE OF BEATS.

minima could be determined. This operation, the calculation of precession frequencies and the preliminary plotting of the data were carried out by the Mathematical Services group of the W.R.E. Some of the results are shown in Figs. 8.10 to 8.13 (in rear pocket).

On the basis of these experiments the following conclusions can be drawn regarding this particular technique of data reduction.

i. Reducing the noise bandwidth during the play-back increases the signal/noise ratio and this in turn enables more of the signals to be measured accurately and leads to a smaller scatter of readings about the mean values. This conclusion is illustrated by a comparison of Figs. 8.10 and 8.13.

ii. There is, however, a limit to the improvement which can be achieved by this technique, as is shown by comparing Figs. 8.12 and 8.13, where it can be seen that the scatter of the observations is greater with the narrower bandwidth. This effect is believed to be due to differential phase changes introduced into the signal and reference channels by the Filter/Mixer unit (Fig. 7.13), as a result of tape "wow" and "flutter". Provided both circuits are tuned to the same degree of accuracy tape speed variations will affect each channel equally, but if VC1 is not precisely adjusted, the changes in phase shift due to tape flutter

will be different in the two channels and errors will result. Thus, using a given tape recorder and for a given value of precession frequency, the bandwidth of the playback system is limited to how accurately the changes in precession frequency can be tracked by manual adjustments of VC1.

iii. A further effect of the use of too narrow a bandwidth is that where there is a very poor signal/noise ratio, due to the proton precession signal being either of low amplitude or well outside the pass band of the play-back system, or due to excessive noise such as occurred during "re-entry", the filter will extract a noisy sine wave which can, in certain circumstances, be mistaken for a true precession signal. Thus in Fig. 8.11, the peaks of the frequency modulations have been compressed (e.g. at +250 sec.) and erroneous "readings" have been plotted during the "re-entry" phase of the flight.

iv. Accuracy of the data. Some indication of the accuracy of the data processing can be assessed from the scatter of the readings of Fig. 8.13. The standard deviation of the readings from a smooth curve varies from 0.161 c.p.s. (during the 20 second period just before impact) to 0.112 c.p.s. (during the 20 second period centred on apogee).

These figures can however be misleading since the reading repetition rate is not sufficiently rapid, as compared with the real modulations in precession frequency,

particularly during the period after re-entry. Since the errors introduced by tape "wow" and "flutter" will be random in nature an improvement by a factor of $\sqrt{n}$ can be achieved by making n determinations of each signal frequency. The accuracy of the "best fit" curves is indicated by a comparison of the data for figures 8.10 and 8.13. The R.M.S. differences between these two sets of data for the two 20 second periods near impact and at apogee are 0.257 c.p.s. (= 6 gamma) and 0.099 c.p.s. (= 2.3 gamma) respectively, and it is reasonable to assume that these figures would be even smaller in the absence of the large frequency modulations.

It can therefore be concluded that, given a favourable orientation of the sensing head, the present technique should be capable of resolving a discontinuity of the order of that anticipated from a typical diurnal current sheet over Woomera as discussed in Chapter 1.

CHAPTER 9

RESULTS, DISCUSSION, INTERPRETATION

9.1 Diurnal Variation

The ground recording magnetometer record for the day of the flight of SL40 is shown in Fig. 9.1 (in rear pocket). The time scale is set on C.S.T. (G.M.T. +9½ hours). The record is fairly typical of the majority obtained during the two months the instrument was in operation at Woomera and shows that the trial took place on a normal magnetically quiet day.

The high speed record showed that during the period of the flight the geomagnetic total force did not change significantly.

9.2 Rocket-borne Data

Summary

The flight measurements of scalar magnetic field show periodic modulations of varying amplitude. In the first instance a successful head separation is assumed and various possible mechanisms, which were located in the instrumented head and which could account for the main features of the results, are critically examined and rejected. It is concluded that the observed effects can only be explained by the close proximity of the spent motor tube

and, furthermore, that the motor must have acquired a considerable permanent magnetisation. This conclusion enables an estimate to be made of the accuracy of the absolute determinations of the geomagnetic field close to the apogee of the rocket's trajectory. The results will now be discussed in greater detail.

A plot of the variation of precession frequency with time is shown in Fig. 8.13 (in rear pocket) and the same data, converted to corresponding heights, are plotted in Fig. 9.2 (in rear pocket). Also plotted in Fig. 9.2 are theoretical values derived by means of a Spherical Harmonic Analysis carried out by S.H. Hall[24] using the Gauss Coefficients calculated by Vestine for the Epoch 1945.0[25].

The height values were taken from the radar trajectory (Fig. 8.1) and have been corrected to allow for the earth's curvature. The flight data after re-entry have not been reduced for plotting in Fig. 9.2 since there is no positive information on the trajectory of the rocket head during this period. The readings have, however, been extrapolated to ground level, by estimating the actual impact time from the known times at which the rocket fell below the radio horizons at Woomera and at Mirikata. The estimated error introduced by this extrapolation is ± 0.5 c.p.s. Also shown in Fig. 9.2 are the value of F in the vicinity of the launcher during the period of the trial, as measured by

the recording magnetometer (Chapter 7, Section 1), and the value close to the impact point, asmeasured during a survey of the range using the portable magnetometer (Chapter 3). This survey is discussed in Appendix II.

The most obvious features of Fig. 8.13 are the periodic modulations of precession frequency which increase to a maximum amplitude and then revert to a comparatively small amplitude during the final few seconds of the flight. The possibility that these large oscillations could be of genuine geomagnetic origin can immediately be discounted by reference to the diurnal record and from the fact that their period agrees precisely with that of the rocket's rotations. The oscillations cannot be attributed to the data reduction technique described in Chapter 8 since the results of the preliminary frequency determinations, which were made using the high speed film records, agree, within the accuracy of the measurements, with the readings of Fig. 8.13. The oscillations can therefore only be attributed to perturbations in the geomagnetic field caused by the rocket itself.

A theory to describe in detail the mechanism by which the frequency modulations were generated must account for the following features of the results.

i. The amplitude of the oscillations increases continuously during the period +168 seconds to +320 seconds to a maximum value of approximately $\pm$20 c.p.s. (= $\pm$ 460 gamma).

ii. During the period +430 to +518 seconds the amplitude of the oscillations is much reduced, as compared with the first period, and the amplitude continues to decrease until signals cease at impact.

iii. The period of the large oscillations is constant at 30.7 seconds, whereas that of the later small oscillations varies from 5 seconds (at +450 seconds) to 9 seconds (at +500 seconds).

It is also necessary to account for the fact that, during the period after 320 seconds and before re-entry, only two usable precession signals were detected (at about +335 seconds) and they were of short duration, in spite of the fact that the instrument was apparently working correctly during this time and was in a favourable attitude. The explanation of this is believed to arise from the same fundamental cause as the magnetic errors. It has already been stated that a magnetic field gradient across the proton sample will cause the signal to decay more rapidly than the normal relaxation time T_2. The effect is discussed quantitatively and in greater detail in Appendix I. Referring to Fig. 8.7 it can be seen that record G displays a much shorter decay time than, say, records E or K. Thus it is established that, at this time, a significant field gradient existed in the vicinity of the sensing head, and it is believed that this was responsible for the failure to

detect precession signals during the above period.

It would appear at first sight, that the only magnetic component of the rocket which could account for the large perturbations (± 460 gamma) is the high tensile steel Raven motor shell (c.f. Chapter 2, Section 2) and, since re-entry would effectively separate the head and motor, this could explain the reduced error in the final section of the flight. However, the following features of the data make it difficult to accept this as a possible explanation.

i. The head release monitor provided a positive indication that the bomb-slip mechanism had worked correctly at +88 seconds (Fig. 8.2). Once released the three separation springs should impart a relative velocity of approximately 1.5 ft./sec. to the two sections of the rocket; thus any magnetic errors attributable to the motor should continue to decrease with time, at least until "re-entry".

ii. The longitudinal axis of the rocket was only 25° from the horizontal at +88 seconds and it is therefore difficult to see how, once separated, the two sections of the rocket could be brought appreciably closer together.

iii. A telemetry fade, followed by a series of signal strength fluctuations, occurred at the time of head release. The character and frequency of the oscillations was consistent with the hypothesis that they were caused by interference between a direct ray and a ray reflected from the

motor tube as the latter moved away.

iv. A small acceleration was registered on the X accelerometer at +88 seconds of the correct polarity to indicate that the headwas being pushed away from the motor. It is, however, possible that this was due to the impulse of the bomb-slip, or even that its origin was merely electrical.

If the source of the magnetic field perturbations was located in the instrumented section of the rocket, in a fixed position and orientation, the 30 second period of the oscillations (Fig. 8.13) implies that the source must have been a permanent magnetic field. Perturbations due to magnetisation induced by the earth's field would result in the appearance of a second harmonic of the rocket's precession frequency. Furthermore, if the magnitude of the permanent magnetisation was constant, the increase in the amplitude of the frequency modulations, during the period +200 seconds to +320 seconds, could only be explained in terms of a change in the angle between the geomagnetic vector and the error vector, which implies a change in the tumbling characteristics of the rocket. Unfortunately the standard sources of accurate attitude information, namely the RAE fluxgates and photocells, had both failed by this time; however some indication of the variations in the angle between the rocket x axis and the geomagnetic vector can be obtained from the amplitude of the proton precession

signal itself. As discussed in Chapter 6, Section 6, the signal amplitude, immediately after switching off the polarizing field, is proportional to $\sin^2\theta$, where θ is the angle between the rocket axis and the geomagnetic vector. A graph showing the variations of θ with time, calculated on this basis, is shown in the lower section of Fig. 9.3 (in rear pocket). In calculating this diagram the following assumptions were made.

i. That the largest signal obtained during the entire flight was with the rocket axis at right angles to $\vec{F}$.

ii. That the polarizing volts, coil resistance, sample temperature, amplifier gain and the gain of the telemetry data transmission, recording and playback systems were all constant throughout the flight.

iii. That the frequency response of the magnetometer amplifier was correctly represented at all times by Fig. 6.8.

The results show that, during the period up to +205 seconds, the round was rotating with a period of 30.7 seconds in such a way that θ passed through the value of 90° twice during each rotation; and that the minimum value of θ was 56°. This agrees closely with the fluxgate attitude data extrapolated to this time. Fig. 9.3 also confirms that the rocket was in a favourable attitude at +320 seconds, when the precession signals first disappeared.

At first sight the attitude data of Fig. 9.3 appear

to confirm that a radical change in the rotational motions of the rocket took place during the period 200 - 250 seconds, which correlates with the period during which the precession frequency modulations were increasing in amplitude. The interpretation of the proton precession attitude data would be that the precession rate increased by a factor of 2; that the angle between the axis of the rocket's cone of precession and the geomagnetic vector changed from approximately 35° to approximately 45° and that the semi-cone angle of the precession cone tightened up from 88° to approximately 10°, which would imply an increase in the roll rate by a factor of approximately 56 . It is very difficult to accept that such a drastic change in the rocket's motion could take place at this time of the flight and it is necessary to look for a different explanation for the decrease in signal during this period.

Also plotted in Fig. 9.3, at the same time scale, are points showing δ Vp, the amplitude of the voltage steps on the monitor record Mm2 of Figs. 8.3 to 8.6. This monitor channel shows the change in the voltage across the terminals of the SZ6/12 polarizing battery, when the polarizing current is switched on, and it can therefore give an indication of the current drain from the battery, though its original purpose was merely as a "go-no-go" indication.

During the period 170 to 230 seconds δVp changes by

approximately 0.16 volts, indicating that during this period the polarizing current was reduced, which in turn implies that the sensing coil resistance was increased. Thus it seems likely that a considerable rise in temperature occurred in the sensing head, during this period, and this is the most probable explanation of the reduction in the amplitude of the precession signals. Such a temperature rise can only be explained in terms of the redistribution of heat which had been generated near the skin of the fibreglass sheath during the rocket's ascent through the atmosphere.

The effect of temperature variations on the data of the lower curve of Fig. 9.3 can be allowed for by assuming that the maximum signal during each fifteen second period corresponds to the position $\theta = 90^{\circ}$, the intervening values of θ are then calculated from the appropriate signal amplitudes, as before. When this adjustment is made to the data, no change can be detected in the period of the rocket's rotation, or in the minimum values of θ, during the period before re-entry. Thus the proton precession attitude data is consistent with the hypothesis that no significant change took place in the attitude characteristics of the rocket during the period immediately following the failure of the rocket's standard attitude measuring devices. The photographic record of solar traverses obtained by the X-ray camera, is also consistent with this view[26].

If no systematic change occurred in the angle between the rocket axis and the magnetic vector, during the period +200 to +320 seconds and, if the field perturbations are to be attributed to a magnetic field associated with the instrumented section of the rocket, then the increase in magnitude of the error during this period can only be explained by a change in the magnetic moment of the source. It is therefore important to determine, so far as is possible, how the magnitude of the error field, in the vicinity of the sensing head, varied during the entire flight, including the period after re-entry.

The comparative smoothness of the record during the last few seconds of the flight (Fig. 8.13) could be explained either by the removal of the field perturbations during the re-entry phase, or by the assumption of a systematic error in all the data of this period. The latter case implies that the source of the error field was located in the rocket head, and also that the head was sufficiently aerodynamically stable to prevent the error field from modulating the measurements appreciably.

The following considerations suggest that, during this period, the head was, in fact, stable, at least to the extent that the centre of the sensing head was at all times higher than the centre of gravity of the rocket.

i. By assuming an inverse cube law for the decrease in

geomagnetic total force during this section of the fall, an approximate value for the height at any time can be derived from the magnetometer data. The results of an analysis based on this assumption are plotted in Fig. 9.4. Thus the vertical velocity can readily be calculated. The values of vertical velocity derived from Fig. 9.3 are 0.19 Km/sec. (623 ft./sec.) at +450 sec. reducing to 0.066 Km/sec. (217 ft./sec) at impact. Taking an average value of 400 ft./sec., it can be shown that the aerodynamic drag which would arise from this velocity would lead to a retardation of the order 10g at an angle of incidence of 90°, whereas the $\mathcal{Y}$ and $\mathcal{Z}$ (lateral axes) accelerometers registered decelerations of only the order 1g (Fig. 8.5 and 8.6). Therefore the rocket head cannot have assumed this attitude during this time.

ii. During the re-entry period the $\mathcal{X}$ accelerometer indicated that the component of the deceleration forces parallel to the longitudinal axis was at all times positive (Fig. 8.5).

iii. The close agreement between the frequencies of the magnetic field modulations (Fig. 8.13) and the variations of θ (Fig. 9.3) is consistent with the view that, during the period +450 seconds to impact, the head was precessing in a vertical cone with a semi-cone angle considerably less than 90°. An angle close to 90° would result in the frequency of the modulations of θ being twice that of the

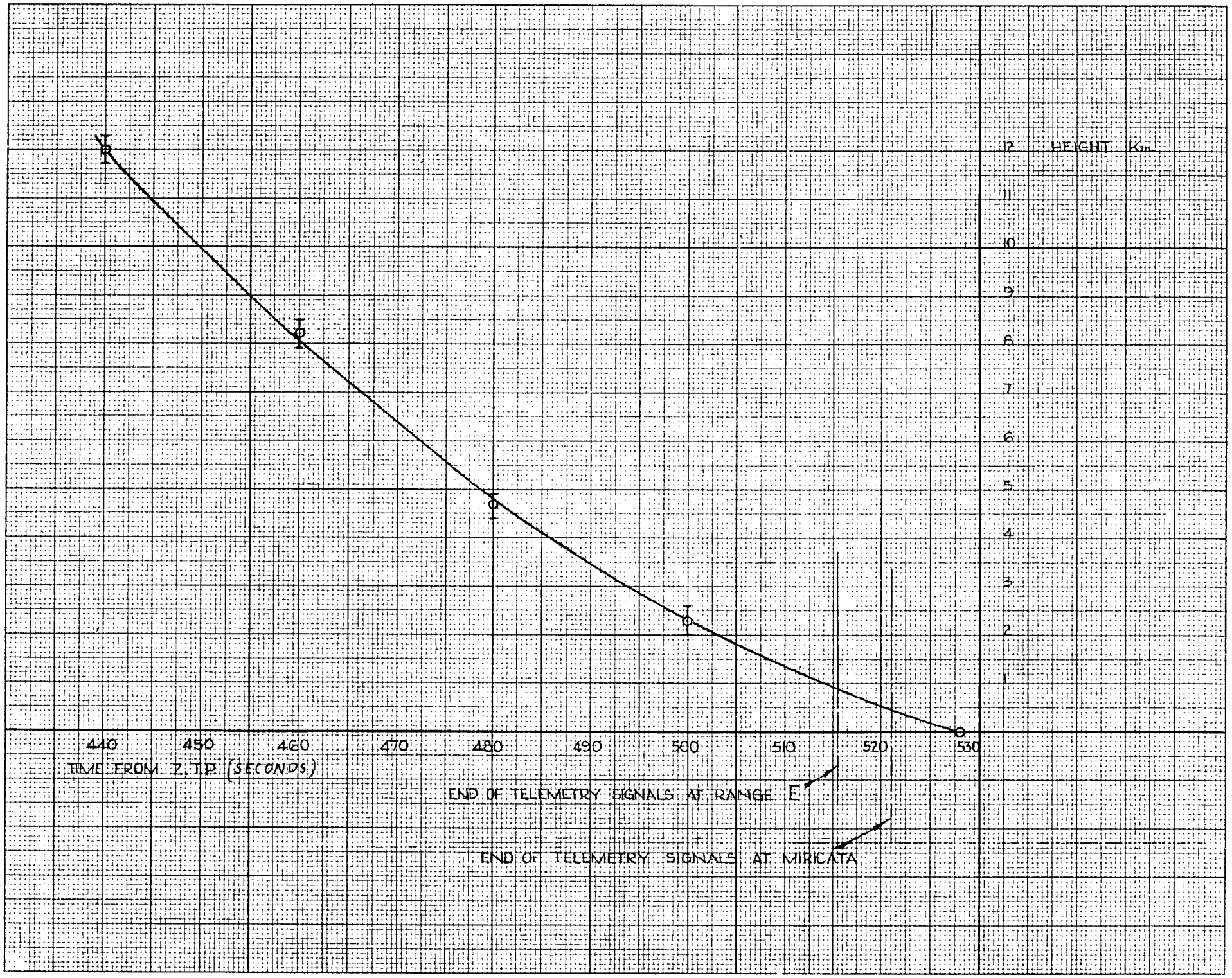


FIG. 9.4. HEIGHT/TIME CURVE CALCULATED FROM PROTON MAGNETOMETER DATA

field modulations. The slight upward trend of the mean value of ϑ during this period in spite of a downward trend of δV_p, suggests that the semi-cone angle increased slightly in the denser lower atmosphere. An examination of the recovered head revealed that it impacted with the probe uppermost.

In view of the conjectured aerodynamic stability of the rocket head the possibility of a systematic error in the data of Fig.8.13 (450 secs. to impact) could not be ruled out. This suggestion is, to some extent, also supported by the fact that the flight measurements, when extrapolated to ground level, do not agree with the value interpolated on the iso-dynamic map of Fig.2.4.

In order to resolve this ambiguity and hence to acquire further evidence as to the possible explanation of the field modulations, it was decided to carry out a ground survey of the Woomera Range, between the launcher area and the impact point of the rocket head, to obtain direct measurements of the geomagnetic field in the vicinity of the impact point. The survey is described in Appendix II and the ground level value of total force at the impact point, as deduced from the survey, is plotted in Fig.9.2. The discrepancy between the extrapolated flight data and the ground measurements is only 2.2 ± 0.5 c.p.s. ($=50 \pm 10$ gamma).

In view of the fact that no direct magnetic measurements were made on the instrumented head prior to flight it is quite reasonable to postulate that this discrepancy resulted from a combination of regional geomagnetic anomalies in the area and magnetic fields associated with the rocket head.

These results indicate that the source of most of the error field was removed during the period when no magnetic measurements were obtained and any theory to account for the field modulations must take this into consideration.

Two mechanisms, which arise from magnetic causes within the instrumented "head" of the rocket and which could conceivably account for most features of the observations, remain to be explored. They are as follows.

i. That the field was generated by a direct current, of changing magnitude, flowing in the rocket wiring.

ii. That the field was due to thermo-remanent magnetisation of the probe.

At +313 seconds the deviation of the measured field from the mean value was approximately +230 gamma (Fig. 8.13) and the angle between the rocket axis and $\vec{F}$ was a minimum at that time (Fig. 9.3). Thus, assuming that the field was due to a magnetic moment orientated along the rocket axis (the only orientation which is compatible with the observed phase of the modulations), the actual field perturbation must have been approximately $230\ (\cos\theta)^{-1} = 411$ gamma. To generate

this field, by means of a single loop of wire positioned near the base of the nose cone, would require a current of approximately 450 amps. Since an SZ6/12 battery is incapable of delivering such a large current the first of the above theories can immediately be discounted.

At first sight the theory based on induced thermoremanent magnetisation of the probe appears to account for all the features of the frequency modulations. The published characteristics of the various types of austenitic stainless steels which were available at the time the probe was manufactured[27], indicated that, from the point of view of its magnetic characteristics, the most suitable material for use in the construction of the probe was BS : En58D. This material was not, however, readily available in tube form and austenitic steel to specification En58B was used. Furthermore it is known that cold working of some austenitic steels can result in a transformation of small areas of Austenite to the magnetic phase, Martensite, with consequent increase in magnetic permeability. Any magnetic field perturbations which would result from the complete probe were measured, by means of the portable magnetometer, prior to its installation in the rocket. Whilst some slight magnetisation could be detected in the vicinity of those sections which had been subjected to cold working (e.g. the shoulder half way along the probe), this was considered negligible and

it was accepted. It is known however[28,29,30] that the heat treatment of some metals in the presence of strong magnetic fields can result in a considerable increase in their magnetic properties. It is thus possible that, as a result of the aerodynamic heating during the rocket's ascent through the atmosphere, followed by a slow cooling in the presence of the intermittent polarizing field from the sensing head, the probe might have acquired an appreciable permanent magnetic moment, which would increase progressively as it cooled. Calculations carried out by the R.A.E.[31] suggest that the temperature of a parallel-sided probe, 1" in diameter and filled with Araldite, might reach about 430°K and would then cool at a rate of between 0.5°K and 1.0°K per minute. The local temperature in the vicinity of the aerodynamic discontinuities, at the shoulder and at the junction between the probe and the sensing head could, however, reach a value considerably in excess of this figure; this hypothesis is supported by the slight temper colour present at these two points of the recovered probe, whereas none can be detected at any other point. Such a mechanism could account for the smooth increase in the error and for the complete disappearance of signals at about +320 seconds; it would also result in an induced magnetic moment orientated, as required, along the rocket's x axis and of the correct polarity to account for the phase of the modulations.

The appearance of two usable signals at about +335 seconds can also be explained by the fact that, at this time, the rocket x axis was orientated at approximately 90° to the magnetic vector (c.f. discussion of Fig. 9.3) and hence the effect of the field gradient arising from the probe magnetisation, would be a minimum at this time.

On recovery and return to England the probe was found to have a remanance comparable with that measured prior to its installation in the rocket. In order to explain this it is necessary to postulate that, on re-entering the dense atmosphere, the probe was re-heated to a temperature in excess of the Curie point of any magnetic domains present and remained at a sufficiently high temperature until the polarizing field was removed on impact with the ground. It is also possible that any residual magnetisation could be reduced by the violent deceleration forces and vibrations when the rocket hit the ground.

Although a mechanism which postulates a significant thermo-remanent magnetisation of the probe would appear to provide a qualitative explanation of the main features of Figs. 8.13 and 9.2, the following considerations make it quite untenable.

i. Since the theory requires a magnetic moment whose orientation is fixed at all times along the x axis of the rocket, the minimum in field gradient, which occurred

at +335 seconds, would coincide with a minimum error; furthermore the oscillations depicted in Fig. 8.13 would be symmetrically situated relative to the true field values and the errors could be partially removed by taking a mean through the oscillations. A plot of magnetic field versus height, calculated on this basis, however, shows unacceptable non-linearities.

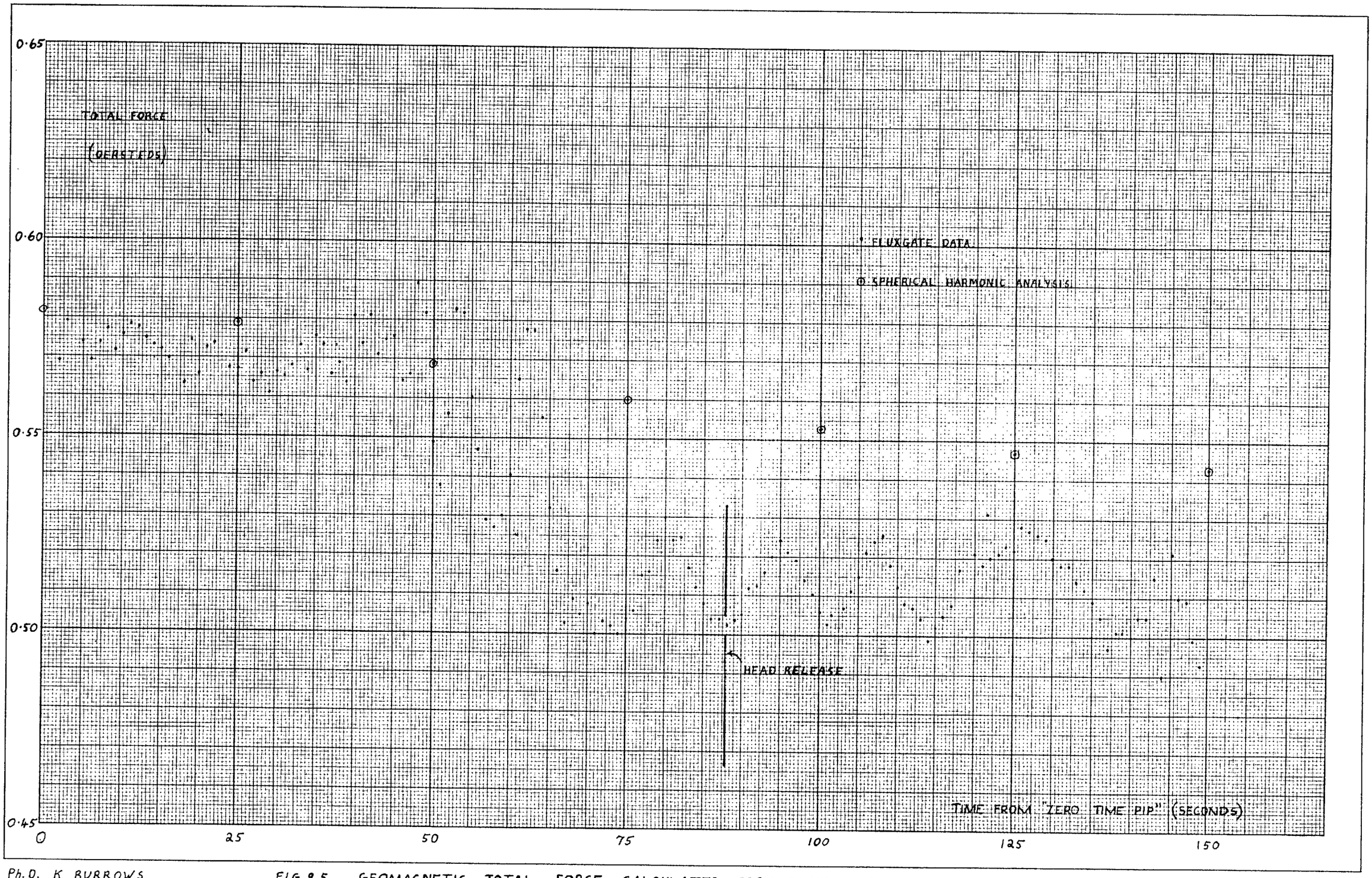
ii. It has been shown experimentally that, if the source of the field perturbations was a dipole orientated along the x axis of the rocket, it must have been situated at a distance of considerably more than 140 cm. at time +314 seconds The experiments which led to this conclusion are described in Appendix I (Gradient Experiments).

iii. A sample of Austenitic stainless steel tubing, to specification EN58B and identical with that used in the construction of the forward section of the probe, was cold-worked to roughly the same degree as the original and heated, in an electric furnace, to a temperature of approximately 700°C. It was then allowed to cool to room temperature in the presence of an intermittent polarizing field identical to that which the original probe experienced in flight; this was achieved by positioning it at the appropriate distance from the SL40 spare sensing head, which was operated as a standard flight instrument. The sensing head, in conjunction with the electronics unit recovered from SL40, then gave a

continuous monitor of the magnetic field. The sample tube did, of course, cool much more rapidly, though from a higher temperature, than the original probe in flight; however, as no thermo-remanent magnetisation could be detected at any stage of the cooling process it seems reasonable to assume that none would have been induced had the actual conditions been simulated more precisely.

It is therefore difficult to accept that any magnetic disturbance in the instrumented head could account for all the features of the results and it is necessary to re-examine the hypothesis that the magnetic field perturbations were due to the Raven rocket motor. In this connection the following facts should be noted.

i. It is particularly unfortunate that no data were obtained from the proton magnetometer at the time of head release, as this should have given unequivocal evidence as to whether or not the head remained within the sphere of magnetic influence of the motor. In an attempt to compensate for this lack of information the data from the R.A.E. three element fluxgate magnetometer have been reduced and are presented in Fig. 9.5. This diagram shows the total scalar force derived by taking the square root of the sum of the squares of the three components, as measured by the three fluxgates, from the time of launch to +150 seconds, when the first element failed (Figs. 8.2 and 8.3); also plotted are points derived



Ph.D. K BURROWS.

FIG. 9.5. GEOMAGNETIC TOTAL FORCE CALCULATED FROM FLUXGATE DATA.

from a spherical harmonic analysis of the field and reduced to a time scale. It will be noted that no discontinuity can be detected at the time of head release, though the large scatter of the readings means that a small change would not be resolved. It is difficult to estimate, with any degree of certainty, the order of magnetic field perturbation which the motor would cause in the vicinity of the fluxgates, and no measurements were made on the particular motor for use with SL40. There is therefore no information regarding any possible permanent magnetisation of the motor tube, furthermore the temperature rise resulting from the fuel burning would reduce any magnetisation present; however the most probable values for the field disturbance at this point are between 100 gamma and 1000 gamma. Fig. 9.5 therefore does not provide any positive evidence either way; but it does not support the view that a successful head release did occur.

ii. It is known that if two sections of a freely rotating body are separated by means of a linear impulse, directed through their respective centres of gravity, then no angular momentum is imparted to either body and they each will maintain the same spin and precession characteristics as the parent body possessed prior to the separation[24]. In practice, however, it is usually found that when a Skylark head is separated from its motor some asymmetry in the

thrust from the three separation springs results in a discontinuous change in the tumbling characteristics as recorded by the three fluxgates. No such discontinuity was recorded with SL40 (Figs. 8.2 and 8.3).

iii. It was stated above that a series of signal strength fluctuations occurred immediately after +87 seconds, followed by a further series at about +95 seconds. The manufacturers of the transmitter are unable to offer any explanation of this effect other than the one outlined above, based on an interference phenomenon, and quoted as an indication of a relative movement between the transmitting antennae and the motor shell[32]. That some alternative explanation is possible, however, is positively demonstrated by Fig. 9.6 which shows the records of R.F. field strength as received at the range head. The diagram covers three sections of the flight: 87 - 98 seconds (including the time of supposed head separation), 366 - 377 seconds (during re-entry) and 464 - 475 seconds (whilst the round was at a height of 6.4 Km and falling at approximately 520 ft./sec.). Two records are shown for each period; the left hand trace of each pair shows the signal strength of the single channel telemetry transmitter (used for the proton magnetometer) and the right hand one shows the signal strength of the 24 channel telemetry transmitter.

It will be noted that considerable and rapid

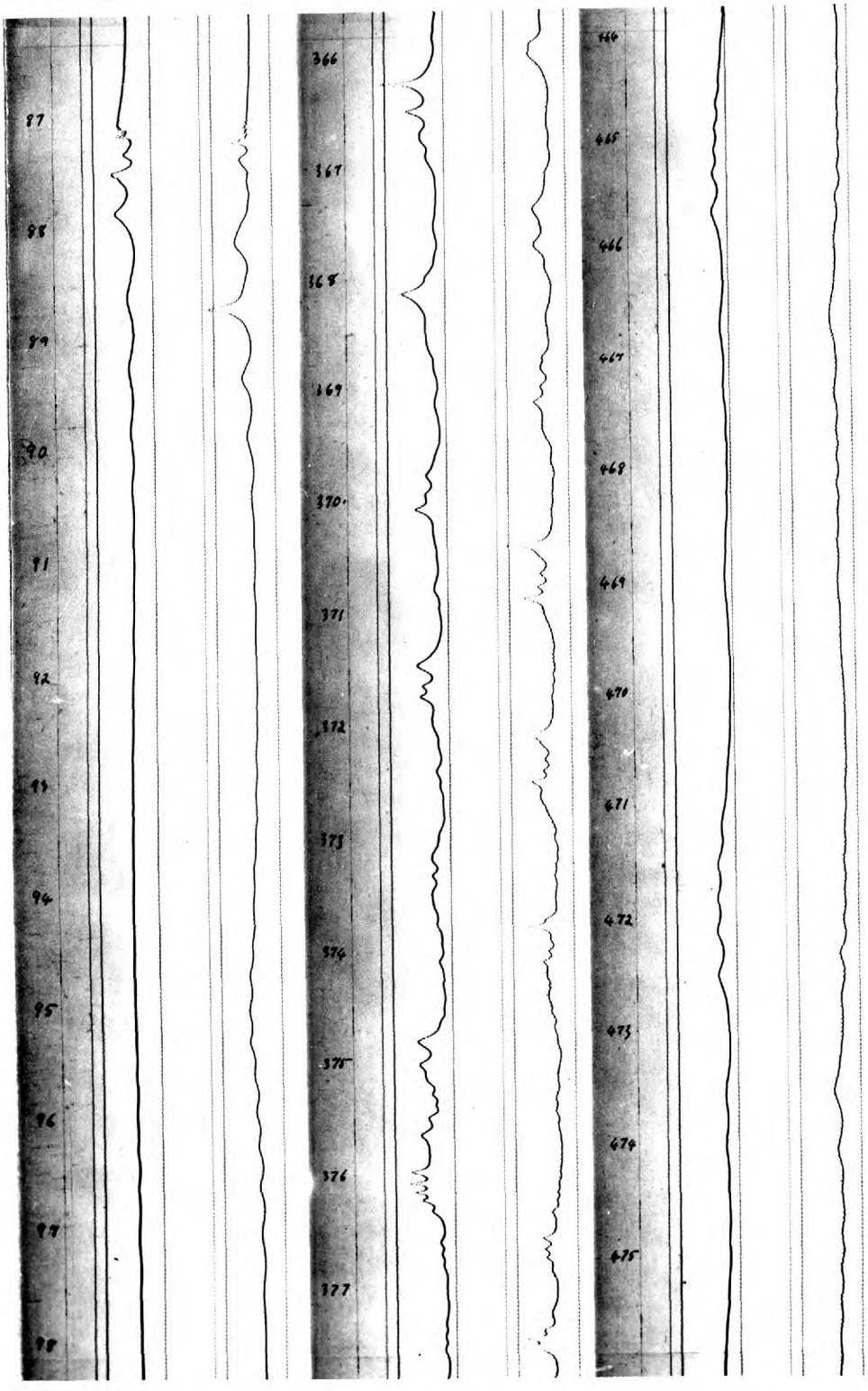


Fig. 9.6. Records of Telemetry Signal Strength.

fluctuations of signal strength occur during the period of severe vibration, whilst the rocket was being retarded to sub-sonic velocities. Whilst the round was falling through the denser atmosphere, very similar patterns of signal strength fluctuation occurred (e.g. at +472 seconds) to those recorded at +88 seconds. Since the motor tube had impacted with the ground at about +400 seconds the oscillations at +472 seconds on Fig. 9.6 cannot possibly be attributed to the mechanism described above; furthermore no similar oscillations occurred at any time during that section of the flight when the round was experiencing a zero-g environment. It is therefore established that the fluctuations in signal strength at +88 seconds could be the result of the severe mechanical shock which would occur when the bomb-slip mechanism fired and they cannot necessarily be interpreted as indicative of a successful head separation.

iv. The fact that the amplitude of the observable frequency excursion at +335 seconds is much smaller than those recorded before +320 seconds suggests that the source of the magnetic field perturbations moved closer to the sensing head during the intervening period (c.f. Appendix I).

The only reasonable self-consistent theory, which can account for all the principal features of the frequency modulations which were recorded during the flight of SL40 is, therefore, that during the period before re-entry, the

sensing head was in too close proximity to the motor for the magnetic effects of the latter to be negligible. The two parts were later separated, during the re-entry phase, leaving only the much smaller errors due to the magnetic material within the head itself.

An increase in magnitude of the field perturbations due to the motor could result from either, a change in relative position of the motor and the sensing head or, a change in the magnetic properties of the steel of the motor resulting from temperature changes, or a combination of both effects. Calculations carried out by R.A.E.[31], together with some measurements during an early Raven static firing, indicate that the maximum temperatures of the various sections of the motor tube during flight would be within the range 300° - 400°C, approximately, and would thereafter fall at a rate of $\leq$ 0.5°C/sec. approximately. Since the temperatures are well below the Curie temperature for high tensile steel (775°C) it can be assumed that the estimated maximum possible change of 50°C during the relevant 100 seconds could not cause the intensity of magnetisation to increase by a factor of 40. The build-up in the amplitude of the frequency modulations must therefore have been due to a change in the relative position of the head and the motor.

It would appear therefore that, either the head separation did not occur when the bomb-slip fired at +87 seconds, perhaps due to the manacle ring remaining jammed,

but that it did occur sometime later, perhaps after the fluxgates had ceased to give any data; or that the operation of the ejection springs was too sluggish to impart an adequate separation velocity. Furthermore, some mechanism must be postulated which could nullify, and even reverse, their relative motions and result in a progressively decreasing distance of separation. At +87 seconds, when head release should have occurred, the rocket was pointing approximately 25° below the horizontal and at a large angle of attack to the relative air flow. In this attitude the drag coefficient of the motor tube would be approximately 6 or 7 times that of the head, whereas its weight, with all fuel burnt, was only about twice that of the head. It is thus conceivable that residual air drag could cause the deceleration of the motor to be slightly greater than that of the head, and, since their initial relative positions when separated were with the motor at a slightly higher altitude than the head, this could lead to a slow drift of the two parts towards each other. It is also possible that gases, resulting from the burning of any residual propellant, might impart a small velocity to the motor tube. On re-entering the denser atmosphere the two sections would rapidly be separated completely, since the fins would quickly stabilize the motor tube in an attitude with a low drag coefficient.

It would be very difficult to derive a unique

solution to the problem of the magnetic interaction between the motor shell and the sensing head, which would enable their relative motions to be described in detail and enable corrections to be applied to the observed data throughout the entire flight, since there is little or no direct information about the many parameters involved. In particular little is known about the direction and intensity of any permanent magnetisation of the motor tube and fins, the relative positions and distance apart of the two sections of the rocket, the orientation of a line joining the centres of gravity of the two sections relative to the geomagnetic vector, the relative amplitudes and directions of the angular momentum vectors of the two sections and the variation with time of all these parameters. It is, however, possible to apply certain qualitative reasoning which will enable an assessment to be made of the absolute magnitude of the total scalar force at a point near the apogee of the rocket's flight.

The magnetic field associated with the rocket motor shell can be considered as comprising "permanent" and "induced" components and, although nothing is known about the permanent magnetic moment vector it can be assumed that its orientation within the motor shell is constant. Furthermore, in view of the comparatively small temperature changes during the period near apogee, the ratio of permanent

to induced magnetisation can also be assumed constant, for any given orientation of the motor relative to the geomagnetic vector. It is also assumed, as discussed previously, that negligible angular momentum was imparted to the two sections of the rocket by the event of head separation. Under these circumstances the permanent component will result in a modulation of the magnetic field about the undisturbed value whereas the induced component will produce a systematic deviation superimposed on which would be a modulation. The systematic deviation, resulting from the induced component, thus determines the probable error which would be introduced into the magnetic field measurements by taking a mean through the 1 c.p.s. precession frequency modulation, which occurred during the first 30.7 seconds of productive signals. The following considerations indicate that any systematic error must be small in comparison with the oscillatory error.

i. Fig. 2.2. gives an approximate indication of the order of magnitude of the effect which might be experienced due to the induced component, though it must be remembered that the measurements illustrated were taken with the geomagnetic vector orientated at 67° to the plane containing the motor tube and sensing head, as compared with 35° in the case of the rocket flight. It can be seen that the $\pm$ 0.5 c.p.s. frequency modulation could result from the translation of

the sensing head between two points 18 ft. apart (i.e. twice the distance between sensing head and the centre of gravity) with a mean distance of about 22 ft., in which case the systematic error would be of the order +0.5 c.p.s. or -0.5 c.p.s., depending on the positions of the head relative to the motor and the geomagnetic vector. It does not, however, seem possible that the induced field alone could cause the ±20 c.p.s. frequency deviations without, at the same time, causing a very pronounced difference in the sharpness of the positive frequency deviation peaks as compared with the negative peaks. Also plotted in Fig. 8.13, at the same time scale as the main diagram, are the modulae of the deviations of the readings relative to a spherical harmonic analysis (curve A) and a graphical mean through the oscillations (curve B). It is immediately evident that, whilst there is a significant difference between the shape of adjacent peaks, this difference is not sufficiently pronounced as to be compatible with the hypothesis that the ±20 c.p.s. frequency excursions could be attributed to induced magnetisation alone. It is therefore necessary to postulate a large permanent magnetisation of the motor shell.

ii. If the contribution to the ±20 c.p.s. amplitude of the frequency modulation arising from the changing orientation of the motor shell can be assumed to be large, compared with that due to the rotation of the rocket head about its

centre of gravity, it can easily be shown that the induced component would introduce a second harmonic component of the rotation frequency into the observed oscillations, whereas the permanent component would contribute only the fundamental frequency. It is therefore, immediately evident from Fig. 8.13 that the permanent magnetisation of the motor shell must have been large compared with the induced magnetisation.

iii. The values of geomagnetic field as a function of height, as calculated on the basis of a simple dipole field, deviate from a linear characteristic by approximately 20 gamma and, if a spherical harmonic analysis is employed, the deviation is only 40 gamma. It seems reasonable to assume, therefore, that the actual values would approximate to a straight line within the same order of tolerance - i.e. ± 2 c.p.s. of precession frequency. It follows that a curve representing the actual decrease of magnetic field strength with height, if plotted on Fig. 9.2, must pass through the large amplitude oscillations recorded at approximately 100 km., since any curve positioned outside the limits of these oscillations would imply that the systematic error in the data was decreasing, whilst the oscillating error was increasing. Assuming, as before, a constant ratio of induced to permanent magnetisation of the motor shell, it follows that the values of precession frequency, which represent true analogues of the total scalar field, must lie within the

observed frequency deviations at all times prior to re-entry.

It can therefore be concluded that the accuracy of the mean of the measurements, during the period from the start of productive signals to just before apogee (height range 148 Km to 152 Km), is better than ±0.5 c.p.s., which corresponds to approximately ±10 gamma. The error in recorded height is mor difficult to assess. Accuracies as high as ±5 meters have been claimed for the FPS16 radar but the accuracy achieved at any given time is mainly dependent on the care with which the equipment has been adjusted. The difference between the positions of the rocket at +60 seconds, as measured by the radar and the kine-theodolites, was less than 0.2 Km and it is considered likely that any systematic error in the radar data would remain of constant magnitude throughout the flight. This error corresponds to approximately ±0.26 cps in precession frequency at a height of 150 Km.

The probable error in the absolute determinations of F at a height of 150 Km is therefore made up of the following parts.

i. Contribution from Height inaccuraces = ±0.3 cps.

ii. Contribution from local magnetic fields = ± 0.5 cps

iii. Inaccuracies due to magnetometer and data processing = ±0.1 cps

Thus the accuracy of the final data is approximately ± 0.$59c.p.s. (= ±14 gamma).

Conclusions

i. The flight of SL40 was primarily intended to act as a test of the proton magnetometer and its associated data processing technique. As such it can be considered highly successful since the breaks in continuity of the data can be attributed to causes not direcly associated with the proton magnetometer itself. It has been demonstrate that it is possible to use the principle of nuclear free precession to obtain accurate measurements of the scalar magnetic field in the upper atmosphere, using a "Skylark" rocket vehicle.

ii. No magnetic discontinuity was detected, as a consequence of the large magnetic field perturbations attributable to the close proximity of the Raven motor. The consistency of the data, however, suggests that, given a suitable environment the techniques employed in the flight of SL40 should be capable of resolving the very small discontinuity, which it is anticipated should be associated with the postulated upper-atmospheric current systems above Woomera.

iii. The absolute magnitude of the total scalar force at a point 150 Km above Woomera, as measured during the flight of Skylark SL40 was 53,807 $\pm$ 14 gamma.

Postscript

Since the completion of the main text a private communication has been received from J.P. Heppner included in which are computed scalar magnetic field values for a selection of points along the trajectory of SL40. These computations have been carried out using coefficients derived from the data of the Vanguard III satellite. This satellite carried a proton magnetometer which was interrogated from various tracking stations including the one situated at Woomera. The value computed for the point, at 150 km. altitude and on the upward section of the trajectory, is $5\overset{3}{\emptyset}$,806 gamma, as compared with the value of $5\overset{3}{\emptyset}$,807 gamma deduced in the main text. Such very close agreement can only be regarded as fortuitous since short period variations could be expected to introduce a discrepancey of a few gamma. It does, however, tend to confirm that the various conclusions, drawn during the discussion in Chpater 9, are in fact valid.

APPENDIX I

GRADIENT EXPERIMENTS

It has already been stated that the frequency of the signal induced into a pick-up coil, by a system of nuclear spins, is proportional to the total magnetic force in which it is situated. Thus, if two discrete samples are positioned in a non-uniform magnetic field and their signals are combined, a series of beats will result, with a beat frequency proportional to the component of the gradient in a line joining the two samples. Similarly, if a single continuous sample is located in a field gradient, the precession signal will comprise a band spectrum, of width proportional to the gradient; this will lead to a loss of phase coherence in the precessing protons in a time shorter than the normal relaxation time, T_2. Some such mechanism is believed to have been responsible for the rapid decay times of the signals which occurred at approximately +335 seconds during the flight of SL40 and for the complete absence of signals at all other times between +320 seconds and re-entry.

The effect is clearly illustrated in Fig. 9.7, which shows a series of decay envelopes obtained from the recovered SL40 rocket-borne magnetometer, using the spare

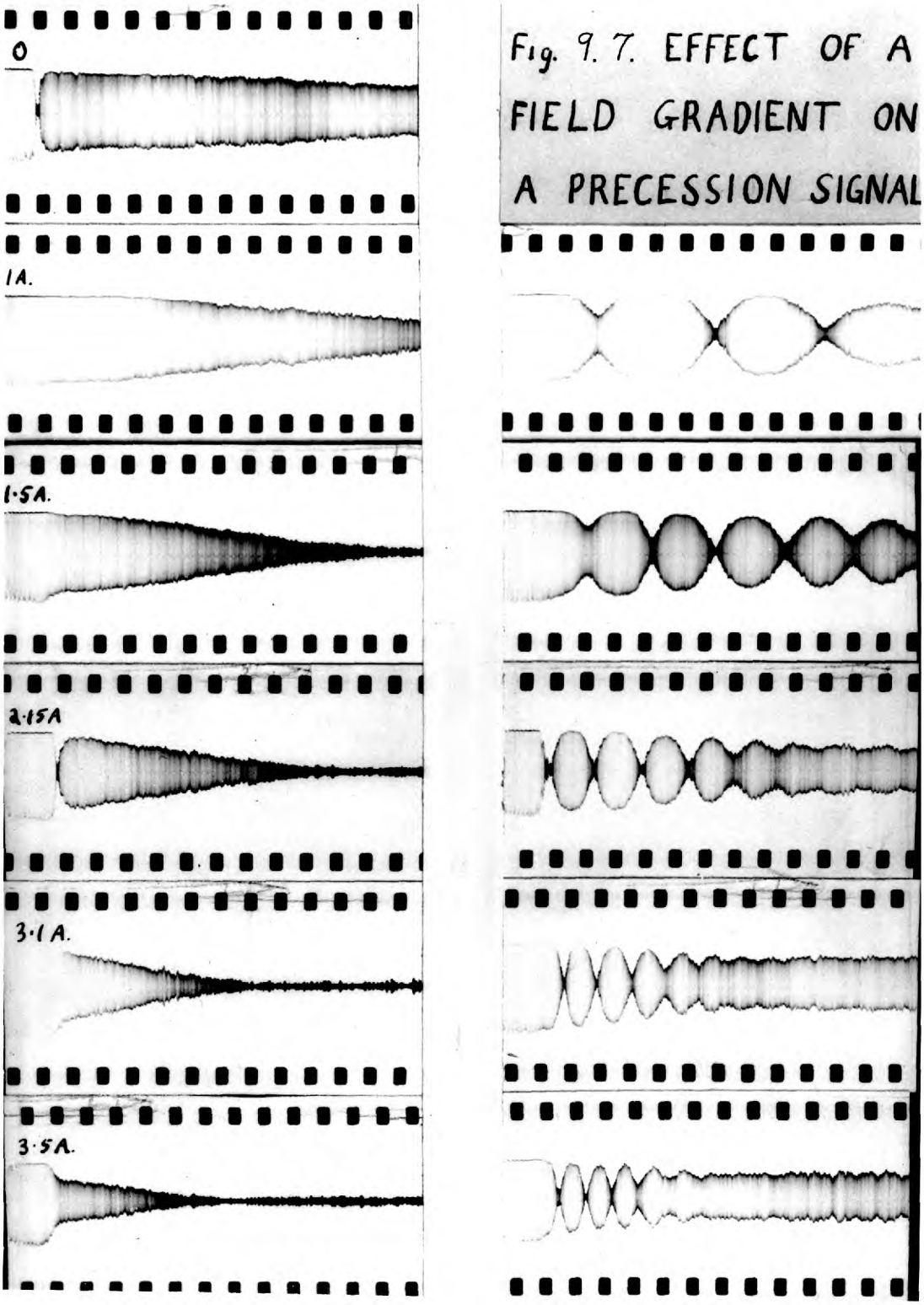


Fig. 9.7. EFFECT OF A FIELD GRADIENT ON A PRECESSION SIGNAL

flight probe. In these experiments the sensing head was positioned in the field coil system (Chapter 6, Section 6), with its axis at right angles to the geomagnetic vector $\vec{F}$ and at right angles to magnetic East-West. A single straight wire, approximately 30 feet long, (defined as the "gradient wire") was positioned in a magnetic East-West direction 100 cm. from the sensing head. The line of the wire, the geomagnetic vector and the line joining the sensing head to the nearest point of the gradient wire were all mutually orthogonal . The circuit through the wire was completed by means of a further wire, which at no point was closer to the sensing head than 15 ft. Thus, at the position of the sensing head, the gradient wire approximates to an infinite line current. Since the field vector resulting from a current in the wire was parallel to $\vec{F}$, the change in the value of total scalar force, as detected by the magnetometer, is given by 200 I gammas and the gradient is given by 2 I gammas per cm., where I is the gradient current in amps. The left-hand column of records in Fig. 9.7 shows the progressively decreasing duration of the signal as the current through the wire was set at 0, 1, 1.5, 2.15, 3.1 and 3.5 amps respectively. The right-hand column illustrates the progressive change in magnetic field strength corresponding to the varying gradients; the beats were obtained by inducing a signal, of constant

amplitude and frequency, into the pick-up coil, by means of a small induction coil energised from a signal generator. The frequency of the reference signal was adjusted to obtain a "zero beat" with no current through the gradient wire.

One theory which could account for some of the features of Fig. 8.13, postulates that a magnetic dipole, of variable moment but orientated permanently along the rocket x axis, might have been induced into the stainless steel probe, by the polarizing field of the sensing head. Now the magnetic field at the position of the sensing head resulting from this induced moment, M, would be $2Mr^{-3}$, where r is the distance in cm., and the field gradient would be $-6Mr^{-4}$. Hence, from a knowledge of the field perturbations and the magnetic gradients, it should be possible to estimate both M and r, or at least to assess limits to their values and hence to test the validity of the above theory.

In order to obtain a quantitative estimate of the minimum magnetic field gradient, which must have been present during the period of the rocket flight when no usable signals were obtained, a series of three experiments were performed, with the gradient wire at two different distances from the sensing head and with the angle between the axis of the sensing head and the magnetic vector orientated at 56° and 90° to the magnetic vector. These angles correspond to the limits of the range of values

which the rocket experienced in flight.

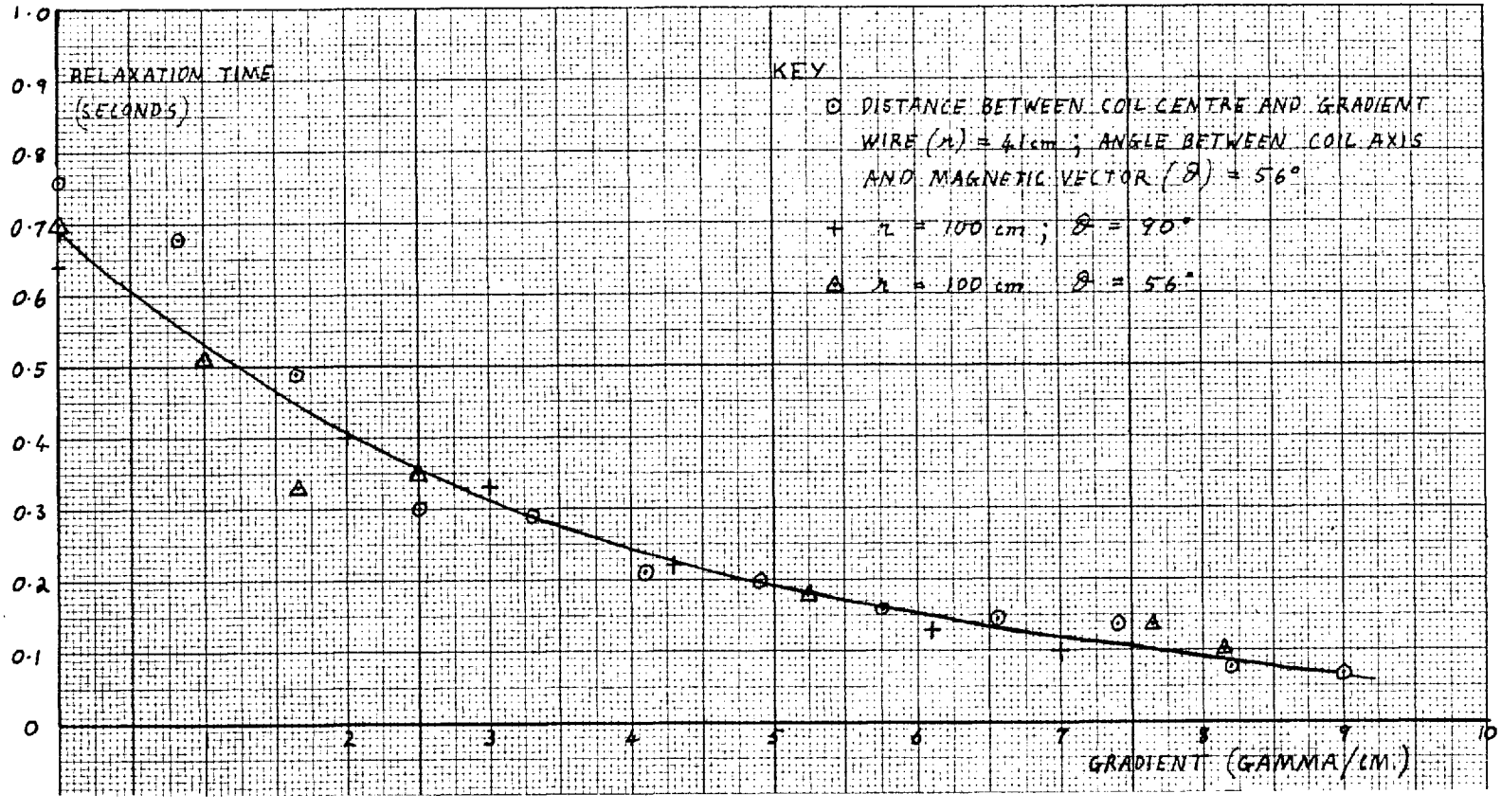
The results of these experiments are shown in Fig. 9.8 which shows how the measured value of the relaxation time constant, of the decaying precession signal, varies with the magnetic gradient, calculated from the geometry of the system and the known current through the gradient wire.

It will be observed that the transverse relaxation time of paraffin (T_2), in the absence of a gradient, is 0.7 ± 0.1 sec. and that T_2 follows a roughly exponential decay with increasing magnetic gradient. Within the limits of the accuracy of the experiments, the decay of the signal is independent of the orientation of the sensing head relative to the geomagnetic vector. The errors in the readings arise from the limit to the accuracy of the signal amplitude measurements, which is determined by the signal/noise ratio, and non-linearities in the amplifier gain with varying signal levels.

These experiments indicate that a gradient of the order of 10 gamma/cm., across the sample, will result in such a short duration of the precession signal that it would be lost in the inevitable large amplitude transient oscillations, which ensue when the polarizing current is switched off; thus a coherent precession signal would not be observed.

Now, since the measured field values during the period just after apogee (Fig. 8.13) oscillate over a range of

FIG. 9.8. VARIATION OF SIGNAL DECAY TIME WITH MAGNETIC GRADIENT.



920 gamma, relative to the mean values, the maximum measured field perturbation must have been $\geq$ 460 gamma. Assuming the source of the error field to be a dipole, orientated along the x axis at a distance r from the sensing head, the maximum field perturbation, δF, is given by

$$\delta F = 2Mr^{-3} \cos 56 = 460 \times 10^{-5} \qquad (1)$$

neglecting the small change in the direction of the resultant total force. The minimum gradient is given by

$$dF/dr = 6Mr^{-4} \cos 56 = 10 \times 10^{-5} \qquad (2)$$

as discussed above.

From these two equations it can readily be shown that the source of the error field must have been situated at least 140 cm. from the sensing head and could not, therefore, have been located in the material of the probe. Furthermore, since at this distance the field from the polarizing coil is less than 10% of the earth's field, it is difficult to accept the hypothesis that thermo-remanent magnetisation might have caused the observed effects.

In the above experiments an "infinite" wire was used to generate the field gradient as, in this configuration, the gradient is less critically dependent on the distances involved, than would be the case with, say, a magnetic dipole; hence it can be calculated more precisely. In order to make a more direct assessment of the minimum possible distance between the source of the spurious magnetic field

and the sensing head, a 680 turn coil, approximately 4.5 cm. in diameter (defined as the "gradient coil") was used to simulate the source of the error field and it was arranged that its distance from the sensing head, in a direction along the axis, could be continuously varied.

To measure the magnetic field resulting from a current, I_c, through the gradient coil, the reference oscillator, referred to above, was adjusted to give an approximate zero beat, with $I_c = 0$. The field corresponding to any given value of I_c dould then readily be calculated, from the mean of the beat frequencies obtained with the two polarities of the moment of the gradient coil. Records were then taken of the decay of the precession signal at various values of gradient current, up to and beyond a value which completely quenched the signal (defined as I_c (crit.)).

Eleven sets of records were taken with d, the distance between the gradient coil and the shoulder of the sensing head (Fig. 6.1) set at, 0, 10, 20, 30, 40, 50, 60, 70, 80, and 100 cm. The results of one of these, with the gradient coil 60 cm. from the sensing head, are shown in Fig. 9.9. The values of I_c(crit.) at the various values of d were as follows:-

d(cm)	0	10	20	30	40	50	60	70	80	100
I_c (crit.) amps.	0.005	0.02	0.05	0.1	0.25	0.45	0.7	1.4	>2.0	>2.5

GRADIENT EXPERIMENTS. 680 turn coil mounted 60cm from SL40 spare coil. Angle between coil axes and $\vec{F}$ = 56°. I_c = current through 680T. coil.

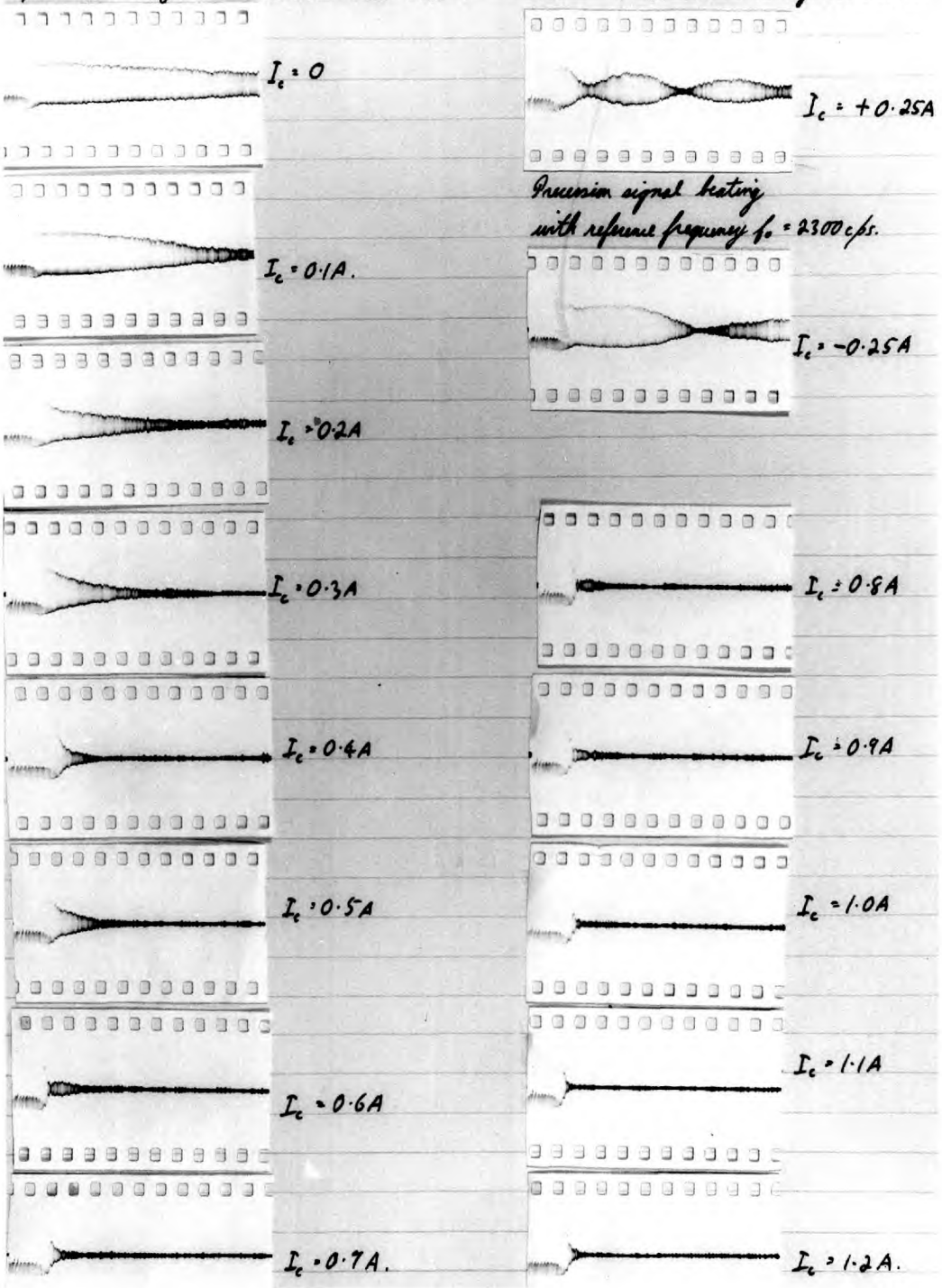


Fig. 9.9.

In each case it was shown that it was impossible to induce a change of ±20 c.p.s. in the precession frequency without, at the same time, completely quenching the signal.

Due to the close proximity of the sensing head to one end of the long, thin probe it is possible that the effect of any thermo-remanent magnetisation on the measured field would resemble more closely that of a magnetic uni-pole rather than a dipole. In this case the magnetic field in the vicinity of the sensing coil would fall off as r^{-2} and the gradient would be proportional to r^{-3}. In order to simulate this state of affairs more precisely the 6 cm. long coil, used in the previous series of experiments, was replaced by one, also of 680 turns, 24 S.W.G. on a 4.5 cm. diameter former but of length 40 cm. In this case the distance d was measured between the end of the "solenoid" closest to the sensing head and the shoulder of the sensing head.

The values of I_c (crit.) at the various values of d were as follows:-

d (cm)	0	5	10	20	30	40	50
I_c (crit.) Amps.	0.02	0.04	0.08	0.3	0.8	1.2	1.7

Again, it proved impossible to produce a detectable change of ± 20 c.p.s. in the precession frequency.

In the light of the results of these experiments it can be stated with some confidence that induced thermo-remanent magnetisation of the probe could not result in a change in precession frequency of 20 c.p.s. without, at the same time, reducing the relaxation time of the decaying signal to such a value that it would be unusable, as an analogue measure of the total scalar magnetic field.

APPENDIX II

MAGNETIC SURVEY OF THE WOOMERA RANGE

Object

The extrapolated proton magnetometer data, from the flight of SL40, yielded a value of 58,115 ± 50 gamma for the total scalar force at ground level; whereas the value interpolated from the, hitherto, best available geomagnetic map is approximately 57,500 gamma (Fig. 2.4). Since a heading effect of ± 460 gamma had been observed in flight, with the angle between rocket axis and the magnetic vector equal to 56°, and since aerodynamic considerations suggest that the rocket head might have been partially stable in falling at sub-sonic speeds; there is a distinct possibility that the magnetic field perturbation, which was observed as precession frequency modulations during the section of the rocket's flight near apogee, might still be present, during the final few seconds of the flight, in the form of a systematic displacement of the measurements from the true values.

The presence of a large error during the post re-entry section of the rocket's flight would provide conclusive proof that the origin of the observed magnetic field perturbations was to be found in the instrumented section

of the round and could not possibly be attributed to the "Raven" motor, since this had impacted with the ground about 118 seconds before the head.

In order to assist in the diagnosis of the cause of the error, and hence in the interpretation of the results, it was therefore decided to carry out a ground survey, to establish the true value of the total magnetic force in the vicinity of the impact point.

Method.

Since the main purpose of the survey was merely to establish whether or not a discrepancy, of the order 500 gamma, existed between the true ground value and that calculated from the flight data, the accuracy required was very low, as compared with that necessary in a normal geophysical survey. It was, therefore, considered that a single traverse between the rangehead and the impact point (or as close to it as possible) would provide sufficient data from which the magnetic field in the impact area could be tied to that, already known, at the rangehead, to within the required accuracy and a full scale two dimensional survey was not necessary.

The portable proton magnetometer described in Chapter 3 was used to obtain a total of 17 absolute determinations of the total scalar force, at 14 stations between the rangehead

and the impact area; the observations at three of the sites were repeated during the return journey. Each determination comprised at least five measurements, which were always self consistent to better than ± 1 count; hence the accuracy of each determination is approximately ± 1 gamma. Each site was chosen to lie as close as possible to a straight line down the range and the magnetometer sensing head was positioned approximately 80 yards from the nearest source of possible magnetic disturbance. The survey was carried out on the 20th July 1962 between 0850 and 1522 hours local time. (Local time = U.T. + 9½ hours). Where it was not possible to fix the position of a station on a map, by reference to local identifiable features, the position was interpolated between two known fixes by reference to the appropriate mileometer readings of the Landrover, used to transport the survey party and equipment; the accuracy of these "fixes" is therefore ± 0.1 mile approximately.

The time of each determination was noted in order that, if required, some allowance could be made, in the final data reduction, for the diurnal variation during the period of the survey.

Results.

Station No.	Local Time	F(gamma)	Local Time	F(gamma)
1	08.50	58209	15.22	58188
2	09.15	58243		
3	09.50	58293		
4	10.07	58206	14.44	58202
5	10.26	58032		
6	10.47	58105	14.08	58085
7	11.05	58014		
8	11.23	58079		
9	11.55	58092		
10	12.44	58037		
11	12.57	58067		
12	13.07	58040		
13	13.16	58035		
14	13.27	58154		

The sites of survey stations are shown on the map of Fig. 9.10 (in rear pocket) and the corresponding values of magnetic field are plotted, at a scale of 1 inch = 100 gamma, using a straight line through the survey sites as the magnetic datum, to which a value of 58,000 gamma is

assigned. By this means some indication of the magnetic trends in the area can be obtained at a glance.

No station magnetometer was operated in the vicinity of Woomera during the survey but the magnetograms recorded at Gnangara (Lat. 31°47'S, Long. 115°57'E, Geomag. Lat. -43.2°, Long. 185.8°) indicate that magnetic conditions were quiet, during the time when the observations were made. A rough indication of the diurnal change in the survey area can be obtained by making an appropriate adjustment to the time scale of the Gnangara magnetograms, to allow for the difference in longitude, and this indicates that the total force at Woomera decreased by approximately 20 - 30 gamma, during the period of the survey, with short period variations of a few gamma. Thus the discrepancies in the measured field values at the three duplicated stations can be attributed to time-dependent changes.

Also plotted in Fig. 9.10, at the same scale and relative to the same magnetic datum, are the following further sets of data.

i. The value of F recorded at 10.00 hours on the 27th September, 1961, (time of trial B67-S040) by the recording proton magnetometer described in Chapter 7, Section 1 (58,223 gamma), together with an indication of the diurnal variation in F recorded during that day.

(58,188 gamma - 58,229 gamma).

ii. Five absolute values of F measured, at five different stations, between 19th and 22nd August, 1957, by the Bureau of Mineral Resources (Melbourne), using an Askania magnetometer. The actual values appropriate to stations 1 to 5 inclusive are 58,167, 58,242, 58,177, 58,086, and 58,115 gamma respectively (mean value 58,157 gamma).

It is immediately evident that all three sets of data are in very close agreement, when due allowance is made for the diurnal and short period magnetic variations and for horizontal magnetic gradients.

Conclusions

1. The absolute value of the scalar magnitude of the total geomagnetic force in the vicinity of the impact point of SL40 can be estimated from Fig. 9.10 as follows. The interpolated value at the point where the survey track approached closest to the impact point is 58,050 gamma; approximating the diurnal variation to a constant rate of change with time, leads to a correction of + 15 gamma, making the final value 58,065 gamma. It is difficult to assess the effect of the displacement of the impact point from the actual magnetic stations, since there are not sufficient readings to make an estimate of the lateral

gradients in the area; however, even if the magnetic gradient at right angles to the survey track were equal to the steepest observed gradient of the survey (i.e. that between stations 13 and 14), this would only introduce an error of 50 gamma and the actual error is probably considerably less than this.

2. Fig. 2.4 shows the hitherto best available ground magnetic measurements in the vicinity of Woomera. The above absolute determination of F has been added to this map (approximated to the nearest 100 gamma, in conformity with the previous figures) and it is immediately evident that the 580 contour requires drastic revision, to accommodate the new measurement.

3. The close agreement between the new measurements and those taken, five years previously, by the Bureau of Mineral Resources, suggests that the mean secular variation, during the period 1957 to 1962, was considerably less than the forecast value of 35 gamma per year [33].

4. The implications of the results of the ground survey on the interpretation of the results of the flight of Skylark SL40 are discussed in the main text.

BIBLIOGRAPHY

1. Balfour Stewart. "Terrestrial Magnetism", Encyclopaedia Britannica, 9th Edition, p.36 (1882).

2. A. Schuster. "The Diurnal Variation of Terrestrial Magnetism", Phil. Trans. Roy. Soc. A, 208, pp.163-204 (1908).

3. S. Chapman and J. Bartels, "Geomagnetism", Vol.2, p.1049, (Oxford University Press, 1940).

4. E.H. Vestine, L. Laporte,, I. Lange and W.E. Scott, "The Geomagnetic Field, Its Description and Analysis", Carnegie Inst. Wash. Publ. 580, p.363, 1947.

5. S. Chapman in "Rocket Exploration of the Upper Atmosphere" p.242, R.L.F.Boyd and M.J. Seaton (Editors), Pergamon Press Ltd., London, (1954).

6. S.F. Singer, E. Maple and W.A. Bowen, Phys. Rev., 77, p.398 (1950) and E. Maple, W.A. Bowen and S.F. Singer, J. Geophys. Research, 55, p.115, (1950).

7. S.F. Singer, E. Maple and W.A. Bowen, "Evidence for Ionospheric Currents from Rocket Experiments Near The Geomagnetic Equator". J. Geophys. Research, 56, p.265, 1951.

8. J.P. Heppner, J.D. Stolarik and L.H. Meredith, "The Earth's Magnetic Field above W.S.P.G., New Mexico, From Rocket Measurements", J. Geophys. Research, 63, p.277, June, 1958.

9. L.H. Meredith, L.R. Davis, J.P. Heppner and O.E. Berg, I.G.Y. Rocket Report Series, No.1, p.169, July 1958.

10. L.J. Cahill, Jr., "Investigation of the Equatorial Electrojet by Rocket Magnetometer", J. Geophys. Research, 64, p.489, (1959).

11. J.M. Conley, "Earth's Main Magnetic Field to 152 Kilometres above Fort Churchill", J. Geophys. Res., 65, p.1074 (1960).

12. R. Hutchinson and B. Shuman, "Rocket Measurements of the Magnetic Field above New Mexico", J. Geophys Res. 66, p.2687, Sept. 1961.

13. H.S.W. Massey, "Rocket Exploration of the Upper Atmosphere", Nature, 177, pp.643-645, 1956.

14. J.F. Hazell and E.B. Dorling, "Sounding Rockets", p.243, McGraw-Hill, New York, 1959.

15. W.M. Rae, "The Airborne Sender for 24-Channel Telemetry" J. Brit. I.R.E., 21, p.57, (1961).

16. J.A. Van Allen, Report No.37 of the Upper Atmosphere Rocket Research Panel, Feb. 4, 1954.

17. M. Packard and R. Varian "Free Nuclear Induction in the Earth's Magnetic Field", Phys. Rev., 93, p.941, 1954.

18. G.S. Waters and P.D. Francis, "A New Method of Measuring the Earth's Magnetic Field", Geophysical Prospecting, 4, No.1, 1956.

19. G.S. Waters and P.D. Francis, "A Nuclear Magnetometer, J. Sci. Instrum., 35, p.88, 1958.

20. J.H. Nelson, "The Gyromagnetic Ratio of the Proton", J. Geophys. Res., Vol.65, p.3826, (1960).

21. S.H. Hall. Private communication.

22. K. Burrows. "A Rocket-Borne Magnetometer", J. Brit. I.R.E., Vol. 19, pp.769-776, 1959.

23. S.M. Rubens. "A Cube Surface Coil for Producing a Uniform Magnetic Field", Rev. Sci. Instr., Vol. 16, pp.243-245, 1945.

24. S.H. Hall. Private communication.

25. E.H. Vestine et al., "The Geomagnetic Field: Its Description and Analysis", Carnegie Institution of Washington, Publication 580, Washington, D.C., (1947), p.10.

26. K. Pounds, Private communication.

27. Firth-Vickers Stainless Steels Ltd., Publication No.108/13.

28. G.A. Kelsall, "Permeability Changes in Ferromagnetic Materials Heat Treated in Magnetic Fields" Physics 5 (1934) pp.169-172.

29. R.M. Bozorth, "Ferromagnetism" (1951) p.117.

30. J.J. Becker. "Mystery of Magnetic Annealing" Metal Progress 1957 (August), p.84.

31. P.J. Herbert. Private communication.

32. W.M. Rae (E.M.I. Ltd.,) Private communication.

33. W.D. Parkinson and R.G. Curedale, "Isomagnetic Maps of Australia for the Epoch 1957.5", Bureau of Mineral Resources Report No.62, 1961.

ACKNOWLEDGMENTS

The author wishes to acknowledge his indebtedness to the following individuals and organisations who have made contributions to the progress of the work.

1. Professor J. M. Bruckshaw, his supervisor, for his advice and encouragement given throughout the research.
2. The British National Committee on Space Research under the auspices of the Royal Society and the Department of Scientific and Industrial Research who have provided, and continue to provide, the financial support for the project.
3. Dr. S. H. Hall who, in addition to taking part in many useful discussions, has:-
   - i) carried out the computations involved in Fig.2.1,
   - ii) assisted in carrying out the rotation experiments (Ch.4),
   - iii) constructed the coil system used to simulate the geomagnetic field at Woomera (Ch.6.Sec.6),
   - iv) corrected the height data of Fig.8.1 for the curvature of the earth and
   - v) carried out the spherical harmonic analysis mentioned in Chapter 9, Section 2.
4. The Royal Aircraft Establishment, Farnborough, who assembled the rocket, and assisted in carrying out the preliminary compatibility tests (Ch.5, Sec.5).

5. The Weapons Research Establishment, Salisbury, South Australia, where the rocket was tested and prepared for firing. Their willing co-operation in providing several facilities, not normally required for a Skylark trial, is particularly appreciated. In addition to providing the play-back facilities and assistance in the routine data analysis (Chapter 8), they took the photographs of the rocket and the ground recording magnetometer installation at Woomera, where private photography is not permitted.

6. Hunting Geophysics Ltd., for the loan of a fluxgate magnetometer with which some preliminary magnetic measurements were carried out.

7. Venner Electronics Ltd., for many useful discussions, particularly in connection with the use of their transistorized plug-in stages.

8. The Bureau of Mineral Resources, Melbourne, who:-
   i) supplied the data from which Fig. 2.4 was drawn and
   ii) supplied copies of the relevant observatory magnetograms for the day of the ground magnetic survey.

9. K. Bullough, of Sheffield University, who, in spite of his own research commitments, found time to carry out the measurements for the ground magnetic survey (Appendix II).

10. P.J. Herbert, of the R.A.E. for many useful discussions in connection with the attitude behaviour of SL40.

11. W. Harrison, of Firth-Vickers Stainless Steels Ltd., for his advice regarding the magnetic properties of stainless steels.

12. F.G. Irving, of Imperial College, for his advice on the aerodynamic properties of a rocket-head with the configuration of SL40.

13. The chief radiographers at University College Hospital, London, and at Heatherwood Hospital, Ascot, for producing the X-rays used for Figs. 5.12 and 6.16.

14. Pergamon Press Ltd., for permission to reproduce Fig.1, from "Rocket Exploration of the Upper Atmosphere", edited by Boyd and Seaton.

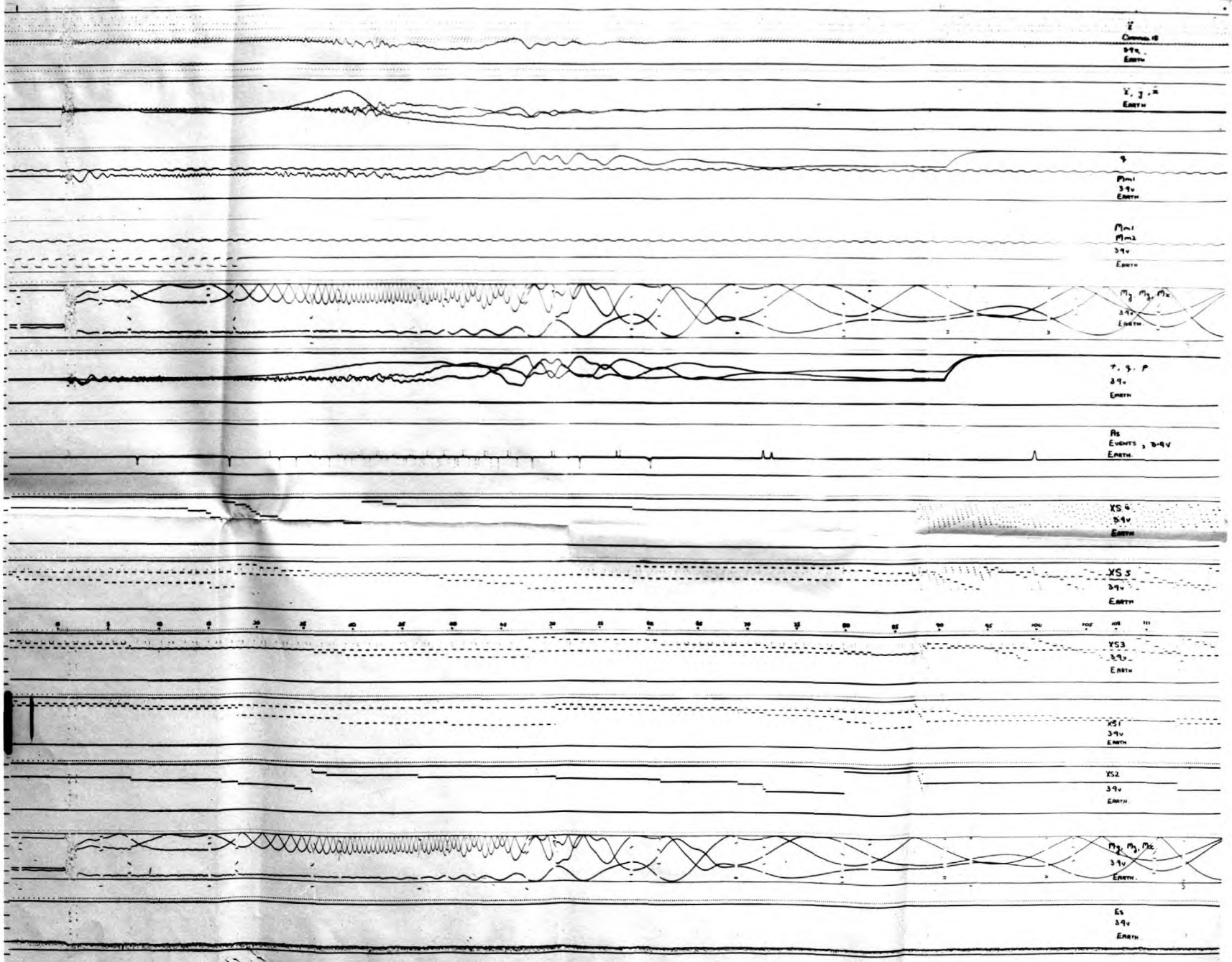


FIG. 8.2.

Ph.D. K BURROWS

Unclassified

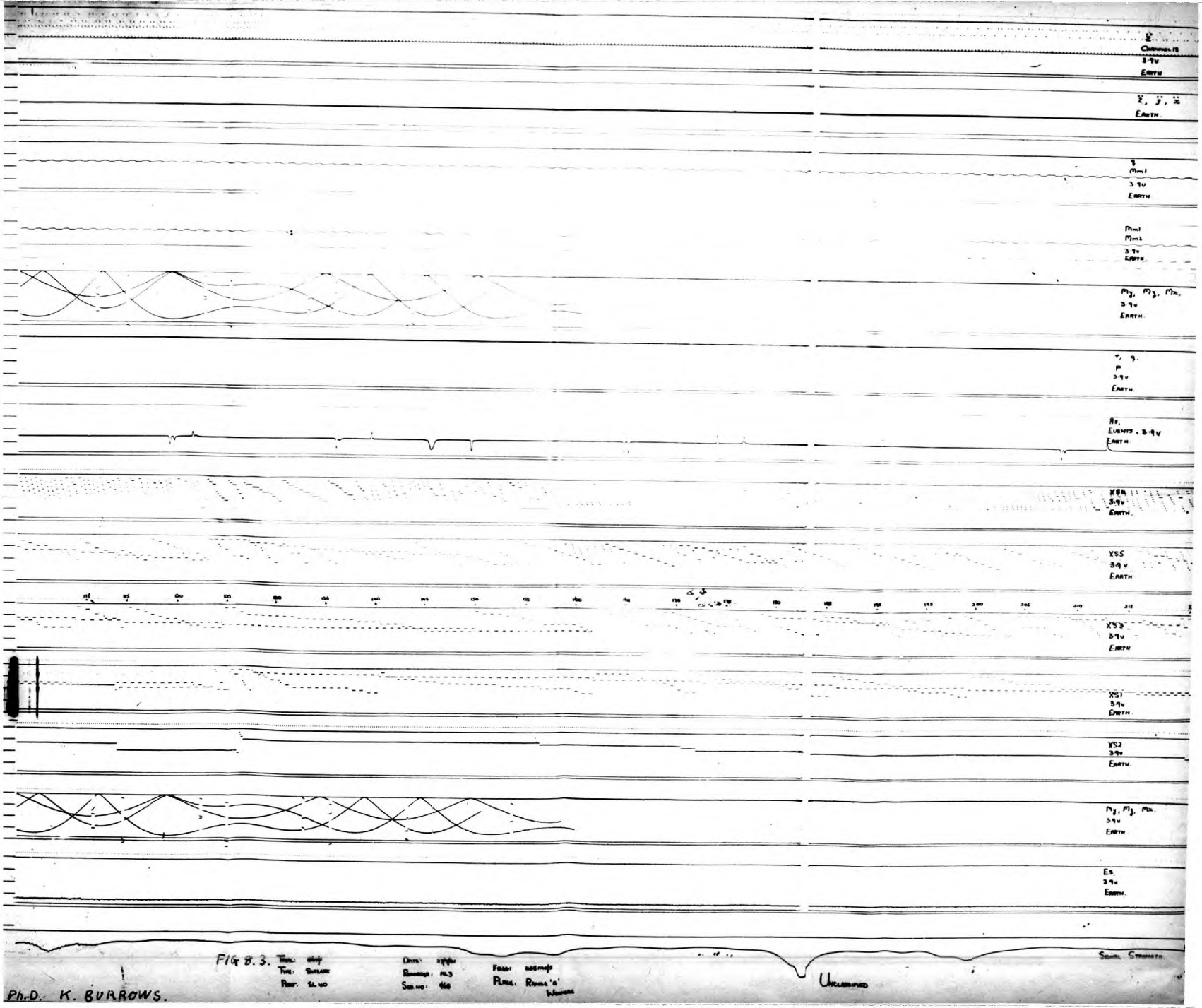
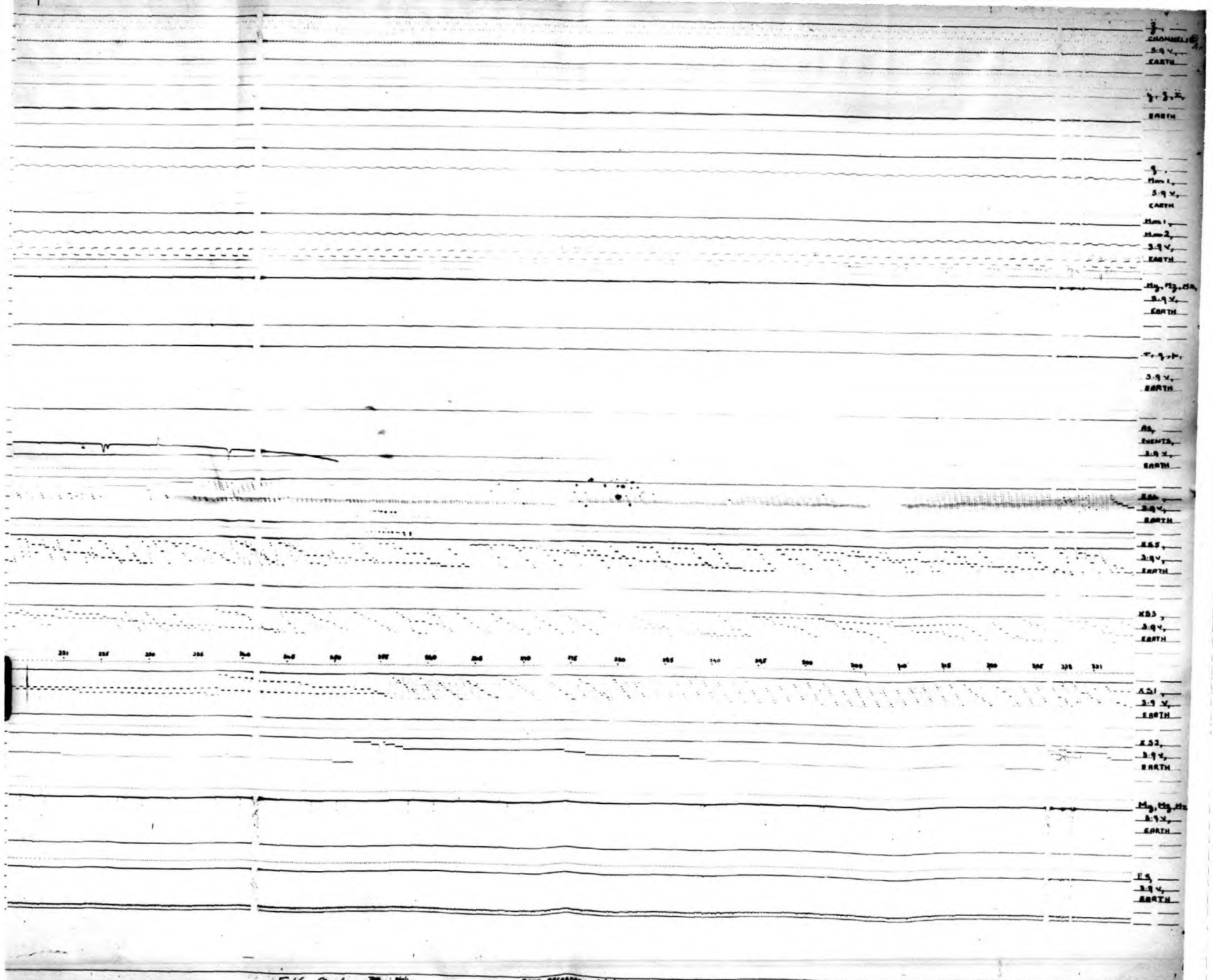


FIG 8.3. Time: 08h
Type: Surface
Rec: SL 40

Date: 23/8/61
Recording: ML3
Seq no: 46

Freq: 400 m/s
Plane: Radial 'a'
Vertical

Ph.D. K. BURROWS.



Ph.D. K BURROWS

FIG. 8. 4.

TAPE : 0611
TYPE : SKYLARK
HEAD : SINGLE

DATE RECORDED : 21/9/61
PLAYBACK FROM : MT16

PLACE : RANGE 'E' WOOMERA
SEA NO : 911
FREQUENCY : 4·75 m/s

UNCLASSIFIED

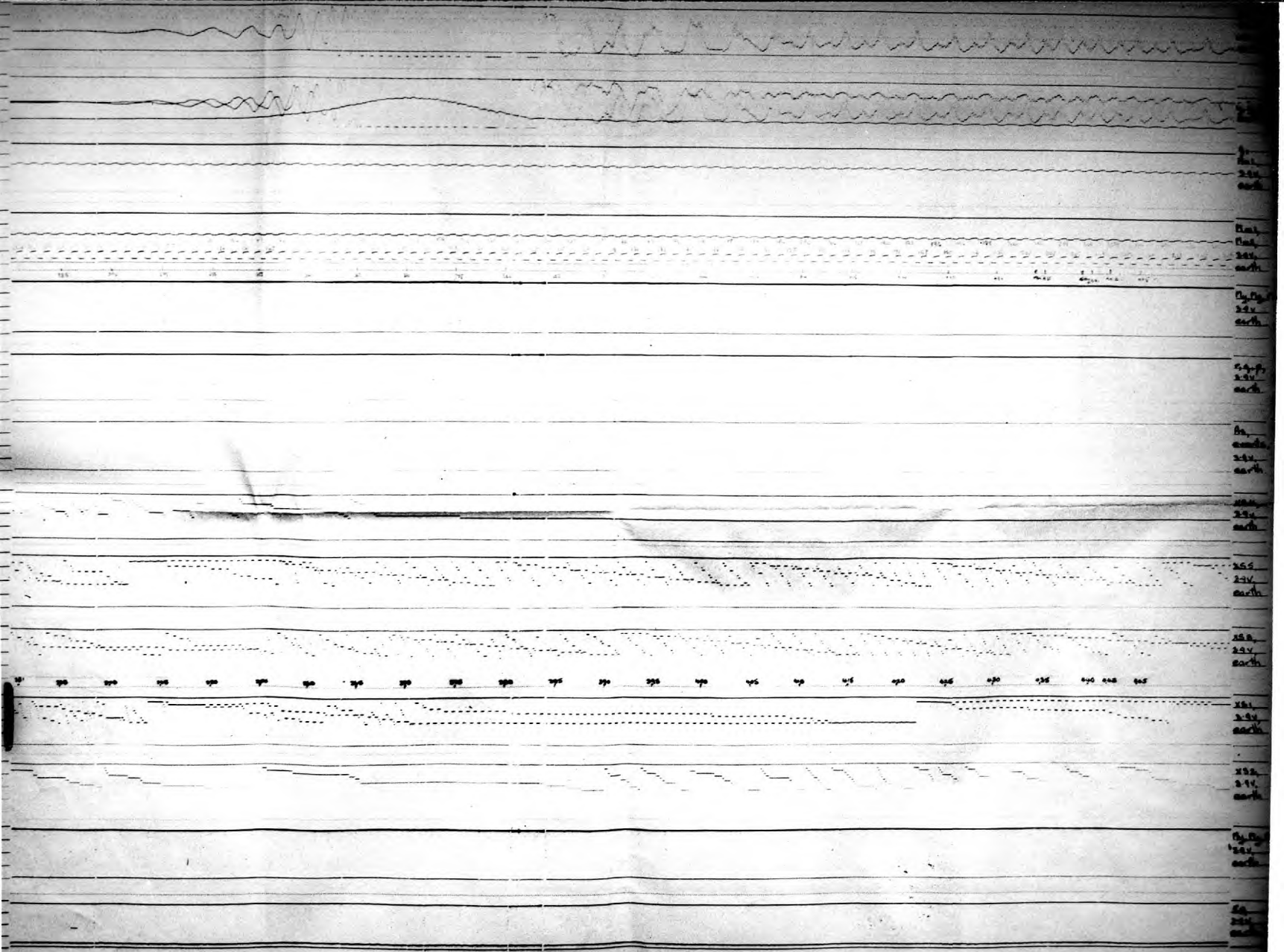


FIG. 8.5 TRIAL: B61/1
TYPE: SHALLOW
PROF: SL 50
DATE RECORDED: 27.5.61

PLAYBACK FROM TAPE
FREQUENCY: 0.65 m/s
SER. NO: 778
PLACE: BOARD 'C' HYDRA

UNCLASSIFIED

Ph.D. K BURROWS

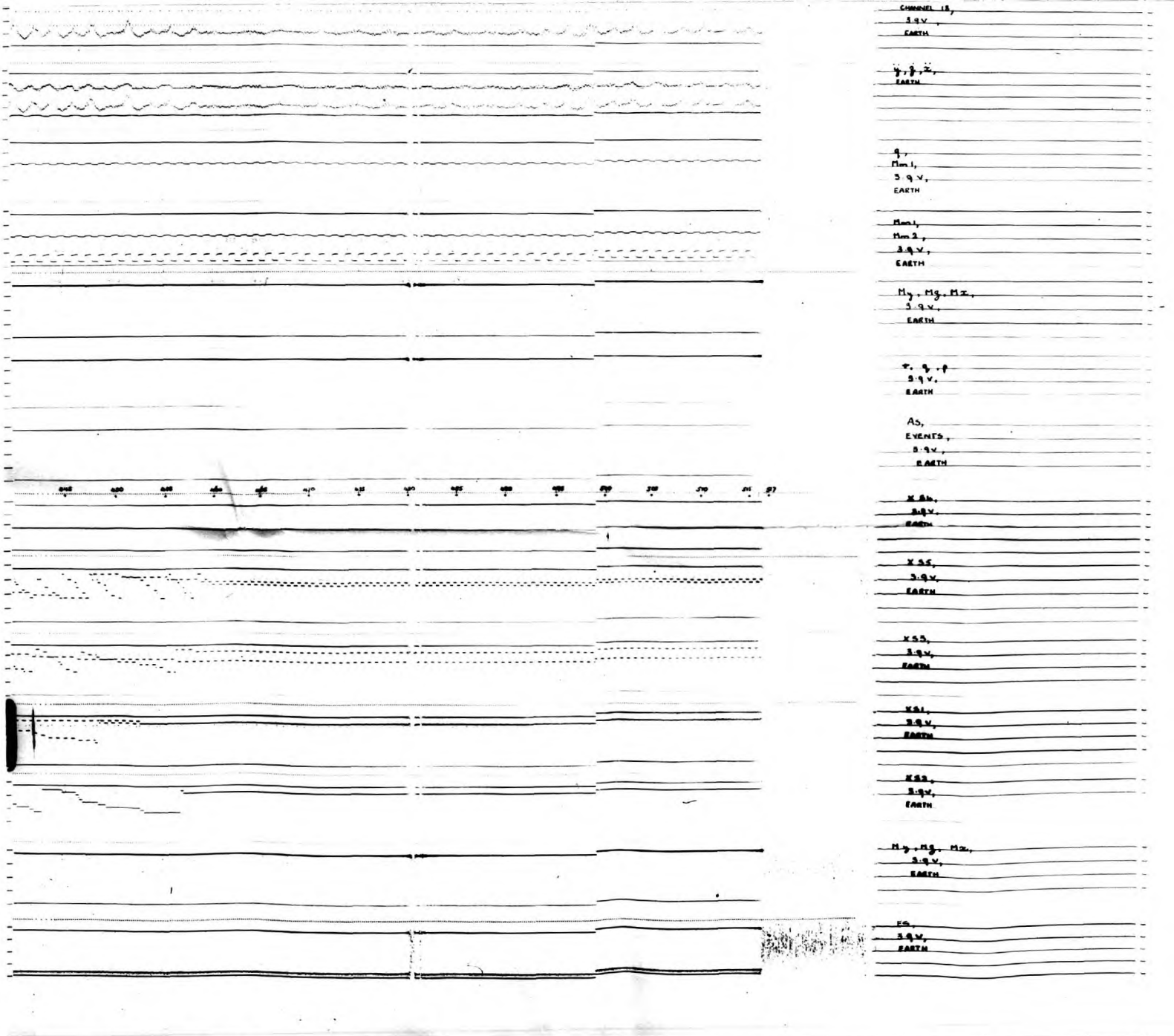
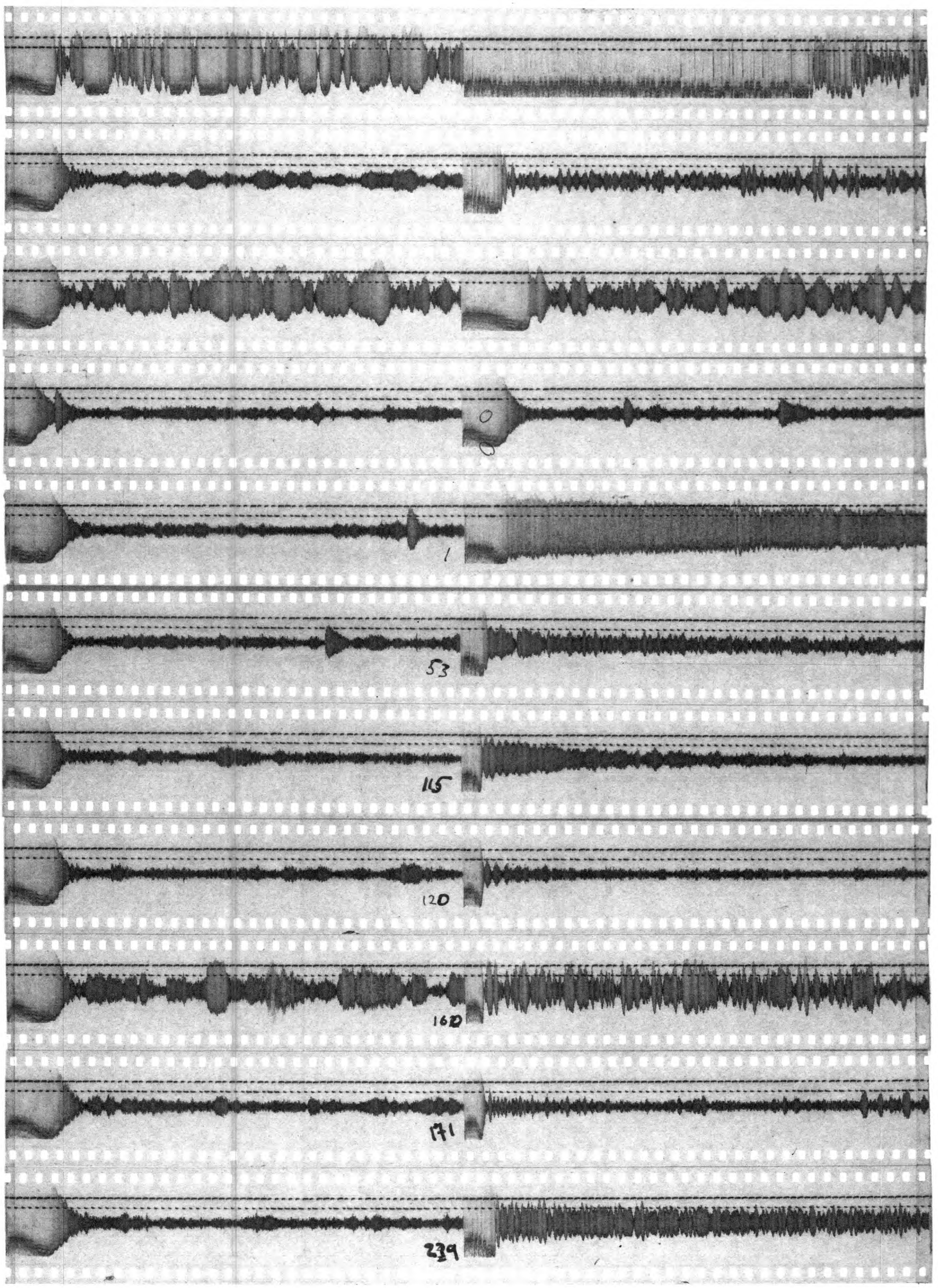


FIG. 8.6. TRIAL: 8149 TYPE: SKYLARK PROJ: SL 40 PLAYBACK FROM MT 96 DATE RECORDED 24/9/70 FREQ: 455 KHz SERIAL: 998 PLACE: Woomera.

UNCLASSIFIED

Ph.D. K BURROWS.



Ph.D. K BURROWS.

FIG. 8.7. SPECIMEN RECORDS

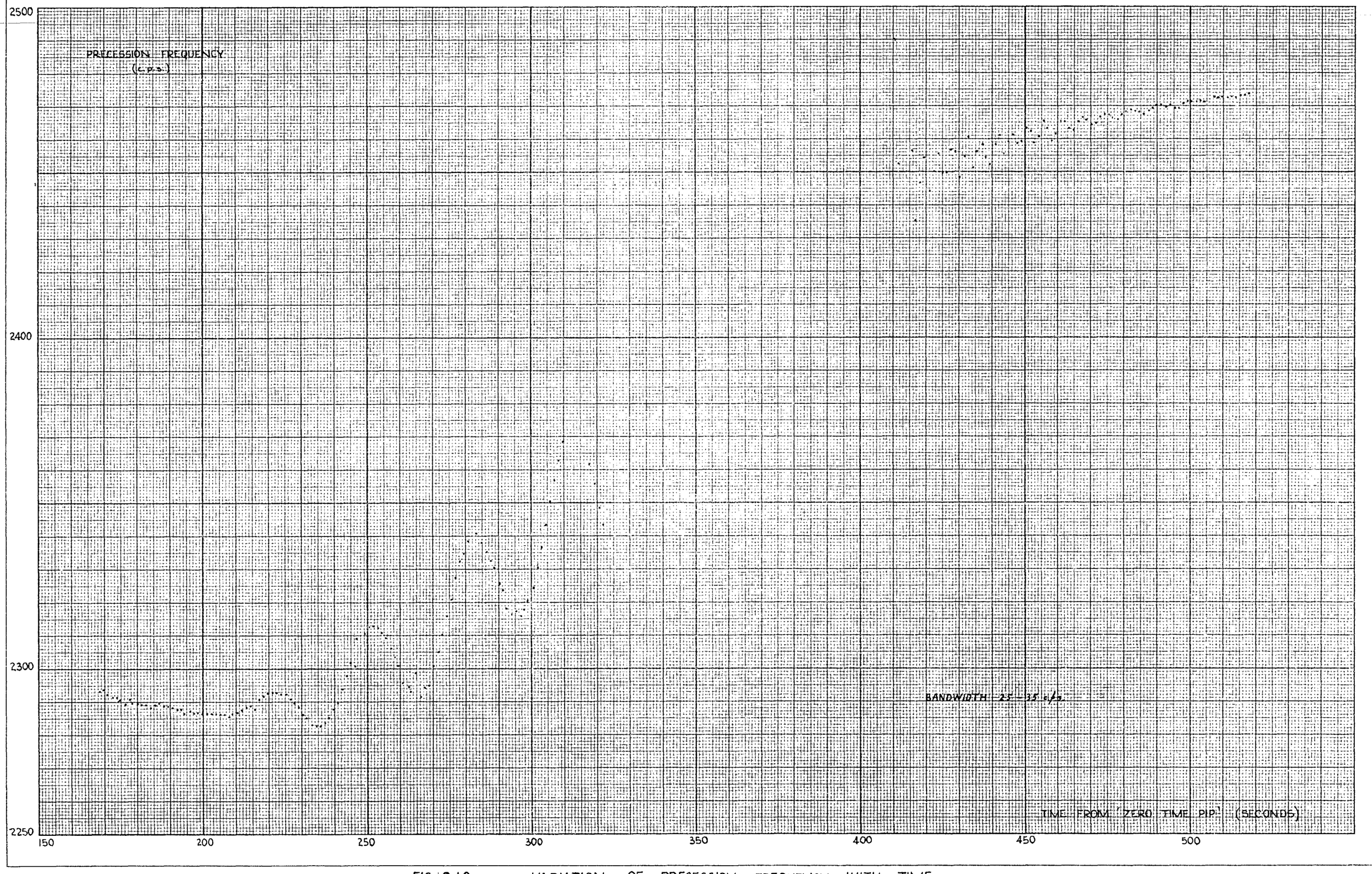


FIG. 8.10. VARIATION OF PRECESSION FREQUENCY WITH TIME

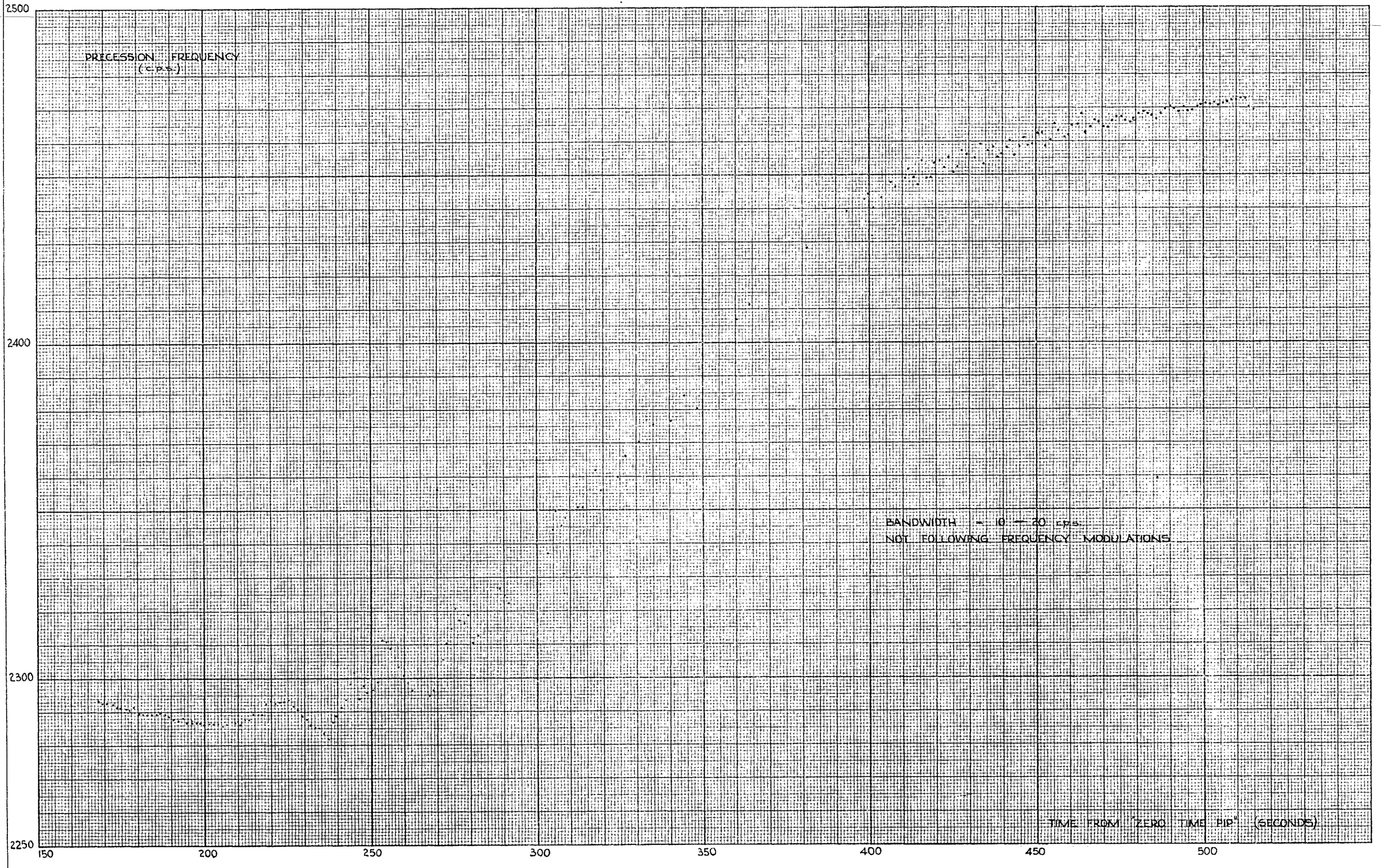


FIG. 8.11. VARIATION OF PRECESSION FREQUENCY WITH TIME.

Ph.D. K BURROWS.

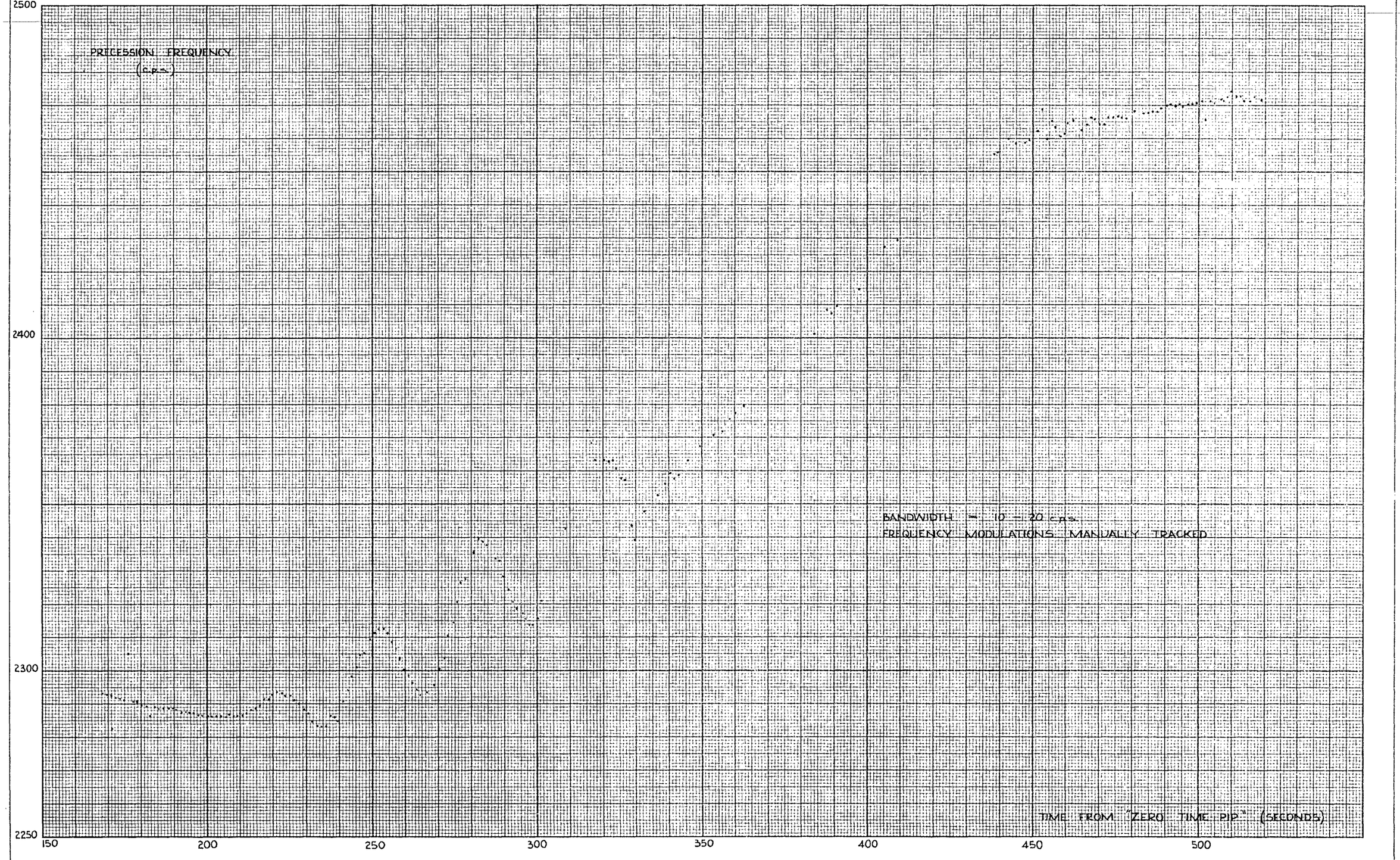


FIG. 8.12. VARIATION OF PRECESSION FREQUENCY WITH TIME

Ph. D. K. BURROWS.

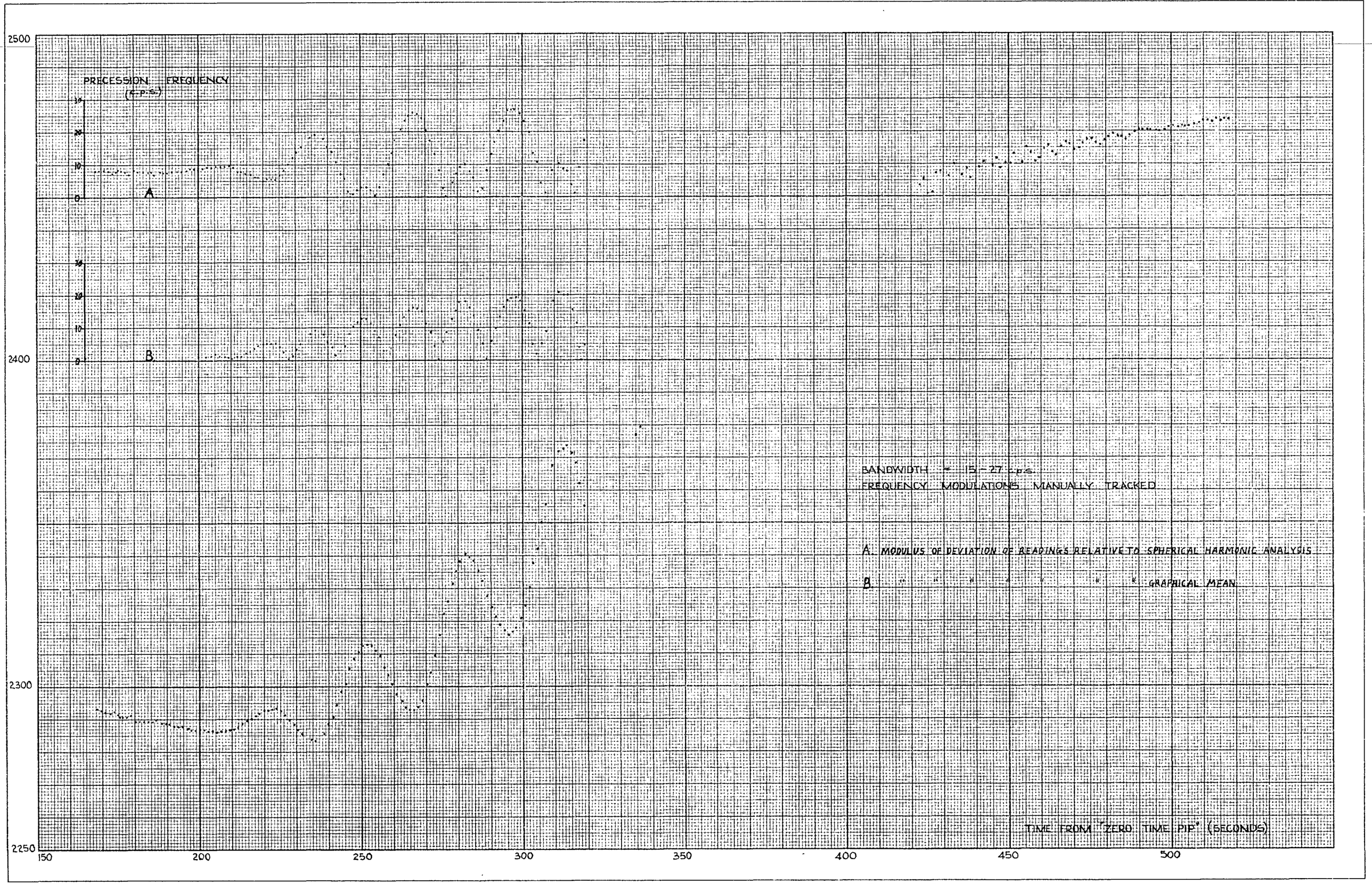


FIG. 8.13. VARIATION OF PRECESSION FREQUENCY WITH TIME

Ph. D. K BURROWS.

24 23 22 21 20 19 18 17 16 15 14 13 12 11 10 9 8 7 6 5 4 3 2 1 24

100 80 60 40 20 0

27/9/61 Vienna

22148 7/59

FIG. 9.1. GROUND RECORD.

Ph.D. K BURROWS.

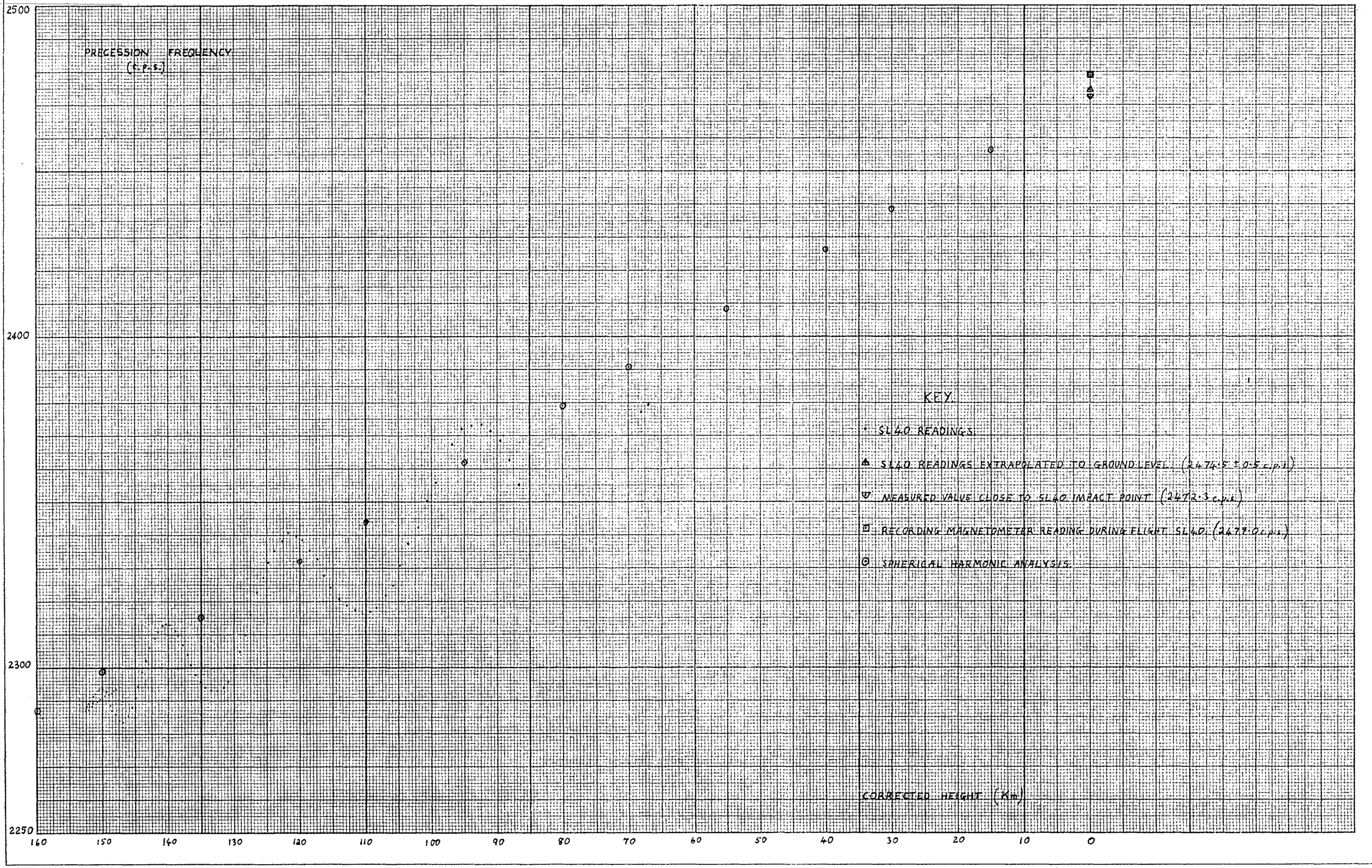


FIG. 9.2. VARIATION OF PRECESSION FREQUENCY WITH HEIGHT.

Ph.D. K BURROWS.

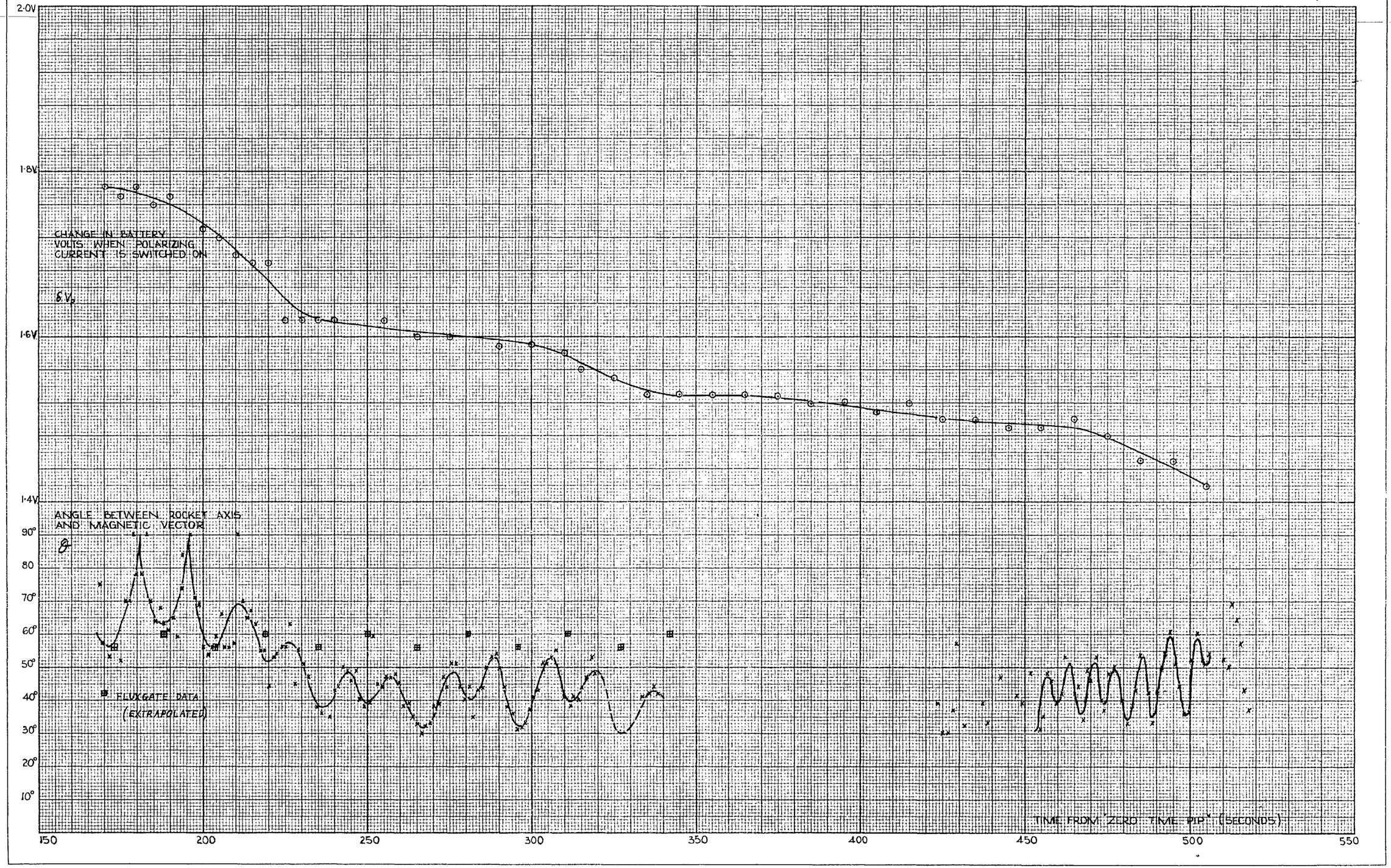


FIG. 9.3. VARIATION OF POLARIZING BATTERY VOLTAGE; ROCKET ATTITUDE CALCULATED FROM PROTON MAGNETOMETER DATA

Ph. D. K BURROWS.

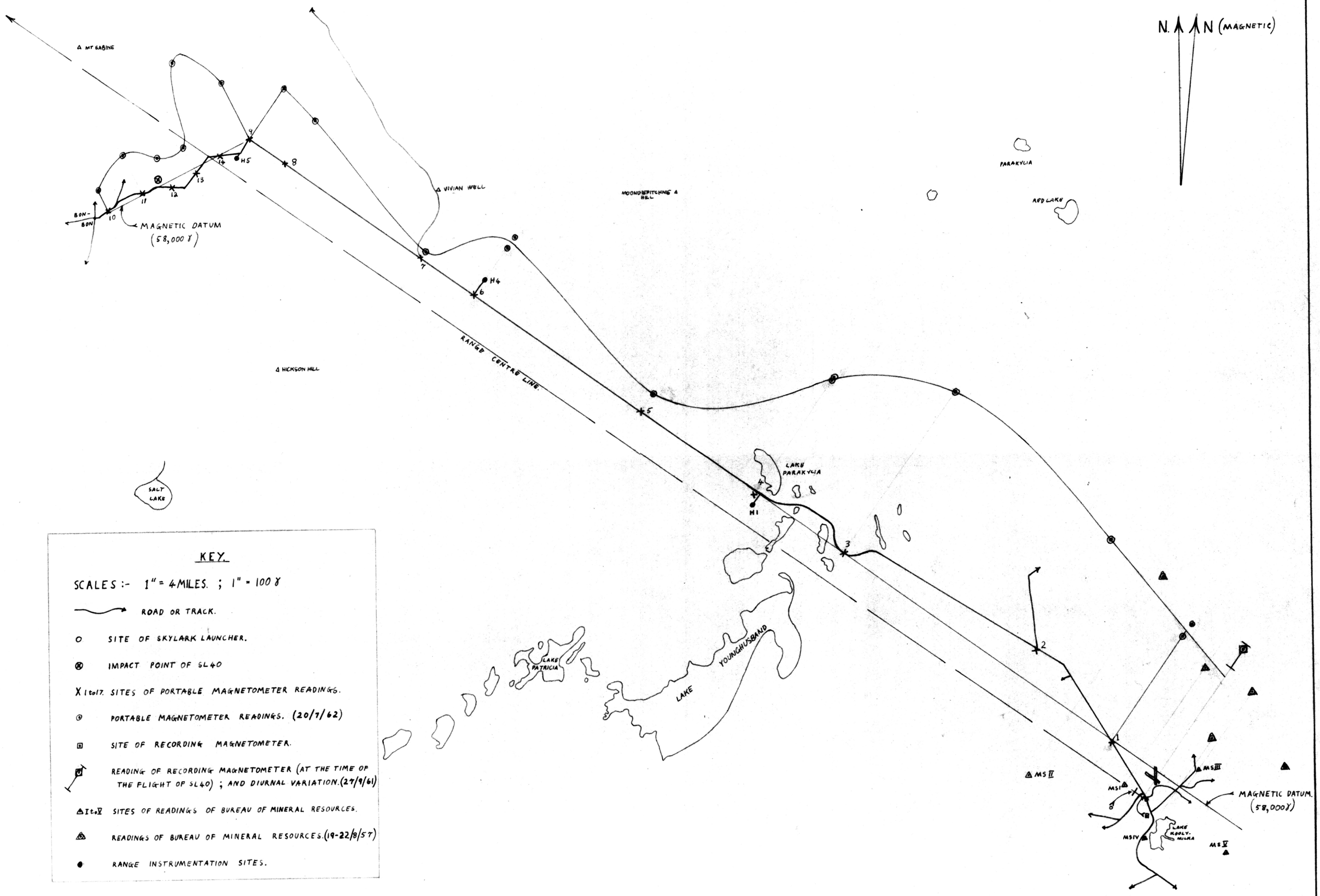


FIG. 9.10. GROUND MAGNETIC MEASUREMENTS AT THE WOOMERA ROCKET RANGE.

Ph.D. K BURROWS.